THE TRANSPORT PROPERTIES OF SUPERCONDUCTING-NORMAL INTERFACES

by

Humphrey William Lean

Kings College

Thesis submitted for the degree of Doctor of Philosophy in the University of Cambridge, March 1987

H. W. Lean

The Transport Properties of Superconducting-Normal Interfaces

The resistive and thermoelectric properties of a series of SNS sandwiches, containing different concentrations of impurity in the superconductor, have been measured. The system used for this work was In/W/In with up to 10% lead added to the indium. A technique was developed in which the interfaces were prepared by melting indium onto tungsten slices in high vacuum. The samples produced in this way were of comparable quality to those used by previous workers.

The samples with pure indium were found to obey a previously developed theory for the divergent temperature dependence of the resistance just below T_c. This theory was extended with more realistic boundary conditions and to include the proximity effect. It was then found to adequately explain the temperature dependence of the resistance over the whole range between $0.3T_c$ and T_c. The thermopower of these samples near T_c was also found to have the temperature dependence predicted by previous theory. The results imply that the thermopower of indium changes in a discontinuous and systematic way at T_c. This is at variance with what is expected theoretically and with previous experimental work on lead.

The low temperature interface resistance was measured as a function of the concentration of lead in the indium. It was found that, for lead concentrations of up to 5%, the interface resistance was proportional to the residual resistivity of the indium as predicted by a theory of Pippard. The magnitude of this resistance was, however, not found to be in agreement with the theory. Above concentrations of 5% Pb, the low temperature resistance data was found to become irreproducible. A theory was constructed which adequately explained the temperature dependence of the resistance of the samples with up to 5% lead in the indium. The temperature dependence of the thermopower of these samples was found to be approximately as expected from theory in the region just below T_c. However, well below T_c, an unexplained divergence in the thermopower was found.

PREFACE

The work described in this thesis was carried out between October 1983 and January 1987 in the Low Temperature Physics group of the Cavendish Laboratory. I would firstly like to thank my supervisor Dr. J. R. Waldram for suggesting the project and for assistance on many occasions, especially with the theory. I would also like to acknowledge helpful discussions with Prof. Sir A. B. Pippard.

On the practical front I would like to thank the following people: Steve Battersby for introducing me to the measurement apparatus, Terry Brown for providing me with high purity tungsten and instruction on the art of spark machining, John Pratt for winding my furnace and all the members of the LTP workshop, especially: Paul Booth for assistance on innumerable occasions with everything from leak testing the cryostat to finding the keys to my desk, Pete Flaxman for supplying liquid helium unfailingly and much assistance with the evaporator, Dave Swainston for never hesitating to drop everything to assist with my problems and Ken Gadsby for supplying liquid nitrogen.

I would like to thank all my contemparies in the Low Temperature Physics group for assorted assistance and friendship. A special mention must go to Lesley Cohen with whom I shared a room, a screened room and many other things (mostly edible) for over three years. I must also thank my other sometime room-mates: Ralph Claessen, Mark Boyd, Wyn Williams and Adrian Porch for providing company. I am grateful to my other friends in the group; John Cockburn, Anne Sleigh, Helen Kibble, James Bellingham, Alison Marshall and all the others, too numerous to mention, who enriched my life in the Cavendish.

Outside the lab, I am extremely grateful to Inderpreet Dhingra for providing a roof over my head and being a very good friend (his one forray into the world of low temperature physics foundered when tomato skin

turned out not to be superconducting!). I have also greatly enjoyed the company of my other flatmates: Mark Deans, Dave Arundel and Henrietta Brougham. I would finally like to thank Andrew Goldsbrough and my many other friends who helped to make my stay in Cambridge enjoyable.

I was supported for three years by a grant from the Science and Engineering Research Council for which I am grateful.

I declare that, except where otherwise stated, this dissertation is the result of my own work and includes nothing which is the outcome of work done in collaboration. This dissertation is not substantially the same as any other which I have submitted for a degree, diploma or other qualification to any other University.

H W Lean.

Humphrey W. Lean

March 1987

CONTENTS

CHAPTER 1

INTRODUCTION

1.1 Historical Review.

The transport properties of superconducting-normal (SN) interfaces have been studied in two types of system. The first of these is metals in the intermediate state which contain normal and superconducting domains. The second and the one with which this thesis will be concerned is SNS sandwiches. These consist of a thin layer of normal metal with layers of superconductor attached on either side. The system is prepared in such a way as to ensure that the SN interfaces are as clean and sharp as possible. Previous work on SNS sandwiches is now reviewed briefly in order to set the present investigation in context.

The first work on SNS contacts was carried out by Meissner (1960) using crossed Sn wires which had been electroplated with various metals. This work was, however, only of slight relevance to the question of NS interface effects since the junctions thus produced were highly oxidised and were also of uncertain area.

SNS sandwiches prepared by soldering or evaporation were first studied by Clarke (1967). A fundamental problem which arises with resistance measurements on such samples is that the sample resistance is very small, being of the order of 10^{-7} Ω in Clarke's samples. These measurements were made possible by the development of superconducting quantum interference devices. Clarke developed the "SLUG" which was also used in several subsequent investigations (more recent work has used SQUIDs). He looked primarily at the supercurrents observed to pass through SNS sandwiches when the N layer was sufficiently thin. This case, in which SNS sandwiches behave as weak links, (see Waldram et. al. 1970) is different from the subject of this thesis. In the present work, the N layer was always thick enough to suppress supercurrents. Clarke also

measured the resistance of these thicker sandwiches (Pb/Cu/Pb and In/Cu/In) below 4.2K. He deduced that the interface resistance had a finite value, but reached no conclusions about the temperature dependence.

This work was extended by Shepherd (1971) who studied the resistance of Pb/Cu/Pb sandwiches in the temperature range up to 7.2K. He observed a sharp rise in the resistance as the temperature approached T_c and a finite interface resistance even at low temperatures. Tindall also observed a resistance anomaly at T_c in intermediate state tin at about the same time. These results were explained by the theory of Pippard, Shepherd and Tindall (1971) which was later extended by Waldram (1975). This theory will be discussed in Chapter 4.

Tomlinson (1973) studied "SNS" sandwiches in which the middle metal was a superconductor with a transition temperature below that of the S layers on either side (denoted SS'S sandwiches in the literature). Harding (1973) looked at SNS sandwiches in which the superconductor was dirty (lead with up to 10% bismuth impurity), and discovered that both the resistance anomaly and the low temperature interface resistance were much larger than with clean superconductors. These effects were partially explained by the theory of Harding, Pippard and Tindall (1974). This will be discussed in Section 1.4. Hsiang and Clarke (1980) investigated the resistance of SNS sandwiches in which S was only slightly dirty (i.e. ~1% impurity).

Van Harlingen (1981a) first used SNS sandwiches to investigate the theromoelectric effect of superconductors. He found that the thermopower of an SNS sandwich shows a divergence below T_c similar to that observed in the resistance. This work was continued by Battersby (1982), who obtained evidence that the thermopower of Pb is continuous across the transition temperature.

The present work is an extension of the work of Harding and that of Battersby. The resistive and thermoelectric properties of In/W/In

sandwiches have been systematically investigated as a function of the dirtiness of the In, to which 0-10 at. % lead impurities were added.

1.2 Basic Theory

1.2.1 Excitations in Superconductors

Before discussing the theory of SN interfaces it is necessary to discuss the basic theory of non equilibrium superconductors. This subsection discusses the general question of excitations in superconductors partly to establish the notation to be used. Fig. 1.1 illustrates the excitation spectrum of a normal (free electron) metal in the notation which is used in superconductivity. The curve ABCDE is the usual $\varepsilon(k)$ curve of the metal measured from the Fermi Energy (i.e. the states represented by the curve BCD are filled at 0K). Electron excitations are formed by moving electrons from the Fermi surface into higher unfilled states, and are represented by the portions of curve AB and DE. Hole excitations are formed by removing electrons from states below the Fermi surface. In the usual way, if an electron is removed which has wave vector **k** the resultant band has a wave vector **-k** so the curve BFD can be built up which represents the hole excitations. The excitation energy E is therefore given by $E=|\varepsilon|$

The theory of Bardeen, Cooper and Schrieffer (1957), (hereafter referred to as BCS) asserts that superconductivity is due to pairing of electrons, which becomes energetically favourable because of electron-phonon coupling. The BCS wavefunction, for zero supercurrent, is a linear superposition of states in which pairs of electron states of equal and opposite momenta are either filled or unfilled.

$$\psi_{BCS} = \prod_p (u_p + v_p c^+_{p\uparrow} c^+_{-p\downarrow})|0\rangle \qquad (1.1)$$

(Where the c^+ are the usual electron creation operators). Here $v_p^2+u_p^2=1$

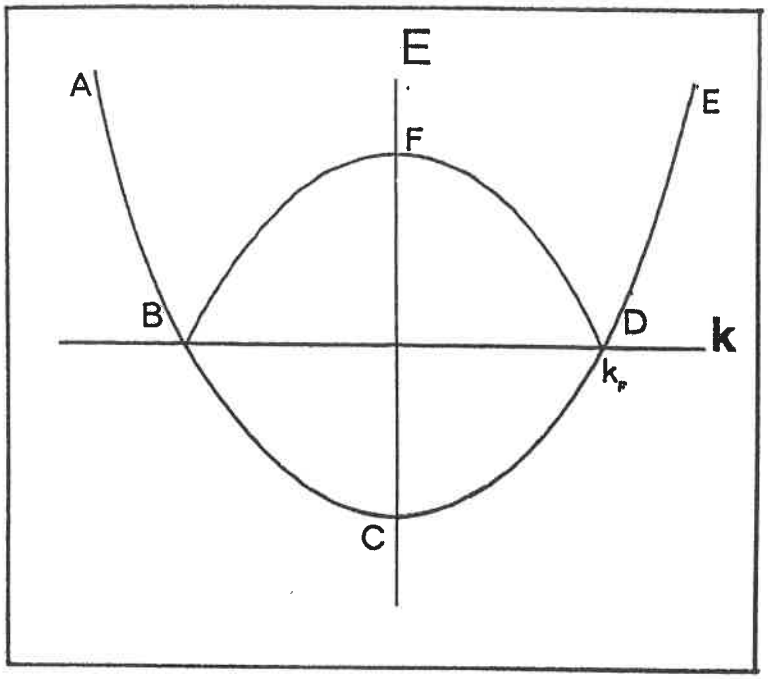

Fig. 1.1 Normal Metal Excitation Spectrum.

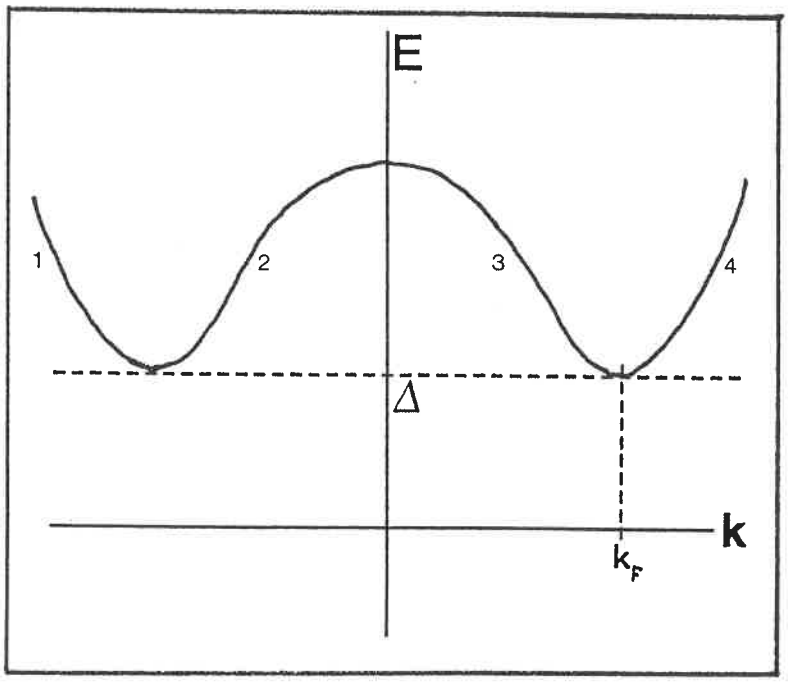

Fig. 1.2 Superconductor Excitation Spectrum. (The numbers 1-4 are the branch numbers as referred to in Appendix 1).

and v_p^2 is interpreted as the probability of the states of momentum $-\mathbf{p}$ and $+\mathbf{p}$ being filled. In the case of a finite supercurrent flowing, the pairing is instead between electrons of momentum $\mathbf{p}+m\mathbf{v_s}$ and $-\mathbf{p}+m\mathbf{v_s}$ ($\mathbf{v_s}$ is the superfluid velocity). The BCS wavefunction contains an indeterminate number of electrons, the usual interpretation being to imagine the pairs in equilibrium with a particle reservoir of chemical potential μ. BCS use the above wavefunction and a simple approximation for the attraction between electrons to derive an expression for the free energy of the system, which is then minimised. They find that v_p is given by

$$v_p^2=(1-\varepsilon/E)/2 \tag{1.2}$$

where E (=E(**p**)) is given by

$$E^2=\varepsilon^2+\Delta^2 \tag{1.3}$$

E(**p**) is the excitation energy of an excitation of momentum **p**. This means that it always takes an energy of at least Δ to create an excitation. Δ is referred to as the energy gap. This explains the fundamental zero resistance of a superconductor, since when a small supercurrent is established it can't relax to a state of zero current by excitation relaxation. The superconductor excitation spectrum derived from (1.3) is shown in Fig. 1.2. Several points about this should be noted:

(a) As T approaches T_c, Δ tends to zero and the excitation spectrum approaches that of the normal metal as would be expected.

(b) In the normal metal, excitations are either electrons or holes, with the two types separated by a singularity in the $\varepsilon(k)$ curve at $\varepsilon=0$. In the superconductor, however, there is no such divide and the localised charge of the excitations is given by $q_p=-e\varepsilon/E$, which goes smoothly from -e to +e as the Fermi wave vector is crossed (and is zero at $k=k_F$). For

this reason excitations in superconductors are referred to as "electron like" and "hole like".

(c) Similarly, the velocities of the excitations are given by $v_s=v_n(\varepsilon/E)$ and are also zero at $k=k_F$.

The above show that the properties of the excitations are substantially different to those of excitations in normal metals (the differences being most marked for particles with $k\sim k_F$). For this reason excitations in superconductors are often referred to as "quasiparticles"

1.2.2 Charge Imbalance

In a normal metal the total number of holes must equal the total number of electrons in order to maintain overall neutrality. This is not true in superconductors, where any excess charge in the excitations can be balanced by changing the number of electrons in the paired state (usually referred to as the condensate). Such an excess charge is known as charge imbalance and is illustrated schematically in Fig. 1.3. The most useful measure of charge imbalance is Q*, defined as:

$$Q^*=\int_{\Delta}^{\infty} -q_E dE \qquad (1.4)$$

where q_E is the total excitation charge at energy E (the reader should be careful to distinguish between Q* as defined above and used throughout this thesis from the other measures of charge imbalance used in the literature). By defining ε_c, the condensate energy, as the energy for which $v_p^2=u_p^2=0.5$, the condition for charge neutrality can be stated:

$$\varepsilon_c - \varepsilon_F = -Q^* \qquad (1.5)$$

Where ε_F is the Fermi energy. The electrochemical potential of the condensate, μ , is given by

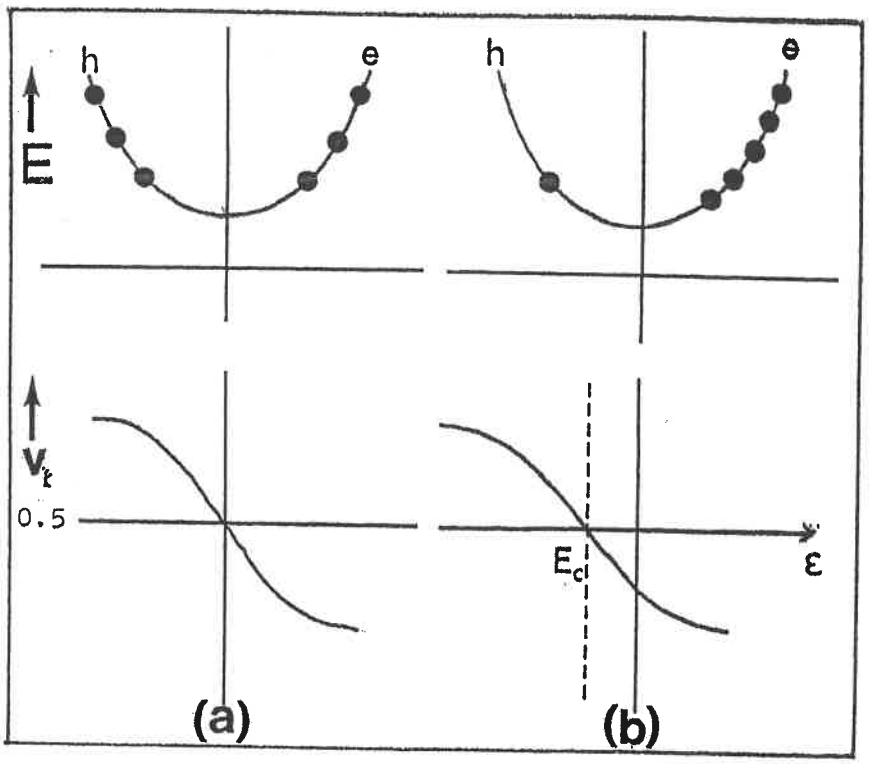

Fig. 1.3 Schematic Representation of Q*. The Upper half of the figure shows two branches of the excitation spectrum and the lower half represents the condensate. (a) shows the equilibrium case where there are equal numbers of electrons and holes and Q*=0. In (b) there is an excess of electrons over holes and Q*≠0, in order to maintain overall neutrality in this case there are less electrons in the condensate. (After Waldram 1975).

$$\mu = \varepsilon_c - e\phi \qquad (1.6)$$

μ is constant, otherwise supercurrent would flow to cancel it. So (1.5) and (1.6) together lead to the conclusion first derived by Waldram (1975) that:

$$eE=-\nabla Q^* \qquad (1.7)$$

ie that a gradient of Q* is always associated with an electric field in the superconductor. It may seem strange that an electric field can occur in a superconductor; the above algebra shows that it is needed to balance any gradient in chemical potential resulting from a gradient in Q*.

Clearly the equilibrium state is that in which Q*=0, and a question of importance in the present work is the rate at which a given distribution of Q* will relax to zero. This has been considered theoretically by several workers (see Pethick and Smith (1980) for a review). Fig. 1.4 shows schematically the possible scattering processes in a one dimensional superconductor. Processes a,b and c are able to occur in both normal metals and superconductors. In the superconductor, however, because of the variation of the excitation charge with energy, processes b and c may change the total charge imbalance. In addition, in the superconductor three more processes are possible, d,e and f, that can not occur in the normal state. As would be expected, it is found from calculations that as T_c is approached, the scattering rates for these processes become very slow. d and e are the "branch crossing" processes by which an electron is scattered directly into a hole or vice versa. It can be seen that the overall rate of relaxation of charge imbalance must become very slow close to T_c. Processes d, e and f which change the charge imbalance by 2e close to T_c become very slow, and processes b and c (which have a finite rate at T_c) do not change the charge imbalance

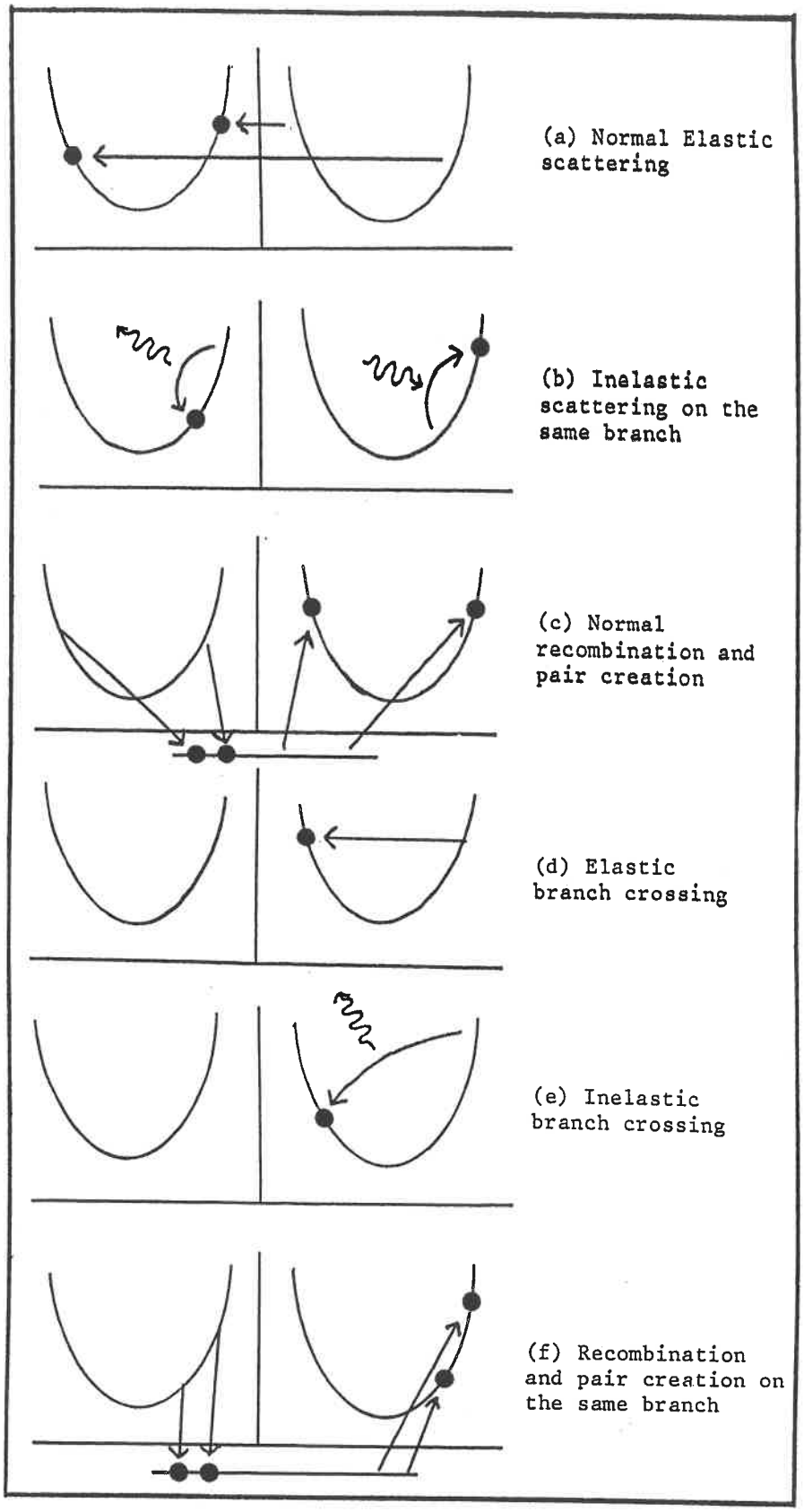

Fig. 1.4 Scattering Processes in Superconductors.

significantly.

1.2.3. Andreev Reflection.

A process of considerable importance in the behaviour of SN interfaces is Andreev Reflection (Andreev 1964). This occurs when an excitation in an inhomogenous material encounters a rising energy gap which eventually reaches an energy greater than that of the excitation. In the context of SN interfaces this means an excitation impinging on the interface from N with energy less than the bulk value of Δ in S. The particle can clearly not be transmitted since there are no states (by definition) below the energy gap for it to go into. The process which occurs is schematically represented in Fig. 1.5 for the case of an incident electron. The local excitation spectrum is drawn at each point. It can be seen that at the point R, at which the electron is classically reflected, the electron can only be at the minimum in the excitation spectrum with corresponding zero velocity. Thereafter, the electron continues round the excitation spectrum and therefore emerges from the interface as a hole as shown.

The net process, therefore, is that an electron has been reflected as a hole, which corresponds to the injection of one Cooper Pair into the superconductor. A charge of 2e crosses the interface and no electrical resistance is measured as a result. It should be noted, however, that this process is not compatible with heat flow, so a large thermal resistance will be measured (this was the subject of the original paper of Andreev).

Another point of relevance to the NS interface problem is the trajectories of the excitations in real space. As is illustrated in Fig. 1.6, in normal reflection the component of **v** parallel to the interface is conserved, and the perpendicular component is reversed. In contrast, in the Andreev process all components of **v** are reversed. This has the consequence that the direction of reflection is independent of the

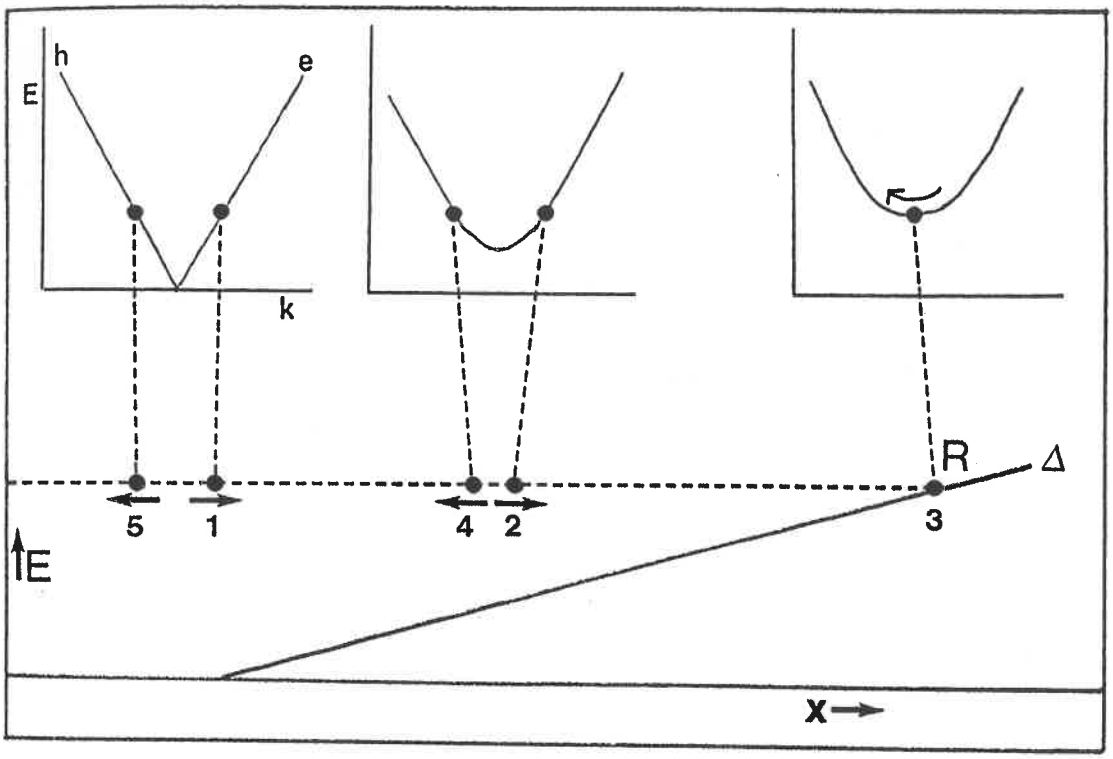

Fig. 1.5 Schematic Representation of Andreev Reflection.

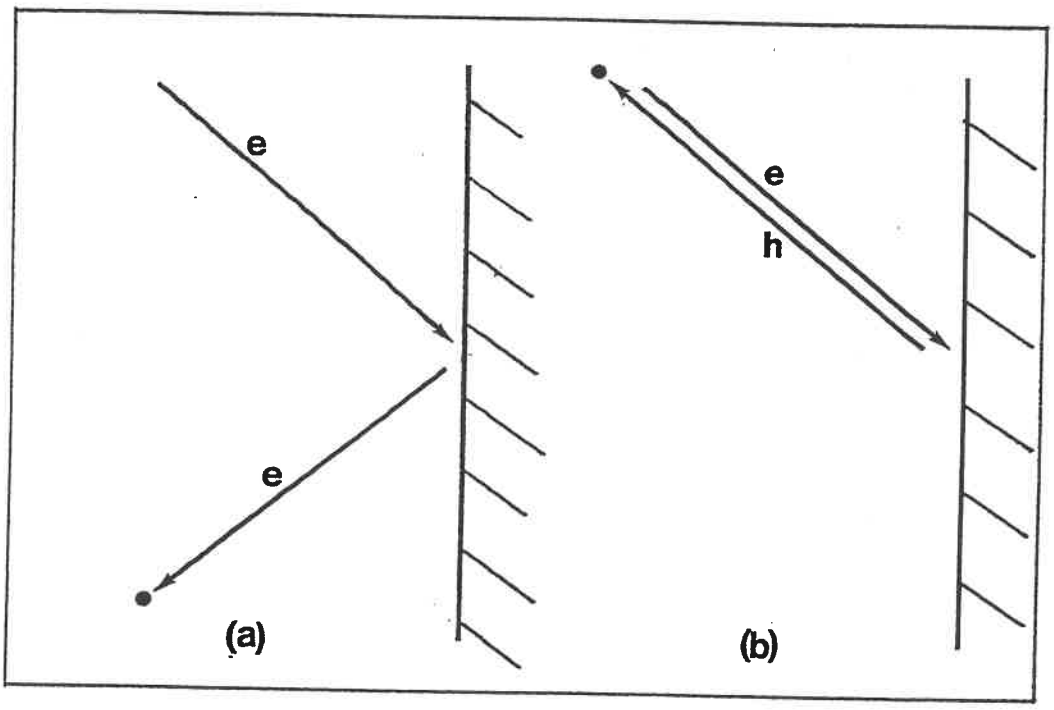

Fig. 1.6 Real Space Trajectories in Andreev Reflection. (a) shows typical trajectories in normal reflection, (b) shows the case of Andreev reflection.

interface orientation, which makes it less likely that the theory will affected if the interface is uneven.

1.3 Resistance of SN interfaces

This section introduces the basic theoretical concepts required to explain the resistive properties of NS interfaces. As was first observe by Shepherd, the resistance of an SNS sandwich, R_{SNS}, has the basic for shown in Fig. 1.7. At low temperatures ($T < 0.8T_c$) the resistance of th sandwich is approximately constant, but as the transition temperature i approached the resistance is seen to diverge.

At temperatures well below the transition temperature the excitati carrying the current in the normal metal have energies much less than Δ S. When these excitations reach the interface they are Andreev reflecte (as discussed in the section above). It might therefore be expected tha zero interface resistance would be observed at low temperatures. Experimentally, however, it is found that the resistance of SNS sandwic at low temperatures is greater than that of the normal layer alone. This is because, in practice a proportion of the excitations are normally reflected (ie without change of character) and this process will clearly cause resistance. The reasons why some normal reflection occurs are discussed at length in later sections.

As the temperature is increased towards T_c, the average energy of t excitations in N increases and Δ gets smaller. Therefore, significant numbers of excitations have energy $E>\Delta$ and penetrate into S. These excitations generate a charge imbalance in S which decays by the process described in Section 1.2.2. As was shown by Waldram (1975), the resultant distribution of charge imbalance in S has Q* decaying exponentially with distance from the interface (Fig. 1.8). The characteristic length of thi decay, following the notation of Waldram, will be denoted λ_3 in this thesis. From (1.7) it can be seen that this Q* distribution corresponds t

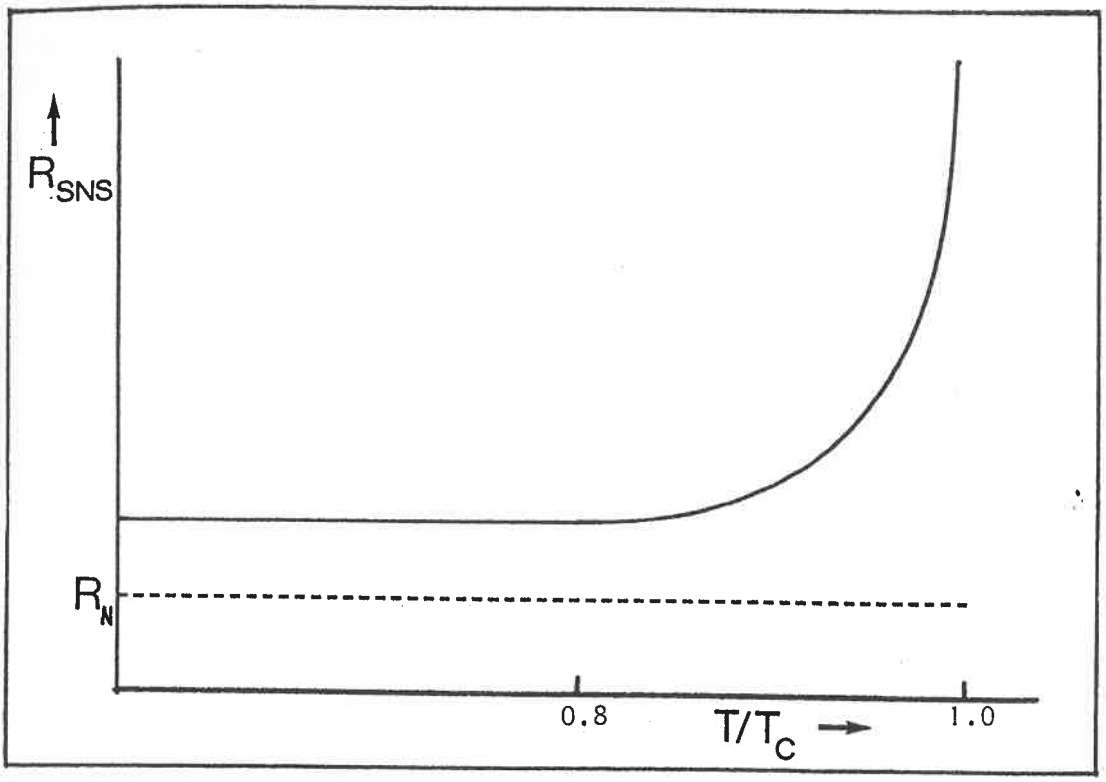

Fig. 1.7 Basic Form of $R_{SNS}(T)$.

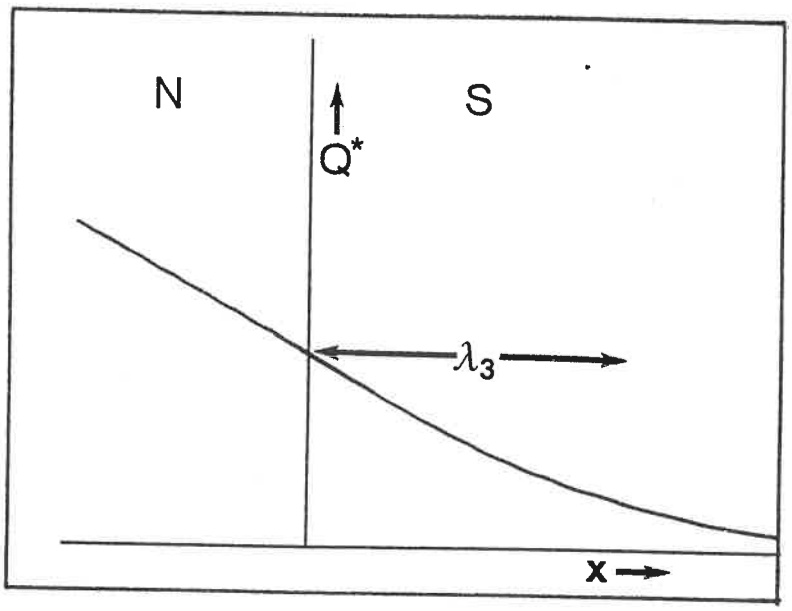

Fig. 1.8 Form of Q* at Interface. It will be noted that Q* rises indefinitely in N. This is a consequence of the definition of ε_c which rises uniformly in N as a result of the electric field.

an electric field decaying into S. This electric field is measured as extra interface resistance. The closer the temperature is to T_c, the slower the Q* relaxation processes become and λ_3 diverges. This is the reason for the observed divergence of R_{SNS}. The quantitative theory proposed by Pippard et. al. (1971) and its modification by Waldram (1975) adequately fit the form of the divergence observed. This is the subject of Chapter 4.

In practice, as was first systematically investigated by Harding, it is often found that the resistance of the junction, instead of being constant well below T_c, falls slightly with increasing temperature before reaching a minimum at $0.7\text{-}0.8T_c$. It is found experimentally that the magnitude of this effect depends on the cleaness of the interface, Harding finding that it was smaller in samples which would be expected to have cleaner interfaces. In common with previous workers, the size of this effect was used by the author as a measure of the cleaness of the interfaces, its mechanism being the subject of Chapter 5.

1.4 Dirty Superconductors.

Harding (1973) carried out the first systematic investigation of SN interfaces in which S was a dirty superconductor. In this context "dirty" means that impurities have been added to the metal to greatly reduce the excitation mean free path. In contrast a pure superconductor with a long mean free path is referred to as "clean". (It should be noted that throughout this thesis a "dirty SNS sandwich" should be taken to mean an SNS sandwich in which the superconductors are dirty, and similarly for "clean SNS sandwich"). The system used by Harding was Pb to which had been added up to 10 at. % Bi. It was found that the $R_{SNS}(T)$ curve was affected in two ways (Fig. 1.9). The most obvious effect was that with dirty superconductors the divergence in the resistance just below T_c was larger and could be seen from lower temperatures. This is qualitatively expected

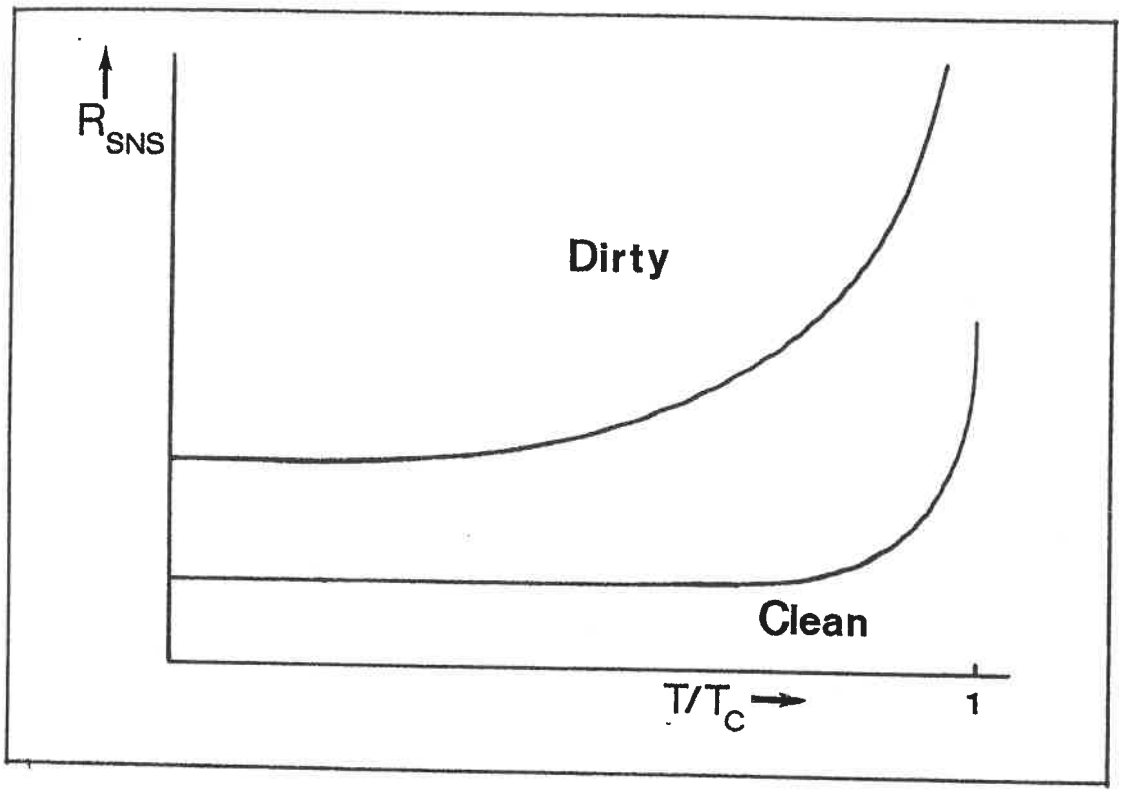

Fig. 1.9 Effect on $R_{SNS}(T)$ of adding dirt to S.

from the theory of Waldram (1975), which predicts that the magnitude of the divergence at T_c will be proportional to $\sqrt{\rho_s}$ (ρ_s=residual resistivity of S). However, attempts to fit the observed curves to theory were unsucessful. The second effect was that the low temperature interface resistance (which as mentioned above is found to be finite in practice) became larger as the dirtiness of S was increased.

This second effect has been qualitatively explained by a theory of Pippard (Harding et. al. (1974) and Pippard (1984)), though quantitative agreement is poor. This theory is based on the fact that the Andreev reflection process involves not only the electron and hole amplitudes, but also decaying evanescent waves which extend into S. The details of the theory are discussed in Chapter 6. The basic physical process is that the evanescent waves are scattered by the imputities in the dirty superconductor and some return to the interface. The effect of this is that the Andreev reflection process is no longer perfect, i.e. there is a finite probability of reflection without change of character which causes an interface resistance. The process is analagous to the phenomenon of frustrated total internal reflection in optics. Harding et. al. gave a one dimensional calculation of the low temperature resistance, and derive a result, quoted in Chapter 6, which implies that the interface resistance due to this effect, R_p, should be proportional to ρ_s. Pippard (1984) gave a three dimensional calculation which also implied a linear form for R_p against ρ_s, but predicted that it would be four times smaller than in the one dimensional case.

Harding's experimental results were consistent with a linear form of R_p against ρ_s except perhaps at low Bi concentrations. The magnitude of the resistance, however, was about a factor of three less than would be expected from the three dimensional theory. This discrepancy is one of the main problems on which it was hoped the present work would shed light. The results are discussed in Chapter 6.

Harding et. al. also attempted to explain the form of the divergence in $R_{SNS}(T)$ below T_c with dirty superconductors. The theory of Pippard et. al. (1971) was modified to take account of the imperfect Andreev reflection below the gap. The resulting theory predicted roughly the right form for the divergence, but expected it to be approximately twice as big as was in fact observed. The present work on this question is discussed in Chapter 7.

1.5 Thermoelectric Effects in Superconductors

As well as looking at the resistance of SNS sandwiches, the present work was also concerned with their thermoelectric properties. This section introduces the subject of thermoelectric effects in superconductors in general and the following one looks at the thermopower of SN interfaces. The three usual thermoelectric effects (Seebeck coefficient, Peltier heat and Thomson heat) are all found to vanish in superconductors. Heat flow drives a current of excitations ($\mathbf{J_n}$) given, as in normal metals, by:

$$\mathbf{J_n} = L(-\nabla T) \qquad (1.12)$$

As will be discussed in Chapter 8, it is expected on theoretical grounds that the coefficient L is continuous across T_c. However as suggested by Ginzburg (1944), inside S $\mathbf{J_n}$ is counterbalanced by a backflow of supercurrent, $\mathbf{J_s}$. This can easily be seen from the second London equation and Maxwell's equations, which together predict that the Meissner effect ($\mathbf{B}$=0 inside bulk superconductor) holds if curl($\mathbf{J_n}$)=0 even in the presence of a heat current. Therefore, in order for B to be zero inside the superconductor, $\mathbf{J_s}$ must exactly cancel $\mathbf{J_n}$ at every point. The conventional thermoelectric effects are effectively short circuited by the supercurrent.

Despite this, a variety of thermoelectric effects have been proposed,

and in some cases seen, in superconductors. Clearly they must all involve some method of separating the thermocurrent from the superfluid counterflow. Three examples are briefly described below; for a more thorough review see Van Harlingen (1981b) or Ginzburg and Zharkov (1978).

(i) Anisotropic Thermoelectric Effect: As mentioned above, the Meissner effect only holds in the presence of a temperature gradient if $\mathrm{curl}(\mathbf{J}_n)=0$. This is not generally true in an anisotropic crystal when there is a heat current. The resultant flux penetration is only expected to be observable close to T_c and, although an effect has been seen (Selzer and Fairbank 1974), good agreement between experiment and theory has yet to be obtained.

(ii) Fountain Effect: First proposed by Clarke and Freake (1972), this is based on the fact that the phase difference across a Josephson junction depends only on the supercurrent, and not on the excitation current. Hence when a heat current is passed through the junction, the resulting flow of $\mathbf{J}_s$ biases the juction despite the fact that the net thermoelectric current is zero. It is therefore expected that the heat current will shift the entire I-V characteristic of the junction by $\mathbf{J}_s$. Experimentally, an inconsistent effect was seen by the above workers; however no effect at all was seen by subsequent investigators (Welker and Bedard 1977).

(iii) Bimetallic Ring: This was proposed by Garland and Van Harlingen (1974a) and Gal'perin et al. (1974) and involves a ring half of which is made of one superconductor and half of another. If a heat current is passed from one contact to the other, the flux in the ring is no longer expected to be quantised. This is because there are differing superfluid counterflows in the two halves of the ring which induce different phase gradients. A number of workers have found poor agreement between experiment and theory for this; see for example Van Harlingen et al. (1980).

In all of the effects mentioned above there are large quantitative discrepancies between experiment and theory. The only method which has given some agreement is measurement of the thermopower of SNS sandwiches.

1.6 Thermopower of SNS Sandwiches.

In this section the effect of passing a heat current across an NS interface is considered. Deep inside S, as discussed in the last section, the excitation current driven by the heat flow is exactly cancelled by supercurrent, ie $J_n=-J_s$. However in N, and at the interface itself, $J_n=J_s=0$. In the intermediate region, in a similar way to the case of electric current flow, J_n generates a region of charge imbalance in which Q* decays exponentially into S with a decay length λ_s. This Q* again produces a voltage, which is measured as the thermovoltage of the interface. The thermovoltage therefore diverges as T_c is approached, in a similar way to $R_{SNS}(T)$, as a result of the divergence in λ_s. This divergence is therefore proportional in magnitude to J_n and therefore to the thermoelectric coefficient of the superconductor. Van Harlingen (1981a) verified experimentally that the thermopower of SNS sandwiches diverges as expected below T_c. Using a simple theory, he showed that the thermoelectric coefficient of the superconductors he used (PbBi eutectic and In) were constant to within an order of magnitude across T_c. Battersby, using essentially the same technique and a more thorough theory obtained evidence that the thermoelectric coefficient in Pb is constant across T_c to within a few per cent. The present work on the thermopower of SNS sandwiches is discussed in Chapters 8 and 9.

1.7 Aims of Present Work

The initial aim of this work was to repeat the measurements of Harding (1971) on the resistance of dirty SNS sandwiches. It was hoped to obtain more reliable data and, hopefully, to explain the discrepancies

discussed in Section 1.4. It was also intended to measure the thermopower of the same samples; a systematic study of the thermoelectric properites of dirty SNS sandwiches had never previously been carried out. For reasons described in Chapter 3 it was decided that a good way to make these measurements would be to use In/W/In sandwiches. This was a system which had never been used before, so comparison with theory of the resistive and thermoelectric properties of samples prepared using clean In with theory was also of interest.

CHAPTER 2

MEASUREMENT TECHNIQUE

2.1 Introduction.

The measurement equipment used in the present work was built by Battersby and only minor modifications were made. For this reason only brief descriptions are given in this chapter; more details may be found in Battersby (1982). In the next section the equipment is described and Section 2.3 discusses sources of noise in the system.

2.2 The Measurement Equipment.

2.2.1. The Insert.

The insert used is illustrated in Fig. 2.1. It was mounted in a standard double enclosure ^{4}He cryostat. The apparatus was able measure the resistance and thermopower of SNS sandwiches in the range 1.2 to 8K. The sample was mounted in a vacuum can on a copper block which was weakly thermally linked to the helium bath. A heater wound (non inductively) on this block allowed the sample temperature to be varied above that of the helium. In the present experiments using In (T_c=3.4K) the temperature of the helium was reduced as much as possible (to about 1.2K) by pumping on it. The sample was in fact mounted on a smaller block held to the larger one by screws to enable easier mounting. It was attached to a copper post on this smaller block with Woods Metal. The melting point of the Woods Metal (about 70°C) is far enough below that of In (155°C) to enable the sample to be attached in this way without damage. This was done using a soldering iron driven from a Variac to allow a low enough temperature to be used. The upper temperature limit at which measurements could be made was fixed by the transition temperature of the Woods metal (about 8K), which was far above what was required for the present work.

For the thermoelectric measurements heat was passed down the sample

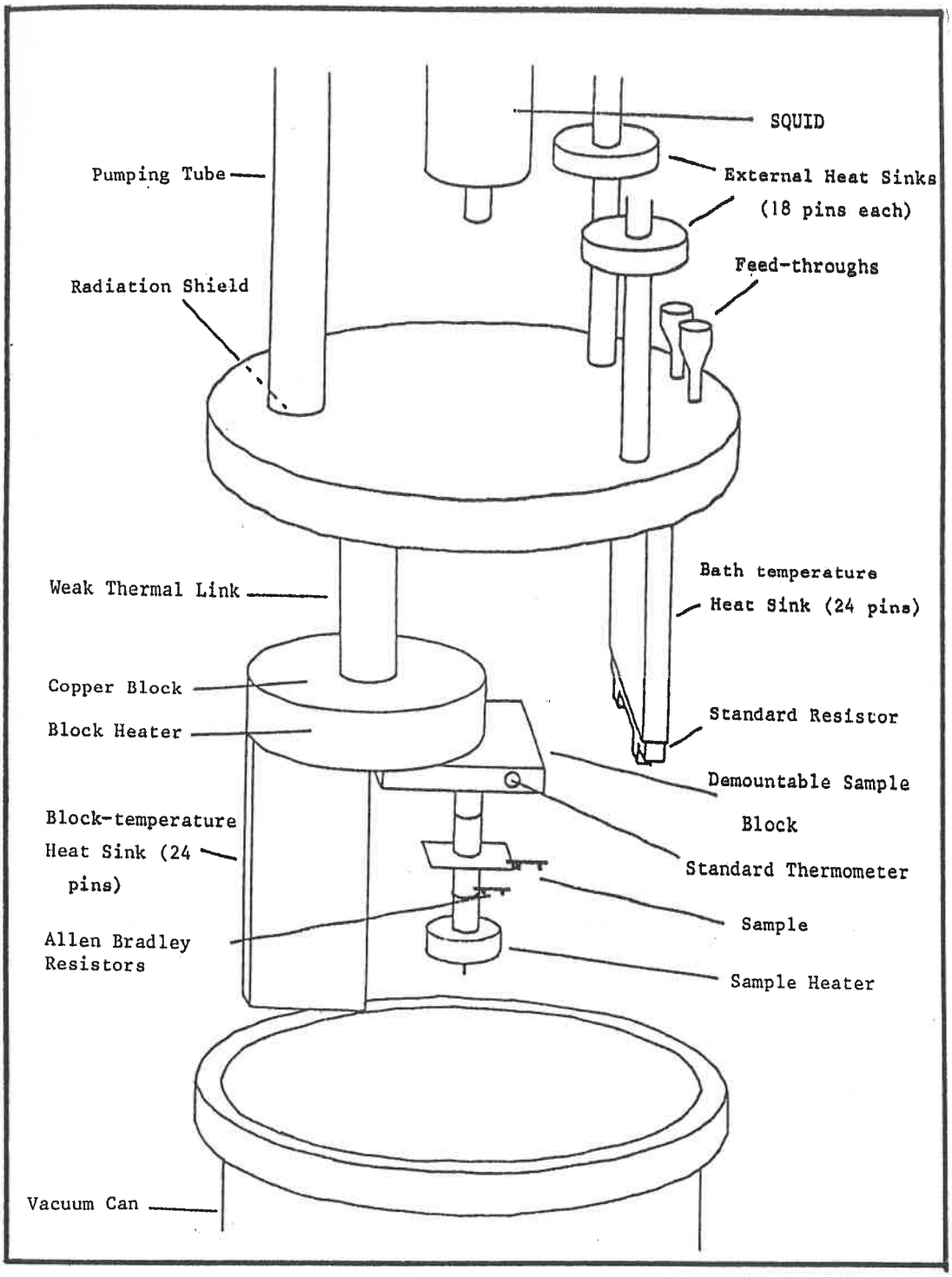

Fig. 2.1 The Lower Part of the Insert with the Vacuum can Removed. For simplicity, the wiring and the radiation shield round the standard resistor are not drawn. (From Battersby 1982).

from a small heater which was mounted on the free end, again using Woods Metal. The resistance was measured by passing a current through the sample from a wire attached to the copper on which the heater was wound. The superconducting voltage leads were sandwiched in the Woods Metal joints. As very small voltages (about 10^{-12}V) were being measured special precautions had to be taken to reduce stray thermovoltages. All of the wires going from the top of the cryostat down into the can (of which there were roughly 30) were heatsunk twice; there were a pair of heat sinks in the helium just above the can and one inside the can. In addition there was another heat sink on the block through which all the wires to the sample passed. This was to reduce thermovoltages due to the block temperature being above that of the bath. The heat sinks inside the can consisted of sheets of copper a few mm thick with holes drilled in. The holes were plugged with Stycast through which metal pins had been pushed before it set. The wires to be heat sunk were soldered to either side of the pins.

2.2.2 Voltage Measurement.

The voltage sensitivity required was determined by the magnitude of the thermovoltages to be measured. The maximum heat current which could be passed down the sample without causing the block temperature to rise too much was limited to a few mW. This meant that the thermovoltages produced were of the order of 10^{-12}V. A SQUID was therefore used to make the voltage measurements. This voltage sensitivity meant that sample resistances, of the order of nΩ at temperatures below T_c, could be adequately measured with measuring currents of a few mA.

The SQUID used was an R.F. device, manufactured by the S.H.E. Corporation and was used in the usual voltmeter configuration; a circuit diagram is given in Fig. 2.2. This arrangement is that of a superconducting bridge in which the SQUID is used as a null detector. The

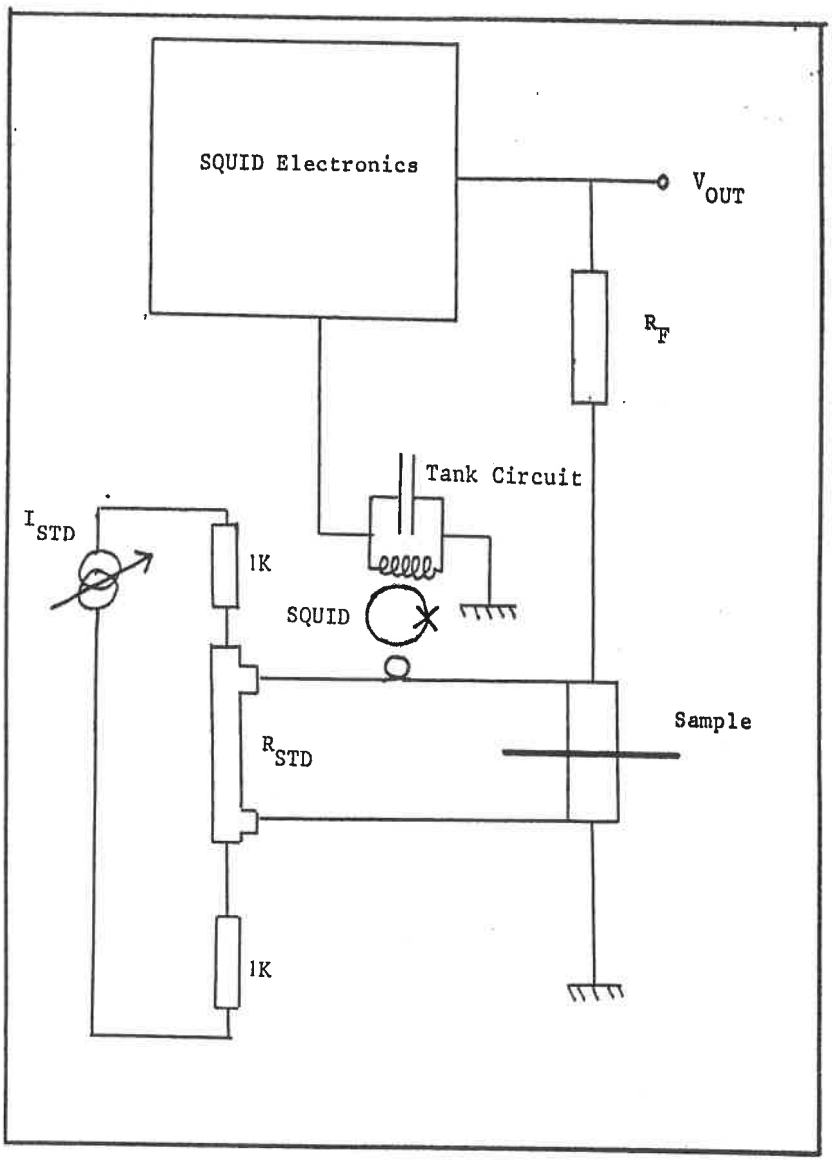

Fig. 2.2 Block diagram of the Voltage Measurement Electronics.

voltage across the sample is balanced by that across a standard resistor, R_{STD}, which was a π shaped piece of OFHC copper with resistance of order 10^{-6} Ω. Clearly no current flows through the SQUID input coil if $I_{STD}R_{STD}=I_{SNS}R_{SNS}$. In practice the most convenient way to measure R_{SNS} was to pass I_{STD} through the standard resistor from a current source and provide I_{SNS} from the external feedback jack of the SQUID electronics via a feedback resistor, R_F. This meant that the bridge in effect balanced itself. It is easy to see that R_{SNS} is given by:

$$R_{SNS}= (R_{STD}I_{STD}R_F)/V_{OUT} \qquad (2.1)$$

Where V_{OUT} is the output voltage measured at the external feedback jack.

At the beginning of the work and also towards the end, R_{STD}, on which the absolute values of voltage measured depended, was recalibrated. This was done in the same way as Battersby using a secondary standard which consisted of 15cm of 26 swg Cu. This secondary standard had a resistance of the order 10^{-4} Ω which was accurately measured four terminally using a nanovoltmeter. R_{STD} was then measured against the secondary standard in the same way as R_{SNS} measurements were made. The resistance of the standard was found to be $(1.116\pm0.004)\times10^{-6}$ Ω.

G_{SNS}, defined as the ratio of electric current to heat current at zero voltage, was measured by passing a heat current through the sample, and is given by:

$$G_{SNS}= V_{OUT}/(R_F V_{SH} I_{SH}) \qquad (2.2)$$

Where the subscripts SH refer to the sample heater. R_F was chosen so that V_{OUT} was of the order of a volt with heat currents of a few mW passing through the sample; it was 2kΩ for most of the present work. In order to analyse the data G_{SNS} was often multiplied by R_{SNS} to give the

thermovoltage across the sample per unit heat current. In practice a majo problem with using the system was the level of noise observed. This is discussed in Section 2.3.

2.2.3 Thermometry and Temperature Stabalisation

The primary thermometer used was a Cryocal Ge device (number 718). Since it was about 6 years since this had been calibrated it was recalibrated against another Cryocal thermometer (number 16381). The four terminal resistance of the thermometers was measured with an AC bridge similar to that described by Ekin and Wagner (1970). The resistance of the Ge thermometer was fitted (using a BBC Microcomputer) to a polynomial of the form

$$\ln T = \sum a_i (\ln R)^i \qquad (2.3)$$

as dicussed by Blakemore (1962). Usually up to 10 terms were used in the fit and the fitting error was less than one mK compared to an error of 6mK quoted by Cryocal in the calibration. The accuracy of measurements of small temperature differences would obviously be expected to be much greater than this. This thermometer was mounted in a hole drilled in the copper block which supported the sample.

In addition to the Ge device, up to 3 Allen Bradley 100Ω resistors were also used as secondary thermometers. The resistances of these were also measured with the Kelvin Bridge. They were recalibrated during each run in which they were used from the Ge thermometer and the R(T) curves fitted to the expression mentioned in White (1968):

$$1/T = A + B\ln R + C/(\ln R) \qquad (2.4)$$

These thermometers were glued to various parts of the sample as required

with Durafix so that they could easily be removed afterwards with acetone.

The properties of SNS sandwiches are very temperature dependent in the region of T_c; accurate temperature control was therefore essential. The temperature of the He bath could be stabilised by a manostat of the type described by Adkins (1961). In this work, however, the He bath was usually required to be as cold as possible and sufficient stability could be obtained by simply pumping as hard as possible on the cryostat. The temperature of the sample was stabilised by an electronic temperature controller. This worked by measuring the resistance of one of the carbon thermometers (which was mounted on the normal metal slice of the sample) and adjusting the sample block heater current. The feedback circuit introduced time constants which were adjusted to give maximimum stability and minimum response time as discussed by Forgan (1974). This arrangement stabilised the sample temperature to within 0.2mK which was adequate for all but temperatures just below T_c. It also had the advantage that when a current was passed through the sample heater for the thermopower measurements, the sample temperature automatically adjusted itself to the correct value. Very close to T_c the block heater was driven directly from a current source and had to be adjusted manually when a heat current was passed through the sample.

2.3 Noise Reduction.

Since voltages of the order of 10^{-13}V were being measured it was important to reduce levels of noise as much as possible. Two sources of noise were intrinsic to the system:

(i) Intrinsic noise from the SQUID point contact and the room temperature SQUID electronics.

(ii) Johnson noise in the sample and R_{STD} and in the R.F. shunt placed across the SQUID terminals (see below).

These are expected to cause about 8×10^{-15}VHz$^{-1/2}$ of noise with

typical sample resistances. However, there are several other potential sources of noise which had to be carefully eliminated:

1. R.F. pick up. This degrades the performance of the SQUID and several precautions were taken to reduce it. All experiments were done in a screened room; on most runs it was found that the noise levels became very high unless the door was kept closed. Certain pieces of equipment were found to radiate unacceptable levels of R.F.. Offenders were often oscilloscopes and DMMs. As suggested in the operator's manual an R.F. shunt was placed accross the SQUID input terminals. This was a piece of wire of approximately 0.01Ω resistance. The combination of this with the superconducting input coil acts as a low pass filter which greatly reduces the R.F. input to the SQUID.

2. Electrical pick up. Care was taken while wiring up the equipment not to introduce earth loops. In particular the insert is earthed via the SQUID electronics. It had, therefore, to be insulated from the rest of the cryostat by a Bakerlite ring which fitted under the top plate and by breaks in the screens of the wires connecting the insert to the distribution box.

3. Magnetic Pick up. This was caused if the wires of the bridge loop vibrated in a magnetic field. The ambient magnetic field was reduced as much as possible by three concentric mu-metal cans placed round the cryostat. In addition the vacuum can was lined with a shielding layer of superconducting lead. The wires were prevented from vibrating as much as possible by clamping them firmly. (Measurements made with the He above the λ point were found to be much more noisy, presumably because the bubbles were vibrating the can. This did not arise much in the present work, but see also 5 below.) The equipment was often found to be very sensitive to external vibrations.

4. Spurious Resistance in the Loop. A frequently encountered problem was resistance (above 10^{-6} Ω) arising at the supposedly superconducting

joints at the SQUID input terminals. When it arose this increased the fluctuations of V_{OUT} since any imbalance between V_{SNS} and V_{STD} then caused less current to flow through the SQUID input. This meant that V_{OUT} was able to fluctuate more without imbalance being detected by the SQUID. The SQUID input connections were originally made by clamping the Nb wires onto Nb bases using Nb screws with Pb washers. It was found, however, that the problem could be eliminated if Woods Metal was used to solder the Nb wires to the Pb washers. It was found necessary to remelt the Woods Metal after each run; otherwise the joints deteriorated.

5. Temperature Effects. Although these did not arise during the work being discussed here they are worth mentioning. It was discovered during preliminary experiments that the SQUID output is very sensitive to small changes in the temperature of the He bath. While operating the system with the He at 4.2K is was found that the SQUID output was greatly affected by small changes in the He recovery system pressure. At lower temperatures it was noted that small changes in the rate of pumping on the He had a similar effect. While measurements were being taken the bath temperature was kept constant so this was not a problem in practice. It is also possible that the additional noise observed with the He bath above the λ point was partly due to temperature fluctuations in the He (discussed by Pankratov et al 1971).

With all these precautions the noise levels in the system were usually found to be about what would be expected from the intrinsic sources only. Despite this, however, some runs suffered from very high levels of noise. The cause of this was never found but was probably external interference of some sort as it was occasionally observed to disappear without any obvious reason.

CHAPTER 3

SAMPLE PREPARATION

3.1 Introduction.

As stated in Section 1.6 the aim of the experimental work was to investigate systematically the resistance and thermoelectric effect of NS interfaces as a function of the dirtiness of S. In order to do this three basic and interrelated questions needed to be faced.

1. What metals to use for N and S

2. How to prepare the samples to ensure that the NS interfaces were as clean as possible.

3. Having established a good sample preparation technique, how to determine the effect of adding impurity to S on the properties of the interfaces, in particular to measure the change in the low temperature resistance.

In the next section question 1 is discussed. Sections 3.3 to 3.7 discuss the work done on 2 roughly chronologically and 3 is discussed in Section 3.8.

3.2 Choice of N and S.

The choice of N and S is a fundamental question in this work and turns out to be remarkably limited. Below is a list of conditions which N and S should satisfy.

(a) S should have a reasonably high transition temperature. As measurements will need to be made down to about $0.3T_c$ to study the low temperature effect, this means that T_c must be above 3K if a conventional ^{4}He cryostat is to be used.

(b) S should not have too high a melting point. S will need to be cast, evaporated and alloyed so metals with high melting points (eg Vanadium) are not very practical.

(c) N, if a superconductor, should have T_c well below the lowest temperature at which measurements are to be made. If this is not satisfied, a fall in the resistance of the sandwich will be seen at low temperatures due to the proximity effect. This would greatly complicate the interpretation of the low temperature resistance data.

(d) N should be available either pure or in thin slices in order to make N as few mean free paths thick as possible. This is so that the resistance and thermopower of the sandwiches is dominated by interface effects and not by N.

(e) N should be non-magnetic.

(f) N and S should not alloy or form intermediates at the temperatures used to apply S to N. This is to ensure that the NS interface is as close as possible to the ideal of a perfectly sharp boundary. If N and S interdiffused the interface would become more complicated in an unpredictable way and the relevance of the theory to the results would be questionable. Previous workers (eg. Shepherd 1971) have found that systems in which N and S have significant mutual solubilities give irreproducible results.

(g) N and S should wet each other to form a good junction. In the present work, casts of S needed to be made on either side of N to form the sample (in contrast to much of the earlier $R_{SNS}(T)$ work which used evaporated films of S on either side of N). This was so that a heat current could easily be passed across the interfaces for the thermopower measurements.

(h) N and S should, if possible, have well behaved and understood elecrical and thermolectrical properties.

These conditions narrow down the choice of N and S to a very few possibilities. (a) and (b) mean that S has to be Pb, Sn or In. (f) greatly reduces the possibilities and with the other conditions leads to the conclusion that the only choices are Cu/Pb or W/Pb,Sn or In. The use of W

was initially suggested by Prof. A B Pippard. Mo could also be usable as N except that its T_c (0.92K but only when very pure) is rather high. Cu/Pb has been used by most previous workers (including Harding and Battersby). It was decided to use W as N in the present work because it was felt that it was time the theories were tested using a weak coupling superconductor which obeys BCS theory more closely. W also has the attraction that by virtue of its high melting point it should be very easy to clean simply by heating in high vacuum. It was in fact found during the course of the work that Sn did not wet W very well so the final system used was W/In.

3.3 Preliminary Experiments.

Having decided to try to use W for N, the basic choice was whether to prepare the samples by soldering to the W (as Battersby did) or whether to clean the W first in high vacuum in some way (as done by Harding and many others). Many attempts were made to solder Pb, Sn and In to W using a wide variety of fluxes but none produced good joints. Most attempts with Pb and Sn didn't produce any adhesion at all. It was felt that cleaning by heating in high vacuum should offer a simple and effective technique so it was decided to try to use that approach. The high vacuum sample preparation technique as originally envisaged is given below:

(i) Clean W sheet by resistively heating ("flashing") it to orange or white heat in high vacuum. This would also possibly increase the resistance ratio if carried on for long enough.

(ii) After cleaning, evaporate films of S onto both sides of the W. This would form the NS interfaces before the W surface had a chance to become covered with any oxide etc.

(iii) Remove the coated W sheet from the evaporator and cast cylinders of S onto either side. This would be done by clamping the W between pyrex rings which would be used as formers as described by Battersby (1982). The bulk S would adhere well to the clean W if the

interfaces were going to be worth using.

(iv) Etch the remaining S film off the W leaving just the two casts. The resulting sample would therefore have NS interfaces of well defined area as required.

It was known from the comments of Harding (1973) that a likely problem was going to be embrittlement of the W after flashing. The first trials therefore simply consisted of resistively heating pieces of 25μm thick Goodfellows W foil in high vacuum. This and all subsequent high vacuum work was carried out in an Edwards 12E3 evaporator. This had a base pressure of around 7×10^{-7} torr. During flashing of foils, however, the pressure usually rose to about an order of magnitude more than this. The foil was clamped between two stainless steel supports and a current of up to 150A passed through it from a high current supply. It was found that the W did indeed become very brittle. It also showed a tendency to sag into an S shape which meant that it was likely to be placed under stress while clamping between pyrex rings for casting. This led to the conclusion that it would indeed be very difficult to use the Goodfellow's W in the method envisaged above. This was confirmed by several attempts to do so.

Embrittlement in W occurs because the grain boundaries are very weak and flashing causes recrystalisation (see eg Smithells (1936)). Hence it was decided that the problem could be solved by using much purer zone refined material. This was expected to be better because it would be single crystal so unless too much recrystalisation took place would contain fewer grain boundaries. Also, since it would be purer, it would be possible to use thicker slices which would be less brittle anyway.

The Goodfellows material was however used for preliminary tests to discover which metals wet W, using pieces of foil which had been coated with S. These were made by clamping the foil in a vertical plane in the evaporator and mounting the evaporation boats containing S on either side. It was therefore possible to evaporate S onto both sides of the W

immediately after flashing it. Each superconductor was tested by attempting to solder a blob of S to a piece of coated W using a soldering iron (driven from a variac to obtain the correct temperature). It was found that both Pb and Sn were very unwilling to form good joints in this manner, partly at least because in these circumstances they tended to oxidise. In was, however, found to form good joints.

3.4 Experiments using Molybdenum for N: The Casting Technique.

Mo was initially used in this work because the zone refined W was available only in relatively small quantities. Goodfellows 25μm thick Mo foil was found not to suffer from the same embrittlement problems as the W. It was therefore decided to use it to develop the method of casting cylinders of S on either side of N. The initial idea was to use the casting technique described by Battersby (1982) except that casting would be onto foil coated with S without the use of a flux. A few modifications were found to be necessary however.

It was felt that the clamp used by Battersby did not hold the Pyrex rings firmly enough around the foil. It was therefore redesigned, the Pyrex tubes being held in place by two copper blocks mounted on long screws as shown in Fig. 3.1. It was found necessary to include springs on the screws as shown to keep the clamp under pressure despite thermal expansion. The Pyrex rings used were about the same size as used by Battersby; about 8mm long and of $9\times10^{-6}m^2$ internal cross sectional area. They were ground flat at the ends which would be in contact with the foil on a lapping wheel. The clamp was heated by placing it in a small furnace which was driven from a Variac. Trials were carried out to ascertain the voltages required to melt the various metals used.

The first cast in each case was made by clamping a sheet of Mo between the Pyrex rings. This Mo foil had been first cleaned in the evaporator and coated with S as described above. The clamp was then put

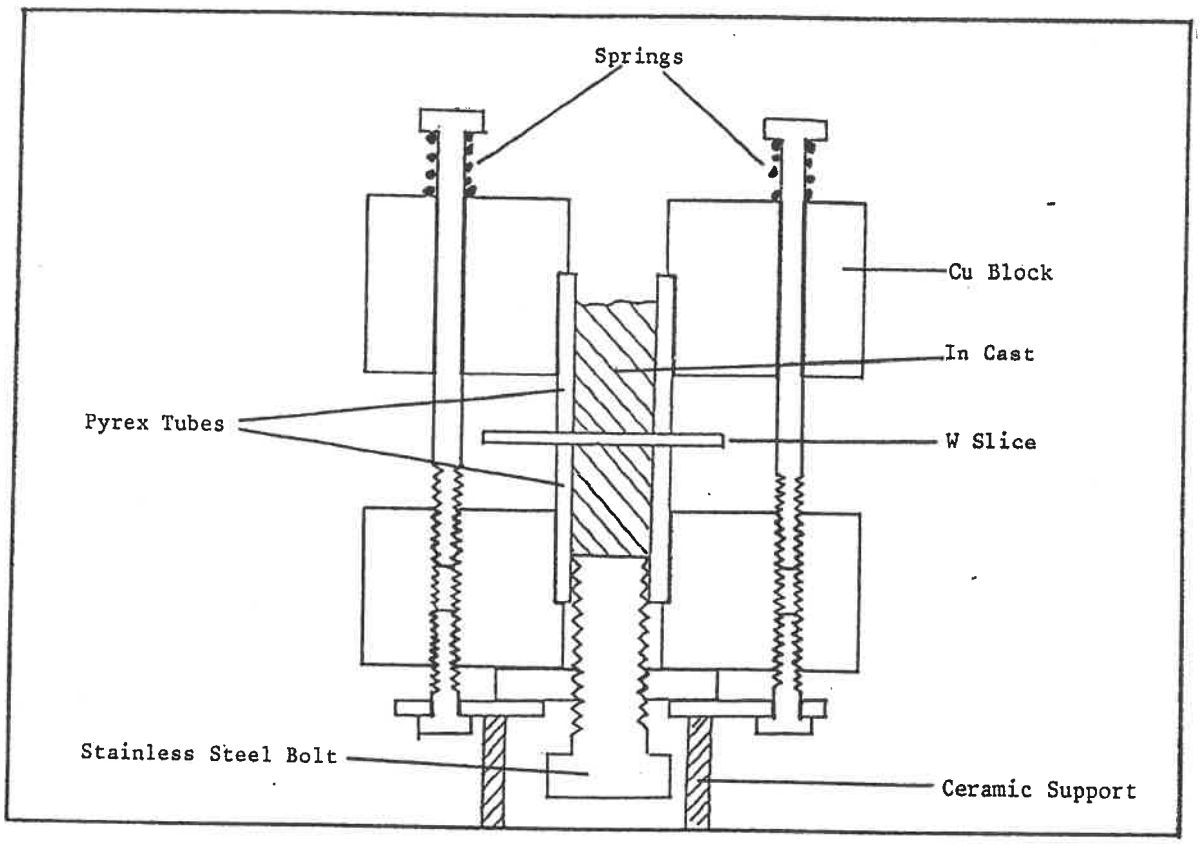

Fig. 3.1 Diagram of Clamp Used for Casting. The whole thing was placed inside a furnace for use.

into the furnace and as it warmed up small, freshly cut pieces of S were put into the uppermost Pyrex tube. When the metal melted it was stirred with a stainless steel rod (this was found not to add any significant impurities; in the case of In material which had been so stirred was found still to have a resistance ratio of about 8,000). More pieces of S were added and the procedure continued until the pyrex tube was full. The clamp was then lifted out of the furnace and allowed to cool. It was found, as with W, that only In reliably produced a good joint by this method. In was therefore used as S for the rest of these experiments.

The result of this procedure was a cylinder of In joined to one side of the foil. The next stage was to repeat the procedure on the reverse side to complete the sandwich. The In film there did not appear to be affected by the heating to produce the first cast. To make the second cast the casting procedure was repeated with the clamp inverted. (This meant that the new cast could be made in the uppermost Pyrex ring.) In order to do this a method had to be found to prevent the first cast falling out when it became molten. This proved to be a problem. The solution adopted by Battersby was to plug the first Pyrex tube with Radio Spares Silicone Rubber compound. This approach was tried by the author but was found to be very unreliable. Sometimes the cast was found to have fallen down and pulled away from the Mo. Another problem encountered was In seeping out under the rings and spreading over the whole surface of the foil. This also sometimes resulted in part of the interface becoming unstuck. Since sample preparation was clearly going to be a lengthy process it was essential to develop a more reliable technique to avoid much time being wasted.

The seepage problem was clearly due to there being a continuous film of In under the rings; it seemed to be more favourable for the bulk In to be spread out over all the foil than to adhere just at the cast. After various other ideas had been tried the problem was eventually solved by

initially making the casts with only small quantities of In (enough to fill about 1mm of the tube). When the first cast was inverted it therefore was too light to pull away from the Mo and there was no need to plug it. This resulted in two small blobs of In on either side of the foil. The rest of the In film was then etched away with HCl before increasing the length of the casts to normal by carrying out the casting technique above. No seepage occurred with the inverted cast because there was now no In film under the rings.

A more reliable method of plugging the inverted cast was found to be the use of a stainless steel bolt. This was chosen so it just fitted inside the tubes. It was mounted as in Fig. 3.1 so that it could be screwed in and out of the inverted tube. The procedure then used for the second cast was to assemble the clamp and screw down the bolt onto the first cast until the clamp was slightly forced apart. On remelting, the inverted cast was therefore under slight pressure so that there was no danger of it pulling away. A little In was usually forced out under the Pyrex tube but this didn't adversely affect the interface. Fig. 3.2 illustrates the form of the final samples.

While these casting methods were being developed a number of In/Mo/In samples were produced. Measurements were made on these in the cryostat in order to assess how clean the interface appeared to be. Typical results for $R_{SNS}(T)$ are shown in Fig. 3.3. The resistance of the Mo is of the order of several nΩ which is low enough not to mask the divergence below T_c. Below about 2.2K the resistance is seen to fall off. This effect was also seen by Harding in Pb/Mo/Pb sandwiches and is due to the proximity effect. As was first observed by Clarke (1972) it occurs if N is a superconductor with T_c not too far below the measurement temperature. In this case a finite Δ extends into N which causes low energy excitations to be Andreev reflected before they reach the interface. This reduces the effective thickness of N (see Clarke (1972) for a detailed discussion) and

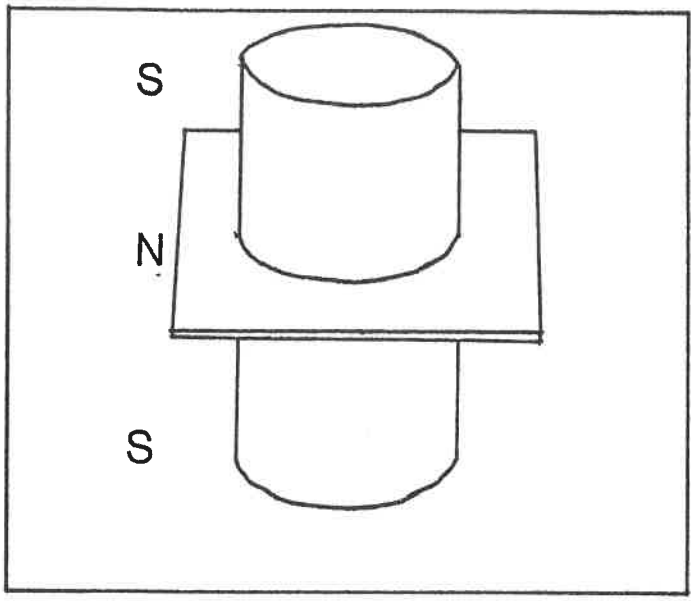

Fig. 3.2 SNS Sandwich.

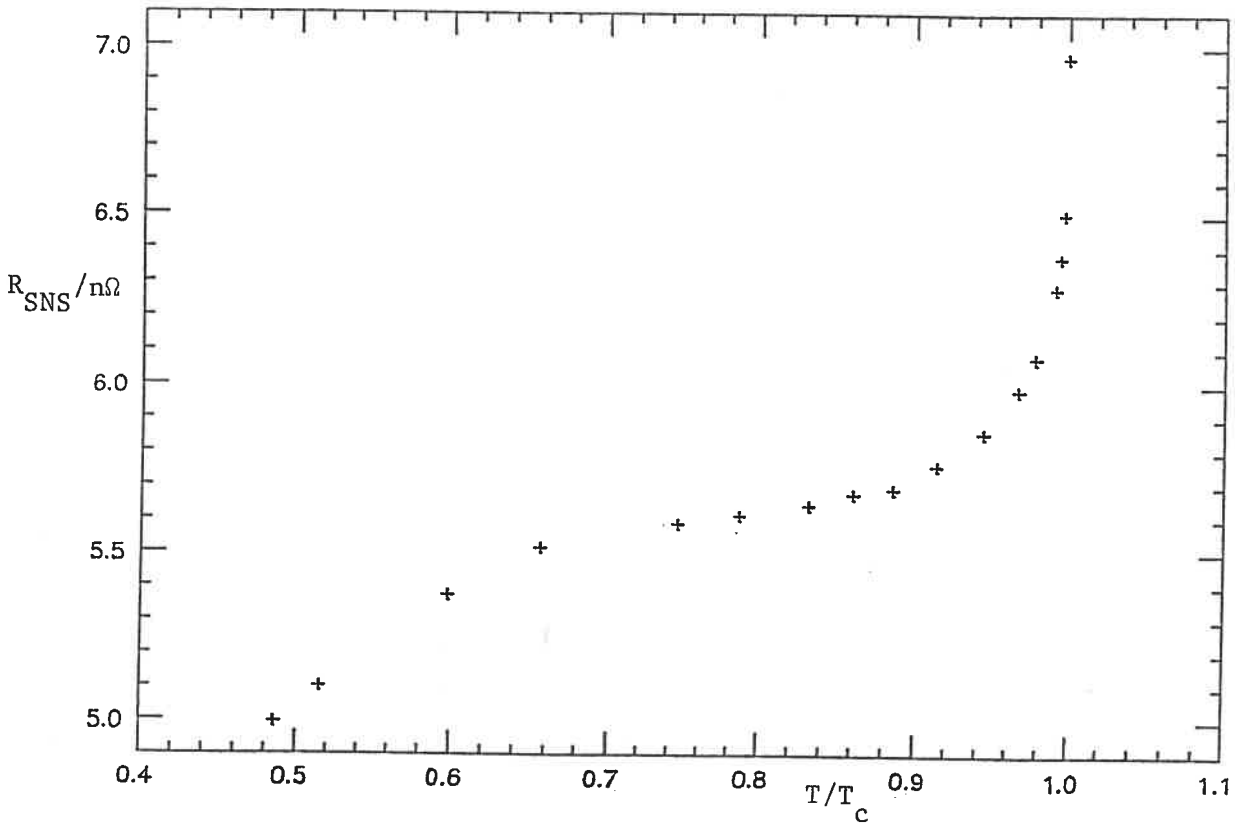

Fig. 3.3 Typical Resistance Data Obtained from In/Mo/In Samples.

also reduces the interface resistance (see Section 5.8).

These results confirmed that as expected Mo would not be suitable for measurements of the low temperature resistance. However the general similarity of this data to Harding's and the absence of a resistance minimum (see Tomlinson 1973) implied that the interfaces being produced by this technique were fairly clean.

3.5 Zone refined W: Preliminary Experiments.

The W finally used in this work was zone refined material supplied by Mr T Brown of Metal Crystals and Oxides Ltd. It had been zoned 4-5 times and was expected to have a residual resistance ratio of over 300, although it was subsequently found to be much purer than this. The crystal was first cut into slices on a spark machine which were further thinned down by spark planing. The slices were then etched in a mixture of HF and HNO_3 to remove the amorphous and impure layer on the surface formed by the spark machining. This resulted in slices of W which were at least 0.15mm thick. Slices thinner than this proved unable to withstand the forces generated during spark planing.

Attempts were made to use this W to make samples using the method described in Section 3.2. This was not successful because brittleness still proved to be a problem. As the W slices were much thicker than the foils which had been used previously, higher flashing currents had to be used. This meant that the current had to be turned up much more slowly to avoid the pressure in the evaporator rising too much as the current carrying strips outgassed. The pressure was required to be below about 6×10^{-6} torr so that the evaporation would produce clean interfaces. In total, therefore, the W was usually flashed for over 2 hours before it reached bright orange heat. Presumably heating for this length of time caused recrystalisation. The resulting W slices usually broke while they were being clamped between the Pyrex rings or even when they were being

removed from the evaporator.

One sample was successfully made using this method. This became superconducting below about 3K for reasons discussed in the next section. As this preparation method was not very reliable it was decided to try cleaning the W by ion bombardment, which was the approach used by Harding. It was hoped that this would produce less embrittlement because the W would not be heated up as much.

3.6 Experiments using Ion Bombardment Cleaning.

In these experiments the W was cleaned by raising it to a negative potential of several KV in low pressure Argon. The positive ions formed in the glow discharge would therefore be accelerated towards the W and would clean it by sputtering off the surface layers. Arranging the evaporator so that the W could be thus cleaned and then evaporated onto on both sides turned out to be fairly difficult. However, after many trials a satisfactory arrangement was found, and it is illustrated in Fig. 3.4. The following specific points about this are worth noting:

(i) The design of a support for the W that was insulated on the outside, and able to stand the relatively high temperatures of the W, proved difficult. The final design had ceramic tube as the last cm or so of insulation. The wire inside was made of stainless steel so that not enough heat was conducted back to melt the insulation further down.

(ii) In the first experiments the W was held in an Al holder. This proved to be unecessary; the anticipated problems of the sharp edges of the foil causing sparks proved to be groundless.

(iii) The large smoothing capacitor in the high tension power supply used was removed from the circuit. It was found (as dicussed by Holland (1956)) that the capacitor made the system much more prone to sparking.

(iv) The Ar supply was led well up into the chamber in a pipe. This ensured that the gaseous products of the sputtering were swept out of the

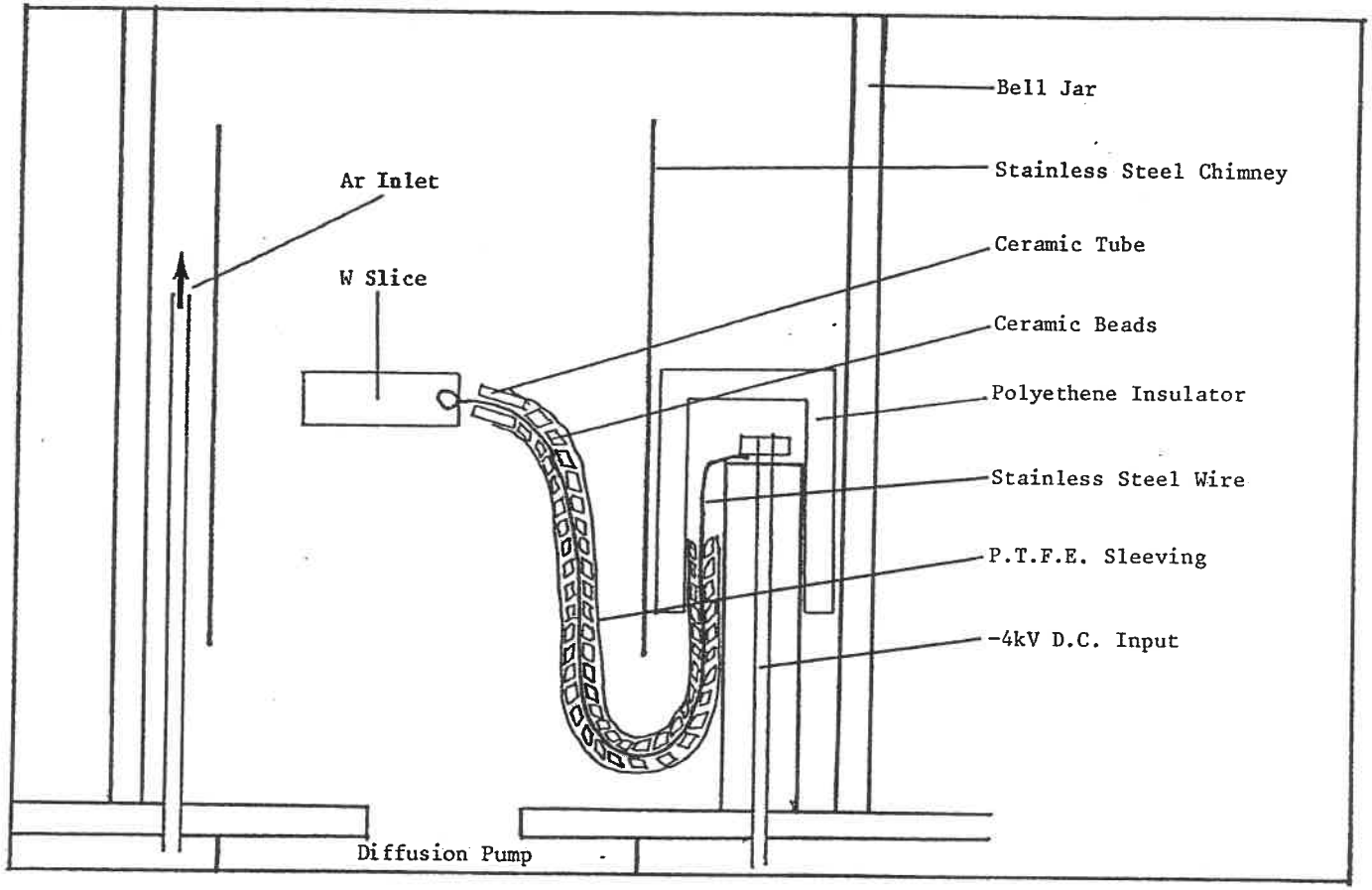

Fig 3.4 Diagram of Sputtering Arrangement. The evaporation boats containing the In were mounted on either side of the plane of this diagram.

chamber. Originally, the Ar entered the evaporator through a hole in the baseplate, the W was then found to become coated with a black deposit.

(v) During the sputtering, the boats were covered by shields of Al foil. This was to avoid W and any other products of the sputtering contaminating the In. The boats were outgassed under the foil before the ion bombardment was started.

After a number of trials, ion bombardment was usually done at a pressure of about 4×10^{-3} torr of Ar with the W at a voltage of about -4kV for about an hour. This caused the W to become dull red hot which didn't cause embrittlement problems.

The first samples made by this technique were found to become superconducting below about 3K. In addition, the resistance below T_c(In) but above 3K was variable, but always higher than was expected. Some typical results are shown in Fig. 3.5. Clearly the superconductivity below 3K was either due to In seeping through small cracks in the W, or a thin film of some sort all over the W surface (or possibly a combination of the two). One of the samples was etched in HF and HNO_3 to remove the top layer of the W in an attempt to find out which. On remeasurement, the transition to superconductivity at 3K was replaced by a sharp fall in the resistance to a much lower value (Fig. 3.6). The implication of this was that the phenomenon was something to do with the surface. At this stage, however, it was fortuitously discovered that the 3K transition completely vanished if the spark planing was missed out of the slice preparation. The results then became much more as was expected. The problem of the exact cause of the 3K effect was never solved. The spark planing subjected the slices to high stresses (as mentioned earlier thin slices were occasionally broken by the forces generated). This possibly caused small cracks in the W which were somehow responsible for this effect. All subsequent samples were made using W slices which had been just spark cut off the crystal and not planed. As the W was purer than expected the rather thicker slices which

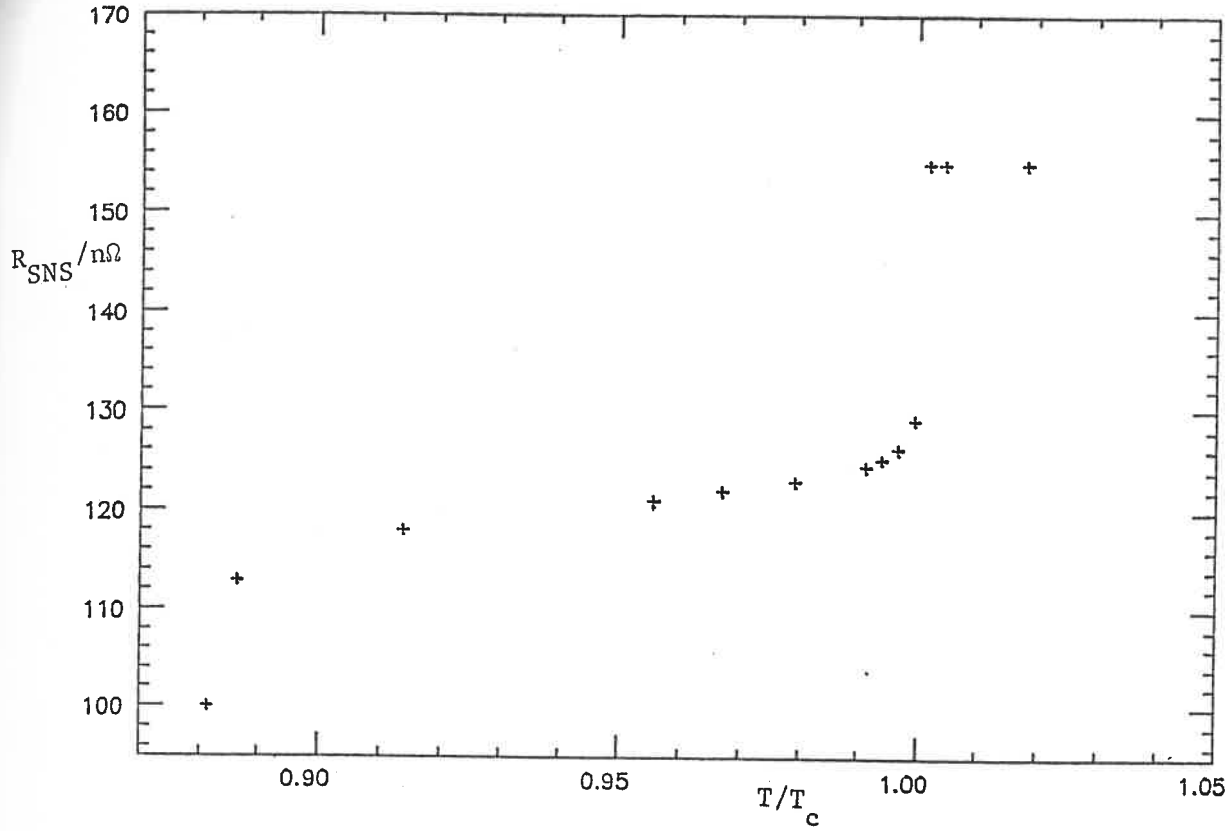

Fig. 3.5 Typical Resistance Data Obtained from Ion Bombardment Cleaned Samples which went Superconducting at about 3K ($\sim 0.88T_c$).

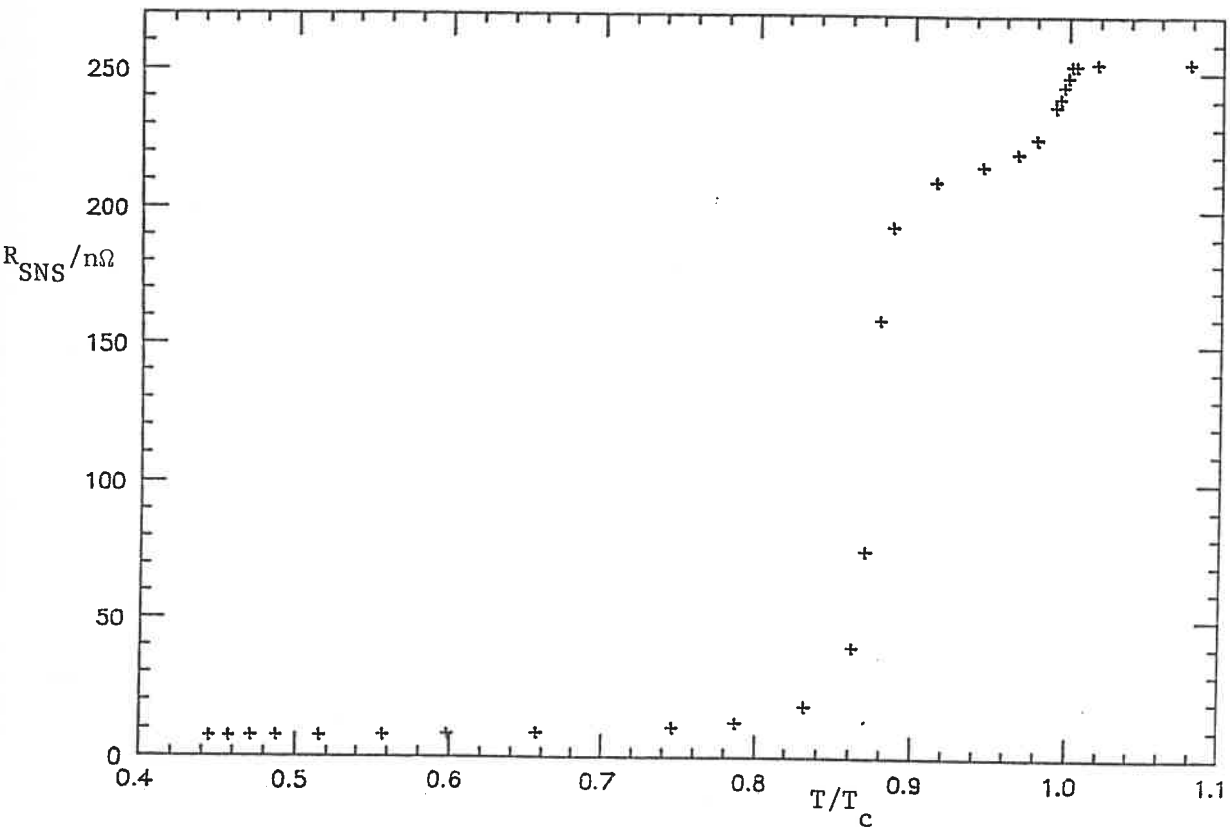

Fig. 3.6 Data from Same Sample as Fig. 3.5 after Etching in HF and HNO_3.

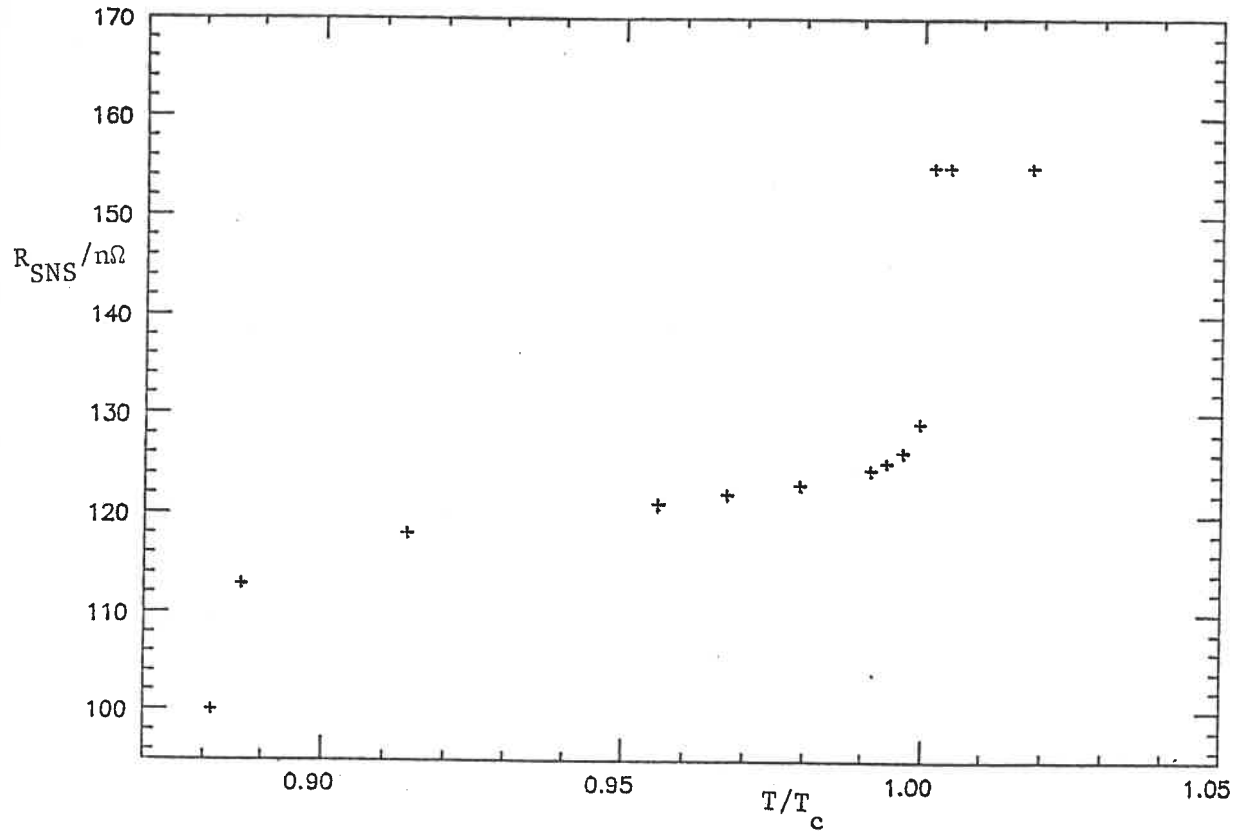

Fig. 3.5 Typical Resistance Data Obtained from Ion Bombardment Cleaned Samples which went Superconducting at about 3K ($\sim 0.88T_c$).

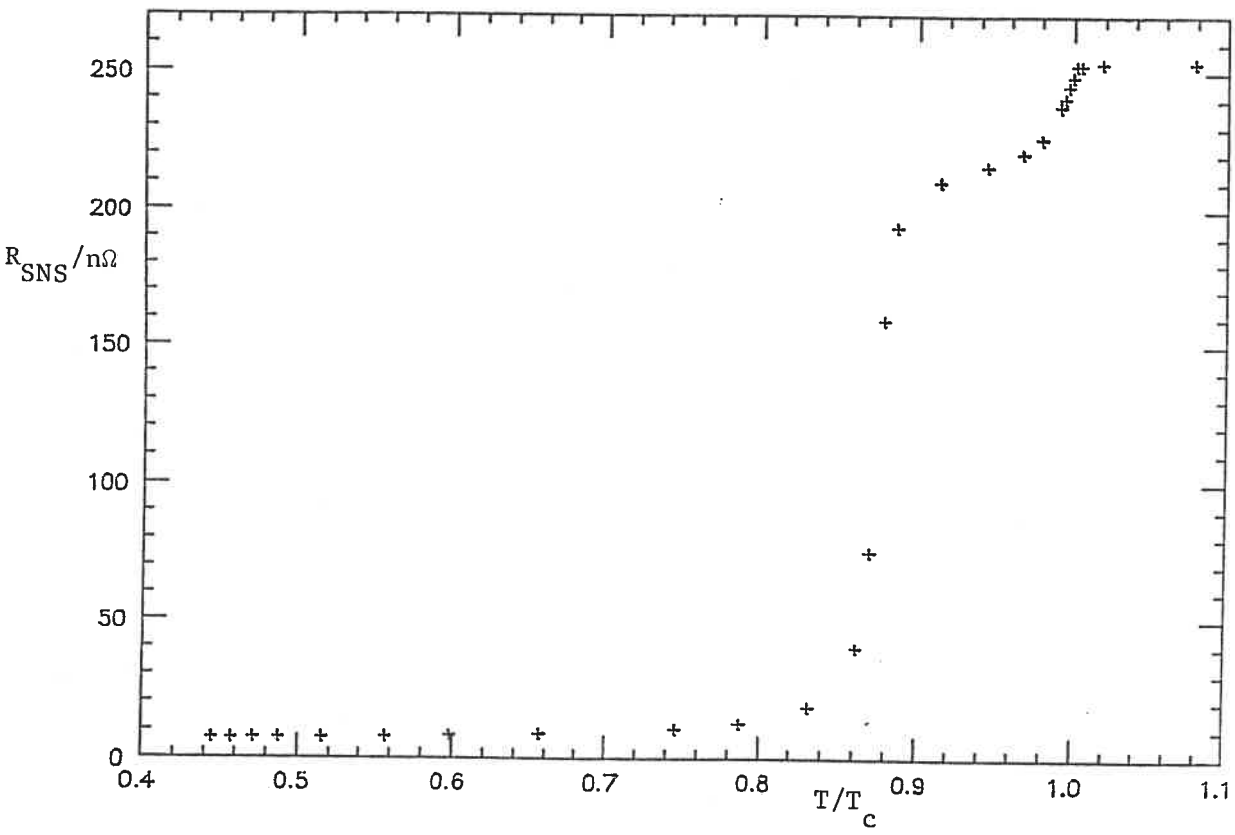

Fig. 3.6 Data from Same Sample as Fig. 3.5 after Etching in HF and HNO_3.

resulted did not adversley effect the results.

Once this problem had been solved, the $R_{SNS}(T)$ results were typically as shown in Fig. 3.7. The minimum resistance was quite low (being typically a few nΩ). However the results showed a distinct minimum at around $0.8T_c$, the resistance at lowest temperatures being 0.2-0.3nΩ greater than at the minimum. This compared with a fall of about 0.03nΩ (when reduced to the same area) observed in the best samples of Harding and of Battersby. This implied that the interfaces being produced were not very clean and so attempts were made to improve the technique.

An obvious thing to do was to modify the cleaning of the W by glow discharge; various different pressures and times of cleaning were tried, but none of these modifications substantially altered the results.

The casting technique was also suspected as being the cause of the problem. During casting the thin film melted before any bulk S was pushed onto it and it could possibly oxidise to some extent in the intervening time. This oxide could then perhaps migrate to the interface. Hence various attempts were made to carry out the casting in high vacuum. These were carried out simply by putting the furnace in the evaporator. (The furnace would clearly not heat up the clamp very well in high vacuum but it worked sufficiently for these trials.) It was found that without being stirred the bulk In seemed very unwilling to wet the film, even in high vacuum. The result was therefore usually that the cast was completely unattached to the foil. A sample was however eventually made by shaking the evaporator to get the casts to wet. The resultant $R_{SNS}(T)$ curve was still the same as before, so it was concluded that casting was not the source of the problem.

3.7 The Final Sample Preparation Technique.

With the failure of the above mentioned modifications to produce cleaner interfaces, it was decided that the problem was more fundamental.

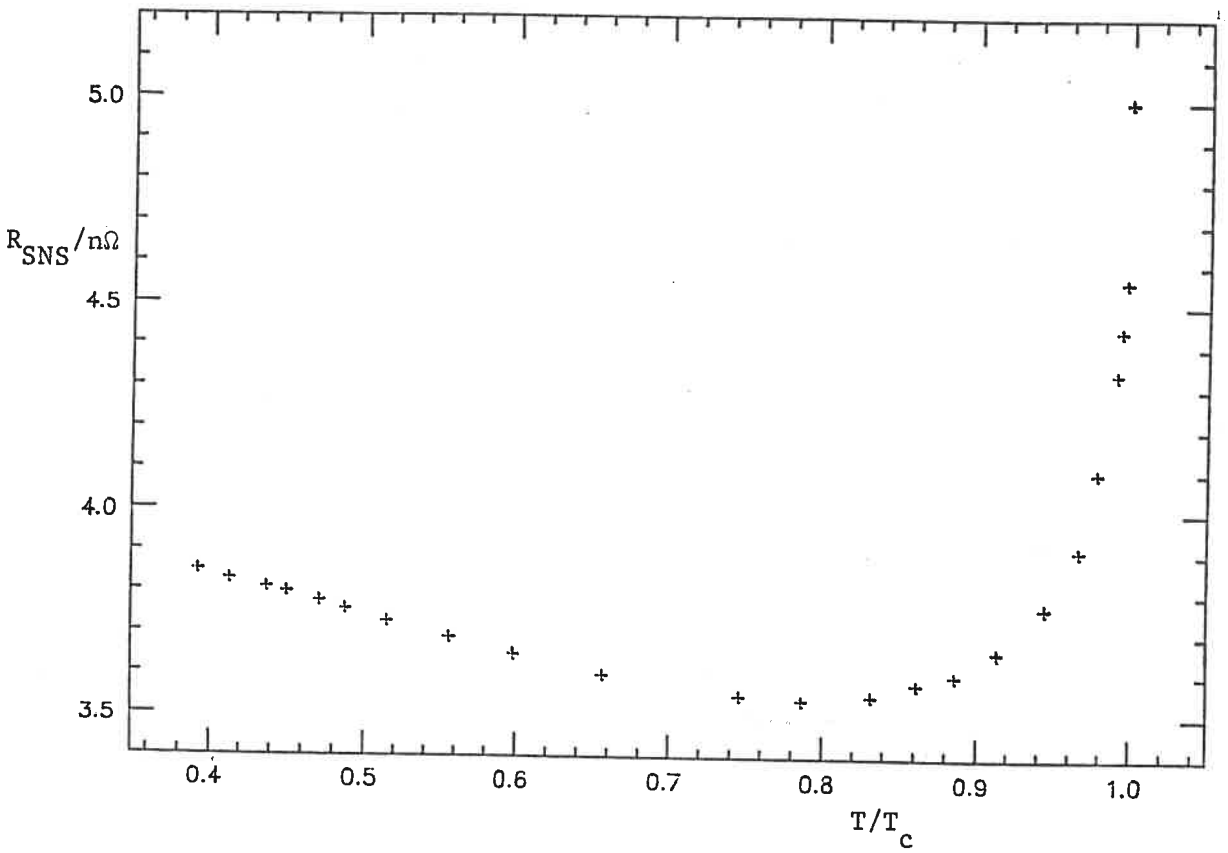

Fig. 3.7 Typical Resistance Data from Ion Bombardment Cleaned Sample.

The most likely explanation seemed to be that the vacuum in the evaporator was simply not good enough to use this sort of technique (Harding and previous workers used UHV systems). The surface of the W was probably becomming significantly contaminated between cleaning and evaporating. Luckily a way round this problem was found which enabled better samples to be prepared in the same evaporator.

The inspiration for the new technique came from watching the behaviour of In in Tantalum boats during the previous experiments. It was noticed that on heating up the boat, the In when it first melted would form a drop which did not wet the Ta. However once the Ta reached orange heat the In would suddenly start to wet the Ta and spread out. This behaviour presumably occured because the contaminant on the Ta surface evaporates at orange heat leaving a clean surface. It was decided to try a similar approch with the W.

In order to do this, the W was clamped in a horizontal plane in the evaporator (in the same way as a boat would be) and pieces of In placed on top. When the slice was resistively heated in high vacuum it was found that the In behaved in the same way as in the boat. Above orange heat it spread out to cover most of the exposed surface of the W. This was encouraging, as it meant that the In had definitely wet the W and therefore probably formed a good interface. After it had cooled, the evaporator was opened, the slice inverted and more In placed on top. (As the W had only been heated for a few seconds there was no problem with embrittlement). The procedure was then repeated to give a slice of W coated on both sides with In. This was converted into a sample with well defined areas of interface by the following process (which is schematically illustrated in Fig. 3.8):

(i) The coated slice was placed in the clamp which was screwed up as much as possible. Because of the thickness of the coating the ends of the Pyrex rings were usually a few mm apart after this had been done.

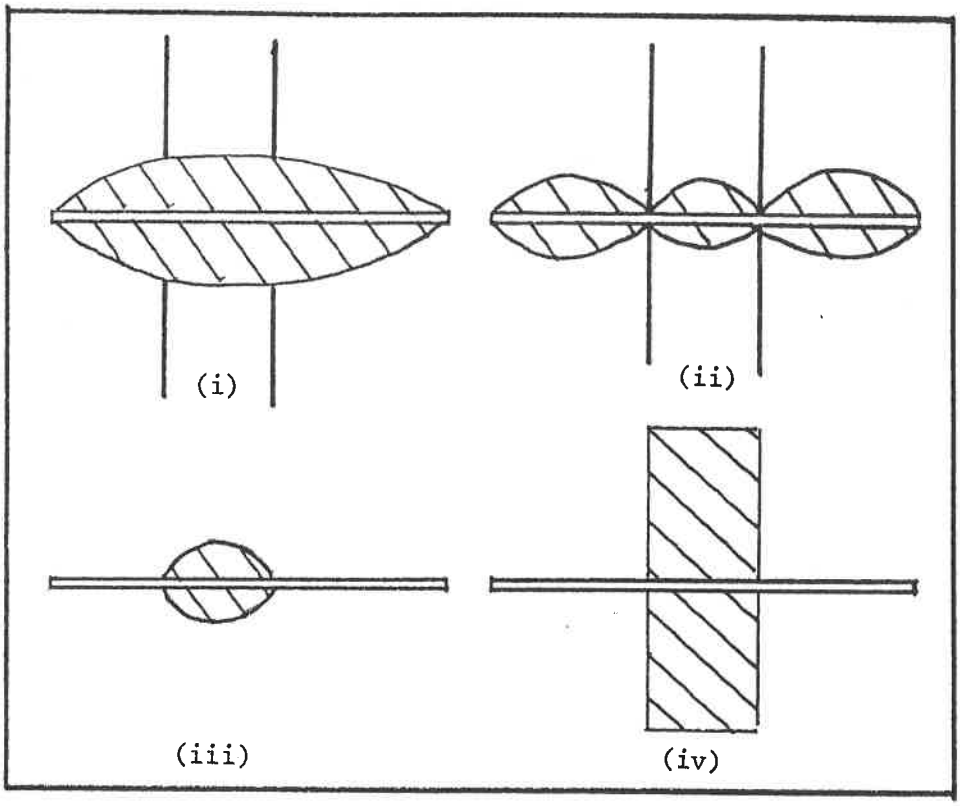

Fig. 3.8 Schematic Illustration of Final Casting Technique.

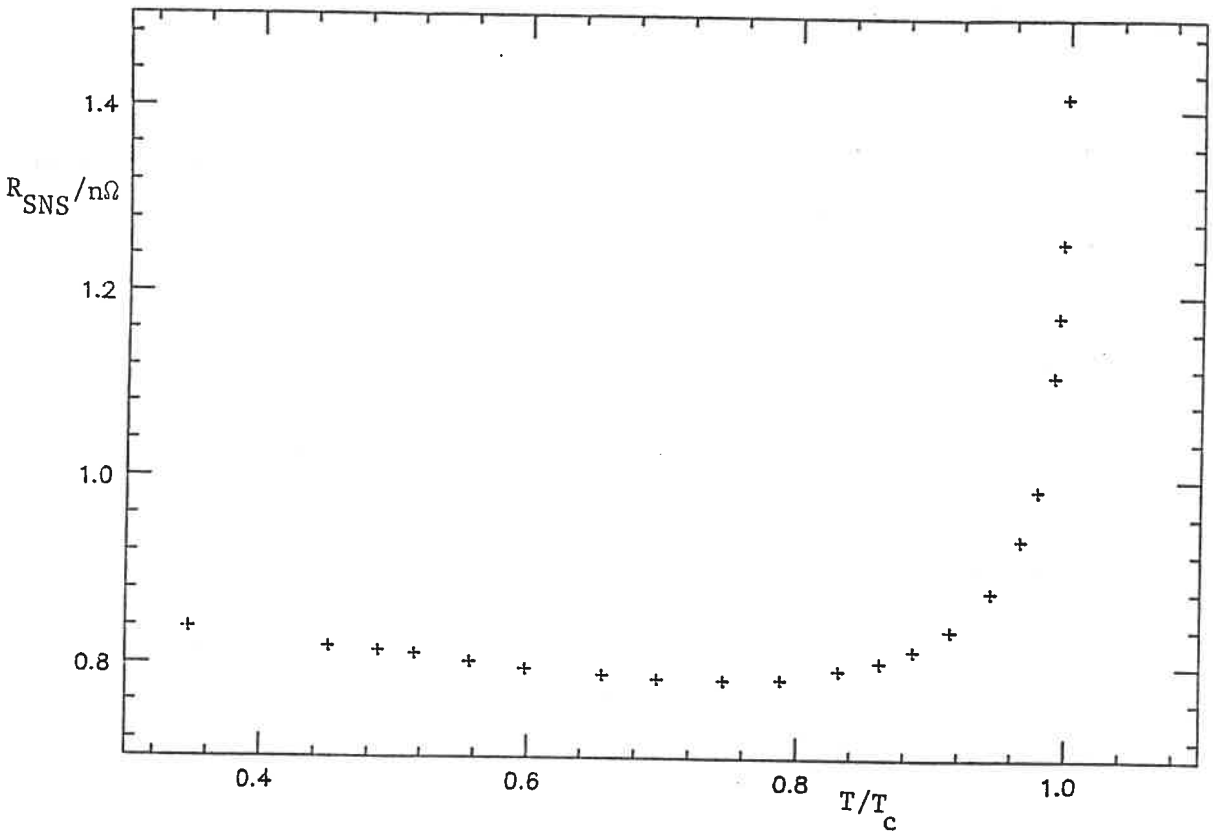

Fig. 3.9 Typical Resistance Data from Samples Prepared with Final Preparation Technique.

(ii) The clamp was then heated in the furnace. When the In melted the pressure of the springs in the clamp forced the Pyrex rings through the molten In onto the W surface.

(iii) After cooling the clamp was removed. The In coating was removed from everywhere apart from where the casts were going to be. This was done using first a scalpel to remove the bulk and then by etching in HCl.

(iv) The result of this was the slice of W with a blob of In attached on each side with the same interface area as the Pyrex rings. The slice was then put back in the clamp and the casts increased to their full length using the usual technique.

Typical $R_{SNS}(T)$ data for samples produced in this way is given in Fig. 3.9. As can be seen, the minimum resistance was now usually below 1nΩ. Also, the fall in resistance from lowest temperatures to the minimum was only about 0.03-0.06 nΩ. This meant that as had been hoped, samples produced in this way had significantly cleaner interfaces than previous ones. The improvement was presumably because the In coated the W while it was orange hot and therefore definitely clean. The quality of the interfaces was very similar to that of previous workers. This preparation technique was therefore the one finally used for the work.

On the assumption that all of the observed resistance at the minimum of the $R_{SNS}(T)$ data was due to the resistivity of the W, these samples imply a W resistance ratio of about 3000. This assumption is unlikely to be correct, however. Harding found that well below T_c, with clean S, the interface contributed an extra resistance of about 0.1nΩ when reduced to the present area. Independent measurements of the resistance ratio were therefore made on small pieces of the W crystal. A dipstick was used to make four terminal resistance measurements at room temperature and 4.2K. The usefullness of these measurements was, however, greatly limited for two reasons:

1. The high values of the resistance ratio meant that very small

resistances needed to be measured at 4.2K. A nanovoltmeter was used to measure the voltages but the drifts in voltage seen (presumably due to stray thermovoltages) were enough to make accurate measurements very difficult. The values obtained were probably only valid to within 10% or so.

2. The material on the dipstick probably had substantially different properties from that in the samples anyway. This was because the small pieces of W for dipstick measurements had to be cut off using the spark cutter which probably strained the material a good deal. In addition the slices used in the samples were flashed which would also have altered the resistance.

(As described in Appendix 3, attempts were also made to measure the properties along the slices of W using the SQUID voltmeter. This method also turned out to be somewhat unreliable, it did, however, give roughly the same results as the dipstick measurements).

Bearing these problems in mind, the resistance ratio of the W measured independently was found to be about 6000. This implies a rather high interface resistance of about 0.4nΩ and would mean that either the intrinsic mismatch in W/In is greater than in Cu/Pb or that the interfaces had more contamination (which is inconsistent with the conclusion above from the low temperature fall in $R_{SNS}(T)$). It can, however, be concluded from this that there is definitely significant interface resistance in these samples, even at the minima of the $R_{SNS}(T)$ curves.

Using this sample preparation technique, it was found that Sn and Pb were still unwilling to wet W. Several attempts were made to make Pb wet, in order to produce a Pb/W/In sample for the remelting experiments described in the next section. Pb was found to stick to the W but it did not spread out over the surface like the In. The Pb/W interface had a resistance of several nΩ decreasing with increasing temperature by about 5% over the range 1.2 - 3.4K.

3.8 Measurement of the Low Temperature Resistance

Apart from the development of a sample preparation technique another problem was how to measure the extra low temperature interface resistance expected when S was dirty (R_p). The fundamental problem was that the extra resistance was expected to be of the order of a few tenths of a nΩ. This turned out to be rather small relative to the possible errors.

Hardings solution to the problem was to measure the resistance of each dirty sandwich at low temperatures and then compare this to an independent estimate of the resistance of the N layer. This estimate had been obtained from the resistance ratio and the thickness of the foil. This approach was found not to be feasible in the present work; as mentioned in the last section it was not found possible to make reliable independent measurements of the resistance ratio of the W. (Hardings method would also have been inapplicable for the reasons mentioned under 1. below).

At an early stage it became clear that there were two possible solutions to the problem of measuring R_p:

1. After making and measuring the sample with pure In clean off the In and make another sample in the same way with the same piece of W. It would be hoped that this process would not change the resistance too much. A few trials would be carried out to determine the resistance of the particular slice of W. It would then be possible to make samples with dirty In and hence measure the extra resistance due to R_p.

2. After making and measuring the sample remelt the casts and add some alloy to them. Again it would be hoped that the remelting would not in itself change the resistance too much. This could easily be tested by remelting the casts but leaving them pure.

Method 1 was tried first, by remaking samples with pure In. It was found that the resistance of the samples was typically increased by about 0.1nΩ by being remelted. This was probably partly because the resistance

ratio of the quite pure W being used was changing significantly during the heating to make the sample. It also seems likely that despite the interfaces appearing to be clean from the $R_{SNS}(T)$ data, that the changes in resistance were partly due to changes of contamination at the surface.

For these reasons method 2 was tried. This is more attractive because in principle the same interface is used for the second run. The only thing which changes is the dirtiness of S which causes the effect of interest. The first trials involved cutting the casts of the first sample down to about 1mm lengths. This slightly simplified the casting because while recasting the first cast the inverted cast did not need to be plugged. It was found however that this process caused quite large rises in the resistance, presumably because it was difficult to cut the casts so short without straining the interfaces. In subsequent experiments only the ends of the casts were cut off (to remove the Woods Metal used to mount the sample) and the inverted cast was plugged at both stages. Pure In was added to the top cast for the trial runs. It was stirred around as the alloy would have to be with a stainless steel rod.

The rise in resistance caused by this process was found to depend on the quality of the sample. With the samples produced by ion bombardment cleaning it was found that remelting caused a rise in resistance of typically 0.08nΩ. However, with the samples made by the finally used technique, the rise was only 0.01-0.02nΩ on the first several remeltings. (It was found to increase if the same sample was remelted and remeasured too many times. New samples were always used in the final experiments). This was found to be adequate for the measurements required.

A decision which needed to be made at this stage was which metal should be used to alloy with the In to make it dirty. The main requirements were that it wouldn't alloy with the W and would be soluble in the In for a fairly large range of compositions. Phase diagrams for many metals and In are given in Hansen (1958). Pb was chosen because it is

soluble in In up to 12 at.% which is more than most metals. The alloys were made by melting together the metals in a test tube containing a He atmosphere. The metals were thoroughly mixed by shaking the tube for several minutes.

The experimental procedure to measure the low temperature resistance was therefore firstly to make the sample with pure In. In the final experiments, about a $1mm^3$ piece of 1 at.% Pb in In alloy was added to the "pure" In samples. This was because the very pure In as supplied was found to have rather irreproducable thermoelectric properties. This is discussed in Chapter 8. The roughly 0.01 at.% alloy finally used was found to have much more reproducible thermoelectric properties. Such a low concentration of lead did not increase the sample resistance noticeably below T_c. After measuring the reistance and thermopower of the sample, the casts were remelted and alloy added. The properties of the sample were then remeasured. R_p was determined by subtracting from the extra low temperature resistance then measured the resistance rise due to the recasting process itself. This latter quantity was taken as the rise seen, in the trial runs, on recasting with pure In (0.01-0.02nΩ as mentioned above; the rather large uncertainty was not important in practice since this was much smaller than the values of R_p). There were two potential problems with this method:

(i) In order to produce readily interpretable data, the concentration of the dilute alloy needed to be the same on both sides of the sandwich. As mentioned in the last section, attempts were made to avoid this problem by making Pb/W/In samples. Once made, the Pb/W interface, it was hoped, would not add a strong temperature dependent resistance or change with thermal cycling. R_p experiments would then use only one interface. This idea proved impractical because the Pb was found not to form a good interface with the W. Another idea to help overcome this problem was to use a more complicated recasting method. This would have involved cutting

off half of each cast after remelting, and then recasting them for a second time, putting the metal from the removed halves into the opposite casts. This would have necessitated a second remelting and would therefore have increased the resistance rise caused by the recasting process itself. Luckily it was found not to be necessary. When removing the Woods Metal the casts were carefully cut to the same length and the same quantity of alloy was then added to each one. Any significant differences between the resulting casts would have been detected during the dipstick resistance measurements (see below). The consistency of the R_p vs concentration data obtained also justifies the assumption that the resistivity of the casts was the same.

(ii) The second likely difficulty was ensuring that the Pb was spread uniformly in the dirty casts. As can be seen from the theory described in Chapter 6, it was necessary that the layer of In within a distance several times the evanescent decay length, l_a, (about 5×10^{-7}m) of the interface contained the same concentration of scattering centres as the bulk. As has been stated, the casts were thoroughly stirred up after adding the alloy. If the Pb was not getting very well distributed to the interface region, it would be expected that the results for R_p would be very irreproducible which is not seen (at least below 5 at.% Pb).

The resistivity of the casts was measured from their length and the jump in the sample resistance at T_c. It was thought that this procedure could lead to error because of the Woods Metal joints at the ends of the sample. While making these, some of the cast probably dissolved making the length difficult to measure. For this reason the resistivity of the casts was also checked independently in some cases. This was done using a dip stick which enabled four terminal resistance measurements to be made at room temperature and at 4.2K. The resistivity was measured on small slices cut from the casts and was always close to that measured in the sample.

Several attempts were made to check the method further. These

involved remelting the dirty samples again and diluting them to see if the resistance fell as expected. It was found that the resistance did fall, but the fall observed was often smaller than would be expected if each remelting caused an extra resistance of 0.02 nΩ. These checks however usually involved cutting the casts shorter than usual to enable the alloy to be significantly diluted. This probably put more strain on the interfaces.

CHAPTER 4

RESISTANCE OF CLEAN SNS SANDWICHES NEAR T_c

4.1 Introduction

The resistance of SNS sandwiches in which S is a clean superconductor close to T_c has been the subject of much previous work. In this chapter the results obtained in the present work are analysed in the light of the theory developed by Battersby (1982). Sections 4.2 and 4.3 introduce this theory. The results are compared with the simplified version of the theory in Section 4.4 and Section 4.5 discusses the fuller variant. Section 4.6 discusses the question of the form of the temperature dependence of λ_3.

4.2 General Theory for $R_{SNS}(T)$

The fundamental theory of the resistance of NS interfaces used in this work was that of Waldram (1975). The detailed mathematical results of this theory are given in Appendix 1. In this section the physics of the model is summarised. Waldram distinguishes three types of scattering of the excitations, elastic, inelastic and branch crossing. The relaxation time approximation is used and the three types of scattering are assigned mean free paths ℓ_1, ℓ_2 and ℓ_3 respectively. The mean free path for any type of scattering is denoted ℓ. The boundary conditions are given by the coefficients R_A, R_N, T_A, T_N which are the probablities of an excitation incident on the interface being Andreev or normally reflected or Andreev or normally transmitted. A Boltzmann equation is hence constructed which is solved subject to the boundary conditions in order to calculate a value of Q* at the interface which is converted to a voltage using (1.7). There are two fundamental mechanisms which produce voltage. Firstly excitations above the gap enter S and cause voltage as discussed in Section 1.3. Secondly if R_N is non zero (either above or below the gap) this will set up a boundary region in N with an excess of electrons which also

contributes to the boundary voltage.

The result of the theory is the rather complicated expression for the boundary voltage (A1.3). This contains numerous integrals over energy of functions of the boundary conditions, R_A, R_N etc., which in general are energy dependent. It is important to note that this result as it stands is generally valid. The central problem in calculating results from this model is making reasonable estimates of the boundary conditions. Much of this thesis is concerned with applying various calculations of these parameters which are valid in different situations.

4.3 Battersby theory of Boundary Resistance.

Battersby (1982) used the following boundary conditions in the theory described in the last section:

(a) $R_N=0$ for all energies, which assumes there is no oxide etc. or mismatch at the interface to scatter back the excitations "normally". This could be a reasonable approximation for clean superconductors if care is taken to prepare very clean interfaces.

(b) $R_A=1$ below the gap which follows from (a) since no transmission is possible.

(c) $R_A=0$ above the gap. Andreev (1964) showed that there is an appreciable probability of Andreev reflection for excitations with energy just above Δ. However this is expected to be a negligible effect near T_c where most excitations will have energies many times Δ and a low Andreev reflection probability.

It is emphasised that becasue of (c) this theory is only expected to be valid close to T_c. Because of (a) all the resistance in this model is caused by charge imbalance in S. With these assumptions the expression for the boundary voltage, (A1.3), simplifies to:

$$2f(\Delta)/Q_i = (\ell/\lambda_3)^S + (\ell/\lambda_2)^N(1 - 2f(\Delta)) \qquad (4.1)$$

Where λ_2 is the diffusion length for all forms of inelastic scattering defined by $\lambda_2=[(1/\ell)(1/\ell_2+1/\ell_3)]^{-0.5}$ and, as mentioned in Section 1.3, λ_3 is a diffusion length for branch crossing processes defined by $\lambda_3=(\ell_3\ell)^{0.5}$. The superscripts imply that the quantity is to be taken in N or S. Following the notation of Pippard et al. (1971), the boundary resistance of the interface is expressed by Q_i. This dimensionless quantity is the thickness in electron mean free paths in N of a slab of N which would have the same resistance as the interface (care should be taken not to confuse this quantity with Q*, or other measures of charge imbalance which are mentioned in the literature). The interface resistance, R_i, is therefore given by $R_i=Q_i(\rho\ell)^N/A$ where A is the area of the interface.

The first term in (4.1) gives the voltage generated by charge imbalance in S which decays by branch crossing. The second reflects the fact that some of the charge imbalance can decay by the excitations returning to N, being inelastically scattered and then Andreev reflected. These two channels for transfer of charge into S act in some sense like resistances in parallel though this analogy should not be taken very literally. This expression was found by Battersby to be a good fit to the data for Pb/Cu/Pb sandwiches near T_c, with pure and slightly dirty Pb (up to 0.1 at.% Bi).

Battersby found that with pure superconductors the $(\ell/\lambda_2)^N$ term is small and may be neglected leading to the simple expression:

$$Q_i = 2f(\Delta)(\lambda_3/\ell)^S \qquad (4.2)$$

Here the $(\lambda_3/\ell)^S$ term reflects the fact that the entropy generation is as if a layer of S of thickness λ_3 had turned normal and the $2f(\Delta)$ gives the number of electrons above the gap.

It should be noted that even in the simple limit (4.2), the

resistance appears as Q_i, ie as an equivalent number of mean free paths in N. This implies that the interface resistance observed depends on the resistance of a mean free path in N, $(\rho\ell)^N/A$, as well as on the properties of S. This is not physically expected since all the resistance is generated by charge imbalance in S in this model. It should, however, be remembered that the theory is one dimensional. This means that it assumes implicitly that $(\rho\ell)^N=(\rho\ell)^S$ in which case the dependence on the properties of N cancel out and the expression becomes that quoted by Battersby and Waldram (1984).

$$R_i = 2f(\Delta)(\lambda_3\rho_s)/A \qquad (4.3)$$

In the three dimensional case where, in general, $(\rho\ell)$ differs between N and S, it turns out that (4.3) can still be derived from (4.2). In this case it is necessary to modify the theory. However, the modification only results in a scaling in λ_3 (and λ_2 in the more general theory). The absolute values of these parameters are not of much interest since the model is essentially one dimensional; a full translation to three dimensions would add several other scaling factors to the parameters. This is not worth considering in detail since an extension to three dimensions would also greatly complicate the boundary conditions described in later chapters. Hence throughout the resistance theory described in this thesis fitting to data is done by calculating Q_i using the real (3D) value of $\rho\ell$ in W. Similarly, ℓ in S is calculated using the real value of $\rho\ell$ in In. The motivation for doing this is that in the theories described in Chapters 5, 6 and 7, part of the resistance genuinely depends on $(\rho\ell)^N$; this is more easily incorporated if the parameters are set up as described.

4.4 Comparison of Results with the Simple Theory.

In this section the comparison of the present results with the simplified expression (4.2) is discussed. In order to do this it is necessary to put into the expression a specific form for $\lambda_3(T)$. The question of the form of $\lambda_3(T)$ is discussed in Section 4.6. In order to fit the results the form used by Battersby (1982) is used:

$$\lambda_3(T) = \lambda_3^{\circ} S(T) \ , \quad S(T)=(T_c/T)(\Delta(0)/\Delta(T))^{0.5}(2f(\Delta))^{0.5} \qquad (4.4)$$

Where $\lambda_3^{\circ}=(\tau_c \ell v_F/23.3)^{0.5}$ and τ_c is defined as discussed in Section 4.6. This form of λ_3 is expected to be valid if $\Delta/k_BT<<1$. Equations (4.2) and (4.4) together imply that a plot of $R_{SNS}(T)$ against $2f(\Delta)S(T)$ should be a straight line of gradient $(2(\rho\ell)^N \lambda_3^{\circ})/A(\ell)^S$. The constant $\rho\ell$ for W was calculated using the formula of Chambers (1952) and the Fermi surface area quoted by Sparlin and Marcus (1966); the value obtained was 8.8×10^{-16} Ωm^2. The intercept of such a plot is expected to give R_W, the value of the resistance due to the W and interface effects other than the charge imbalance in S (assumed temperature independent).

The data for two In/W/In sandwiches plotted with the above axes are shown in Fig. 4.1. T_c has been adjusted to give the best straight line. This is reasonable since the adjustments required are of the order of a mK which is over an order of magnitude less than the width of the transition. Throughout this work the form of $\Delta(T)$ used was obtained by interpolating between the values calculated by Muhlschlegel (1959) (although close to T_c, as in this case, the approximate form $\Delta(T)=1.76\Delta(0)(1-T/T_c)^{-0.5}$ is adequate). It can be seen that close to T_c the expected linear form is observed. Below about $0.8T_c$ deviations are seen which is to be expected in view of the simple nature of the theory. This is in contrast to the findings of Battersby, whose results on Pb/Cu appeared to obey the theory down to much lower temperatures. It is worth noting that the temperature

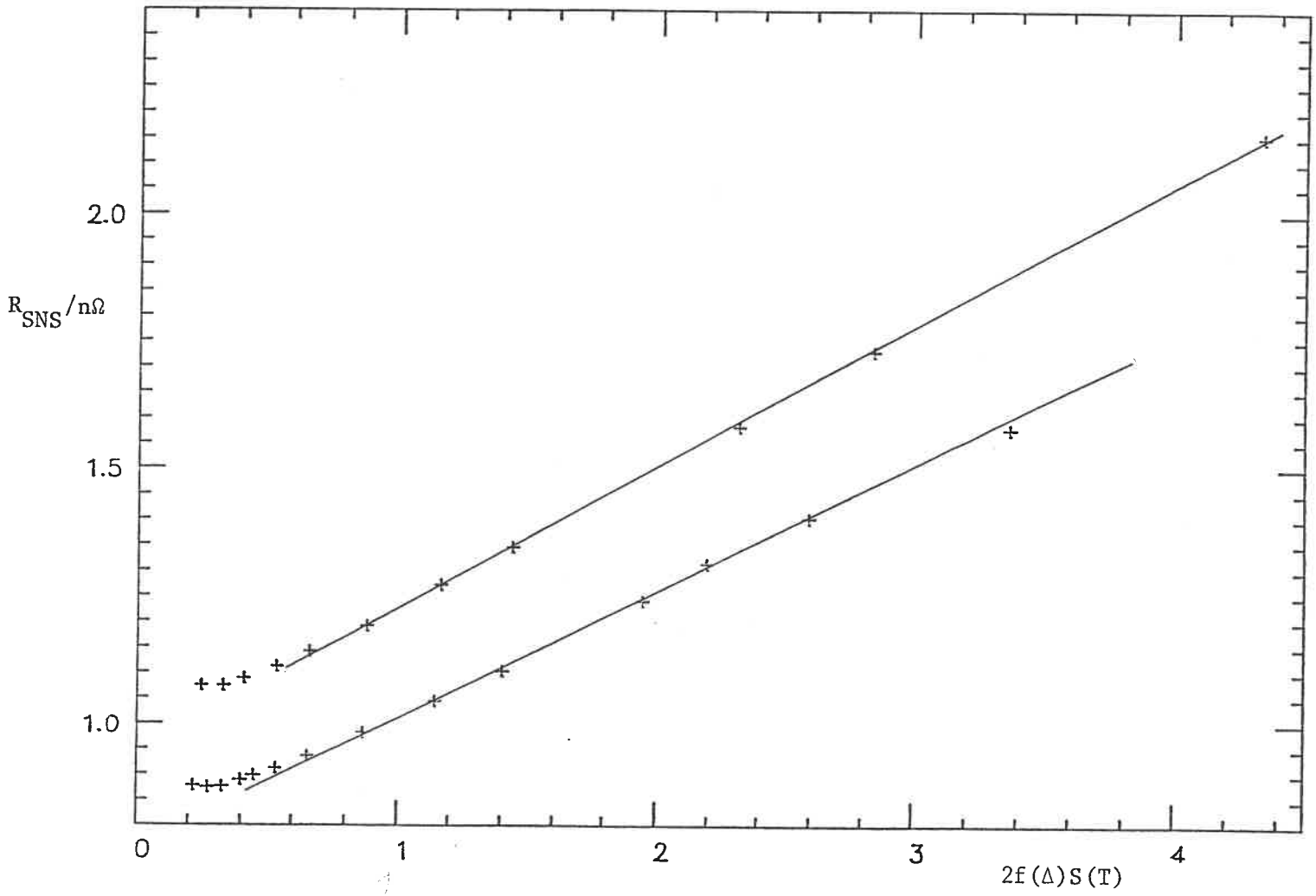

Fig. 4.1 Fit to the Simple Theory For Two Samples.

dependence predicted by this theory is very similar to that expected from some earlier theories (Hsiang and Clarke 1980) so the present data can be assumed to fit those theories also.

The values of λ_3° obtained are best considered in terms of ℓ_3 and ℓ since ℓ varies significantly between the specimens, which were very slightly dirty as discussed in Section 3.6. ℓ was calculated in each case using $\rho\ell = 5.7\times10^{-16}\ \Omega m^2$ for In from Dheer (1960). ℓ_3° was calculated using $\lambda_3^\circ = (\ell_3^\circ \ell)^{0.5}$; it is expected to be a constant quantity if the theory is valid. The results for four samples are given in Table 4.1

Table 4.1

Sample No.	$\ell/10^{-5}$m	$\ell_3^\circ/10^{-5}$m
91	2.0±0.1	2.5±0.3
97	1.2±0.1	2.0±0.2
99	1.6±0.1	2.0±0.2
108	0.8±0.1	2.0±0.3

It can be seen that the values of ℓ_3° are indeed fairly constant. The rather large errors in the data stem from difficulty in measuring the normal resistivity of the In; the dimensions of the samples were somewhat uncertain because there was probably some alloying between the In casts and the Woods Metal used to mount the sample.

It is also possible to compare the value of ℓ_3° thus obtained with a theoretical value. This is deferred until Section 4.6 where the question of the form of $\lambda_3(T)$ is discussed.

4.5 Comparison of results with the Battersby theory.

Battersby analysed his data on Pb/Cu/Pb sandwiches in terms of the full expression (4.1). An important point is that Q_i in this expression, as before, gives the resistance due to the interface only. This means that

the resistance of the W etc needs to be subtracted off the total before fitting to the theory (as opposed to appearing as the intercept in the simplified theory). R_W is not measurable directly since it includes temperature independent interface contributions (eg mismatch as discussed in Chapter 5) as well as the W resistance. It therefore has to be treated as a second adjustable parameter (T_c being the first).

The present In/W data was fitted by plotting $(R_{SNS}-R_W)^{-1}2f(\Delta)/(1-2f(\Delta))$ against $(S(T)(1-2f(\Delta)))^{-1}$ following Battersby. By comparison with equations (4.1) and (4.4), it can be seen that such a plot is expected to be linear with a slope proportional to $(\ell/\lambda_3{}^o)^S$ and intercept proportional to $(\ell/\lambda_2)^N$. Battersby chose the parameters T_c and R_W (R_C in his notation) to give the best fit to the theory. It was not, however, found possible to do this uniquely with the present data; different values of R_W were found to produce equally good fits by making small adjustments to T_c. Fig.s 4.2 and 4.3 show curves for the same sample, calculated with different values of R_W. It can be seen that the linear portions have intercepts which differ by a factor of roughly 3. For this reason no very definite conclusions could be drawn from the intercepts and gradients of these curves. The values are therefore not discussed here beyond commenting that the intercepts were found to imply a value of $(\ell/\lambda_2)^N$ between about 0.4 and 1.2 which is relevant to the discussion in Chapter 5.

It can also be seen from Fig.s 4.2 and 4.3 that, as with the simpler theory, the data only fits down to about $0.8T_c$. Large deviations are observed below that temperature; the exact form of these depends sensitively on the value of R_W used. Battersby saw agreement with the theory down to lower temperatures which was, however, surprising in the light of the approximations described in Section 4.3. The reason for these apparent differences between In/W and Pb/Cu is not known; the approximations in the theory appear to hold down to lower temperatures in

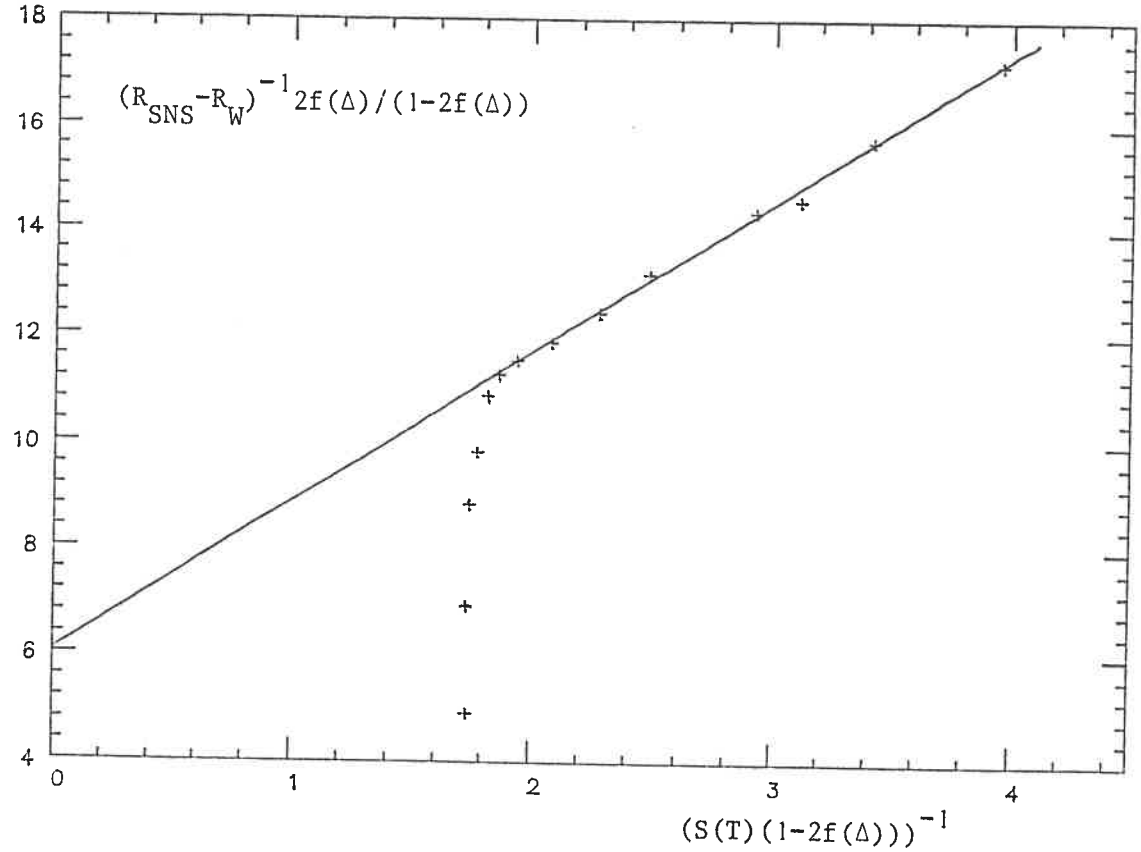

Fig. 4.2 Fit to the Battersby Theory. In this case R_W taken to be 0.74nΩ.

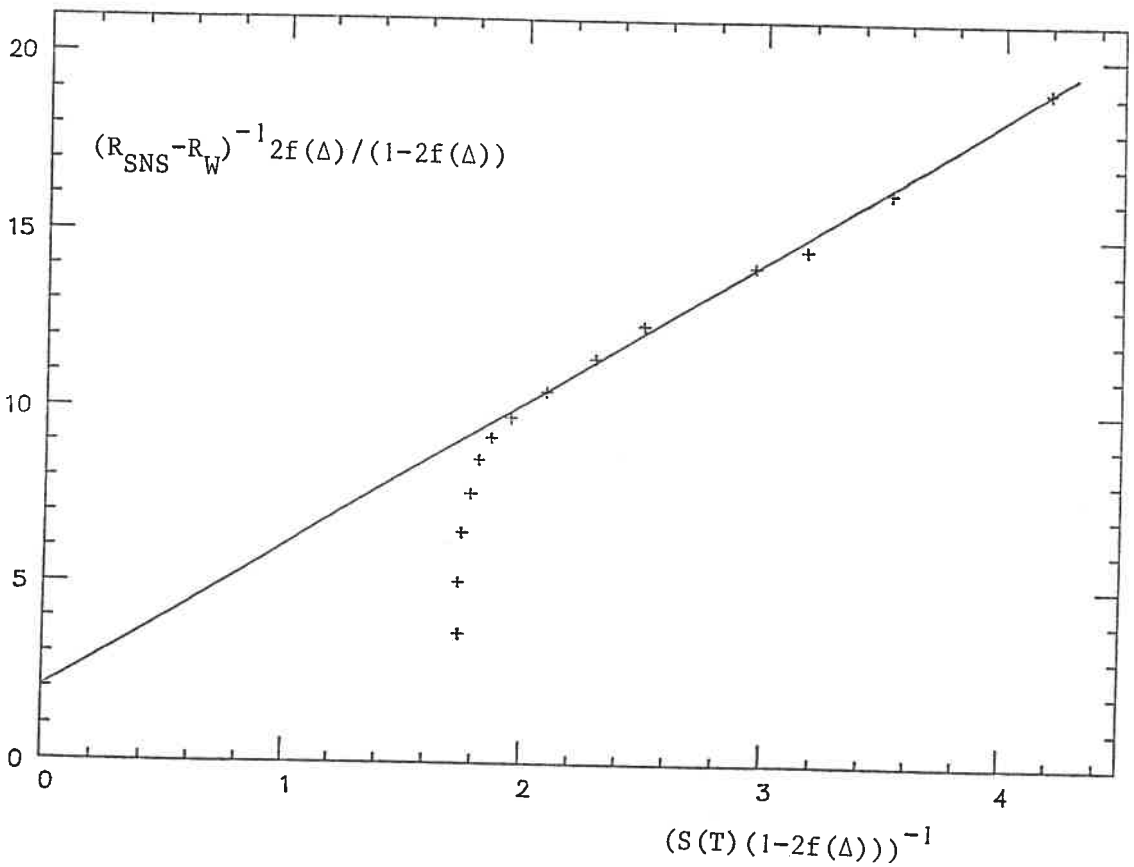

Fig. 4.3 Fit to Battersby Theory for same Sample as Fig. 4.2 but with R_W=0.72nΩ.

the latter case.

4.6 Form of $\lambda_3(T)$

The form of the temperature dependence of λ_3 is an important question and is worth discussing further. In this section the derivation of the form used above (due to Battersby) is examined and is compared with an alternative form which has been more recently proposed.

$\lambda_3(T)$ is the diffusion length for scattering processes which relax the charge imbalance, Q*, in S. Battersby's calculation started from the work of Chang (1979). Chang considered a perturbation to the excitation distribution at just one energy, E, with the rest of the distribution left at its equilibrium value, f_o. He calculated the rate of decay of charge imbalance in this case assuming that the phonon distribution was in equilibrium and that T is close to T_c.

$$\tau_{Q*}^{-1}(E) = \tau_c^{-1}(kT_c)^{-3}(\pi/2\ \Delta E^2 \coth(E/2kT)) + O(\Delta^2) \qquad (4.5)$$

where τ_c^{-1} is a theoretical quantity related to the assumed form of the electron-phonon interaction. In order to arrive at a result for λ_3, $\tau_{Q*}^{-1}(E)$ needs to be energy averaged over some distribution of charge imbalance. The distribution used is that assumed in the Boltzmann equation:

$$q_{Q*}(E) = -f'(E)Q*/f(\Delta) \qquad (4.6)$$

(q(E) is a measure of the charge excess at a given energy as defined in Waldram (1975) and Appendix 1). q_{Q*} is the equilibrium value of q in the presence of a given Q* assuming each branch is seperately in thermal equilibrium. Averaging over this distribution gives the result for λ_3, equation (4.4). Two points about this should be noted:

(i) The form given by equation (4.4) is only expected to be valid

close to T_c where $\Delta/kT<<1$. This is because second and higher order terms in (4.5) are neglected and because of a similar approximation while averaging.

(ii) The distribution (4.6) is probably not very realistic. In reality the distribution as Q* relaxes should be obtained self consistently from the Boltzmann equation.

The difficulty is avoided by an alternative approach to calculating λ_3 suggested by Battersby and Waldram (1987). This is based on the work of Chi and Clarke (1980) who studied forms of q(E), denoted q_0, which decay uniformly ie

$$dq_0(E)/dt = -q_0(E)/\tau_{q_0} \quad (\tau_{q_0} \text{independent of } E) \tag{4.7}$$

and they find $q_0(E) \propto -(\epsilon/E)f'(E)$. Such a distribution can be considered to be more realistic since any deviations from q_0 can decay by ordinary processes and will therefore be expected to decay more quickly. Chi and Clarke's result for τ_{q_0} thus defined is:

$$\tau_{q_0} = (4kT\tau_i/\pi\Delta))\Theta(\Delta/k_BT) \tag{4.8}$$

Where τ_i is the inelastic scattering relaxation time at the Fermi surface and at T_c, $\Theta(\Delta/kT)$ has been calculated by Chi and Clarke. The details of the derivation are in Battersby and Waldram but the result finally arrived at for the temperature dependence of λ_3 is:

$$S(T) = [(Q^*/Q)(T/T_c)\Theta(\Delta/kT)(\Delta(0)/\Delta(T))]^{0.5} \tag{4.9}$$

where:

$$Q^*/Q = 1/2f(\Delta)\int_{\Delta}^{\infty} -f'(E)(\epsilon/E)dE$$

and

$$\lambda_3^{\circ} = (0.72\tau_i \ell v_F)^{0.5}$$

Figure 4.4 shows this form of $\lambda_3(T)$ as calculated by the author with the Battersby form (4.4) for comparison. It can be seen that the two forms give the same result for the divergence close to T_c but differ substantially below about $0.95T_c$. As has already been mentioned the Battersby form is not expected to be valid except close to T_c because of approximations made in its derivation. In addition neither form is strictly applicable for In/W below about $0.95T_c$, if the values of ℓ_3° given in Table 4.1 are taken seriously. This is because in order for the reasoning above to be applicable it is necessary that $\ell_3 >> \ell_2$, otherwise the distribution of q will will not be in thermal equilibrium (as was assumed) in the region of S where the Q* exists. Calculations described in the next chapter, show that $\ell_3 = \ell_2$ at roughly $0.95T_c$ if ℓ_3° has the value expected from Table 4.1. However, with the models described in the next chapter ℓ_3° is found to be several times larger with the result that ℓ_3 remains larger than ℓ_2 down to about $0.6T_c$.

Luckily, however, the form of $\lambda_3(T)$ is not critical except close to T_c where the two forms are the same anyway. At lower temperatures there are very few electrons above the gap so charge imbalance in S is responsible for a correspondingly small resistance. To illustrate this point, figure 4.5 shows $R_{SNS}(T)$ curves obtained from the simplified expression (4.2) using both forms of $\lambda_3(T)$. It can be seen that despite the differences between the $\lambda_3(T)$ forms, the two curves are very similar. In the more complicated cases discussed in later chapters the form of $\lambda_3(T)$ well below T_c is expected to be less important still. This is because, in these more complex models, charge imbalance in S is responsible for only part of the observed resistance as opposed to causing all of it here. In conclusion, therefore, either form of $\lambda_3(T)$ may be used in calculations with almost the same results. This is the justification

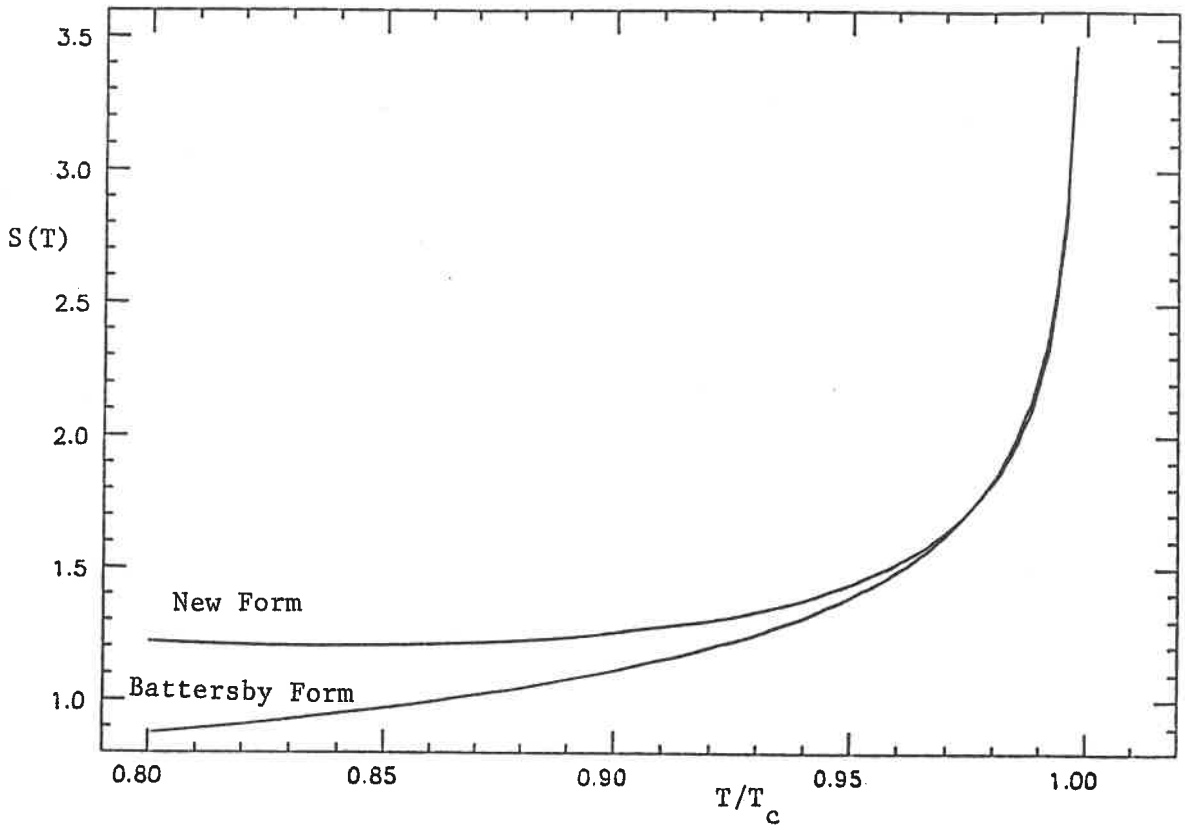

Fig. 4.4 Comparison of the Two Forms of $\lambda_3(T)$.

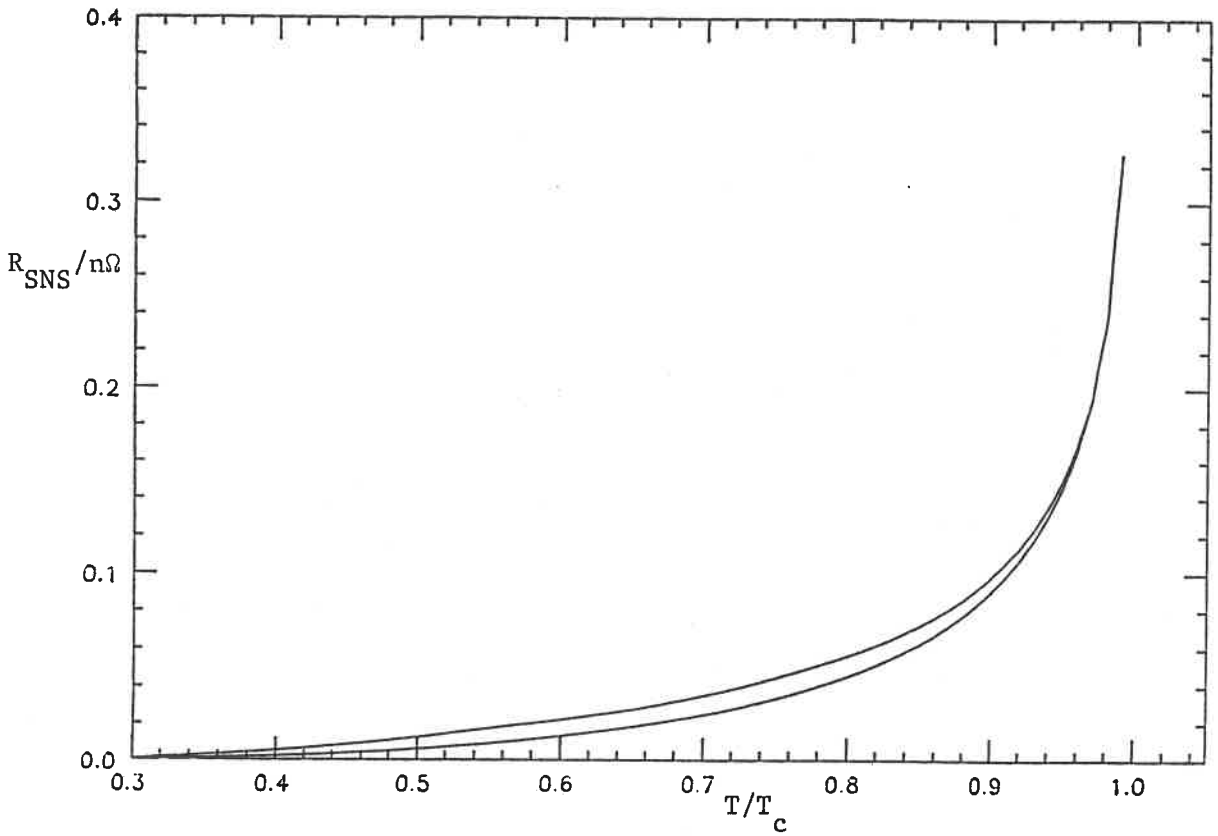

Fig. 4.5 Two $R_{SNS}(T)$ curves calculated from the simple theory using the different $\lambda_3(T)$ forms.

for using the Battersby form in the work described in this chapter. In the calculations described in the rest of the thesis, however, the new form is used.

The Battersby and Waldram calculation of λ_3 allows theoretical estimates to be made of λ_3^0 since it contains τ_i which has been experimentally and theoretically determined for a number of metals. These values are tabulated in Pethick and Smith (1980) and for In is quoted as 0.11ns. Using the above expression for λ_3^0 this gives a value of ℓ_3^0 of 2.7×10^{-5}m which agrees fairly well with the values given in Table 4.1 (about 2×10^{-5}m). The comments about the absolute values of ℓ_3^0 in Section 4.3 must be remembered while making the comparison; the only conclusion which should be drawn is that the theoretical value obtained is of the right order of magnitude.

CHAPTER 5

RESISTANCE OF CLEAN SNS SANDWICHES WELL BELOW T_c

5.1 Introduction

The simplified boundary conditions described in Chapter 4 are unable to explain the behaviour of R_{SNS} below about $0.8T_c$. This chapter discusses the extension of the theory with more realistic boundary conditions in an attempt to make it applicable to lower temperatures. In particular an explanation is sought of the form of the fall in R_{SNS} between the lowest temperatures and about $0.8T_c$. This, as mentioned in Section 1.3, has been seen by many previous workers as well as in the present work.

The next section examines the deficiencies of the simple theory in more detail. The calculation of the boundary conditions for a step potential is described in Sections 5.3 and 5.4. The calculation of the parameters in the resulting theory and its comparison to the experimental data is discussed in Sections 5.5 and 5.6. Section 5.7 describes the theory using a delta function potential and Section 5.8 discusses its modification to include the proximity effect. Section 5.9 describes the effect of a thin layer of heavy scattering at the interface.

5.2 Deficiencies of the Simple Theory

Fig. 5.1 shows a typical $R_{SNS}(T)$ curve obtained for a In/W/In sample compared to the best fit to (4.3). As is expected from the simplified nature of the boundary conditions, the fit to the experimental data is poor below about $0.8\ T_c$. The theory curve continues to fall steadily as the temperature is decreased. This reflects the decreasing number of electrons above the gap which reduces the amount of Q* generated in S and therefore the resistance. The experimental curve, however, levels out and begins to rise again as the temperature is decreased. This rise shows signs of levelling out again at the lowest temperatures at which data were

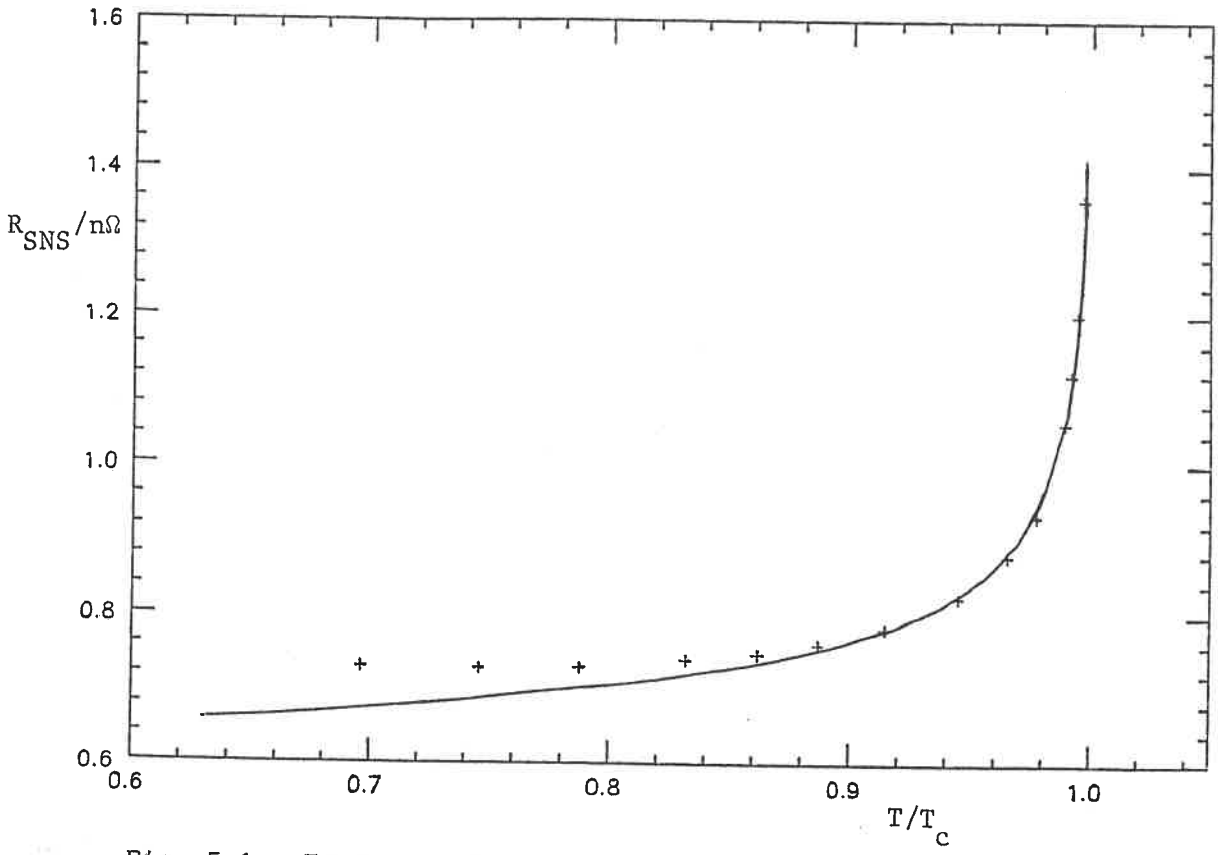

Fig. 5.1 Experimental $R_{SNS}(T)$ Curve Compared to Best Fit using Simple Theory.

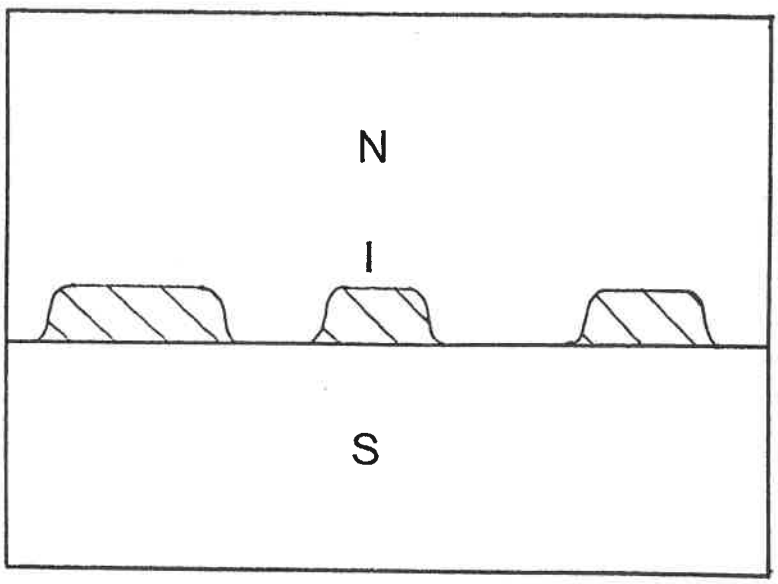

Fig. 5.2 Hardings Model of Imperfect SN Interface.

taken.

Harding (1973) explained the low temperature behaviour by a model in which only part of the interface consists of SN contact (Fig. 5.2). The rest of the interface has a layer of insulator (probably oxide) between N and S which acts as a tunnel barrier. The total resistance of the interface, therefore, is that of "perfect" SN interfaces in parallel with tunnel junctions whose resistance increases quickly as the temperature is decreased. By assuming that the tunnel barrier had the BCS zero bias tunneling resistance Harding was able to obtain reasonable fits between this model and his data. This may be criticised, however, because the assumed structure does not seem very likely; if there is significant oxide in some regions of the interface, it is questionable that other areas would be perfectly clean. A theory in which the low temperature behaviour is explained by an imperfect interface of some sort over the whole area would seem much more natural. As mentioned by Harding simple tunnelling theory is not able to explain the relatively slow change in $R_{SNS}(T)$ at low temperatures without assuming some areas of perfect contact.

The aim of the calculations described in this chapter, therefore, was to develop more realistic boundary conditions for the interface. In particular two points are worth noting:

1. The fundamental assumption of the Battersby and Waldram theory, $R_N=0$ is clearly not valid. This assumption leads to the conclusion that the only source of interface resistance is Q* above the gap which implies that the interface resistance at low temperatures is negligible. In fact all workers to date, including the author, have seen appreciable interface resistance at the lowest temperatures at which data was taken. The fact that R_{SNS} falls with increasing temperature at low temperatures in the experimental data confirms that another resistance producing mechanism must be in operation, associated with a non zero R_N.

2. As the temperatures now under consideration extend to well below

T_c, the second approximation in the theory, $R_A=0$ above the gap, must also be discarded. This is because there may now be appreciable numbers of excitations just above the gap which will have a non negligible probability of Andreev reflection. Pippard et al. (1971) introduced an enhanced value of Δ into their theory to take account of this approximately. They multiplied Δ by a factor p at all temperatures and treated p as an adjustable parameter. The best fits to their data used values of p between 1.2 and 1.4. This seems reasonable since at an energy of 1.2Δ the Andreev reflection probability as given by the formula of Andreev (1964) is 0.45. In the theory to be described, however, such approximations as this prove unecessary. The fuller calculations motivated by the need to insert a more realistic form of R_N also give expressions for R_A which reduce to that of Andreev in the limit of a perfect interface.

5.3 Solutions of Bogoliubov Equations in Bulk Metals.

The next section discusses the first attempt to calculate more realistic boundary conditions for the SN interface. This section introduces the simple (bulk material) solutions to the Bogoliubov equations which are used in the calculations. The notation given here is that of Waldram (1986).

According to the BCS theory excitations are described by the Bogoliubov amplitudes $u(\mathbf{r})$and $v(\mathbf{r})$. These obey the Bogoliubov equations, first derived by Bogoliubov (1958):

$$Hu + \Delta v = Eu \qquad (5.1)$$

$$-Hv + \Delta u = Ev$$

where

$$H = -(\hbar^2/2m)\nabla^2 + V - \mu$$

V is the "normal" potential and μ the electrochemical potential as before. As the rest of the theory used is one dimensional this calculation is restricted to one dimension. In general, inhomogenous superconductors the solutions are complicated. Here, however, the calculation proceeds by matching relatively simple bulk solutions at a sharp interface. In homogenous materials the solutions are of the form:

$$u(x) = u_0 \exp(i(k_0+k)x) \qquad v(x) = v_0 \exp(i(k_0+k)x) \tag{5.2}$$

where $k_0=+k_F$. Substituting these into (5.1) gives:

$$v_0/u_0 = (E-\varepsilon)/\Delta = \Delta/(E+\varepsilon) \tag{5.3}$$

where $\varepsilon = (\hbar^2 k_0 k)/m$

This means that:

$$E^2=\varepsilon^2+\Delta^2 \tag{5.4}$$

which is the usual BCS result. The following simple solutions hold:

(i) In N $\Delta=0$, $u_0=1$, $v_0=0$ for electrons and $v_0=1$, $u_0=0$ for holes.

(ii) In S for $E>\Delta$, (5.4) implies ε is real. $u_0=u_B$, $v_0=v_B$ for electron like excitations and $u_0=v_B$, $v_0=u_B$ for holes where u_B and v_B are the usual BCS u and v. (ie $u_B^2=(1+\varepsilon/E)/2$ and $v_B^2=(1-\varepsilon/E)/2$). The solutions, as in N are running waves. k_0 and k can both be either positive or negative which correspond to the four branches on the excitation spectrum.

(iii) In S for $E<\Delta$ (5.4) implies that ε and hence k are both imaginary The solutions in this case are therefore either decaying or growing slightly evanescent waves with:

$$k=+i(\Delta^2-\varepsilon^2)^{-0.5}/\hbar v_F \qquad (5.5)$$

In this case (5.3) can be written:

$$v_0/u_0 = \Delta/(E+i\varepsilon_o) = e^{+i\phi} \quad , \quad \varepsilon_o=(\Delta^2-\varepsilon^2)^{0.5} \qquad (5.6)$$

so that $\phi = \cos^{-1}(E/\Delta)$

also define: $u_B' = 1/\sqrt{2}$ and $v_B' = (1/\sqrt{2})e^{-i\phi}$

Following the notation of Harding et. al. (1974) the evanescent modes are classified as either A modes which decay in the same direction as k_0 (in 1D this means that k_0 has the same sign as k) or B modes which grow in the direction of k_0. Superscript + or - indicate the sign of k_0. In the present problem it is assumed that x<0 is N and x>0 is S. Clearly when matching solutions at the interface, solutions which grow into S can be neglected since they are unphysical. The only solutions of interest in the present problem are therefore A^+ for which $u_0=u_B'$, $v_0=v_B'$ and B^- for which $u_0=v_B'$ and $v_0=u_B'$.

5.4 Calculation of Boundary Conditions for Step Potential.

The first calculation of the boundary resistance, assumed the simple potential illustrated in Fig. 5.3. Δ and V are both assumed to have steps at x=0. The step in V will tend to reflect excitations normally. It is hoped that this will adequately represent the non zero R_N which is observed in real interfaces. The step is represented by the parameter γ which is defined as the ratio k_{FS}/k_{FN}.

The calculation proceeds in the same way as the usual quantum mechanical calculations of reflection and transmisson coefficients. It is described below. The algebra, which is tedious but not difficult, is not

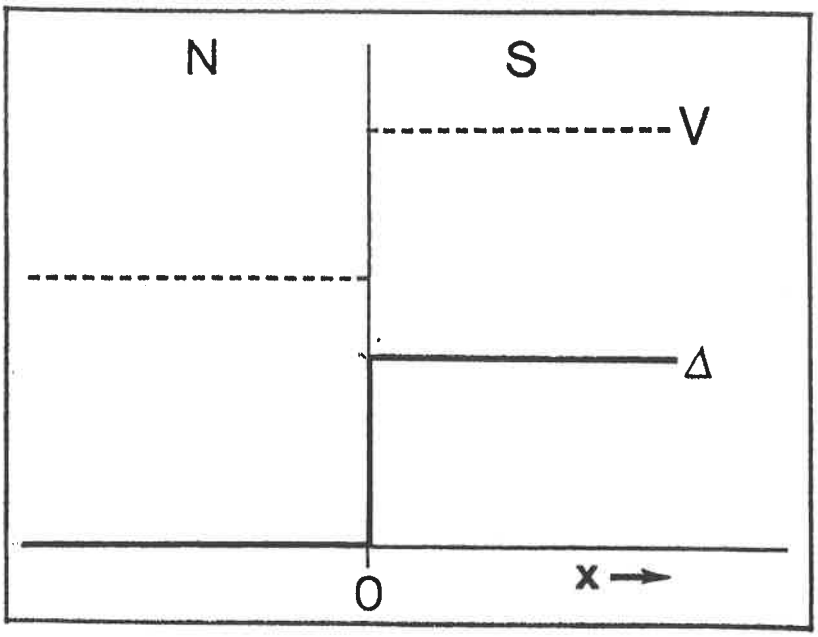

Fig. 5.3 Illustration of Model Potentials Used in Mismatch Theory.

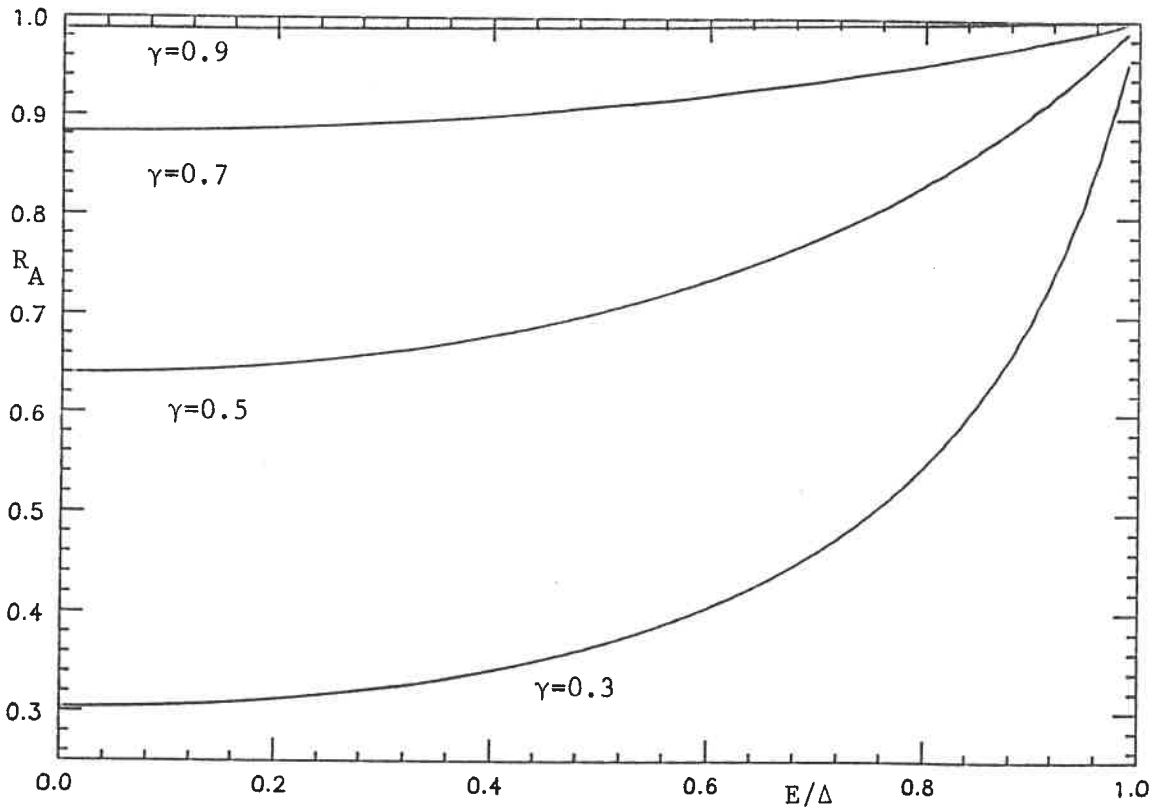

Fig. 5.4 $R_A(E)$ For Several Values of γ.

reproduced.

(i) The total wave function is written down on either side of the interface. The incoming electron wave is assigned amplitude unity. The Andreev and normally reflected waves in N are given amplitudes r_A and r_N respectively. In S above the gap the transmitted holes and electrons are given amplitudes t_A and t_N. Below the gap the A^+ and B^- modes are given amplitudes t_{A+} and t_{B-}.

(ii) The wavefunctions and their slopes are set to be continuous across the interface. This results in 4 equations (the wave functions have two components, u and v) both above and below the gap.

(iii) These equations are solved to give expressions for r_A, r_N, t_A and t_N in terms of γ and E.

(iv) The amplitude reflection and transmission factors thus obtained are converted to flux amplitudes, denoted by R_A, R_N, T_A, T_N as before. This is done by multiplying them by their complex conjugates. In the case of the transmission coeficients they also need to be multiplied by $\gamma v_S/v_N$ where the v's denote excitation velocities.

The results obtained in this way by Waldram (1986) were:

for $E>\Delta$:

$$R_N = (\varepsilon/E)^2(1-\gamma^2)^2/D$$

$$R_A = 4(1+\varepsilon/E)(1-\varepsilon/E)\gamma^2/D \qquad (5.7)$$

$$T_N = 2(1+\gamma)^2(1+\varepsilon/E)\gamma(\varepsilon/E)/D$$

$$T_A = 2\gamma(1-\gamma)^2(1-\varepsilon/E)(\varepsilon/E)/D$$

where $D = [u_B^2(1+\gamma)^2 - v_B^2(1-\gamma)^2]^2$

for $E<\Delta$:

$$R_A = [1 + (A-1)(1-(E/\Delta)^2)]^{-1}$$

$$R_N = 1 - R_A \qquad (5.8)$$

where $A = (1+\gamma^2)^2/4\gamma^2$

Several points about these results are worth mentioning:

1. The particle conservation relations, $R_A+R_N+T_A+T_N=1$ above the gap and $R_A+R_N=1$ below it are obeyed.

2. The relation derived in Appendix A of Battersby and Waldram (1987) by assuming electron-hole symmetry, $R_AR_N=T_AT_N$ is obeyed above the gap. Below the gap where $T_A=T_N=0$ it breaks down. This is probably related to the fact that the interface is not idealy thin as was assumed by Waldram.

3. If $\gamma=1$ is put into these results (ie no mismatch), the expected results are regained: $R_A=1$ below the gap and has form of Andreev (1964) above, $R_N=0$ at all energies.

4. For $\gamma \neq 1$ (5.8) implies that $R_A=1$ for $E=\Delta$ but decreases as E is reduced. $R_A(E)$ is plotted for several values of γ in Fig. 5.4. This is important since it provides a mechanism for the fall in resistance observed from 0.3 to $0.8T_c$. As the temperature is increased in this range the average energy of the excitaions increases and there are therefore more excitations with lower values of R_N.

5.5 Calculation of Parameters

Before the boundary conditions (5.7) and (5.8) could be used in the basic theory (A1.3), it was necessary to consider the values of the other parameters in the theory. As can be seen from (A1.3) these are $(\ell/\lambda_2)^N$, $(\ell/\lambda_2)^S$ and $(\ell/\lambda_3)^S$. The comments of Section 4.2 about the absolute values

of parameters need to be remembered here. It turns out, however, that the results obtained from this model are only weakly dependent on the values of λ_2. $(\lambda_2)^N$ is found to be larger than the thickness of N and $(\lambda_2)^S$ is not relevant except near T_c where the value of λ_3 is much more critical. The approach which has therefore been adopted is to estimate ℓ_2 from independent results and leave the magnitude of ℓ_3 as an adjustable parameter. This theory is the same in this respect as the simpler ones which were described in Chapter 4.

The value of $(\ell/\lambda_2)^N$ was estimated using thermal conductivity data. In N $\lambda_2=(\ell\ell_2)^{0.5}$, if the material is very pure so that $\ell=\ell_2$ (ie no elastic scattering by impurities) then $\lambda_2=\ell_2$. λ_2 can therefore be taken as the mean free path for thermal conduction of ideally pure material. This was obtained, for W (at T_c for In), from the thermal conductivity data of Wagner et.al. (1971). and found to be about 4×10^{-4}m. This is however longer than the thickness of the W slice, typically 3×10^{-4}m. In these circumstances, as shown by Pippard et.al. (1971), λ_2 must be taken as $\lambda_2\tanh(d/2\lambda_2)$ where d is the thickness of the W (which tends to d/2 for $\lambda_2>>d$). This means that in this case λ_2 needs to be taken as about 1.45×10^{-4}m. ℓ for the W used was calculated from the dipstick resistance ratio measurements described in Section 3.6 and was found to be typically 10^{-4}m. $(\ell/\lambda_2)^N$ was therefore estimated to be 0.7 and this was the value assumed for the calculations in the rest of this thesis. This value is nearly independent of temperature because λ_2 is greater than d for all temperatures of interest. It should be noted that this estimate is in agreement with the very approximate estimate of this quantity mentioned in Section 4.5.

The estimation of $(\ell/\lambda_2)^S$ is more complicated because in S both ℓ_3 and ℓ_2 are finite and temperature dependent. In addition the temperature dependence of λ_2 needs to be taken into account in this case. ℓ_2 for In was calculated in the same way as described above for W. The thermal

conductivity data used was that of Guenault (1960). The result found was $\ell_2=2\times10^{-3}/T^3m$. ℓ_2 therefore increases quickly with falling temperature which reflects the falling number of phonons available to be involved in inelastic processes. This form of ℓ_2 is plotted in Fig. 5.5. ℓ_3 is plotted twice on the same graph, both curves have been calculated assuming the Waldram temperature dependence (Section 4.6). The lower curve assumes that $\ell_3{}^0$ has the value implied by the simple theory (Section 4.4) and the upper that it has the value implied by the fits of the experimental data to the mismatch theory described in the next section. λ_2 for the In was therefore calculated from these forms of ℓ_2 and ℓ_3 (using the definition given in Section 4.3).

5.6 Comparison of Mismatch Theory with Experiment

Once reasonable values for the parameters $(\ell/\lambda_2)^{S,N}$ had been calculated theoretical curves for $R_i(T)$ were calculated by inserting the boundary conditions (5.7), (5.8) into (A1.3). These curves were generated by numerically integrating to calculate the W_i factors using a BBC microcomputer. In order to do the integration, the reflection and transmission factors (5.7) were put into (A1.9) and (A1.6) to obtain rather complicated expressions for u_{1-4} in terms of E and γ for $E>\Delta$. These expressions are given, for reference, in Appendix 2. The subgap boundary conditions are much less complicated and an expression for P(E) was obtained from (A1.10) and u_1 calculated from this in the program.

There were 4 adjustable parameters in this theory. R_W, the non temperature independent resistance of the sandwich was adjusted so that the theoretical and experimental curves had the same value at the minimum. Since this theory includes mismatch at the interface it seems likely that R_W should now be simply the resistance of the slice of W. Unfortunately this quantity was not easy to measure directly in the present work for reasons mentioned in Chapter 3. $\ell_3{}^0$ and T_c were adjusted, as before, so

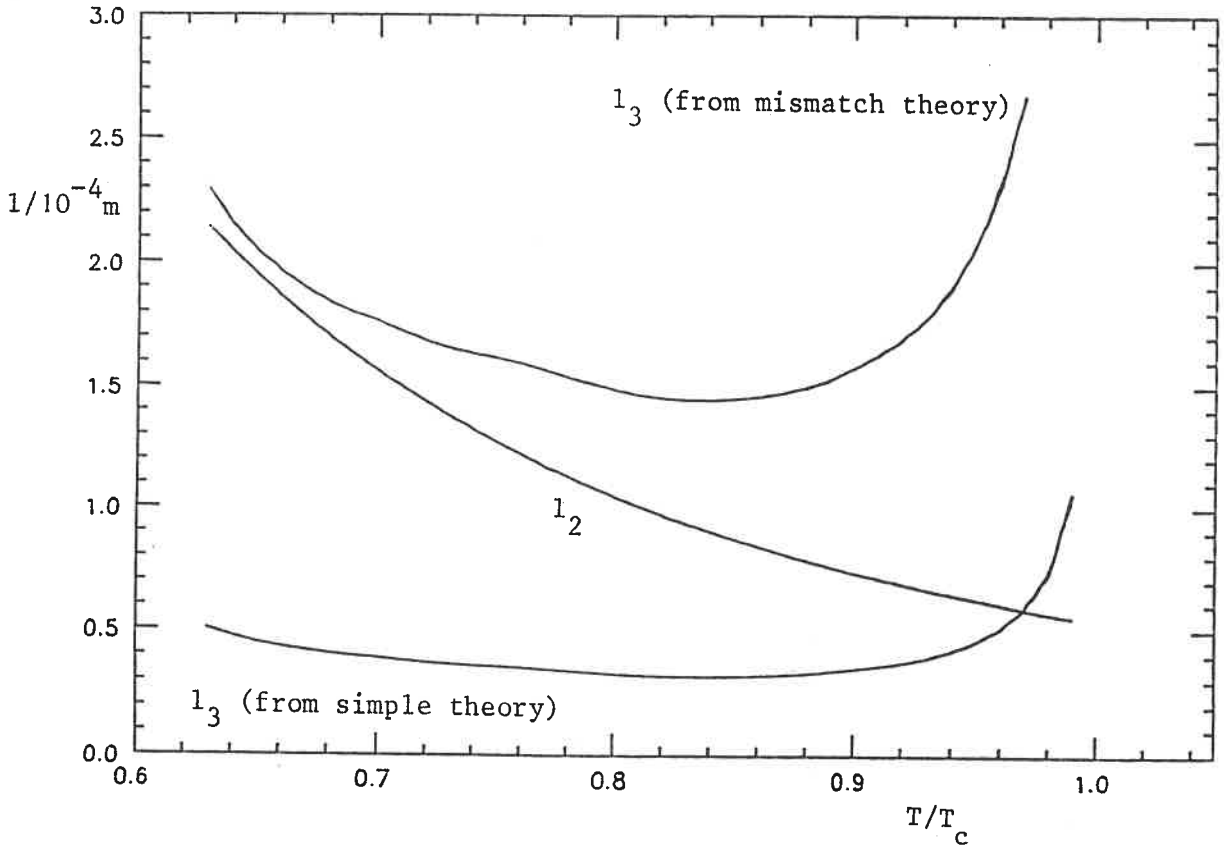

Fig. 5.5 Calculated Forms of l_2 and $l_3(T)$ for In.

that the theoretical fit to the divergence below T_c was a good fit to the data. γ was adjusted so that the size of the decrease in the resistance from low temperatures to the minimum was correct. It should be noted therefore that, although there are 4 adjustable parameters, each one of them corresponds to an independent characteristic of the system.

Typical fits to the experimental data with this theory are given in figs 5.6 and 5.7. It can be seen that it fits well from the minimum in the curve up to T_c. At low temperatures, however, the fit is not very good. The experimental curve shows signs of levelling out as the temperature is reduced below about $0.6T_c$ whereas the theoretical fit has the opposite curvature. The reason for the poorness of the fit at low temperatures is discussed in Section 5.8. The values of ℓ_3° and γ found for the best fits to the data for four samples are given in Table 5.1.

Table 5.1

Sample No.	ℓ_3° 10^{-4}m	γ
91	1.4±0.1	0.315
97	1.0±0.1	0.305
98	1.4±0.1	0.325
99	1.4±0.1	0.325

The large errors quoted for ℓ_3° in this case reflect the fact that the magnitude of the divergence below T_c is only a fairly slow function of ℓ_3°. This is expected because the important quantity is λ_3 which depends on $\sqrt{\ell_3}$. The values of ℓ_3° are again found to be fairly constant from sample to sample. In this case, however, the values are about a factor of six higher than those found by the simple theory described in Section 4.4. (They are also about a factor of five higher than the theoretical estimate given in Section 4.6, though as mentioned in that section this should not be taken too seriously). It is easy to see the physical reason for this

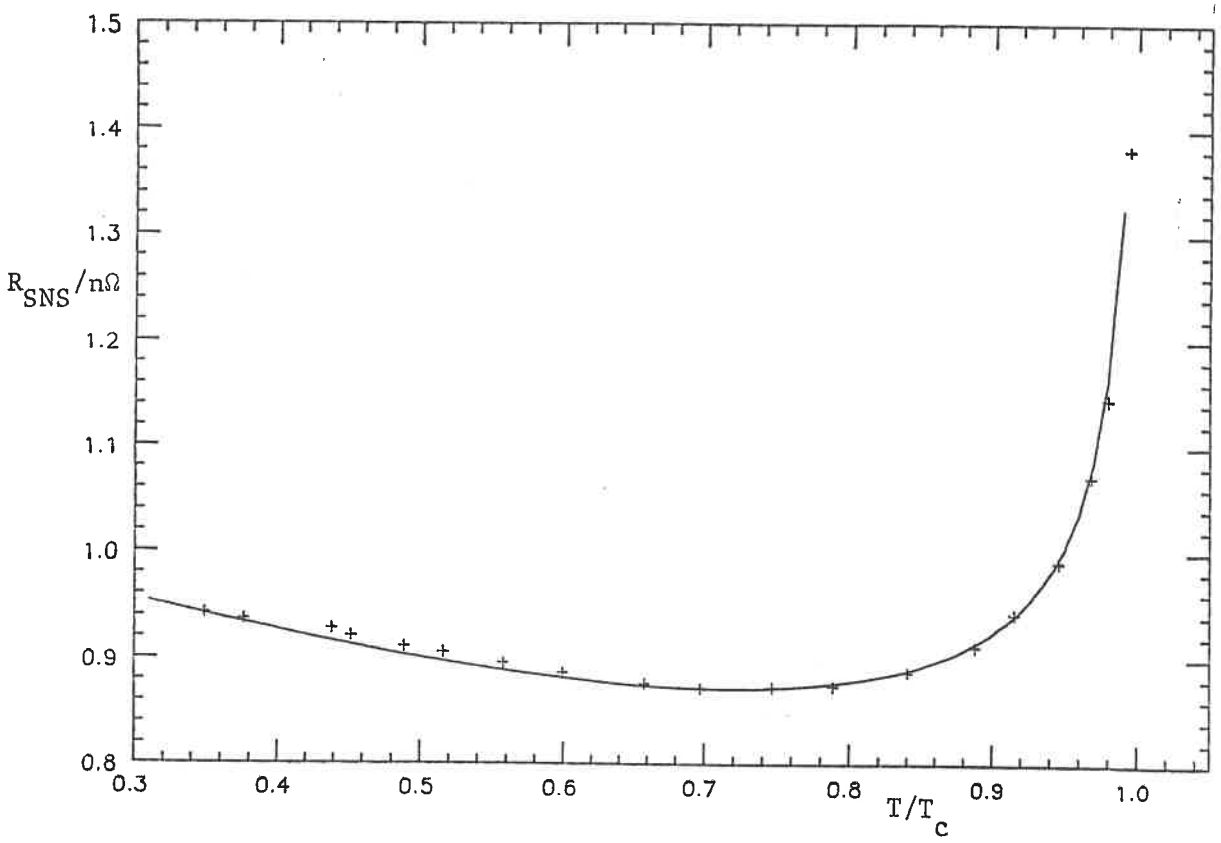

Fig. 5.6 Fit of Mismatch Theory to $R_{SNS}(T)$ of Sample 97.

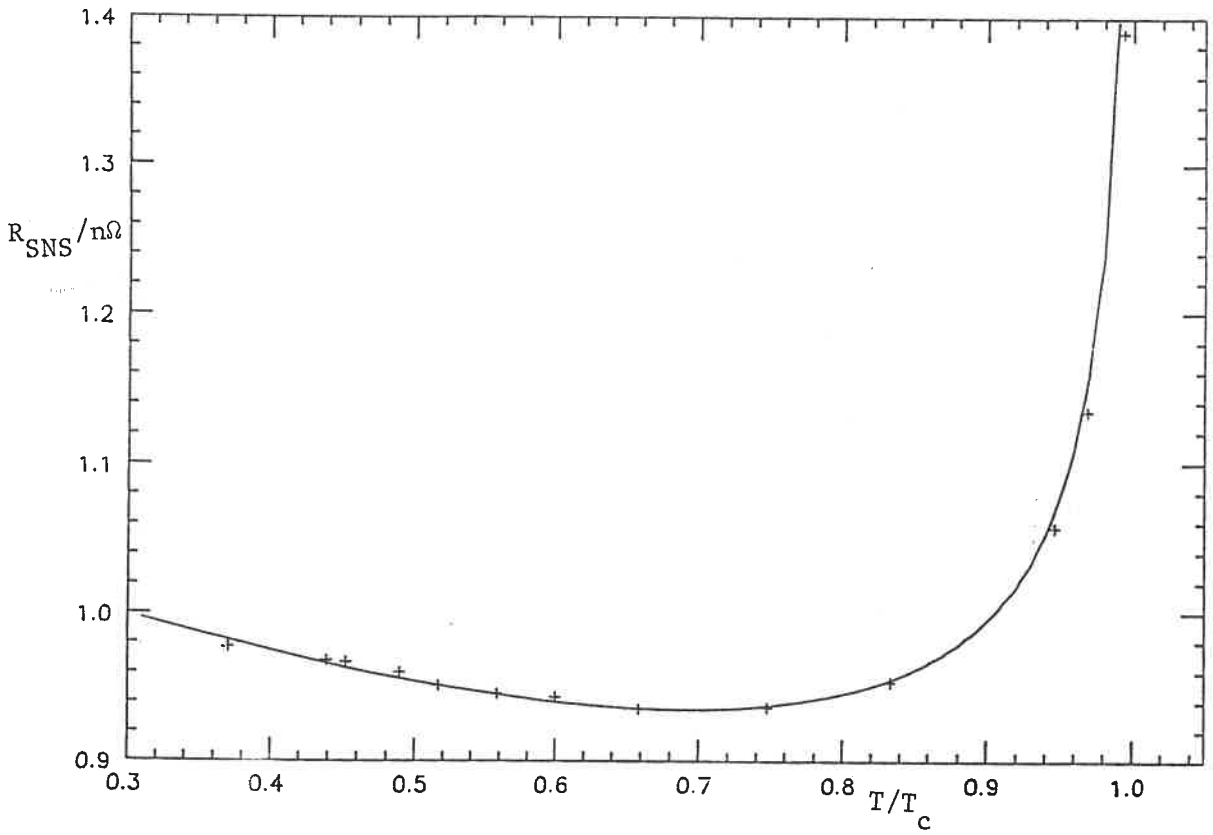

Fig. 5.7 Fit of Mismatch Theory to $R_{SNS}(T)$ of Sample 99.

difference. In this model there is a finite R_N which means that less supergap excitations penetrate into S. Just below T_c, where charge imbalance in S is the dominant source of resistance, the only way that the same voltage can be generated is to assume that ℓ_3 is longer. This means that the same Q* can be set up at the interface even though less excitations are entering S.

The values of γ vary significantly from sample to sample. It should be noted that the low temperature behaviour is sensitive to the value of γ; the fall in resistance from low temperatures to the minimum, in the data quoted, ranges from 0.041nΩ in sample 99 to 0.070nΩ in sample 97. This tallies with the conclusions of previous workers that the low temperature behaviour is very sensitive to the amount of dirt etc. on the interface, which would be expected to differ from sample to sample. The major critisism which can be made of this model is that the non zero R_N is due to mismatch between the Fermi wavevectors of N and S. This is a fundamental property of N and S and would not be expected to vary from sample to sample. This model strictly represents a perfect interface between the two metals. The fact that γ is observed to vary significantly from sample to sample and that a fairly low value of γ needs to be used implies that the present samples were not ideally clean. A model in which there is a scattering potential at the interface only is therefore deiscussed in the next section. The question of making theoretical estimates of the value of γ from a knowlege of the Fermi surfaces of W and In is difficult since W has an extremely complicated Fermi surface.

5.7 Imperfect Interface Theory.

This theory was developed in order to avoid the critisism of the mismatch theory mentioned at the end of the last section. In this case the potentials are assumed to be as illustrated in Fig. 5.8. Δ as before is assumed to be a step function. V is assumed to have the form $V(x) = f\delta(x)$,

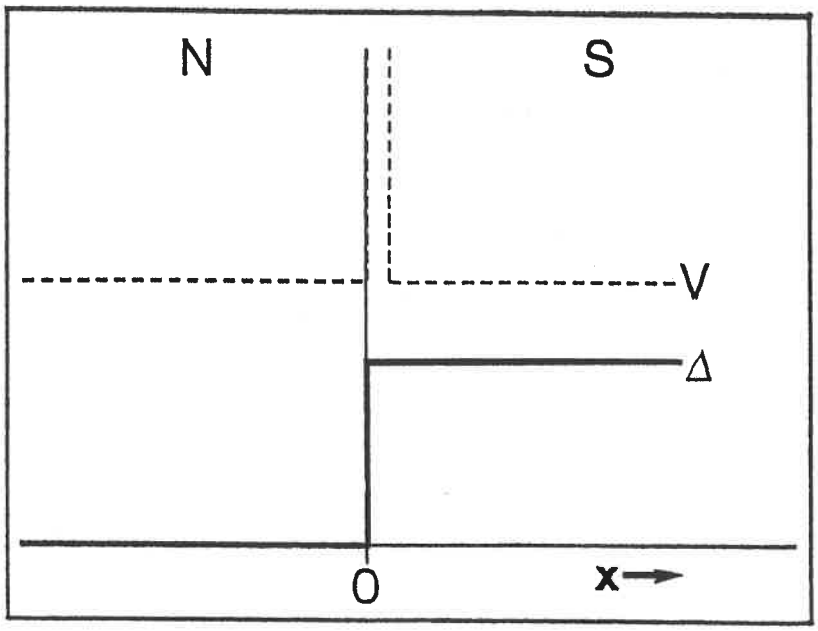

Fig. 5.8 Illustration of Model Potentials Used in Imperfect Interface Theory.

which is the form assumed by Tomlinson (1973). The delta function V represents dirt, etc. at the interface. This theory is in this sense the opposite of the mismatch one. The finite R_N is now assumed to be entirely due to imperfections of the interface whereas before it was assumed to be entirely due to intrinsic mismatch. The real situation is somewhere between the two; comparison is therefore of interest.

The theory now proceeds in a similar way to that described in Section 5.4 for the mismatch theory. The algebra is rather more complicated since there are now three regions and two boundaries at which the wavefunctions and their derivatives are to be matched. Only at the end of the calculation is the top hat function of V allowed to tend to a delta function. The results of the theory below the gap were obtained from Tomlinson (1973) while above the gap they were calculated by the author.

The results thus obtained are given below:

For $E>\Delta$:

$$R_N = F^{-1}[a^4+4a^2]$$

$$R_A = F^{-1}[16b(1-b)^{-2}] \qquad (5.9)$$

$$T_A = F^{-1}[2a^2(1-\varepsilon/E)(E/\varepsilon)]$$

$$T_N = F^{-1}[2(1+\varepsilon/E)(E/\varepsilon)(4+a^2)]$$

where $F = [4(1-b)^{-1}+a^2]^2$, $a=2mf/\hbar^2k_F$

and $b = (v_B/u_B)^2 = (1+\varepsilon/E)/(1-\varepsilon/E)$

For $E<\Delta$:

$$R_A = [1 + (4R/(1-R))(1-(E/\Delta)^2)] \qquad (5.10)$$

$$R_N = 1 - R_A$$

where $R = a^2/(4+a^2)$

The important point here is that the expression for R_A below the gap is of the same form as (5.8) which was obtained using the mismatch theory. In order to convert one to the other the parameter A involving γ must be replaced by R, involving a, according to

$$A-1 = 4R/(1-R) \qquad (5.11)$$

This means that well below T_c the two theories will give the same results. In particular the fit to the fall in R_{SNS} from the lowest temperatures to the minimum will not be any better with this theory than it was with the mismatch theory. The expressions above the gap are different, however, so that differences may be expected close to T_c. The new expression for R_A, however, still tends to that of Andreev in the case of a perfect interface, a=0.

This theory was fitted to the data in the same way as the mismatch one. The functions u_{1-4} derived are again given in Appendix 2 for reference. Two examples of fits to experimental data using this theory are given in figs 5.9 and 5.10. It can be seen that again the fit below T_c is good and, as expected, the low temperature fit is no better than before. The values of $\ell_3{}^\circ$ and a for the best fits are given in Table 5.2. The values of $\ell_3{}^\circ$ are even greater than those required in the mismatch theory. They are now about a factor of 20 greater than in the simple theory discussed in Section 4.4. However it should again be remembered that the physically important quantity (which is proportional to the resistance generated by the Q*) is λ_3 which goes as $\sqrt{\ell_3}$. λ_3 in this case will,

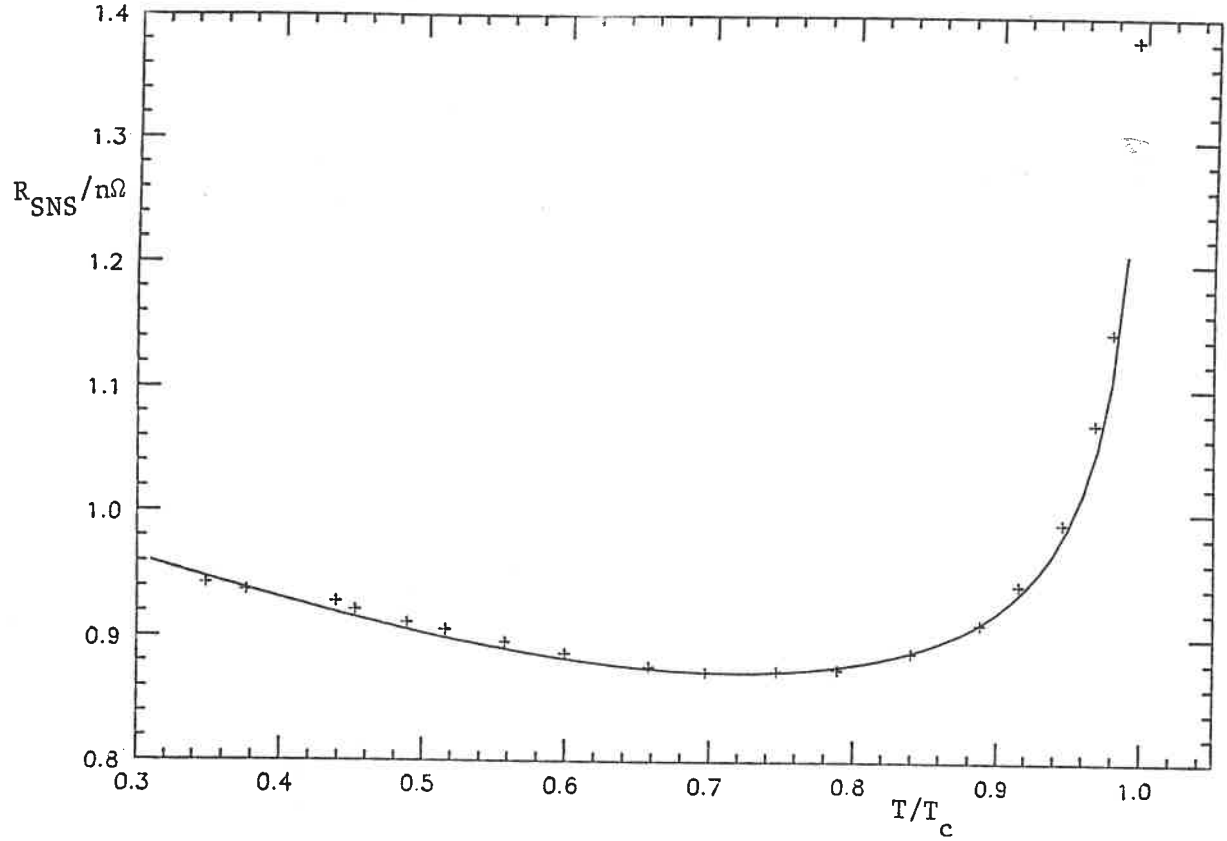

Fig. 5.9 Fit of Imperfect Interface Theory to $R_{SNS}(T)$ of Sample 97.

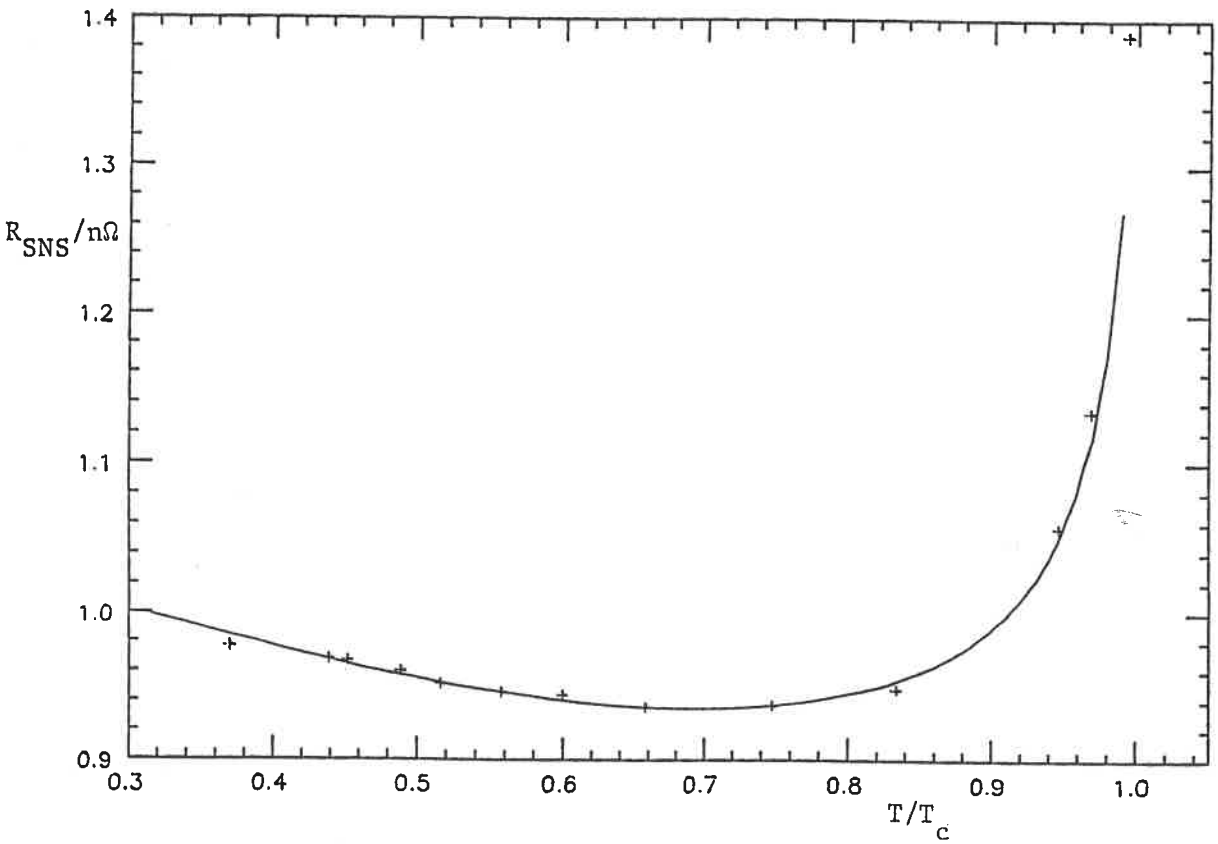

Fig. 5.10 Fit of Imperfect Interface Theory to $R_{SNS}(T)$ of Sample 99.

Table 5.2

Sample No.	$\ell_3 \circ 10^{-4}$m	a
91	4±0.6	1.45
97	3±0.6	1.53
98	4±0.6	1.40
99	4±0.6	1.40

therefore, only be about a factor of 4.5 greater than in the simple case. The values of a obtained for the best fits are in all cases close to those implied by (5.11) and the fits to the mismatch theory (Table 5.2). These results confirm that, as expected, this theory is essentially the same as the mismatch one at low temperatures. The reflection and transmission factors obtained above the gap are different, however, and this leads to differences in the magnitude of the divergence below T_c.

5.8 Proximity Effect Calculation.

This section discusses attempts to improve the fit of the theories to the data at low temperatures. As discussed above, in the range 0.3 to $0.6T_c$ the theoretical curves are found to have the wrong curvature (Fig.s 5.6 etc.). Fig. 5.11 shows curves generated by the mismatch theory, for two values of γ, including the temperature range right down to 0K. It can be seen that as the temperature is reduced towards 0K the R(T) curve does start to level out below about $0.3T_c$. This is to be expected since all the temperature dependent parameters in the theory ($\Delta(T)$, f' etc) become constant at low enough temperatures. The experimental data shows signs of becoming constant at a much higher temperature, i.e. below about $0.6T_c$. The discrepancy is therefore more a question of scale rather than form.

Much better fits to the experimental data at low temperatures have been obtained by including the effect of a non zero Δ extending into the W, the proximity effect. It will be shown that when the magnitudes of the

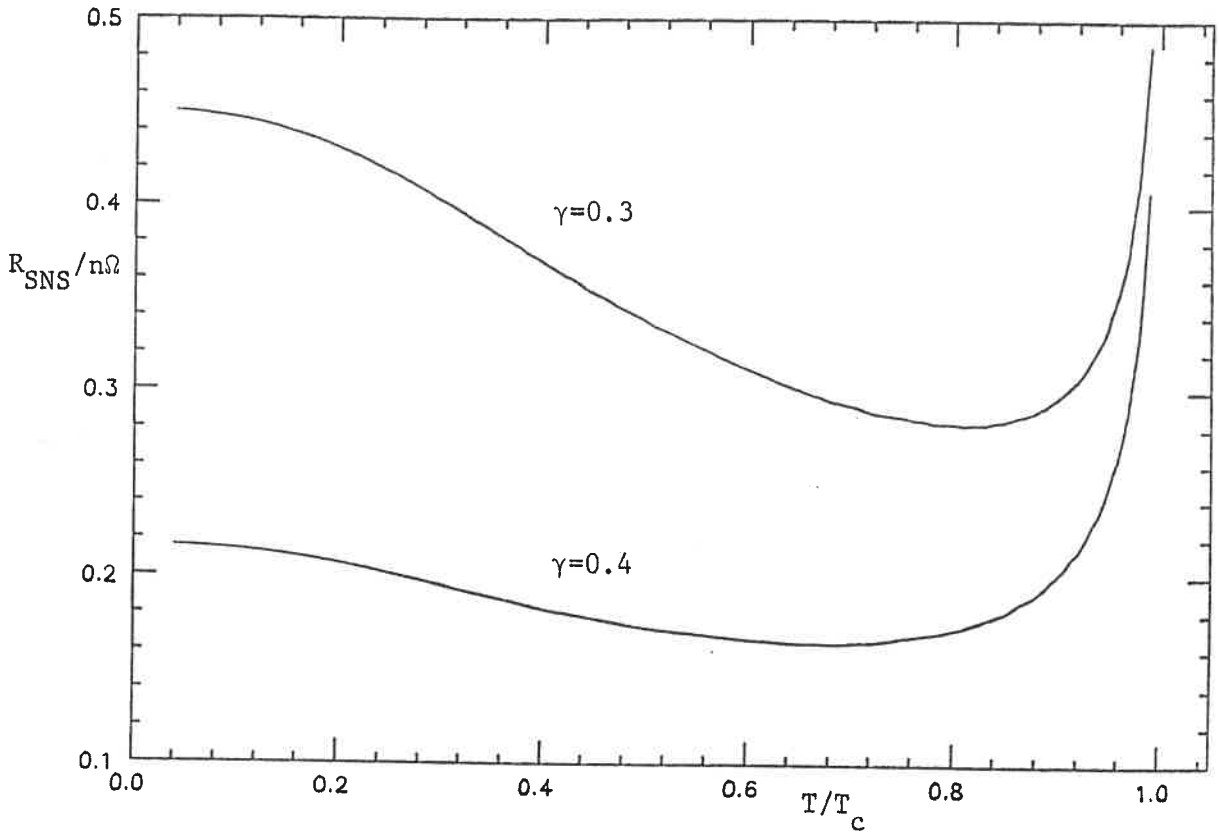

Fig. 5.11 Mismatch Theory Curves down to 0K.

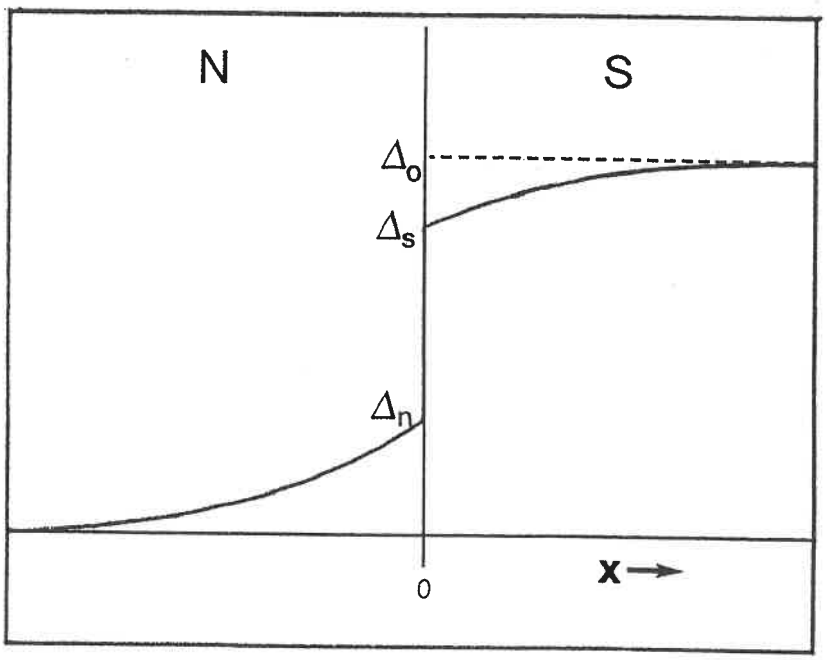

Fig. 5.12 Form of Δ(x) at the Interface.

quantities concerned are considered, this is expected to be a significant effect in In/W. The general form of Δ in the region of the interface is illustrated in Fig. 5.12. In S, Δ is pulled down from its bulk value, Δ_o, close to the interface and has a value Δ_S on the S side of the interface. At the interface there is a discontinuous change in Δ to Δ_N. In W Δ decays approximately exponentially with a decay length k_N^{-1}.

The effect of the tail of Δ extending into N is that excitations of energies less than Δ_N are Andreev reflected some distance inside N rather than at the physical interface. This means that in the present models the potential step in V at the interface no longer directly affects the normal excitations but instead only interacts with the evanescent modes. It is easy to see physically that the result of this must be to diminish R_N. In the extreme case, if the potential step was many times the evanscent decay length from the point of reflection, R_N would be zero since perfect Andreev reflection would take place. The effect on R_N will be important if K_N^{-1} is large enough for the evanescent modes to decay significantly between the point of reflection and the interface. This effect in which the boundary conditions are altered by the scattering of evanescent modes is very similar to the effects discussed in the next chapter with dirty superconductors.

It should be noted that this is a different effect from that discussed by Clarke (1972) which occurs even if R_N is assumed to be always zero and relies on K_N^{-1} being a sizeable fraction of the thickness of the foil; it turns out to be completely negligible in this case.

K_N^{-1} was calculated from the result of Hook and Waldram (1973) in the clean limit. This was:

$$K_N^{-1} = 0.42\hbar v_F/\pi k_B T \qquad (5.12)$$

Inserting values for In leads to the result $K_N^{-1}=2.5\times10^{-7}/T$ m. So at the lowest temperatures at which data was taken K_N^{-1} will be about 2×10^{-7}m.

Estimates can be made of the evanescent decay length close to the interface, using (5.5) and realistic estimates of the size of Δ. These lead to the conclusion that it will typically be about 5×10^{-7}m for zero energy excitations so the effect on R_N is expected to be significant.

In order to calculate the exact effect of the proximity effect on the resistance at low temperatures, estimates also need to be made of the parameters Δ_o/Δ_S and Δ_S/Δ_N which together give the value of Δ_N. The former was calculated using the boundary condition derived by de Gennes (1964):

$$\Delta_S/\Delta_N = (N_0V)^S/(N_0V)^N \qquad (5.13)$$

Although Hook and Waldram have pointed out that this boundary condition is not very rigorous, it will be used here since it only scales an adjustable parameter in the final theory. N_0V was calculated for In and W from the values of T_c and the Debye temperature using the BCS expression. It is found that the ratio Δ_S/Δ_N is expected to be about three. The ratio Δ_o/Δ_S which gives the extent that Δ is pulled down in S by the interface is harder to estimate. The theory of McMillan (1968) suggests it is approximately two. In view of these uncertainties, two values of the ratio $\Delta_o/\Delta_N(=X)$ were tried in the theory.

The imperfect interface theory described in the last section was modified to include this effect. This was done by using the results of Tomlinson (1973) who did exactly this calculation. The supergap boundary conditions are, of course, unchanged. The subgap ones for $E<\Delta/X$ are modified, as shown in Appendix 2. It should be noted that the function θ represents the total decay of the evanescent wave amplitude from the point of Andreev reflection to the interface. Fig. 5.13 compares curves (for a=1.5) with and without this effect. It can be seen that, as expected, the proximity effect significantly decreases the resistance at low temperatures but has little effect near T_c.

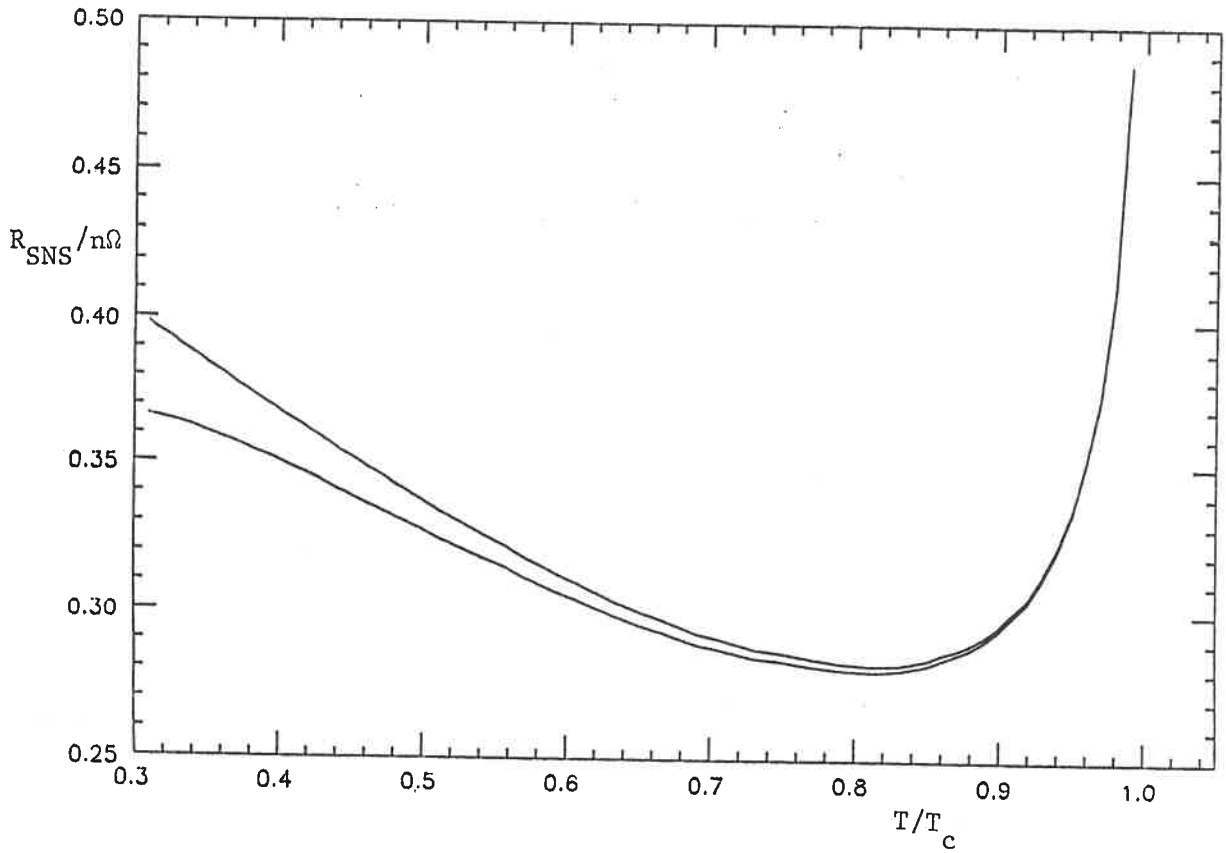

Fig. 5.13 Theoretical Curves With (lower) and Without the Proximity Effect.

The modified theory was fitted to the experimental data. Two values of Δ_o/Δ_N were tried, 3 and 6. The fits are shown in figs 5.14-5.17. In order to balance the depression of the resistance at low temperatures it is found that slightly higher values of a than previously are required for the fits. It can be seen that the fits at low temperatures are much better than in the unmodified theory; the theoretical curves have the correct curvature at low temperatures. It turns out, rather surprisingly, that the $\Delta_o/\Delta_N=3$ curves fit the data better than $\Delta_o/\Delta_N=6$ ones. If (5.13) is taken seriously this implies that Δ is not pulled down significantly in S close to the interface.

It seems, therefore, that the shape of the $R_{SNS}(T)$ curve in In/W/In at low temperatures is strongly influenced by the proximity effect. It would be interesting to extend measurements on this system to lower temperatures. It would be expected that the resistance would be observed to go through a maximum and begin to fall again. This was not tried in the present work through lack of time.

It is worth mentioning that previous low temperature data on Pb/Cu/Pb, in which the proximity effect is definitely negligible (because Cu is not a superconductor), nevertheless also seems to flatten out noticably at the lowest temperatures attainable with a ^{4}He cryostat. There are two reasons for this. Firstly, in Pb Δ/k_BT_c has a larger value than the In (BCS) value. This will make the low temperature flattening out of $R_{SNS}(T)$ predicted in the mismatch theory without the proximity effect (Fig. 5.11) occur at higher values of T/T_c. Secondly, T_c for Pb is higher than for In so the measurements extend to lower values of T/T_c. The flattening out at low temperatures is therefore more likely to be observed. The fact that the proximity effect must be taken into account to produce a good fit of this theory to the In/W/In data does not, therefore, mean that it would not fit Pb/Cu/Pb data without it. Shelankov (1985) has recently reported agreement with low temperature data on Pb/Cu/Pb using a

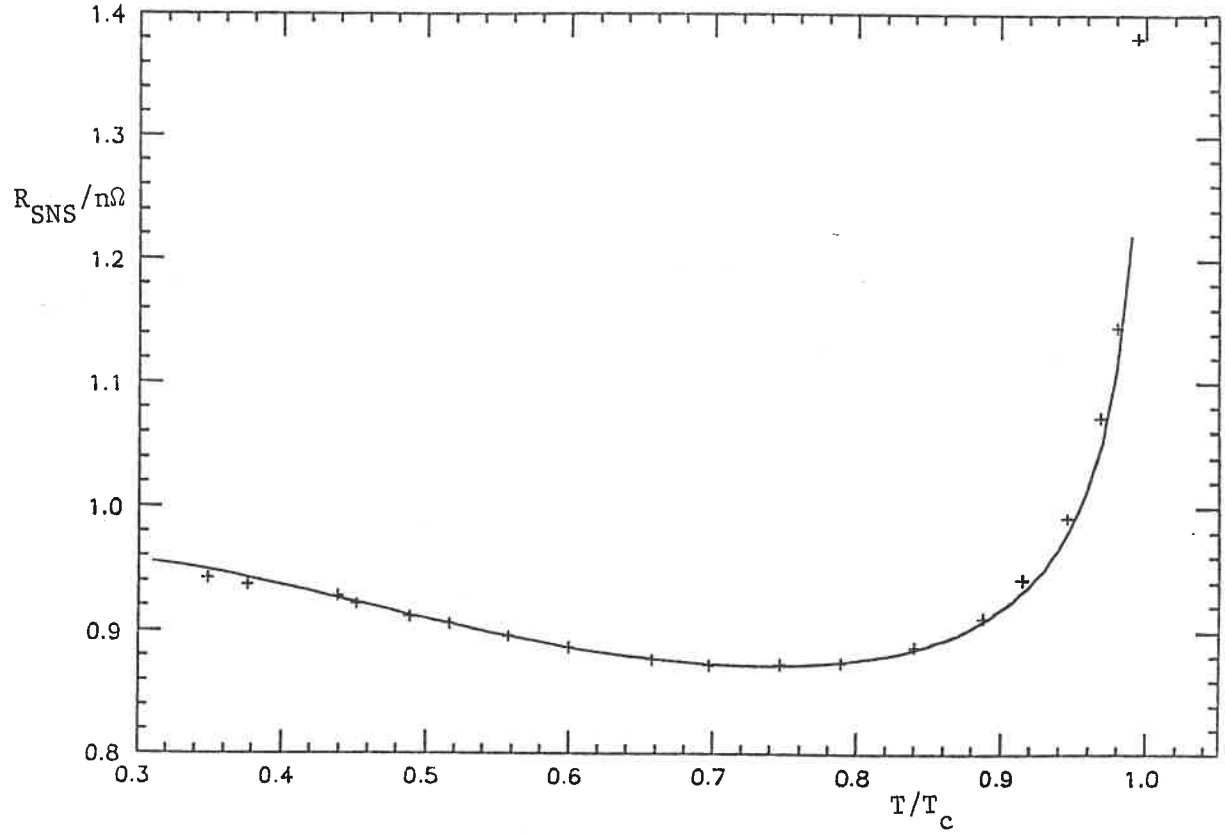

Fig. 5.14 Fit of Proximity Effect Theory with $\Delta_0/\Delta_N=6$ to Sample 97.

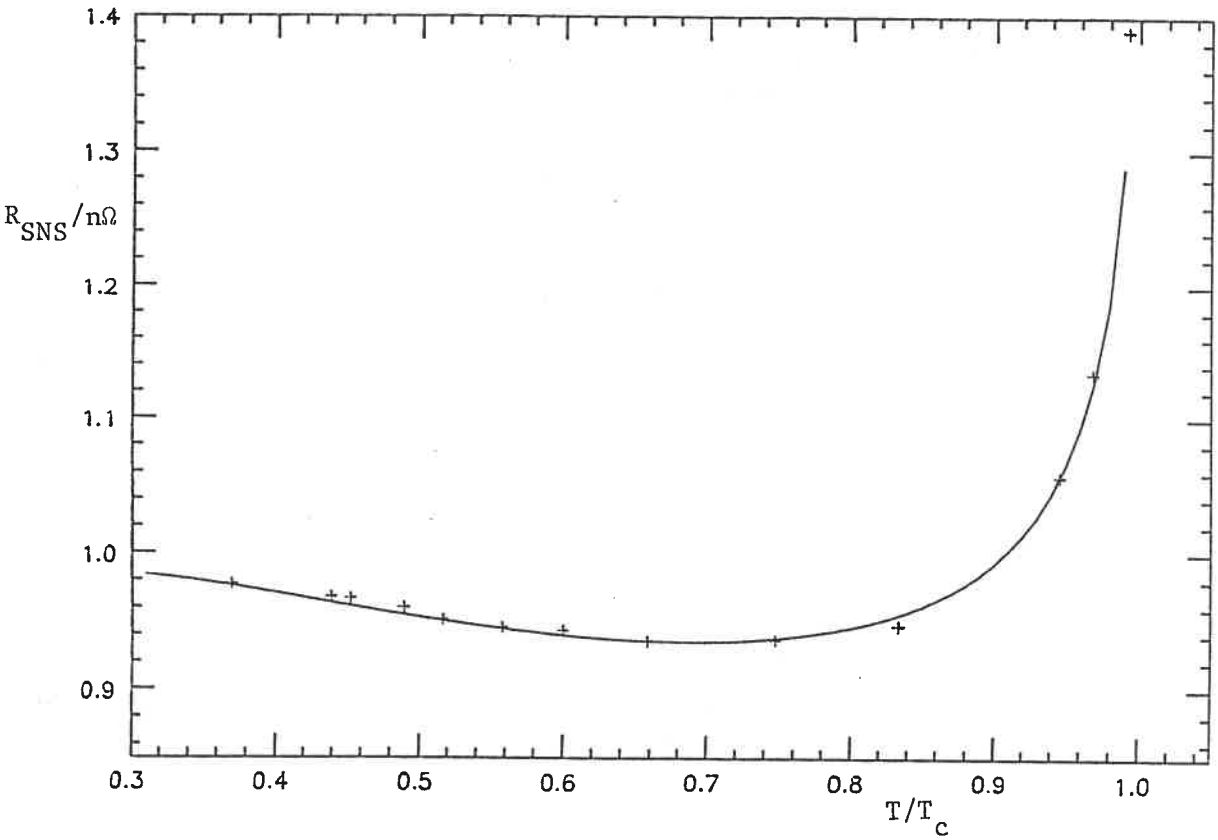

Fig. 5.15 Fit of Proximity Effect Theory with $\Delta_0/\Delta_N=6$ to Sample 99.

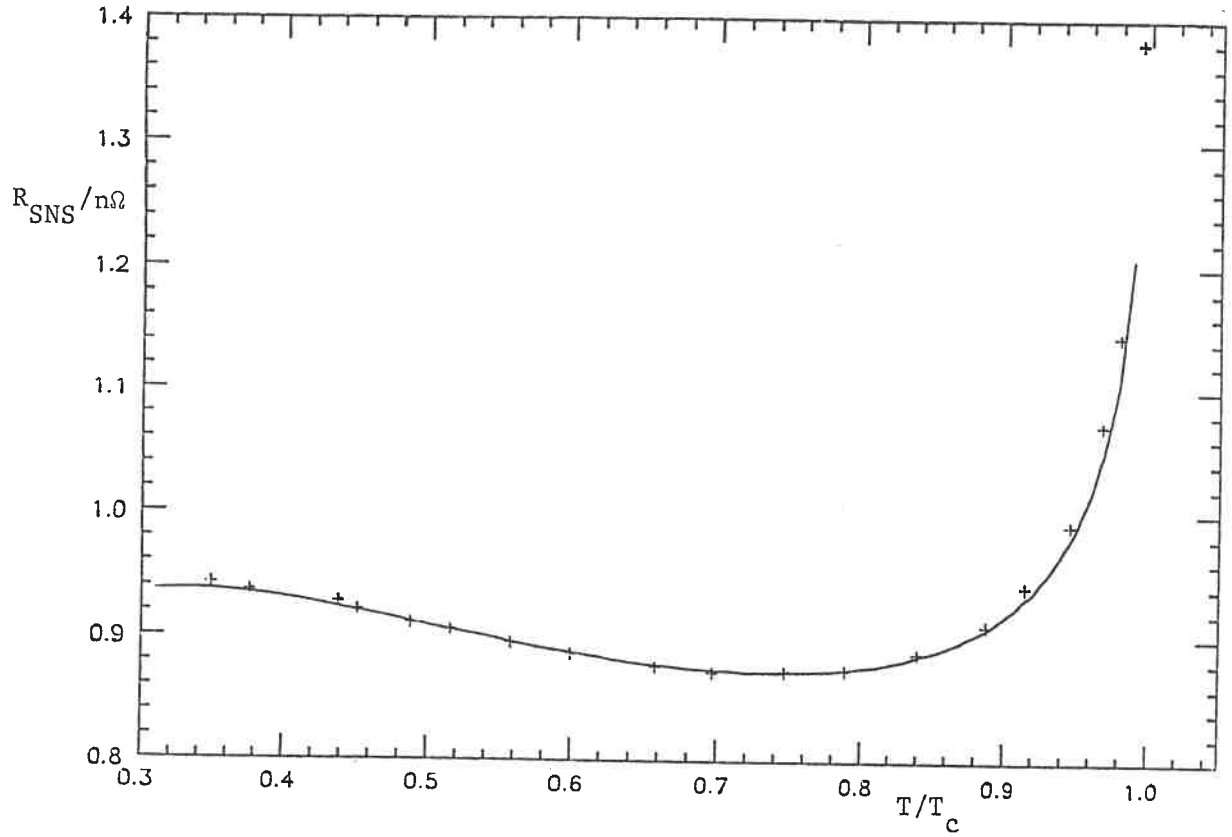

Fig. 5.16 Fit of Proximity Effect Theory with Δ_0/Δ_N=3 to Sample 97.

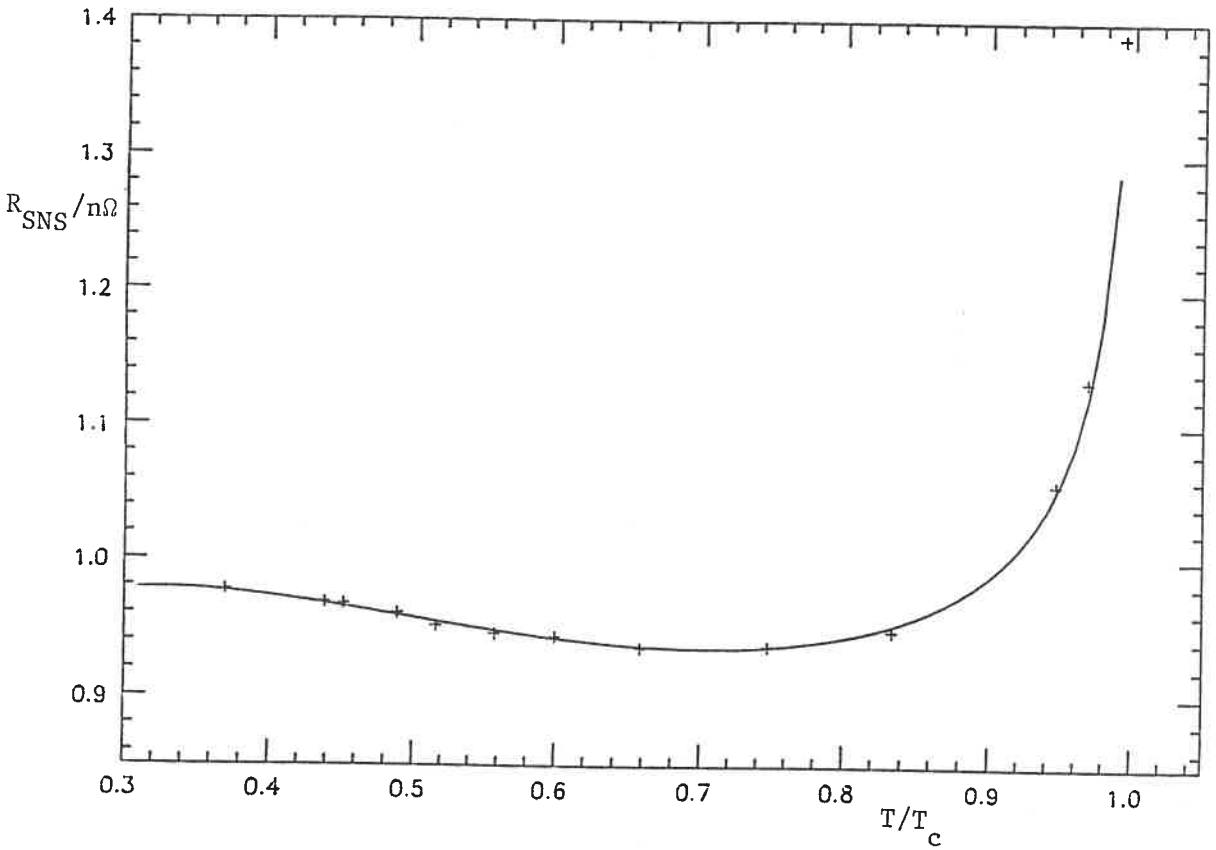

Fig. 5.17 Fit of Proximity Effect Theory with Δ_0/Δ_N=3 to Sample 99.

theory similar to that described here which did not include the proximity effect.

5.9 The Effect of a Scattering layer at Interface.

Pippard et. al. (1971) included a layer of heavy elastic scattering at the interface in their boundary conditions. Such a layer would be expected to be formed if the two metals interdiffused to some extent. Such a layer turns out to be easy to incorporate in the theories discussed in this chapter. This is the subject of this section. The calculation was originally carried out in the hope that it would reduce the discrepancy between experiment and the theories of Sections 5.6 and 5.7 at low temperatures. It did not do this but is worth mentioning nevertheless.

The layer of scattering is assumed to have the resistance of I_B mean free paths in N and to be much thinner than λ_2 and just on the N side of the interface (Fig. 5.18). The boundary conditions of the interface without the scattering layer are denoted by the γs above the gap and P below defined by (A1.1) and (A1.2). The aim of the present calculation is to relate these to the total boundary conditions for the interface, including the scattering layer, denoted by γ's and P'. The values of q and j (as defined in Appendix 1) are similarly denoted q^N, j^N and $q^{N'}, j^{N'}$. Waldram (1975) derives the equations which govern q and j:

$$dj/dx=(q-q_{Q*})/\ell_2+(q+q_{Q*})/\ell_3 \ , \quad dq/dx=j/\ell \qquad (5.14)$$

Since the thickness of the scattering layer is much less than λ_2 $j^N=j^{N'}$. The second half of (5.14) gives the result $q^{N'}=q^N-I_B j^N$. Substituting these relations into the definitions of the boundary conditions (A1.1) gives the required results:

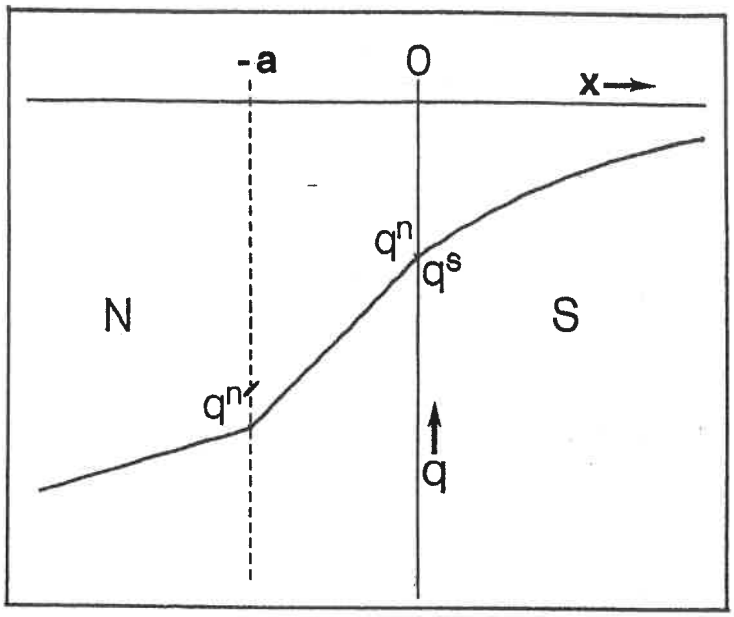

Fig. 5.18 Illustration of Layer of Heavy Scattering Calculation.

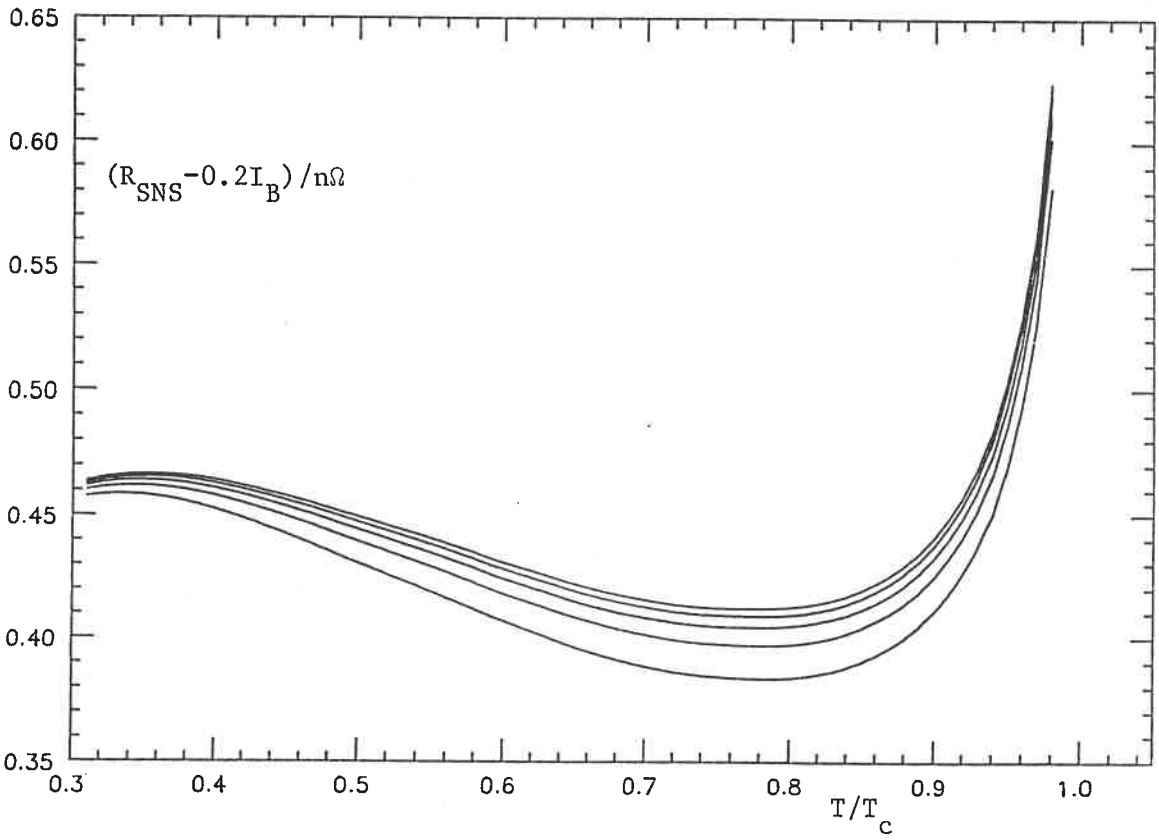

Fig. 5.19 Results of Heavy Scattering Layer Calculation with I_B=0,1,2,3 and 4 (I_B=0 lowest curve).

$$\gamma_{11}'=\gamma_{11}-\gamma_{21}I_B, \qquad \gamma_{21}'=\gamma_{21}$$

$$\gamma_{12}'=\gamma_{12}-\gamma_{22}I_B , \qquad \gamma_{22}'=\gamma_{22} \tag{5.15}$$

For $E>\Delta$

$$P' = P + I_B \tag{5.16}$$

For $E<\Delta$

These relations have been used to modify the boundary conditions put into the theory discussed in the last section. It was found that, as expected, the most noticable change was that the overall resistance increased by about $0.2I_B$ nΩ. (The equivalent resistance to one mean free path in N for each interface is 0.196 nΩ). Fig. 5.19 shows the resultant R(T) curves. It can be seen that even if $I_B=4$ the shape of the curve is not drastically altered, the minimum becomes rather shallower. (In most samples $I_B=4$ is sufficient to account for most of the low temperature resistance by this effect alone). It should be noted that if the thin scattering layer was deep inside N it would simply add a temperature independent resistance corresponding to I_B. The temperature dependence is only affected because the q and j values are not in equilibrium at the interface. This calculation shows that there could, in fact, be significant interdiffusion in the present samples since it would not greatly affect the predicted R(T) curves.

CHAPTER 6

RESISTANCE OF DIRTY SNS SANDWICHES AT LOW TEMPERATURES

6.1 Introduction.

This chapter looks at the question of the low temperature resistance of NS interfaces as a function of the amount of impurity in S. The next section introduces the basic theory. Section 6.3 looks at the experimental data obtained at low impurity concentrations and Section 6.4 discusses higher concentrations.

6.2 Theory of Low Temperature Resistance

In this section the theory of the extra interface resistance observed at low temperatures when S is dirty is discussed. The approach will follow that of Harding et. al. (1974) but includes a correction of an error related to the phase which has been pointed out by Waldram (1986).

It is first necessary to look at the subgap boundary conditions in some detail. These may be calculated, in one dimension, from the Bogoliubov equations as described in Section 5.4, from where the notation used in this section is derived. If $\gamma=0$ (an approximation discussed later) it turns out that the amplitude reflection and transmission coefficients derived are:

$$r_N=0, \quad r_A=e^{-i\phi}, \quad t_{A+}=\sqrt{2}, \quad t_{B-}=0 \tag{6.1}$$

It should be remembered that these were derived in a practical calculation of boundary conditions. The possibility of evanescent modes growing into S was not included since it was not physically reasonable. It is, however, equally possible to carry out the calculation for these modes. In particular, as can be seen from the definitions in Section 5.3, if B^+ modes are substituted for A^+ ones, and A^- for B^- the algebra is the same

with ϕ replaced by $-\phi$. This gives:

$$r_N=0, \quad r_A=e^{+i\phi}, \quad t_{B+}=\sqrt{2}, \quad t_{A-}=0 \tag{6.2}$$

The result (6.1) means that an electron and a hole wave combined with suitable phases in N can be coupled with a pure A^+ mode in S. Harding et. al. represented this process by:

$$e^+(1) + h^+(1) = A^+(1) \tag{6.3}$$

As before superscripts refer to the sign of k_0. The complex numbers in brackets give the amplitude and phase of the wave. It can be seen that the origins have been chosen so that in this case they are all in phase. (6.2) shows that if the phase relations are different, an electron and a hole can generate only a B^+ mode. If the origins are kept the same as in (6.3) it is easy to show that the phase relation is given by:

$$e^+(e^{i\phi}) + h^+(e^{-i\phi}) = B^+(1) \tag{6.4}$$

Harding et. al. incorrectly gave the hole component phase as $-e^{i\phi}$. This does not, however, make any difference at low temperatures since most excitations then have E~0 which means that $\phi=\pi/2$. It does make a difference when the temperature dependence of R_{SNS} is considered (Chapter 7).

Applying time reversal to these relations, it is easy to derive the boundary conditions for the "reflection" of evanescent modes incident on the interface from S:

$$\begin{gathered} h^+(-e^{i\phi}+e^{-i\phi}) = A^+(-e^{i\phi}) + B^+(1) \\ e^-(e^{i\phi}-e^{-i\phi}) = B^-(e^{i\phi}) - A^-(1) \end{gathered} \tag{6.5}$$

It is now possible to describe in more detail the processes which lead to interface resistance appearing in this theory. It will be noted that the argument treats the evanescent modes as if they are travelling waves (ie they are "scattered" etc). The justification for this is that their wavevectors are only slighly complex; the real part is k_F, of order $10^{10}m^{-1}$ and the imaginary part from (5.5) is of order $10^{5}m^{-1}$. The process may be described in stages as follows (although the real situation is time independent with each of these "stages" adding a component to the overall wave field).

1. An incident electron from N is reflected as a hole and also generates an A^+ mode in S according to (6.3).

2. This A^+ mode is scattered by the impurities in S, and eventually some of the scattered modes return to the interface as A^- waves.

3. The A^- modes, when they reach the interface, are "Andreev reflected" according to (6.5) to give a B^- mode and eject an electron into N.

4. The process (6.5) is similar to Andreev reflection in that the **k** vector remains the same. Therefore the B^- modes produced retrace exactly the scattering processes which the A modes underwent. As a result, when the scattered B^+ modes reach the interface they produce a hole wave which is exactly π out of phase with the original one produced in stage 1. It is also slighly weaker because of the progressive attenuation of the evanescent modes. A new A^+ wave is produced and the steps described begin again at stage 2.

This process repeats many times until the evanescent waves have been attenuated to the stage of being negligible. The hole wave produced by the original Andreev process is sucessively weakened by the addition of successive components whose phase changes by π each time. In addition some electron amplitude is also produced at each stage so the total result is that the Andreev process is no longer perfect; an incoming electron now

has a finite probability of being reflected as an electron. This is the origin of the interface resistance at low temperatures.

It should be noted that, although as described it relates to the 1D case, the argument above also holds for 3D. As a result of the "Andreev reflection" process for evanescent modes described in stage 3 above, the reradiated hole components are coherent and change in phase by π at each reradiation (assuming the original incident electron wave was plane). The radiated electron waves, on the other hand, are incoherent.

The conversion of the above physics into a quantitative theory turns out to be fairly easy in one dimension and is described in detail by Harding et. al. The result of the calculation in terms of the subgap boundary parameter P (defined in Appendix 1) is:

$$P(E) = 2(l_a/\ell)^S \sin^2(\phi) \qquad (6.6)$$

Where $l_a = \hbar v_F/2\Delta$ is the amplitude decay length of the evanescent waves. This gives the following result for the resistance at low temperatures where all the excitations have effectively zero energy:

$$Q_p = (2l_a/\ell)^S \qquad (1.D.) \qquad (6.7)$$

(As in Chapter 4, the resistance is expressed as the dimensionless quantity Q_p which is the equivalent number of mean free paths in N). Since l_a is independent (approximately) of amount of impurity, this predicts that the low temperature resistance will be proportional to $1/\ell$ ie to the residual resistivity of the superconductor.

The three dimensional calculation is much more complicated but has been carried out by Pippard (1984) by using an analogy with optics. His result was:

$$Q_p = (l_a/2\ell)^S \qquad (3.D.) \qquad (6.8)$$

The extension to three dimensions reduces the expected resistance by a factor of four but does not alter the form.

6.3 Experimental Results for Low Temperature Resistance; 0-5% Pb.

The results of the experimental determinations of the Low temperature resistance are given in Fig. 6.1 and also in Table 6.1. The approximate percentage compositions given are derived from the composition of the alloys used to remake the casts. In the graph, the y axis shows the increase in low temperature resistance on recasting with the alloy, and the x axis the residual resistivity of the superconductor, ρ_s, (measured just above T_c). The interface resistance of interest, R_p, is the interface resistance attributable to the dirtiness of S. This is given by the rise in resistance on recasting with the dirty In minus the rise seen on recasting with pure In (the point at zero concentration). As mentioned in Section 3.8, this latter quantity was generally small compared to R_p and gives an idea of the likely errors in the data.

It can be seen immediately from Fig. 6.1 that there are two distinct regions. At lower Pb concentrations (below $\rho_s \sim 25 n\Omega m$ which corresponds to approximately 5 at. % Pb) a linear relation is seen, as is expected from (6.8). At higher concentrations this breaks down. The rest of this section discusses the lower concentration region of the curve; the part at higher concentrations is the subject of the next section.

In the range 0-5 at. % Pb, the experimental R_p vs ρ_s curve is a good fit to a straight line, with the exception of two points (samples 79 and 94 at about 1 and 3% Pb respectively). The reason why these two points did not fall on the line was never discovered. Given the accuracy with which the other points appear to fit the linear form, random errors are unlikely to be responsible. The experimental plot of T_c against ρ_s, Fig. 6.2

Table 6.1

At.% Pb	Sample No.	ρ/nΩm	Resistance Rise/nΩ	T_c/K
0	91	<0.01	0.024	3.41
0.5	115A	2.64	0.081	3.40
1	89A	5.46	0.154	3.42
1	79A	5.21	0.179	3.42
2	114A	9.73	0.234	3.48
3	97A	12.6	0.308	3.53
3	94A	12.9	0.232	3.53
4	76A	16.0	0.397	3.57
4.3	86A	18.0	0.431	3.60
5	85A	21.5	0.516	3.67
6	117A	26.8	0.524	3.79
7	113A	33.2	0.482	3.86
7	111A	33.7	0.530	3.87
7	99A	35.2	0.687	4.07
9	104A	43.1	0.577	4.32
9	98A	44.9	0.380	4.32
10	108A	47.5	0.350	4.39

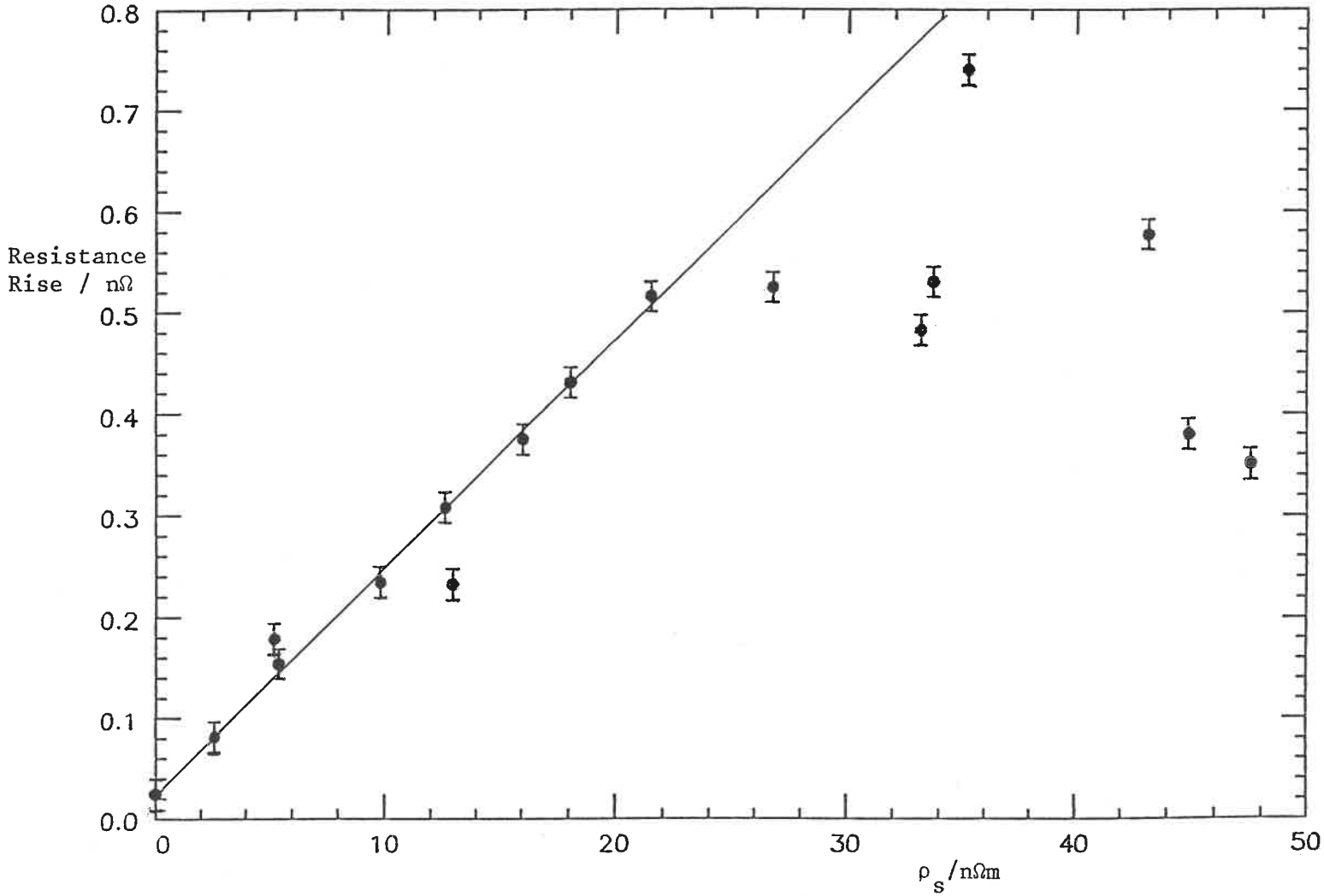

Fig 6.1 Low Temperature Resistance Rise on Recasting vs Residual Resistivity of S.

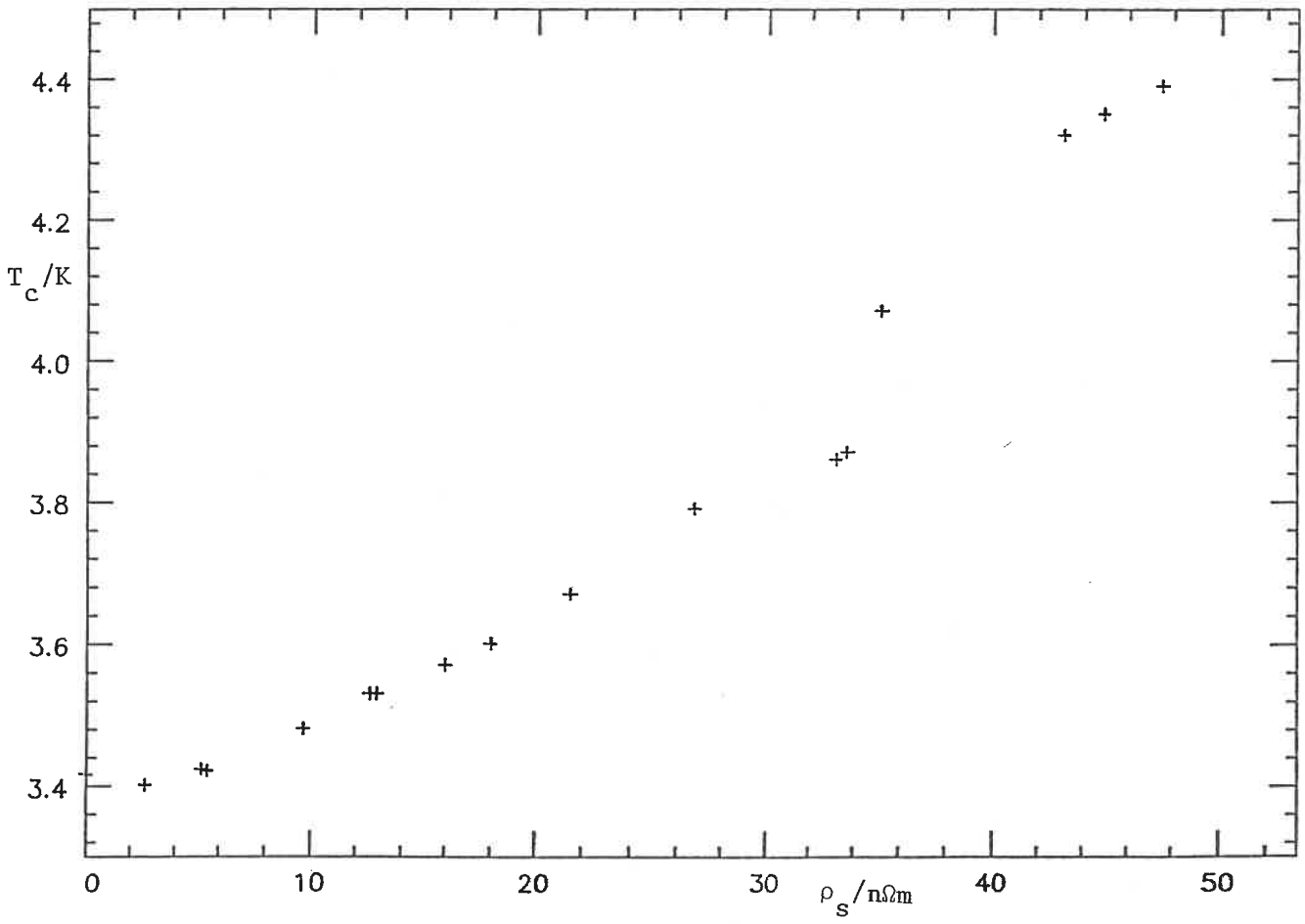

Fig. 6.2 Transition Temperature of $In_{1-0.9}Pb_{0-0.1}$ vs Residual Resistivity.

(discussed in more detail in the next section), is a smooth curve in this range including these points so gross errors in measuring the residual resistivity are ruled out. It is likely that the point which is too high was so because the remelting process for some reason changed the resistance more than usual (eg the inverted cast pulled away slightly). The point which is too low is harder to explain. It is possible that the piece of W used was cracked and that the In seeped in during remelting. In any event the closeness with which the remaining points appeared to obey a linear relation showed that these two points were spurious for some reason.

It can, therefore, be concluded that, in the 0-5% Pb region, the theoretical prediction of a linear dependence of R_p on ρ_s is verified experimentally. The comparison of the gradient found to the theoretical value is now discussed. Linear regression was performed on the points which lie close to the line. The best fit was found to be:

$$R_p = (0.023\pm0.001)\rho_s \quad \text{(experimental)} \tag{6.9}$$

where R_p is given in nΩ and ρ_s in nΩm. The calculation of the theoretical value was carried out in the following stages:

(i) As mentioned in Chapter 4, the resistance of a mean free path of W of the area of the present samples is 0.098nΩ. Since sandwiches contain two interfaces this gives: $Q_p=R_p/0.196$

(ii) $l_a=\hbar v_F/2\Delta$ whereas $\xi=hv_F/\pi\Delta$, ie $l_a=\xi\pi/2$. Dheer (1960) quotes $\xi=4.4\times10^{-7}$m which gives $l_a=6.9\times10^{-7}$m.

(iii) For In $\rho\ell=5.7\times10^{-16}$ Ωm^2 as mentioned in Chapter 4. This means that $\ell=5.7\times10^{-16}/\rho_s$.

Combining these results with (6.8) gives the result:

$$R_p = 0.119\rho_s \quad \text{(theoretical)} \tag{6.10}$$

It can be seen that this gradient is about a factor of five larger than that found experimentally. (It is also worth noting that the one dimensional theory,which leads to (6.7), gives a gradient a factor of 20 too large).

For Hardings results on Pb/Cu/Pb the three dimensional theory gave a gradient which was three times greater than the experimental gradient. The present discrepancy is, therefore, somewhat larger than that found in Hardings work. This suggests that the problem is related to the properties of the pair of metals involved rather than some consistent error in the theory.

One assumption which might be questioned is that the proximity effect discussed in Section 5.8 can be safely neglected. As can be seen from Fig. 5.15, the reduction in resistance due to this effect at the lowest temperatures used is only about 5%. This is about 16 times smaller than the discrepancy observed and, although a valid correction, it is therefore not worth considering in detail here. A related point, which was pointed out by Pippard (1984), is that if Δ is pulled down significantly in S as is also discussed in Section 5.8, the discrepancy between experiment and theory would get even worse. This is because the evanescent modes would be less attenuated before returning to the interface in which case the theoretical resistance would be even greater.

Another possibility is that the discrepancy is due to the imperfections of the interface discussed in Chapter 5. Dirt or alloying at the interface, which (because of the proximity effect) for zero energy excitations would be on the S side of the point of Andreev reflection, could strongly scatter the evanescent modes. As a result the amplitudes penetrating into S would be reduced and the effect on the resistance of alloying S would correspondingly decrease. The problem with this explanation is that, as seen in Chapter 5, the amount of scattering at the interface varies significantly from sample to sample. If this was a

significant effect the low temperature resistance results would be irreproducible and a good linear relationship would not be seen at all.

As mentioned in Chapter 3, another possible problem is that the concentration of Pb within a distance l_a of the interface may not be the same as in the bulk casts. It may be postulated that the Pb migrates to the interface or is repelled from it. Again it seems likely that if there was some concentration gradient it would not form reproducibly. The fact a linear relation is seen, therefore, makes this seem unlikely. In addition the fact that the temperature dependence (which involves variations in the size of l_a) is correctly predicted (see next chapter) implies that the concentration of Pb is uniform in the region of interest.

A likely source of the discrepancy is mismatch at the interface. As was discussed by Pippard (1984) this arises if the Fermi surfaces of N and S are of different sizes (Fig. 6.3). In this case incident excitations are refracted as illustrated, assuming that the component of **k** parallel to the interface is conserved. For electrons in some states in the metal with the larger Fermi surface, there is no corresponding state on the other side. Such excitations, corresponding to high angles of incidence, therefore can not cross the interface. (It should be noted that this is a different effect from the one dimensional $\gamma \neq 1$ reflection described in Chapter 5: in that case the reflection was caused by the change in potential across the interface).

The system discussed by Pippard was Pb/Cu (the one on which Harding obtained data). In this case both the Fermi surfaces were approximately spherical and the ratio of the surface areas S_{Cu}/S_{Pb} was 0.75. Excitations incident on the interface from N were therefore refracted so that there were no evanescent modes with high angles of refraction. This meant that the modes which eventually returned to the interface were more strongly attenuated on average than they would have been if all angles were present. Pippard estimated the size of this effect and concluded that the

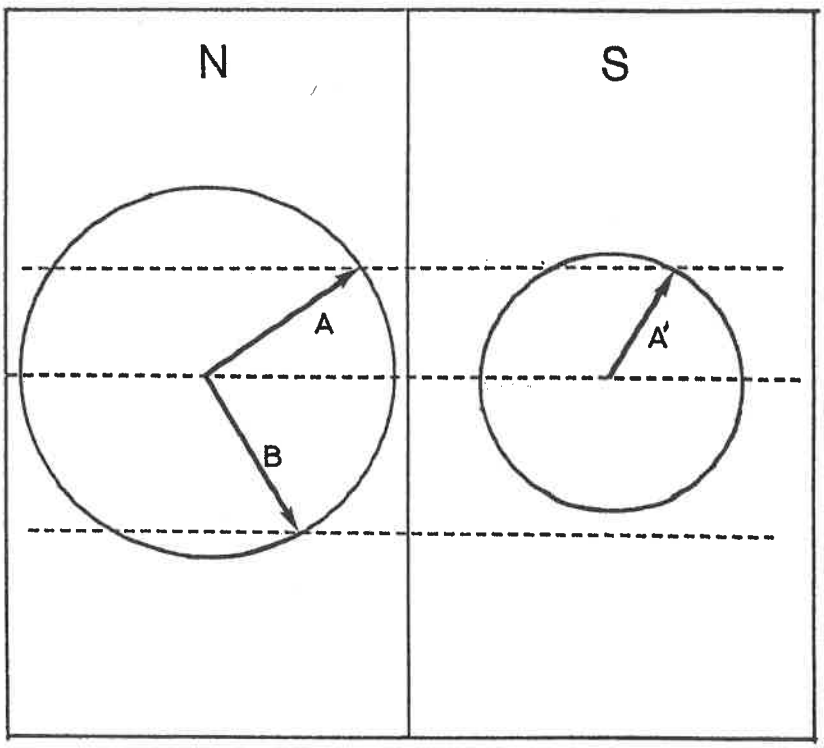

Fig. 6.3 Illustration of Effect of Fermi Surface Mismatch in 2D. It can be seen that the excitation A incident on the interface is refracted into state A'. The excitation B has no correspnding state on the S side of the interface.

gradient of the theoretical relation would be approximately halved. This was, however, insufficient to bring experiment into coincidence with theory in that case.

In the present case it is not possible to make a simple estimate of the likely size of the effect. The reason is that, although the Fermi surface of In is approximately spherical, that of W is very complicated (see, for example, Shoenberg (1969) p112). This makes the analysis of the likely effect on the interface resistance extremely complex and it has not been attempted. There is definitely appreciable mismatch since the ratio $S_W/S_{In}=0.68$, so it seems likely that this effect is significant. The results of the Pb/Cu case mentioned above suggest that there is probably also yet another mechanism reducing the resistance observed.

So, to summarise, the reason for the discrepancies between the theoretical and experimental magnitudes of R_p in this work and that of Harding is not known. It seems likely that they are at least in part due to mismatch between the Fermi surfaces of N and S. However, it is clear that more work needs to be done to clear up this problem. It would not be surprising if there were a completely different, as yet unthought of, mechanism reducing the experimentally observed resistance.

6.4 Experimental Results on Low Temperature Resistance; 5-10% Pb.

Above concentrations of about 5 at.% Pb the linear relation is observed to break down completely. The reason for this is not known, the purpose of this section is to discuss some possibilities. There are two basic types of explanation; firstly there are those in which it is assumed that the greater concentration of Pb in some way interferes with the recasting so that the interfaces formed are no longer the simple system which is treated by the theory. Secondly it is possible that the theory for some reason breaks down for W/In interfaces.

The idea that the high Pb concentration somehow interferes with the

quality of the samples is supported by the fact that the most obvious characteristic of the data above 5% Pb appears to be irreproducibility. It is easy to speculate that above a certain Pb concentration the Pb either migrates to the interface or is repelled from it; such a process would probably be quite irreproducible from sample to sample. It is, however, difficult to explain why this should start to happen suddenly at a certain concentration with the theory being obeyed well at slightly lower ones. Harding found that his results became irreproducible above the alloy concentration at which phase changes took place. This does not, however, arise in the present work since the first phase change in the In/Pb system takes place at about 12 at. % Pb (eg. Hansen 1958) which is is well above the concentration at which the present data begins to behave irreproducibly. It is possible, however, that the interface somehow nucleates formation of the more concentrated phase so that the alloy is a two phase system in the region of importance.

Another point is that as the Pb concentration of the alloy is increased, so does its melting point. It is known that In begins to oxidise in air at temperatures slightly above its melting point (Rosebury 1965). Above a certain concentration of Pb, therefore, the casts could have started to oxidise significantly during recasting. This oxide would then have been stirred into the cast being remade and could possibly have migrated to the interface. This could be the cause of the observed irreproducibility. It should be noted however that oxide at the interface would tend to increase the resistance. This effect alone could therefore not explain the fact that the general departure from the linear trend is downwards. It would be necessary to assume that at about the same concentration as the oxide begins to cause irreproducibility another factor causes deviation from the linear form.

There are several theoretical reasons why there could be deviation from the linear form at higher concentrations. An obvious feature as the

concentration of Pb is increased to relatively high values is the increase in T_c of the alloy (Fig. 6.2). Assuming the usual BCS relation ($\Delta=1.76k_BT_c$) holds this implies that Δ also increases which means that l_a will get shorter. However when the numerical values are put into the theory, it is found that the decrease in resistance expected from this effect would only be a few per cent. The change is therefore negligible compared to the gross deviations from theory observed.

It can be seen from the T_c against ρ_s curve, Fig. 6.2, that there is a discontinuity at $\rho_s \sim 34 n\Omega m$. It seems likely that this is a real effect since Merriam (1963 and 1964) saw a discontinuity in the rate of change of T_c with concentration at exactly the same place. It is unlikely to be due to experimental error since it is hard to see how major errors could occur in measuring T_c. In addition the curve seems smooth on both sides of the discontinuity. This effect has been ascribed to an interaction of the Fermi surface with the Brillouin zone. It should be noted that it occurs just above the point at which the linear R_p v. ρ_s relation breaks down. In fact as the departure of T_c from a smooth curve can be seen somewhat below the jump so the departure from linearity probably coincides reasonably closely with the beginning of these effects. If the R_p data could be taken literally rather than being assumed to be irreproducible, which is very doubtful on the present data, it would be noticable that the discontinuity in T_c corresponds to a large jump in R_p.

Exactly how Brillouin zone effects could affect the interface resistance is not certain. The most obvious point is to return to the mismatch argument in the last section. Which excitations can cross the interface and how those that do are refracted, depends on the details of the Fermi surfaces of the two metals. The discontinuity in T_c found corresponds to a change in the topology of the In Fermi surface. It therefore seems likely that this change would affect the interface resistance. Unfortunately because of the complexity of the problem it is

impossible to estimate even roughly the size of the effect.

As pointed out by Pippard (1984), the theoretical result (6.8) assumes that the Fermi surface area, S_{In}, remains constant. In addition, if it doesn't the resistance varies as S_{In}^{2}. This could clearly also be a mechanism for the Brillouin zone effect changing the resistance. The question is whether the changes in S_{In} are large enough to have a significant effect. The linearity of the $R_p(\rho_s)$ below about 5% Pb implies that the constant S_{In} approximation is adequate in that region. This implies that the order of the changes in the S_{In} occuring in this system are of negligible size; it is not very likely that the discontinuous changes which are under discussion here are much larger.

It would be useful to repeat these measurements with In-Sn alloys in which a similar T_c effect has been seen at a different concentration (about 9 at.% Sn). If there was a similar breakdown of the linear R_p curve at that point it would clearly imply correspondence between the two effects. There are problems with this, however, since the In-Sn system undergoes a phase transition at about 3 at.% Sn which would further complicate matters.

In summary, the irreproducibility of the low temperature resistance results at higher Pb concentrations strongly suggests that the breakdown of the linear form is due to some sort of imperfection occuring in the SN interfaces. It is, however, found that the breakdown occurs at around the same concentration as an anomaly in the T_c curve due to a Fermi surface-Brillouin zone interaction. It is possible that the same interaction is also responsible for the unexpected behaviour of the low temperature resistance.

CHAPTER 7

TEMPERATURE DEPENDENCE OF RESISTANCE OF DIRTY SNS SANDWICHES

7.1 Introduction.

This chapter looks at the form of $R_{SNS}(T)$ in the dirty In samples whose low temperature behaviour was discussed in Chapter 6. It will be shown that, despite the fact that the fundamental theory of the scattering of the subgap excitations is not perfectly understood, a theory can be constructed which adequately describes the form of $R_{SNS}(T)$. The next section describes this theory and it is compared to the experimental data in Section 7.3.

7.2 Theory of $R_{SNS}(T)$ in Dirty Samples.

The approach to this problem is exactly the same as that used in previous chapters. Boundary conditions relevant to this system are developed which are then inserted into the Waldram theory, equation (A1.3).

Fig. 7.1 shows the experimental R_{SNS} curves obtained in the present work for 0-5% Pb alloys. It can be seen that as lead is added to the casts the divergence in the resistance below T_c increases greatly in size. There are two mechanisms by which adding dirt to S will alter the interface resistance:

(i) The subgap excitations are no longer perfectly Andreev Reflected due to the scattering of the evanescent tails described in Chapter 6. The excitations will now have non-zero energy so l_a will be enhanced according to (5.5). In addition the phase factor in (6.6) needs to be taken into account.

(ii) The supergap excitations encounter much heavier elastic scattering when they enter S. As mentioned earlier the contribution to the interface resistance is expected to increase as $\sqrt{\rho_s}$.

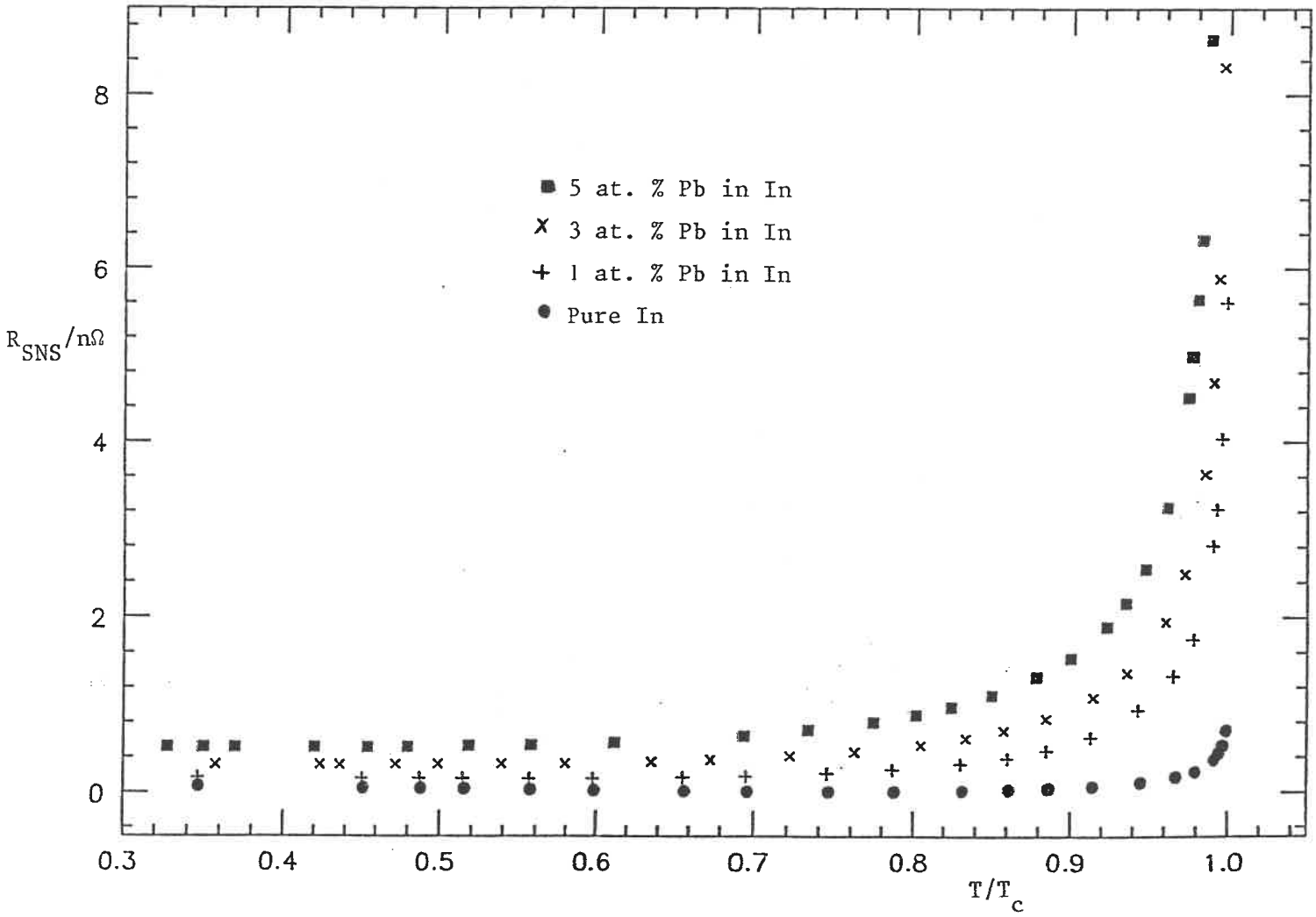

Fig. 7.1 $R_{SNS}(T)$ Curves for Dirty Samples.

Of these, (ii) is included in all the theories described so far if suitable values of ℓ and λ_3 are inserted; (i) however is new and needs to be added. The simplest theory which can be constructed which takes both of these effects into account has boundary conditions as follows:

1. Above the gap, the same boundary conditions as used by Battersby and Waldram and described in Chapter 4, namely: $R_A=0$ and $R_N=0$.

2. Below the gap, the P boundary condition given by (6.6) remembering that l_a is energy dependent.

It should be noted that this is in a sense a step backwards compared with the theories described in Chapter 5. Normal reflection due to mismatch or dirt at the interface is neglected as is supergap Andreev reflection. It turns out, however, that these effects are much less important in this case. It is easy to see that the $R_N=0$ approximation is less important since the overall interface resistance is much higher than with pure S. The effect of the $R_A=0$ approximation above the gap is less clear. However it can be seen that this approximation will be better the larger the subgap contribution to the boundary voltage becomes relative to the supergap one. The supergap boundary voltage increases as $\sqrt{\rho_s}$ whereas the subgap voltage goes as ρ_s so the dirtier the sample is the better the approximation will be.

If the above boundary conditions are put into (A1.3) some algebra leads to the result:

$$Q_i = \frac{2f(\Delta)+I_p}{(\ell/\lambda_3)^S + (\ell/\lambda_2)^N[1-2f(\Delta)-I_p]} \qquad (7.1)$$

where:

$$I_p = 2[(\ell/\lambda_2)^N+(\ell/\lambda_3)^S]\int_0^\Delta -f'(E)\ P\ dE/(1+P(\ell/\lambda_2)^N)$$

P, the subgap boundary condition, is obtained from (6.6), the definition of

ϕ in Section 5.3 and the energy dependence of l_a from (5.5) and is given by:

$$P(E) = 2(E_s/\Delta)(1-(E/\Delta)^2)^{0.5} \qquad (7.2)$$

where:

$$E_s = \hbar v_F/2\ell$$

E_s is a parameter which gives the magnitude of the resistance generated by the scattering of the evanescent tails. It should be noted that it contains $1/\ell$ and is therefore proportional to the resistivity of S. The one dimensional form of P has been used in this theory. This is reasonable since the rest of the theory is one dimensional. The extension to three dimensions is known to only scale P at low temperatures (Section 6.2) and it is assumed here to scale it by the same factor at higher ones (see next section).

The following points should be noted about this result:

(i) In the limit of clean S, $E_s=0$ and $I_p=0$. The expression then reduces to the result of Battersby, (4.1), as it must since the boundary conditions are then identical.

(ii) If T=0 the expression reduces to $Q_i=2E_s/\Delta$ which is the same result as (6.7); again this is necessary for the theory to be consistent with previous ones.

(iii) The extra resistance resulting from the scattering of evanescent tails appears only as an addition to $2f(\Delta)$, ie as if there are more electrons above the gap. This seems wrong since it appears to imply that there is a dependence on $(\lambda_s)^S$ even at low temperatures where there are no electrons penetrating into S. It should, however, be remembered that λ_s appears in the definition of I_p. If $2f(\Delta)$ is assumed to be negligible relative to I_p it is easy to derive the result:

$$Q_i = S/(1-(\ell/\lambda_2)^N S) \qquad 2f(\Delta) << I_p \qquad (7.3)$$

where $S = 2\int_0^{\Delta} -f'(E)\, P\, dE/(1+P(\ell/\lambda_2)^N)$

which means that there is no dependence of Q_i on λ_3 at low temperatures, as is expected. The expression contains $(\lambda_2)^N$ which is to be expected physically since the voltage is generated by an excess of electrons on the normal side of the interface.

(iv) It is noticeable that (7.2) implies that P gets smaller as E is increased, becoming zero at $E=\Delta$. This is a direct consequence of the $\sin^2(\phi)$ factor in (6.6) and means that a minimum could be seen in $R_{SNS}(T)$ similar to that observed in the mismatch theories. It is, however, found that with realistic values of the parameters the charge imbalance contribution to the resistance just dominates so a monatonic curve is expected. This is borne out experimentally: all the dirty $R_{SNS}(T)$ curves were found to be monatonic, except those with low Pb concentrations; in these cases the minima were more likely to be due to the mismatch effects discussed in Chapter 5.

(v) The parameter $(\ell/\lambda_2)^S$ in (A1.3) cancels out in this case; ie it does not occur in (7.1). This should improve the agreement with experiment since one less temperature dependent parameter needs to be estimated.

The fundamental difference between this result and the work of Harding et. al. (1974) on $R_{SNS}(T)$ is that the phase factor $\sin^2(\phi)$ in (6.6) is included. Before this was noticed it was attempted to fit the data to the theory without the phase factor; the discrepancy between experiment and theory then found was very similar to that seen by Harding et. al.

7.3 Comparison of Theory with Experiment

This section describes the comparison of the theory described in the last section with the experimental data. Only the data in the range 0-5%

Pb (ie that which qualitatively obeyed the low temperature theory) was seriously fitted to this theory. The data in the range above 5% Pb is not expected to fit the theory since the low temperature data did not behave as expected in these samples (this was confirmed by the 10% Pb sample as discussed at the end of this section.)

Before the theory could be compared with the experimental data, the values of the various parameters involved had to be estimated. These are discussed in turn:

(a) $(\ell/\lambda_2)^N$: The calculation of this quantity for W was described in Section 5.5. The estimate derived in that section, $(\ell/\lambda_2)^N=0.7$, was used while fitting this theory.

(b) $(\ell/\lambda_3)^S$: This has also been discussed in earlier chapters, the temperature dependence used was that derived by Battersby and Waldram (1987) and discussed in Section 4.6. The values of $(\ell/\lambda_3{}^\circ)^S=(\ell/\ell_3{}^\circ)^{0.5}$ were derived using the values of ℓ calculated from the resistivity of the alloy and $\ell_3{}^\circ$ from Table 4.1. The $\ell_3{}^\circ$ value was taken from the $R_N=0$ theory, described in Chapter 4, because that is the assumption used in the present one.

(c) R_W: As in previous chapters a temperature independent resistance had to be subtracted from the experimental data to bring it into coincidence with the theoretical curve. The procedure which it was originally intended to use was to choose R_W so that the low temperature resistance tended to the value of R_p found with that alloy concentration. R_W would then represent all the sandwich resistance except that due to the effects included in the theory. It was found however, that better fits were obtained if R_W was chosen to be smaller than this by between 0.02 and 0.08nΩ depending on the sample. This is to be expected since the mismatch effects etc. discussed in Chapter 5 have been neglected. This is discussed in more detail below.

(d) E_s: This is the parameter which represents the extra subgap

resistance due to scattering of the evanescent tails. The estimation of this parameter is complicated by the lack of quantitative agreement between the low temperature behaviour and the theory discussed in Chapter 6. There are clearly two possible approaches; either estimate E_s directly from the theory or estimate it from the observed low temperature behaviour. The first approach will give results a factor of five too large at low temperatures as discussed in the last chapter. It is in fact found that agreement at higher temperatures is then poor even if R_W is adjusted for coincidence at low temperatures (which is difficult to justify anyway). This is shown in Fig.. 7.2 for the 3% Pb sample. (It may seem surprising that the divergence in R_{SNS} below T_c gets larger when E_s is increased because the contribution to the resistance from the subgap excitations then falls off more sharply as T_c is approached. The reason is that the inelastic relaxation of charge imbalance in S via N (as described in Section 4.3) is reduced because R_A below the gap is smaller. This latter effect turns out to dominate.) The lack of agreement using this approach is not surprising for it is clear from the discrepancy in the low temperature behaviour that something is wrong with the theory of the subgap excitations.

The second approach of estimating E_s from the low temperature behaviour was therefore used. This seems more reasonable if it is noted that l_a and ℓ appear in the form of P(E) used, (6.6), solely as the ratio l_a/ℓ (the phase factor is a function of energy only). The observed linear low temperature behaviour can therefore be taken as implying that the dependence of P on l_a/ℓ is as expected if the empirical value of E_s is inserted. In comparing this theory with experiment the main assumption which is being tested is that the dependence of P on l_a/ℓ continues to be as expected from (6.6) when E (and therefore l_a) are varied rather than ℓ. It will be shown below that agreement with experiment is indeed obtained using this theory. This means that whatever the reason for the

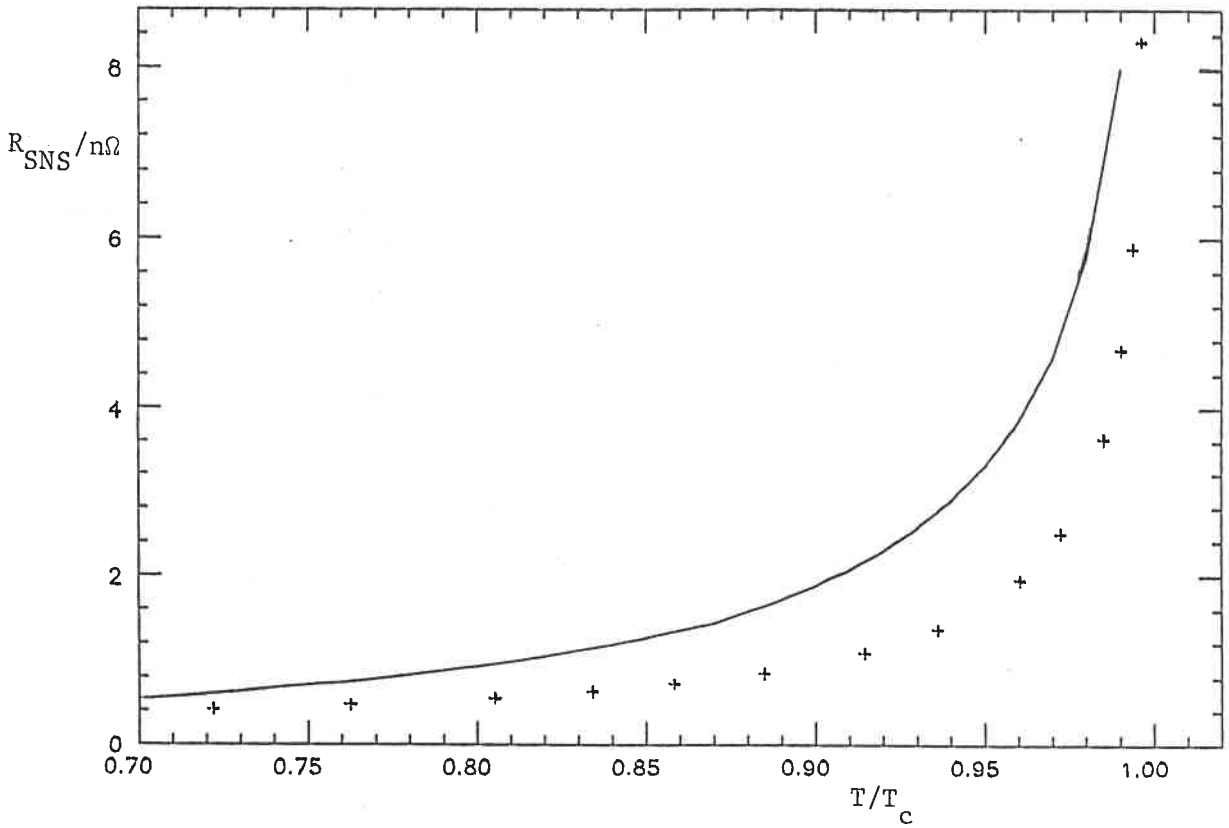

Fig. 7.2 Theoretical $R_{SNS}(T)$ Curve for 3% Pb Sample Calculated Assuming Theoretical Value of E_s with Experimental Points.

low temperature factor of five discrepancy using the theoretical values of E_s, it only scales P(E) rather than altering its form. E_s was therefore obtained from the gradient of the experimental low temperature resistance against residual resistivity line, (6.9) and the low temperature limit of (7.2) $Q_i=2E_s/\Delta$. The value thus derived was $E_s=\rho_s/2.9\times10^{-9}$ using energy units such that $k_B=1$ in common with the rest of the theoretical work.

The values of the parameters derived as above for the various samples used are given in Table 7.1.

Table 7.1

At. % Pb	E_s/k_B	$\ell/10^{-8}$m	$(\ell/\lambda_3)^S$
0.5	0.91	21.6	0.116
1	1.85	10.6	0.078
2	3.37	5.83	0.060
3	4.34	4.50	0.052
4.3	6.42	3.16	0.045
5	7.40	2.65	0.040

The theoretical curves were computed in the same way as those in Chapter 5. The integral I_p was calculated using Simpsons rule, the Waldram form was used for $\lambda_3(T)$ and $\Delta(T)$ again calculated from the data of Muhlschlegel. The resultant curves (using the parameter values given in Table 7.1) and the corresponding experimental points are shown in Fig.s 7.3-7.8 (as before T_c has been adjusted slightly in the experimental data for the best agreement). It can be seen that there is generally good agreement. This justifies the assumption made in calculating E_s discussed above. In several cases slightly better fits than those shown can be obtained by making small adjustments to the parameters, it is, however, more meaningful to look at what is obtained with a consistent set of

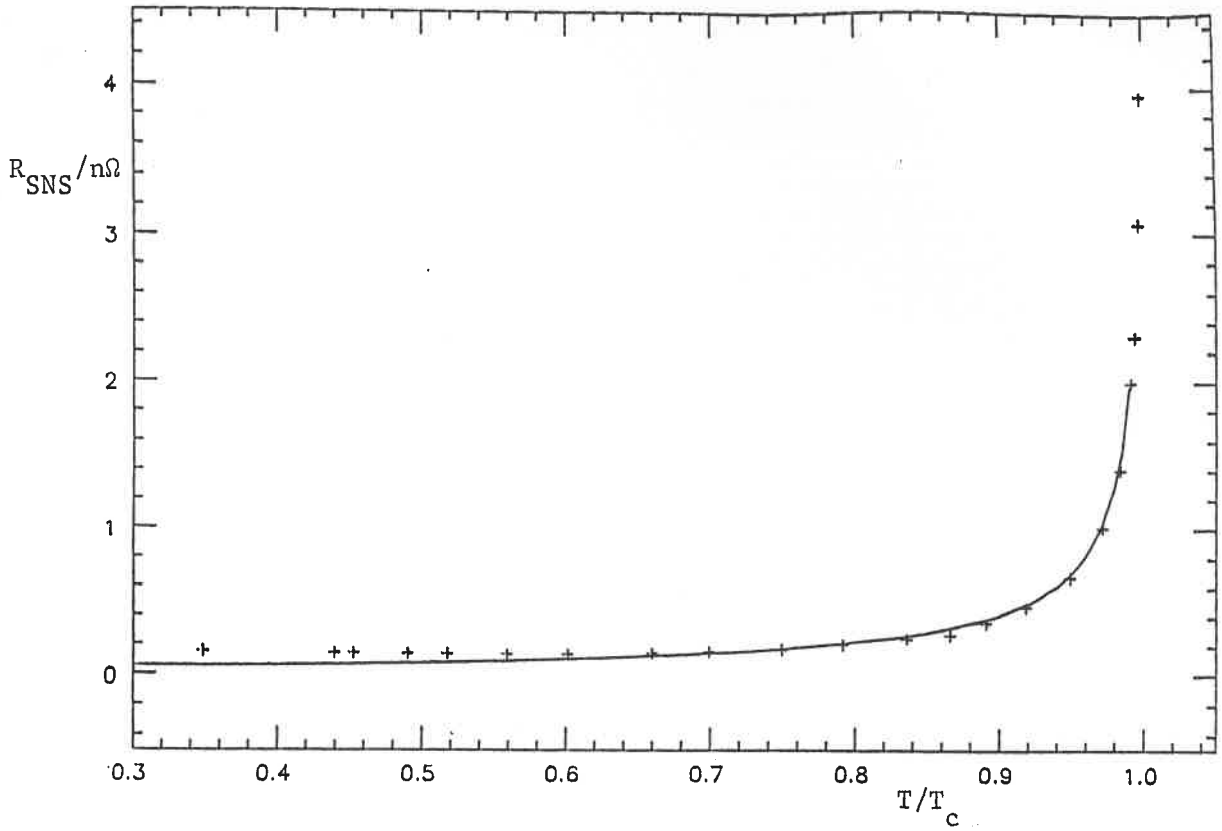

Fig. 7.3 Experimental and Theoretical $R_{SNS}(T)$ For 1/2 at.% Pb.

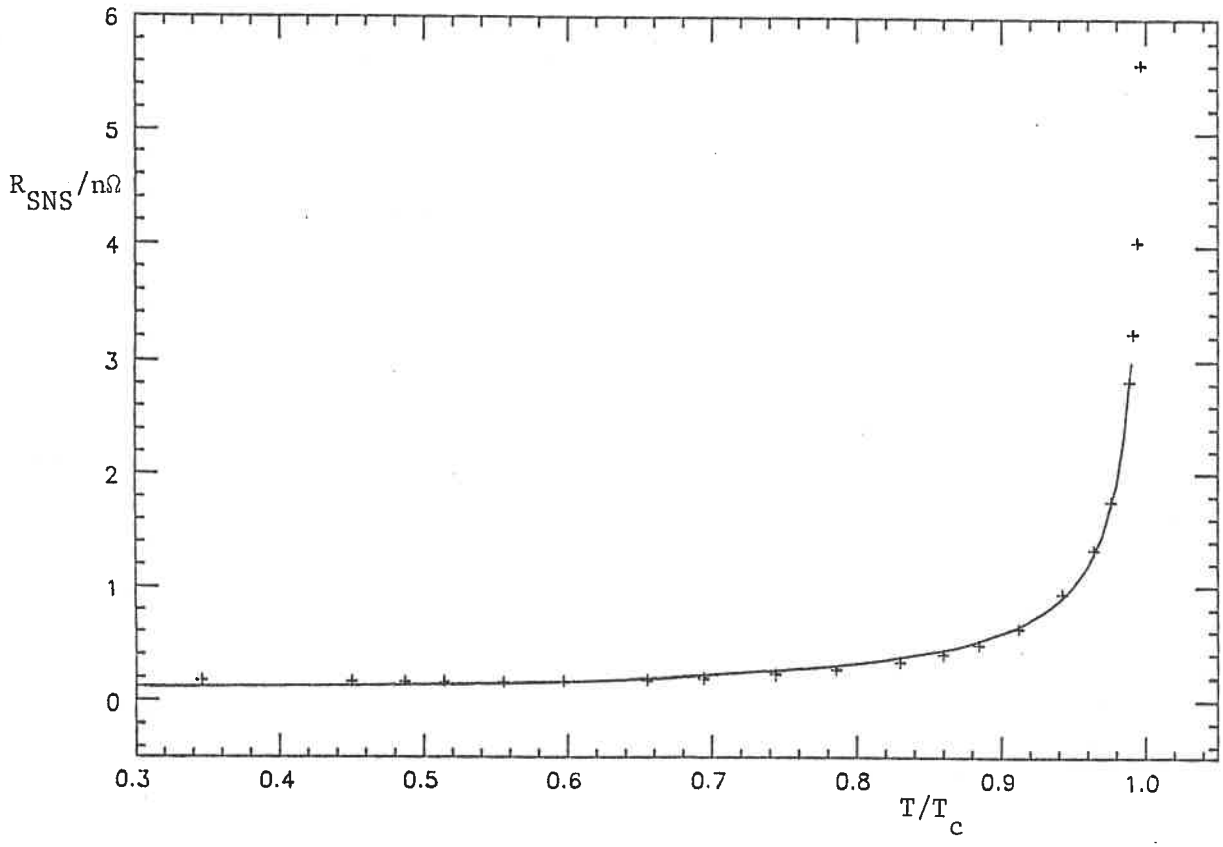

Fig. 7.4 Experimental and Theoretical $R_{SNS}(T)$ For 1 at.% Pb.

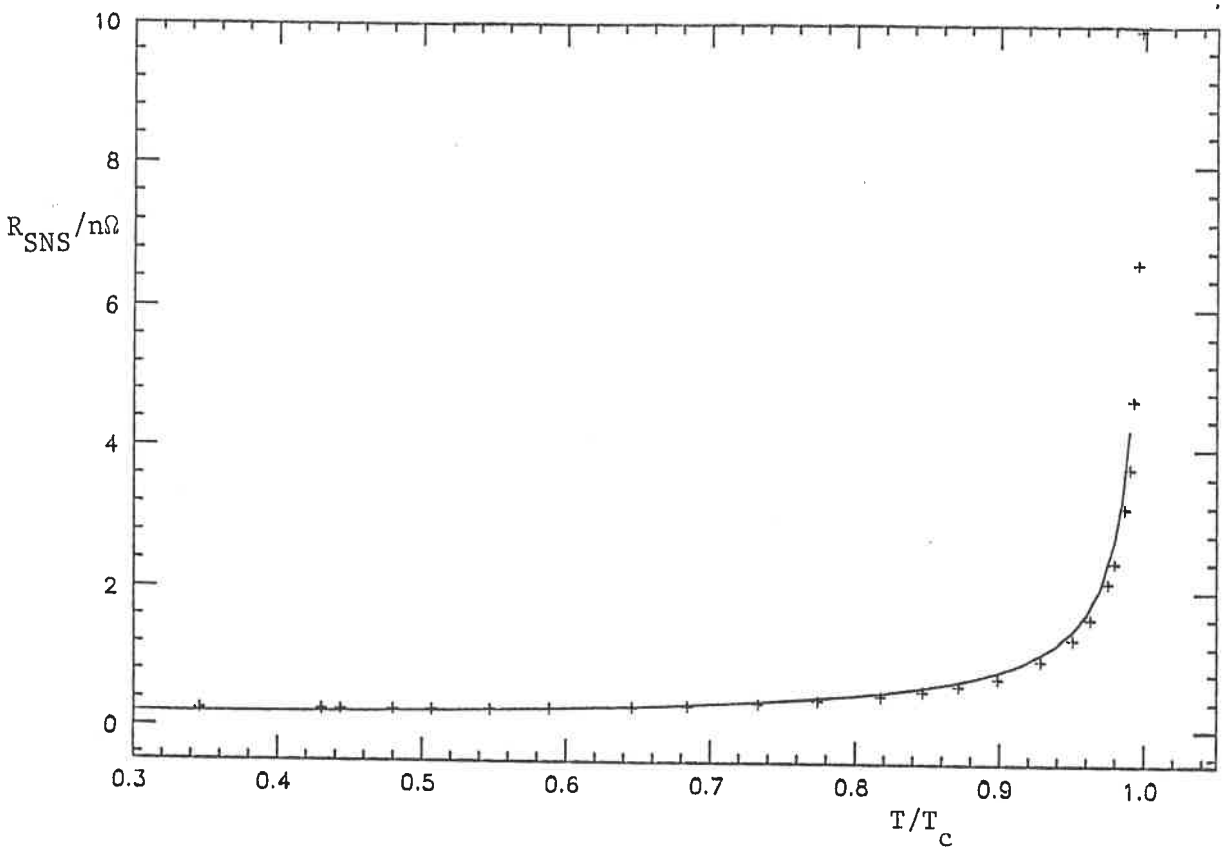

Fig. 7.5 Experimental and Theoretical $R_{SNS}(T)$ For 2 at.% Pb.

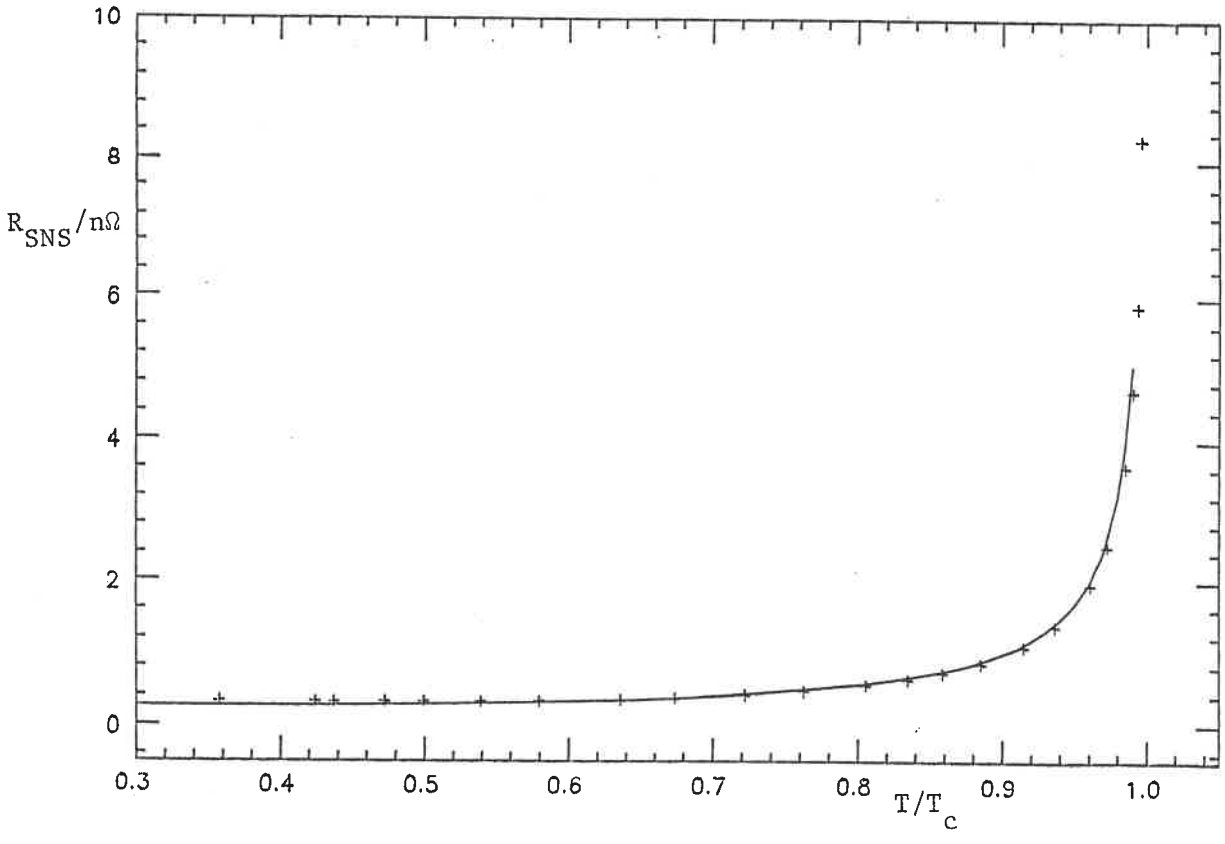

Fig. 7.6 Experimental and Theoretical $R_{SNS}(T)$ For 3 at.% Pb.

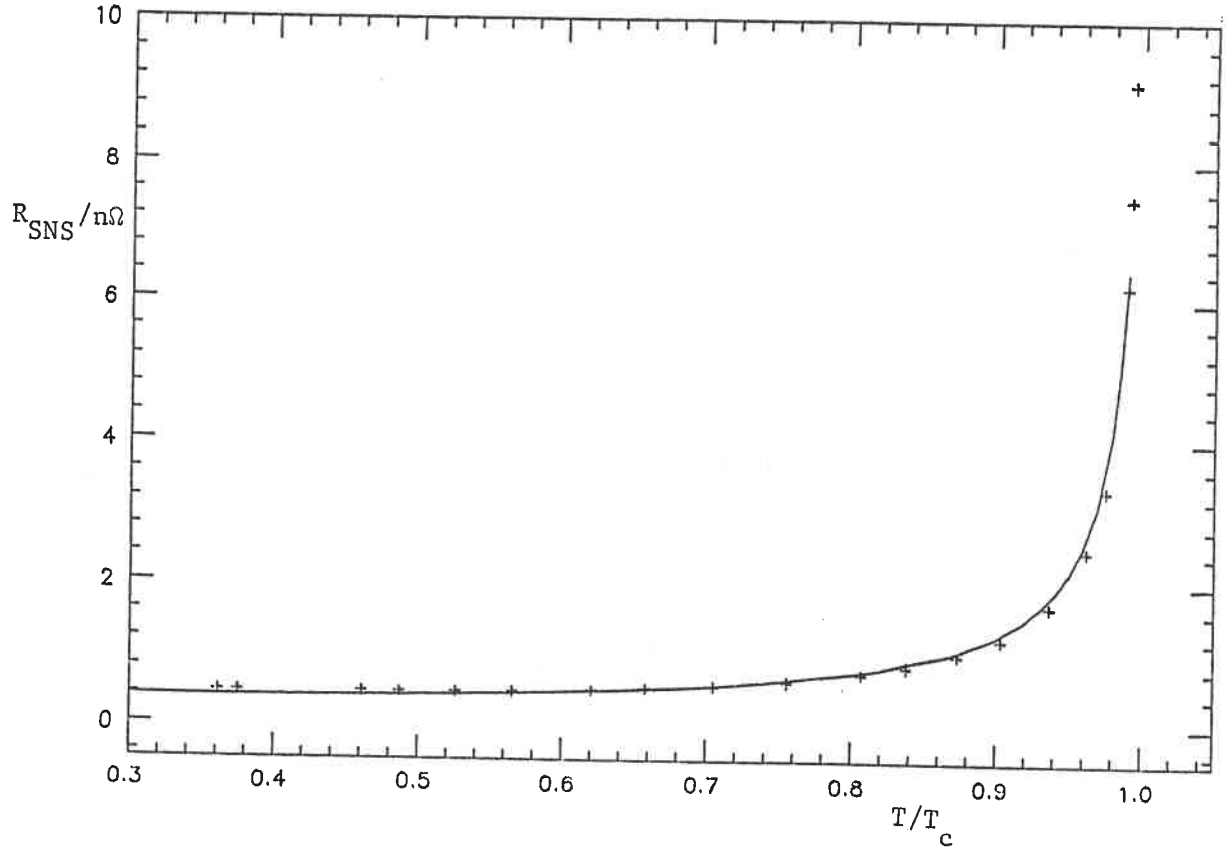

Fig. 7.7 Experimental and Theoretical $R_{SNS}(T)$ For 4 at.% Pb.

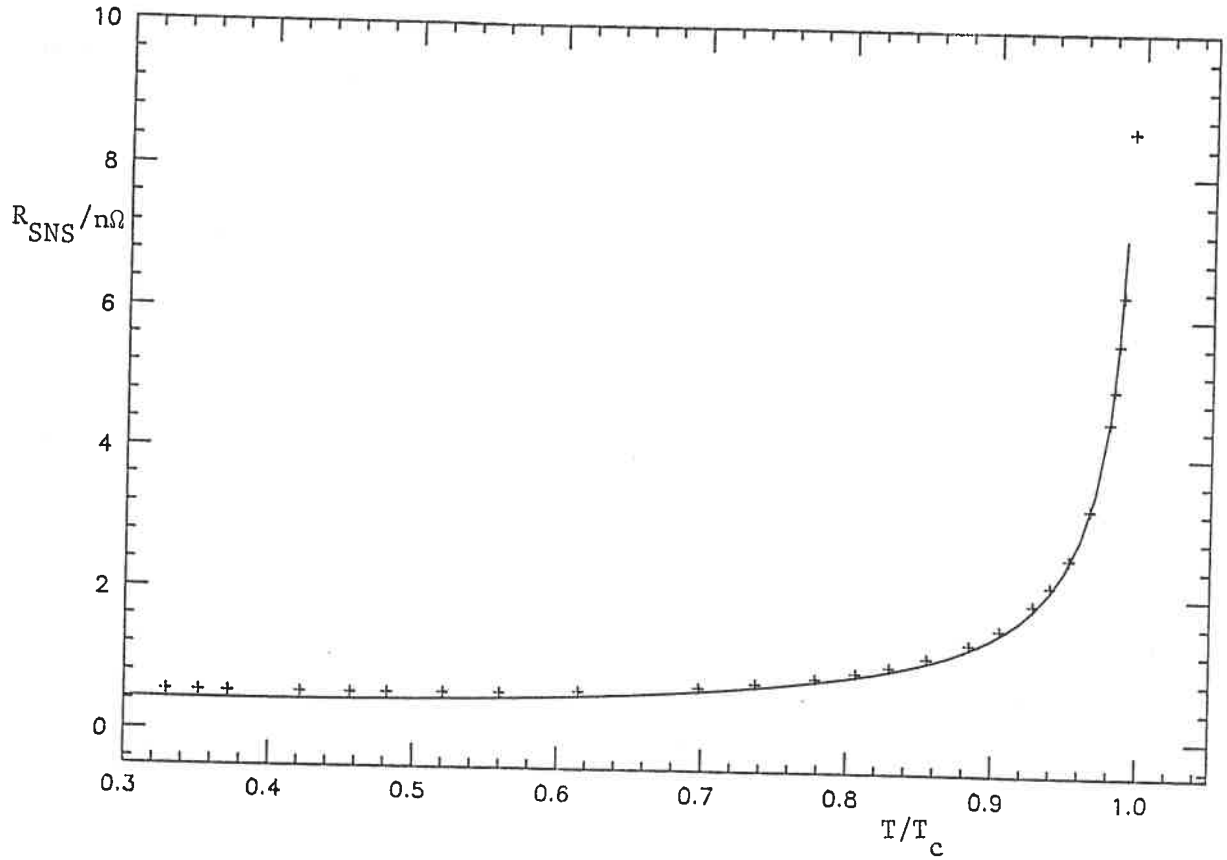

Fig. 7.8 Experimental and Theoretical $R_{SNS}(T)$ For 5 at.% Pb.

calculated values.

It can be seen, in several cases, that theory and experiment deviate slightly at low temperatures. As already mentioned, this is due to the mismatch effects discussed in Chapter 5 being neglected. The fact that the deviation has the same range of magnitudes as the low temperature falls in $R_{SNS}(T)$ observed in pure samples is evidence for this. The discrepancies are, as discussed in the last section, relatively much smaller than in the case of pure superconductors (Section 5.2).

Fig. 7.9 gives the R_{SNS} curve for the 10% Pb sample and a theory curve generated by calculating the parameters as above. It can be seen that agreement is poor. The theory, in this case, is being applied outside its range of validity. The low temperature behaviour from which the empirical value of E_s is calculated completely breaks down above 5% Pb as discussed in Chapter 6. There is therefore no reason to expect the form of P(E) in the theory to be correct for the 10% Pb sample; the lack of agreement implies that it is not. Similar results were found when attempts were made to fit to other samples with alloys more concentrated than 5% Pb.

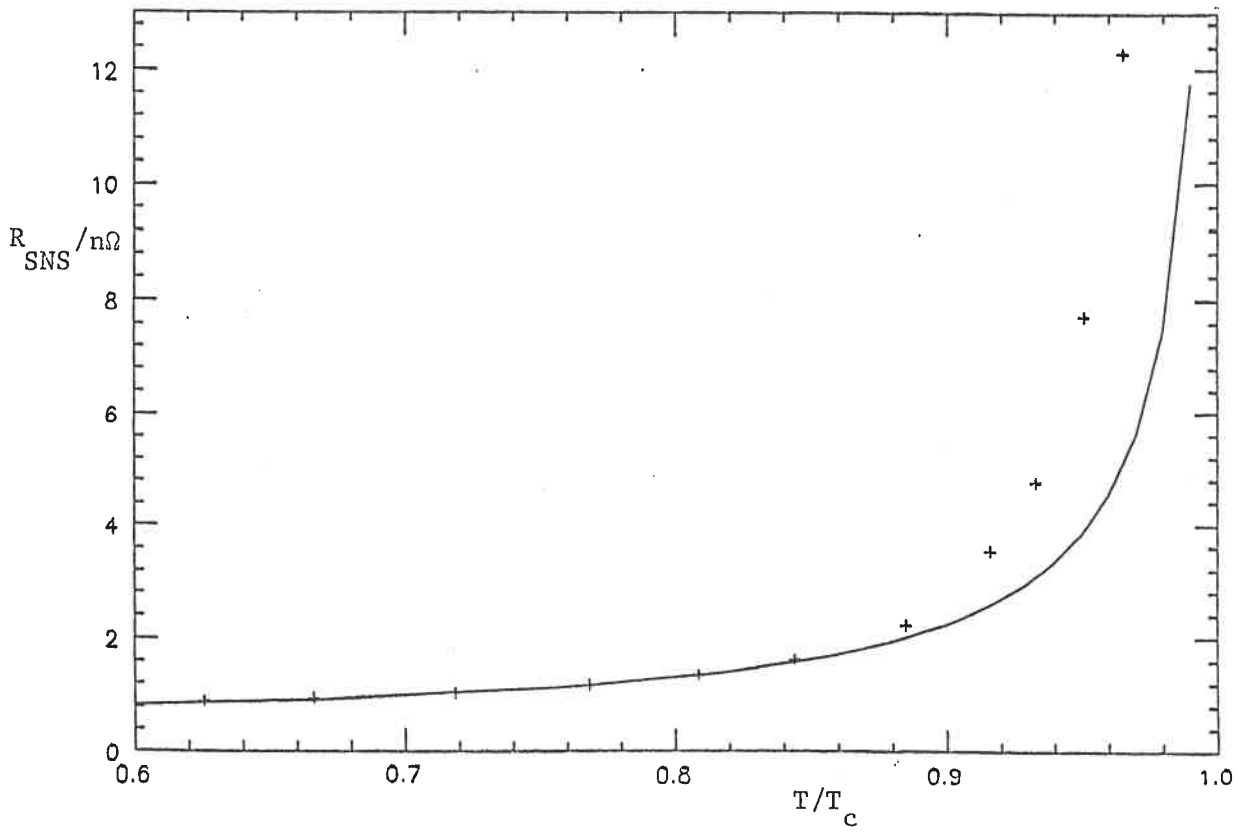

Fig. 7.9 Experimental and Theoretical $R_{SNS}(T)$ For 10 at.% Pb.

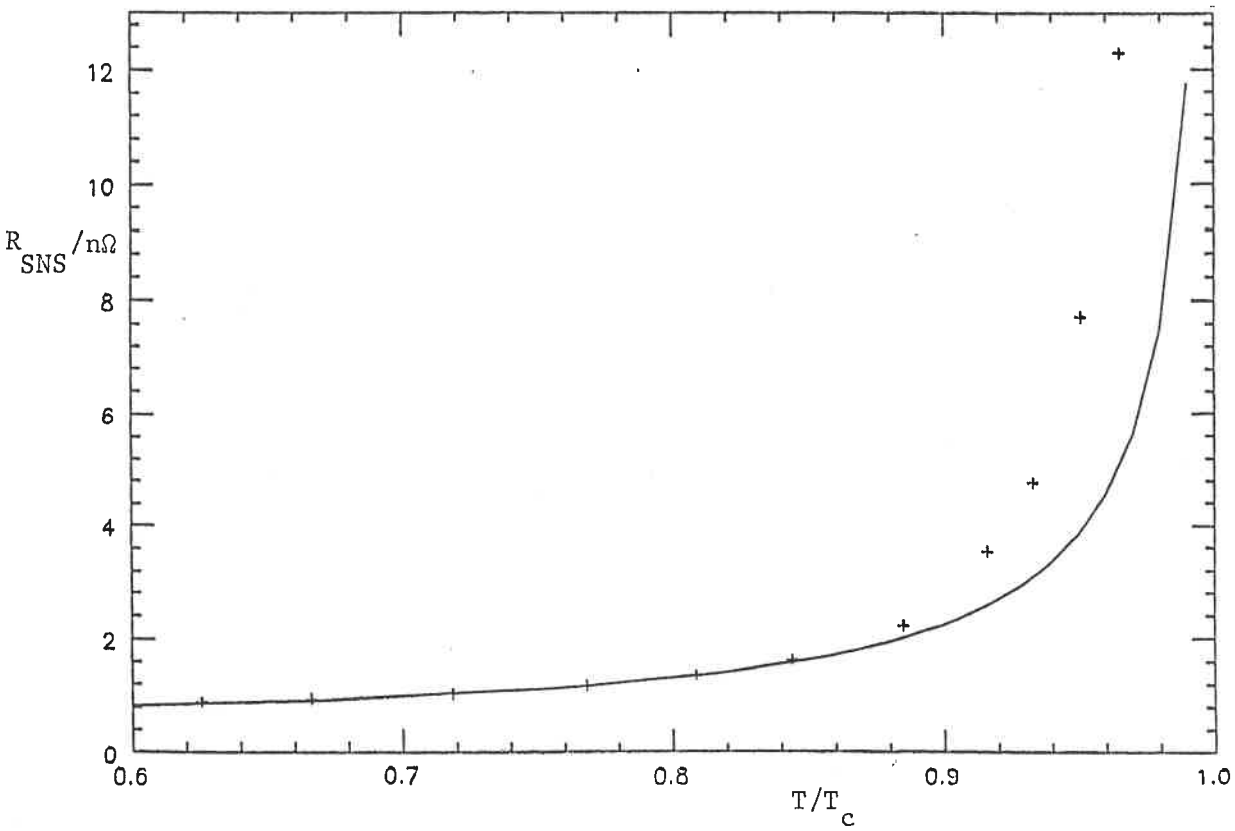

Fig. 7.9 Experimental and Theoretical $R_{SNS}(T)$ For 10 at.% Pb.

CHAPTER 8

THERMOPOWER OF CLEAN SNS SANDWICHES

8.1 Introduction

This chapter begins the discussion of the thermopower data obtained on the same samples as gave the resistance results discussed in previous chapters. It is generally true that the thermopower is a more difficult problem than the resistance. The analysis of thermopower data given in this chapter and the next is necessarily less complete and more speculative than was the case with the resistance data. The next section discusses the Battersby and Waldram theory of thermopower at SN interfaces. Section 8.3 discusses the data obtained with the very slightly dirty In and its comparison with the theory. The data from samples with the purest In is discussed in Section 8.4 and Section 8.5 looks at possible reasons for the discrepancy observed between the thermopower of normal and superconducting In.

8.2 Battersby and Waldram Theory of Thermopower of SNS Sandwiches

The most thorough attempt to develop a theory of the thermopower of NS interfaces has been that of Battersby and Waldram (1987). The physics of this theory is now discussed, partly because it is used to analyse the data in the next section. It is also useful to introduce the theoretical problems which arise when thinking about thermopower at SN interfaces. The theory is an extension of that of Waldram (1975) for R_{SNS} (which is summarised in Appendix 1). The Boltzmann equation is extended to take into account the possibility of a temperature gradient across the system and heat transport by the excitations. Because of the temperature gradient the previously used symmetry relations between the excitation distribution functions, $g_1=-g_3$ and $g_2=-g_4$ no longer hold. As a result the equations are now formulated in terms of four parameters:

$$
\begin{aligned}
q &= 0.5(g_1 - g_2 - g_3 + g_4) \\
j &= 0.5(g_1 + g_2 - g_3 - g_4) \\
n &= 0.5(g_1 + g_2 + g_3 + g_4) \\
h &= 0.5(-g_1 + g_2 - g_3 + g_4)
\end{aligned}
\tag{8.1}
$$

as previously, q and j are the contributions to charge imbalance and electric current at given energies. n and h are similarly the contributions to the total excitation number and the heat current. The steps in the derivation of the result for the boundary voltage are now summarised. For details of the theory the reader is refered to the original paper.

1. Four equations analagous to (5.15) involving the variables q,j,n and h are derived from the Boltzmann equation. In these equations q and j are coupled to n and h only via relatively small terms involving the differences in the mean free paths of electrons and holes of the same energy. These terms are responsible for the thermopower in this theory.

2. The boundary conditions used for q and j are the same as before, ie given by (A1.1) and (A1.9). The boundary conditions for n and h can be shown to be:

$$
\begin{aligned}
n^n &= n^s + h^s 2R/T \\
h^n &= h^s
\end{aligned}
\tag{8.2}
$$

where $R=R_A+R_N$ and $T=T_A+T_N$. The important point is that the boundary conditions themselves do not couple q and j to n and h; they do not in themselves cause any thermoelectric effects.

3. The two equations involving n and h are considered neglecting the small terms involving j and q. This is justified assuming that the electric current does not affect the heat current significantly which is

reasonable since h is expected to be much larger than q and j. In bulk N and S there is the very simple solution n=0 and $h=h_T$ where h_T is an (energy dependent) function which represents the distribution of heat flow. For the purposes of this theory this simple solution is assumed to hold right up to the interface. This is probably reasonable close to T_c where Δ is very small but is a poor approximation otherwise and will be discussed later.

4. The above solution for h and n is inserted into the equations for q and j. Solving the equations in a similar way to that used in Waldram (1975) leads to a complicated expression for the boundary voltage (equation (7.5) of Battersby and Waldram 1987). This is an extension of (A1.3) containing several additional energy integrals of functions of the boundary conditions.

An important point here is that, although this result seems analagous to (A1.3), it is not as generally applicable; it is not possible to obtain theories valid for different situations by putting in different boundary conditions as was done in the case of the resistance. The reason for this is the assumptions which have been used in the theory. There are two assumptions about the heat flow:

(i) That the distribution of heat flow is given by $h=h_T$ even right up to the interface.

(ii) That all the heat is carried by the excitations.

Both of these assumptions are likely to be valid with pure superconductors close to T_c which is the situation in which the theory was applied by Battersby and Waldram. The former is certainly not true for temperatures at which there are significant numbers of excitations below the gap. As was mentioned in Section 1.2.3 Andreev reflection, although compatible with electric current flow, does not allow the flow of heat. At low temperatures this Andreev thermal boundary resistance results in a significant temperature drop across the interface. h must, therefore, be

zero close to the interface below the gap on the N side. This results in an excess of heat accumulating at low energies in N which is transferred to higher energy excitations by inelastic phonon scattering. A more complete theory would, therefore, need to take account of the form of h(E) near the interface.

The assumption (ii) is also likely to be a poor approximation well below T_c. In a superconductor the condensate is unable to carry heat. Near T_c where there are many excitations it is carried by the quasiparticles in a similar way to in a normal metal. As the temperature is reduced, however, the number of excitations falls rapidly which causes the observed drop in thermal conductivity below T_c (see for example Guenault (1960)). Below a certain point the thermal conductivity will be reduced to the point at which a significant fraction of the heat can be carried by phonons. The thermal conductivity of superconductors was first investigated in terms of the BCS theory by Bardeen, Rickayzen and Tewordt (1959). It would be expected that towards the low temperature end of the range over which the present data was taken, virtually all the heat was carried by phonons rather than by excitations.

Battersby and Waldram continued by inserting into the expression for the boundary voltage the simple boundary conditions which are given in Section 4.3 (and are expected to be valid close to T_c). The result for the boundary voltage, ϕ_i, then reduces to:

$$\phi_i = \frac{2f(\Delta)(I-G^N H) + (G^N-G^S)H}{1 + (1-2f(\Delta))(\ell/\lambda_2)^N/(\ell/\lambda_3)^S} \quad (\lambda_3\rho)^S \qquad (8.3)$$

Here I is the elctric current and H is the heat current. Two of the integrals in the original expression have been simplified assuming T is close to T_c. G^N and G^S are the values of the thermoelectric ratio in N and S respectively. (As was mentioned in Chapter 2 the thermoelectric ratio,

G, is defined as the ratio of heat current to electric current at no overall voltage. The product GR therefore gives the thermoelectric voltage per unit heat current). From the resistance data it is known that the term in the denominator containing $(\lambda_2)^N$ is negligible with pure In. Battersby and Waldram also assumed that close to T_c the term in G^N in the numerator is also negligible; this approximation was used in the present work (its validity was tested as described in Section 8.3.2). The resulting expression for the resistance has already been quoted, (4.3). The expression for the thermopower of the interface is:

$$(GR)_i = G^S(\lambda_3\rho)^S/A \qquad (8.4)$$

This expression was used by Battersby and Waldram to show experimentally that the thermopower of Pb was continuous across T_c. It is also used in the analysis of the present data described in Section 8.3.2.

8.3 Thermoelectic Data from Samples with Slightly Dirty In

As was mentioned in Section 3.6 samples containing the very pure In as supplied were found to have rather irreproducible thermoelectric properties. Most of the experiments therefore used samples with In casts to which very small amounts of Pb (about 0.01 at. %) had been added. By making one scattering mechanism dominant it was found that the properties of the In could be made more reproducible. It turns out, however, that the properties of the samples with pure In are also of interest and these are discussed in the next section. This section is in two parts: firstly the general thermoelectric properties of the slightly dirty samples are discussed. Secondly the behaviour close to T_c is compared with the theory described in the last section.

8.3.1. General Properties

Fig.s 8.1-8.3 show three typical $(GR)_{SNS}(T)$ curves obtained from

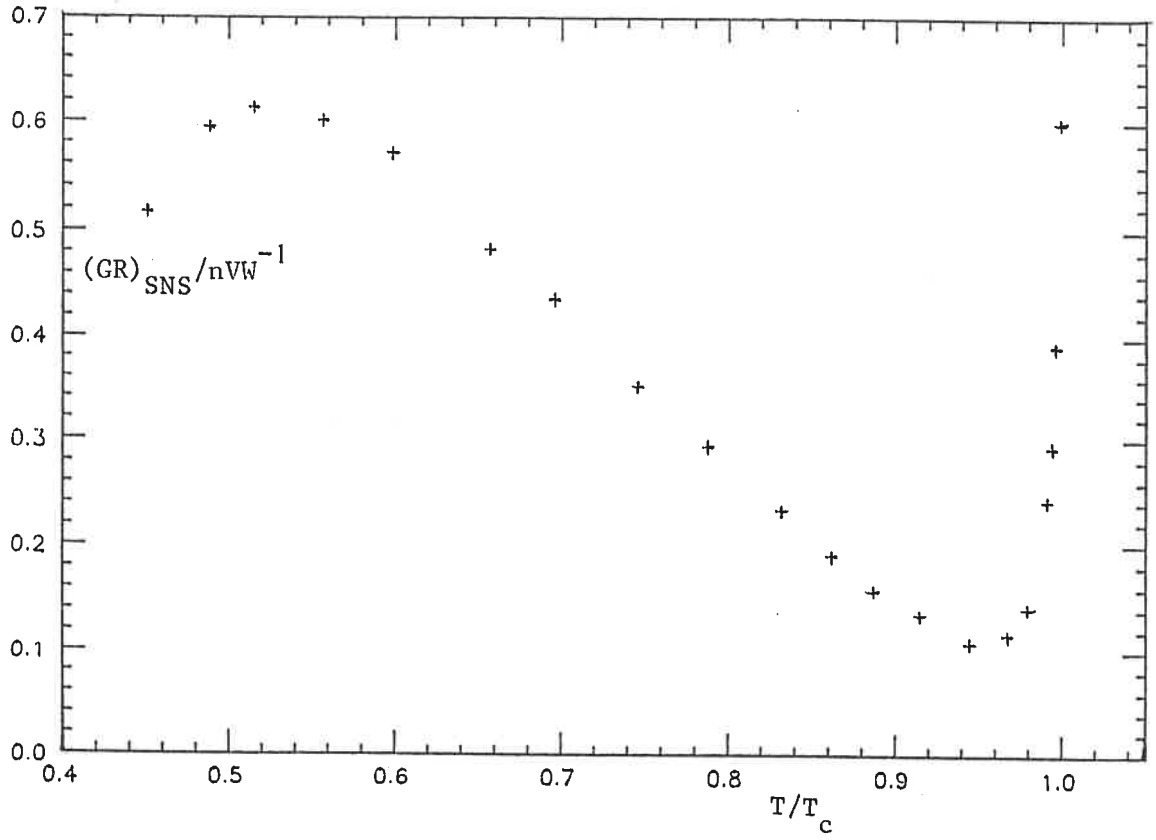

Fig. 8.1 Typical Clean Sample $(GR)_{SNS}$ curve (sample 91).

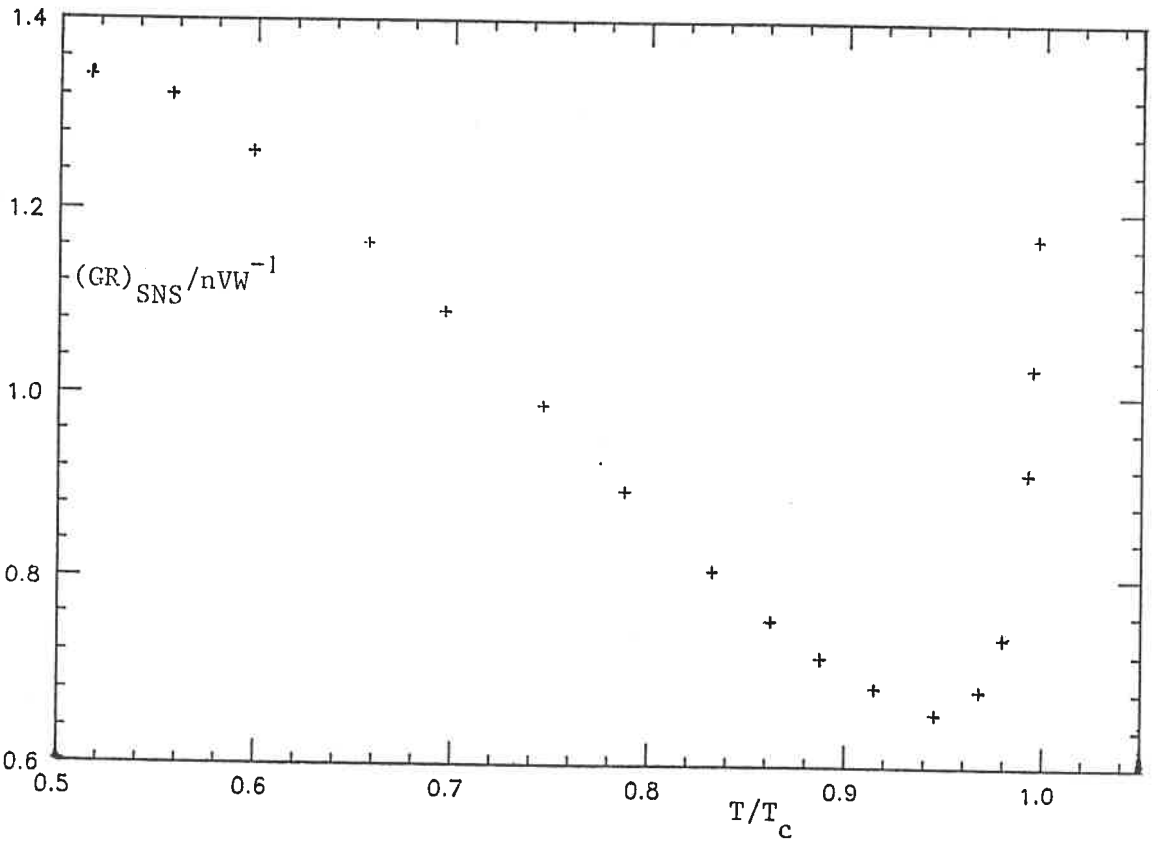

Fig. 8.2 Typical Clean Sample $(GR)_{SNS}$ curve (sample 97).

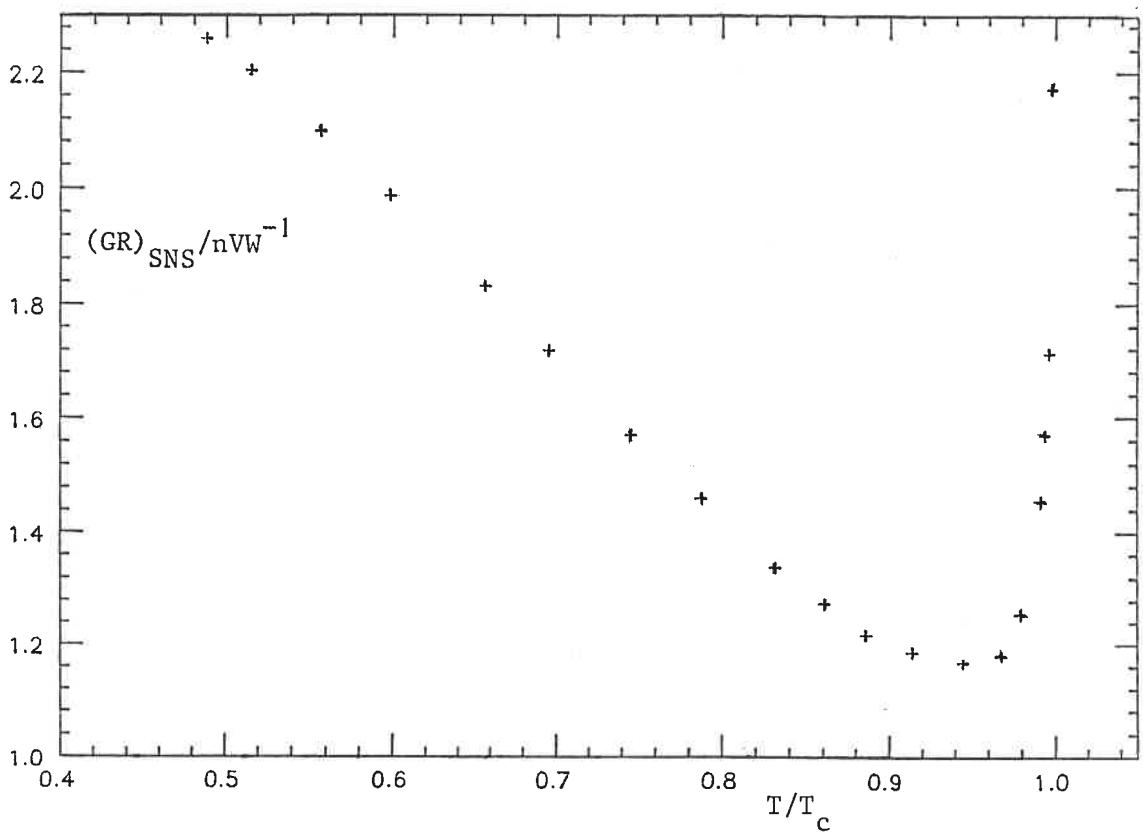

Fig. 8.3 Typical Clean Sample $(GR)_{SNS}$ curve (sample 108).

these samples. As mentioned above, the thermoelectric properties of the slightly dirty In were found to be reasonably reproducible. The thermopower of In just above T_c was estimated from the value of G_{SNS} just above T_c. At this temperature the properties of the sandwich are assumed to be dominated by the In. The values of G for the In above T_c (denoted G_{In}^N in this thesis) in the three samples in Fig.s 8.1-8.3 were +1.8, 2.0 and 2.0 V^{-1} respectively.

It can be seen that the form of $(GR)_{SNS}(T)$ was also fairly reproducible. As expected from the simple theory above, there was a positive divergence below T_c. As with the $R_{SNS}(T)$ this divergence did not begin to appear till above $0.8T_c$. Between about 0.5 and $0.8T_c$ there was a strong fall in $(GR)_{SNS}$ with increasing temperature. The behaviour below $0.5T_c$ was found to be rather less consistent from sample to sample. However, in most samples there was at least a suggestion that the strong rise in $(GR)_{SNS}$ as T was decreased began to level off and in many cases reached a maximum and began to fall again.

It is natural to assume that the strong temperature dependence below $0.8T_c$ is due to the thermoelectric properties of the W. Clearly it is important to verify this by comparison with independent measurements. Garland and Van Harlingen (1974b) have measured G for five different crystals of W of differing purity (see their Fig. 6). For their purest crystals (resistance ratio up to 77,000) G was found to increase strongly with temperature in the range 1-4K. However, with decreasing purity it was found that the reverse trend began to appear. Their most impure crystal (resistance ratio about 9000) was found to have a strongly decreasing G in the temperature range of interest. In all cases the overall sign of G was positive. This is consistent with the present $(GR)_{SNS}$ data; the resistance ratio of the W used in the present work was around 6000. Attempts were made to check this conclusion by making direct measurements of the thermopower of slices of the W used in the present work. The thermopower

of very pure materials is sensitive to the impurities which are present and it is conceivable that the material used in the present work had completely different properties. Unfortunately it was not found possible to independently measure GR for the W reliably. These experiments, and their results, are described in detail in Appendix 3.

The most likely conclusion, therefore, is that the observed trend in $(GR)_{SNS}$ in the range $0.5\text{-}0.8T_c$ is predominantly due to the thermoelectric properties of the W (as opposed to some sort of interface effect). This conclusion is supported by the fact that Van Harlingen (1981a) also ascribed observed temperature dependence of the thermopower well below T_c to the normal metal. (In particular, in the Pb/Cu/PbBi system he ascribed a bump in $(GR)_{SNS}$ at about 4K to the Kondo effect in the Cu).

The reason for the levelling off and sometimes turnover of the $(GR)_{SNS}$ curve below $0.5T_c$ is not known. The fact that this feature appears to be less reproducible than the others from sample to sample implies that it may be something to do with the imperfections of the interface. It could possibly be analagous to the effect related to the proximity effect discussed in Section 5.8. A major complication in this temperature range is that most of the heat is carried in S by phonons rather than by excitations. In addition it is expected that there will be significant temperature drops across the interfaces at these temperatures. The theory discussed in the last section does not apply at all and it is possible that there are various other interface effects. The previous workers (Van Harlingen (1981a) and Battersby (1982)) who made measurements on $(GR)_{SNS}$ using Cu as the normal metal did not see a similar effect at low temperatures. This could be taken to imply that the effect is related to the proximity effect but it should be noted that Van Harlingen did not see an effect with an In/Al/Sn sample (T_c for Al is 1.2K).

8.3.2 Divergence Below T_c

In this section the divergence in $(GR)_{SNS}$ in the slightly dirty samples is compared with the theory discussed in Section 8.2. The approach which has been used is the same as that of Battersby and Waldram (1982). The expressions used for the interface resistance and thermopower have already been quoted but are repeated here for convenience:

$$R_i = 2f(\Delta)(\lambda_3\rho)^S/A \ , \qquad (GR)_i = G^S(\lambda_3\rho)^S/A \ . \qquad (8.5)$$

It should be noted that, as discussed in Section 4.3, these expressions were derived using the one dimensional theory, ie assuming that $(\rho\ell)^N=(\rho\ell)^S$ which is not true in the real materials. They have been used in this chapter in order to be consistent with Battersby and Waldram (1982). As discussed in Section 4.3, the use of a one dimensional theory only results in a scaling of λ_3 and, as long as it is used consistently throughout, it will not affect the value derived for G^S (which is the result of interest in this chapter). This does mean, however, that the values of λ_3 derived in these calculations will not be consistent with those given in Chapter 4.

The method used was firstly to plot R_i against $2f(\Delta)S(T)$ (as before, $S(T)$ is the function which gives the temperature dependence of λ_3 ie $\lambda_3(T)=\lambda_3{}^\circ S(T)$). Such plots are shown in Fig. 4.1 and gave good straight lines for the present samples. These plots enabled $\lambda_3{}^\circ$ to be calculated in each case using (8.5). The next stage was to plot the divergent contribution to $(GR)_{SNS}$ against $S(T)$ using the values of T_c found to give the best fit for $R_{SNS}(T)$. (The divergent contribution to $(GR)_{SNS}$ was obtained by subtracting a background temperature dependent contribution which was probably due to the W (as discussed in the last section). In order to do this a straight line was fitted to the approximately linear region below $0.8T_c$, and the extension of the line up to T_c was taken to be

the background for subtraction) . The resultant plots are expected to be linear with a gradient $G^S(\lambda_3{}^\circ\rho)^S/A$. The intercept is expected to be zero since the subtraction procedure above should leave only the contribution from the Q* in S. Typical plots of this type are given in Fig. 8.4. It can be seen that they are indeed straight lines confirming the theoretical form for the divergence. The intercept is, however, non-zero implying that the subtracted background is not exactly linear in T as was assumed. G^S, the value of G in the superconductor implied by the theory was calculated from the gradient in each case. $G_{In}{}^N$, the value of G just above T_c was measured from the value of G_{SNS} above T_c. The values determined for $\lambda_3{}^\circ$, G^S and $G_{In}{}^N$ for four samples are given in Table 8.1.

Table 8.1

Sample No	$\lambda_3{}^\circ/10^{-5}$m	G^S/V^{-1}	$G_{In}{}^N/V^{-1}$
91	3.4	1.1±0.1	1.8±0.1
97	2.5	1.0	2.0
99	2.8	1.0	1.7
108	2.0	1.2	2.0

The values of $\lambda_3{}^\circ$ vary from sample to sample, as is expected since ℓ varies. It can be seen that the values of G^S and $G_{In}{}^N$ are substantially different in each case. G^S is consistently smaller than $G_{In}{}^N$ by about 0.7 V^{-1}. This is in contrast to the findings of Battersby and Waldram (1984) who found that for their Pb/Cu/Pb samples $G^S=G_{In}{}^N$ within experimental error.

One possible cause of the discrepancy is the fact that the term in G^N in the numerator of (8.3) was discarded. This approximation proved to be reasonable in the case of Pb/Cu but this is no guarantee that it is applicable to In/W in which the values of G^N and G^S are different. If this term is not neglected instead of (8.4) the expression for $(GR)_i$ becomes:

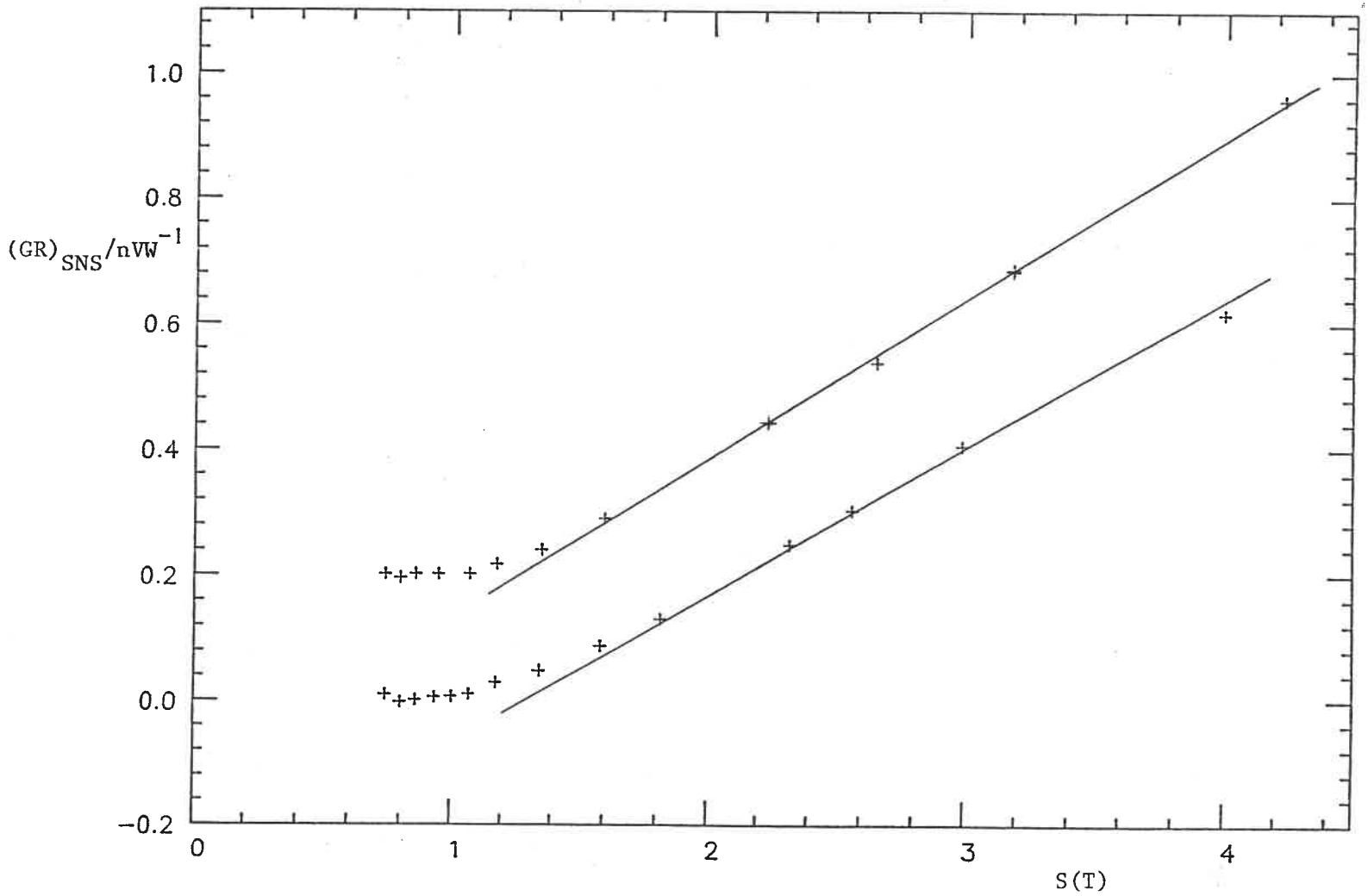

Fig. 8.4 Fits to Theory for Samples 91 and 97. The curve for sample 97 has been displaced upwards by 0.2 nVW^{-1} for clarity.

$$(GR)_i = (\lambda_3\rho/A)[G^S+(1-2f(\Delta))G^N] \qquad (8.6)$$

It can be seen at this stage that the G^N term (which adds another divergent contribution to $(GR)_i$) is unlikely to be very important. If it were significant the plots of the form in Fig. 8.4 would not be observed to be linear (T_c may not be adjusted to improve the fit here since it is fixed at the value which gave the best fit for the R_{SNS} data). However, it is worth checking this conclusion in more detail. This is done by plotting $(GR)i/((1-2f(\Delta))S(T))$ against $1/(1-2f(\Delta))$. It can be seen that this plot is expected to be linear with gradient giving G^S and intercept G^N. The same problem here arises as did with the R_{SNS} data (Section 4.5) that it is necessary to subtract all other contributions to $(GR)_{SNS}$ to give $(GR)_i$. It would be expected that the divergent contribution calculated as above gives $(GR)_i$. Non zero (negative) intercepts are, however, found in the plots using the theory which neglects G^N (the plots in Fig. 8.4) due to errors in estimating the background value of GR. This implies that an additional constant needs to be added to the calculated divergent contribution. This constant was set, in each case, to the value of the intercept obtained using the theory neglecting G^N.

Examples of two of these plots are given in Figs 8.5 and 8.6. It can be seen that the curves are linear, except for the points furthest below T_c (as in the case of the Fig. 8.4 plots). The gradients are found to be the same as in the previous theory which means that the estimate of G^S is the same, as would be expected. This justifies the above conclusion that the term in G^N is not important very close to T_c. The intercepts of these curves can be seen to be small and positive. They imply values of G^N many times smaller than those of G^S.

8.4 Thermoelectric Data from Samples with Pure In

This section discusses thermoelectric data from samples whose casts

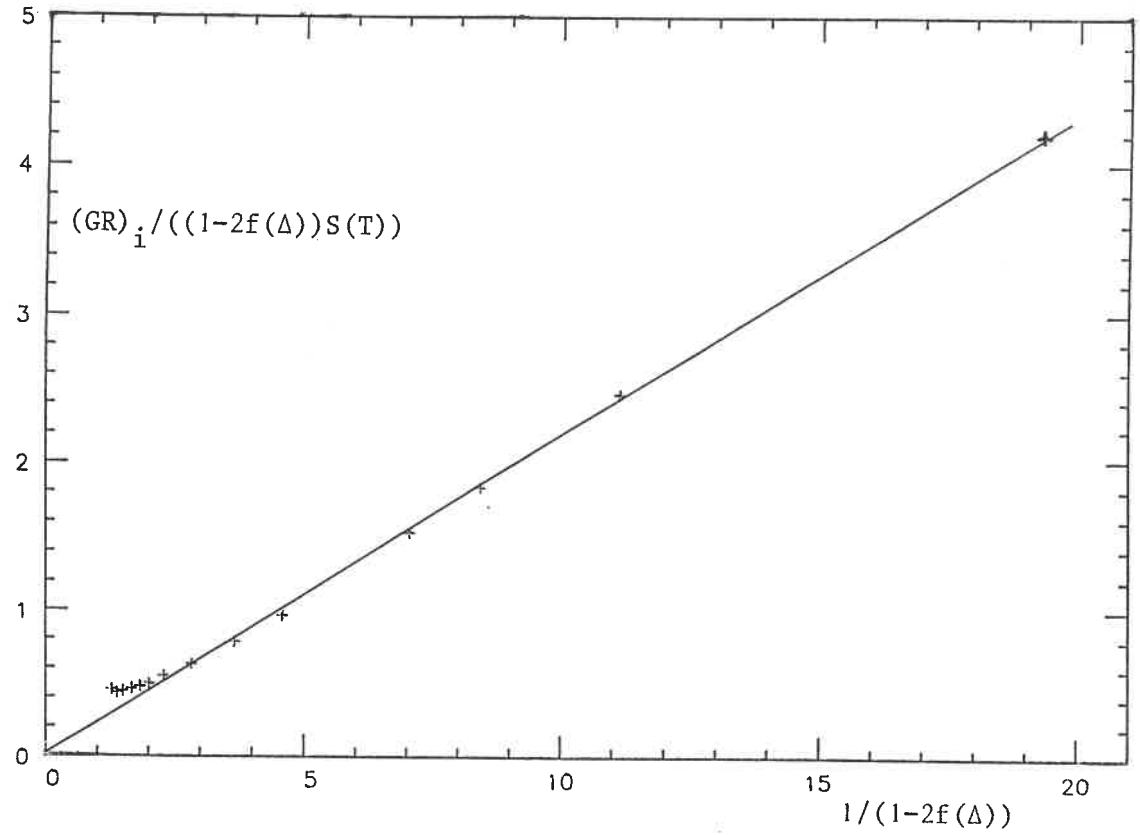

Fig. 8.5 Fit to Fuller Theory (including G^N) for Sample 91.

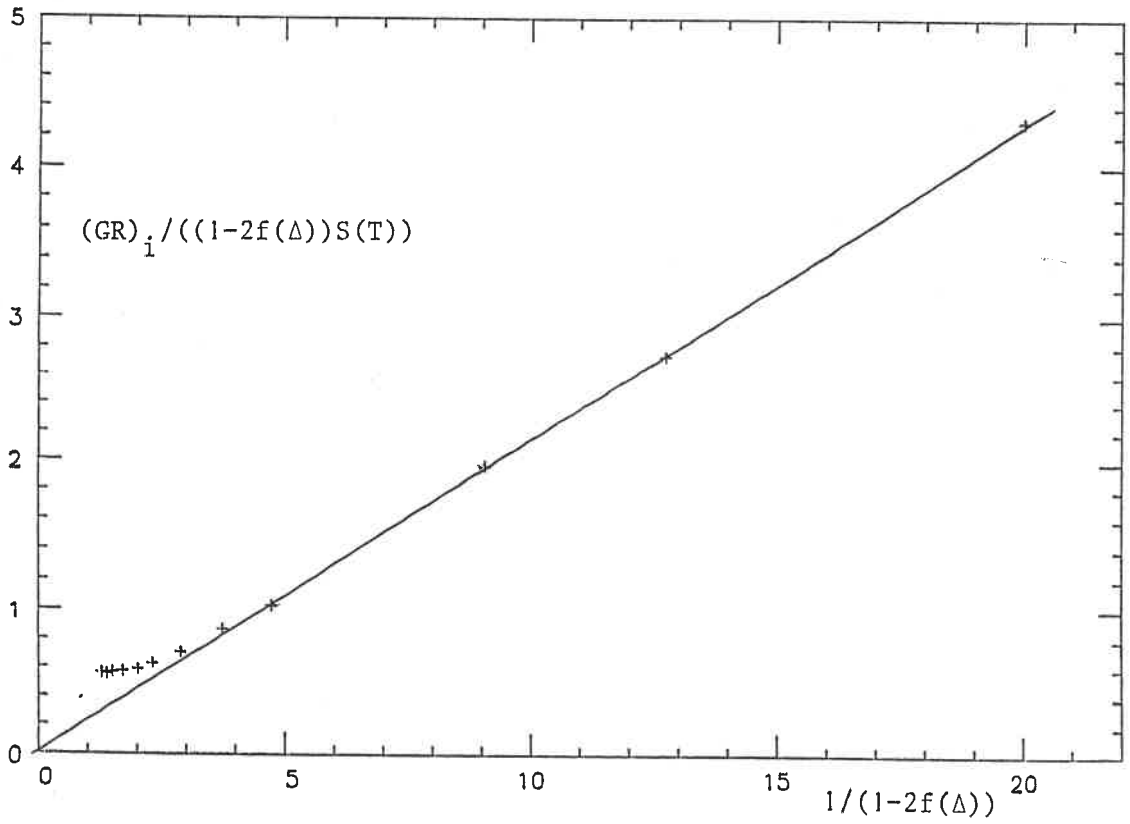

Fig. 8.6 Fit to Fuller Theory (including G^N) for Sample 97.

were made using the In as supplied without any impurities deliberately added. The resistance ratio of this material inferred from the jump in R_{SNS} at T_c was found to be between 8000 and 10000. This seems very high but it should be remembered that In has a very low melting point (about 150 °C) so any metallic impurities would be unlikely to dissolve in it while casting. (Attempts to verify independently the resistance ratio on small pieces with the dipstick proved abortive due to the small values of resistance to be measured).

The thermopower of the In just above T_c (from $(GR)_{SNS}$ just above T_c) was variable: G_{In}^N varied from about -0.2 to +1.0 V^{-1}. This seems a very large range but it should be noted that a similar variation (also including positive and negative values) was observed by Van Harlingen et. al. (1980). Figs 8.7-8.10 show the $(GR)_{SNS}$ curves obtained for sandwiches with various values of G_{In}^N between -0.14 and +1.0 V^{-1}. It can be seen that the behaviour is consistent with the thermoelectric coefficient of the superconducting In being always more negative than that of the normal material. Fig. 8.7 shows the data for the sandwich in which G_{In}^N=1.0 V^{-1}, and it can be seen that in this case there is a positive divergence below T_c as would be expected. However in Fig. 8.8 which shows data for a sample with G_{In}^N=0.7 V^{-1} it can seen that except extremely close to T_c there is no divergence. In a sample with G_{In}^N still lower (Fig. 8.9, G_{In}^N=0.14 V^{-1}) it can be seen that the divergence actually becomes negative, even though the thermopower still jumps to a positive value above T_c. If the normal thermopower is negative (Fig. 8.10) the divergence remains negative and becomes larger.

This data, therefore, is explained if G_{In}^N has an additional negative component relative to G^S. This is consistent with the results for slightly impure In discussed in the last section. There even appears to be some measure of quantitative agreement since the sample in which there is no divergence below T_c (which implies G^S=0) had G_{In}^N=0.7 V^{-1}. As can be seen

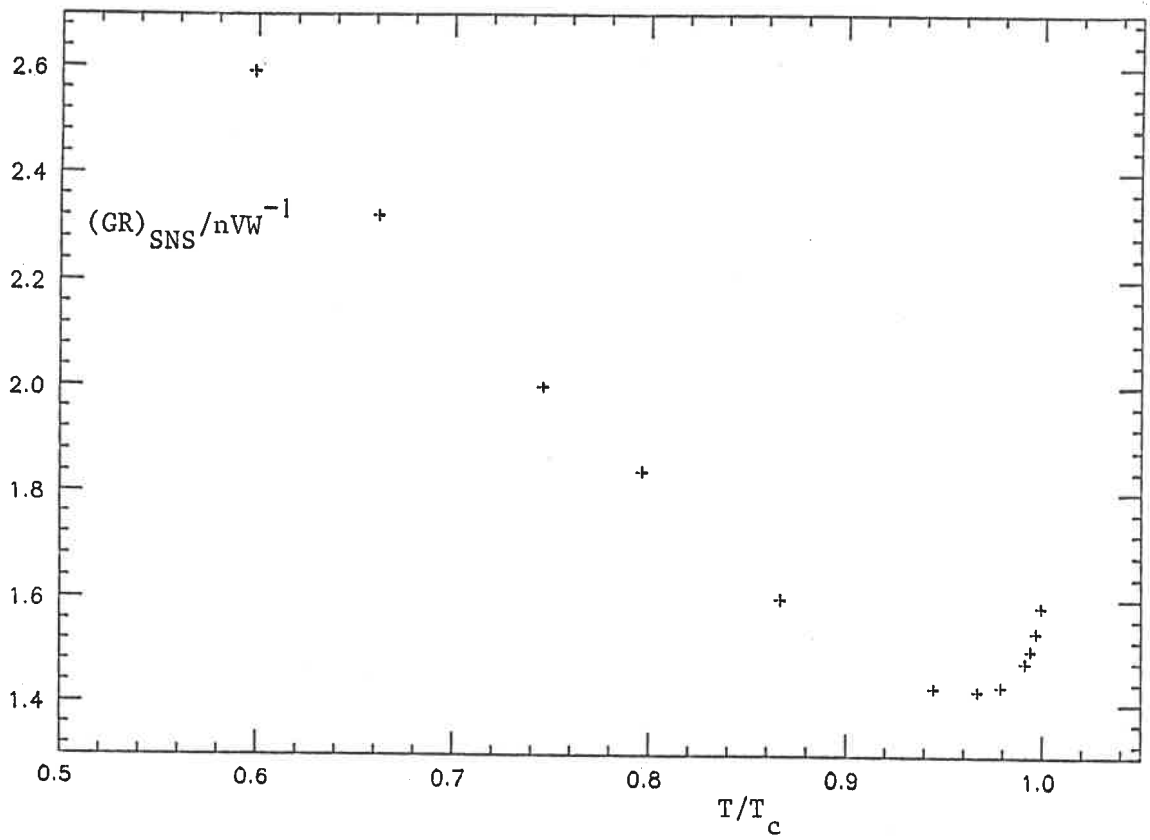

Fig. 8.7 $(GR)_{SNS}$ Curve For Sample with $G_{In}{}^{N}$=+1.0 V^{-1}.

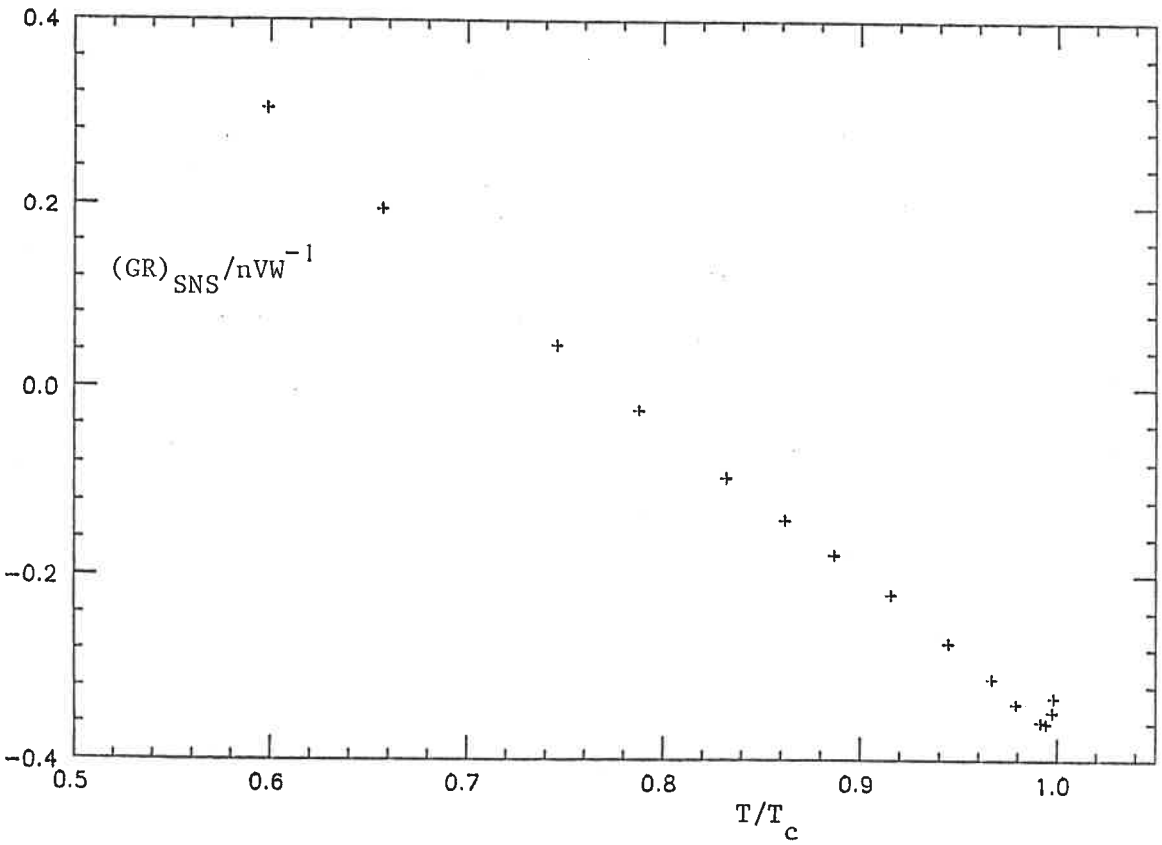

Fig. 8.8 $(GR)_{SNS}$ Curve For Sample with $G_{In}{}^{N}$=+0.7 V^{-1}.

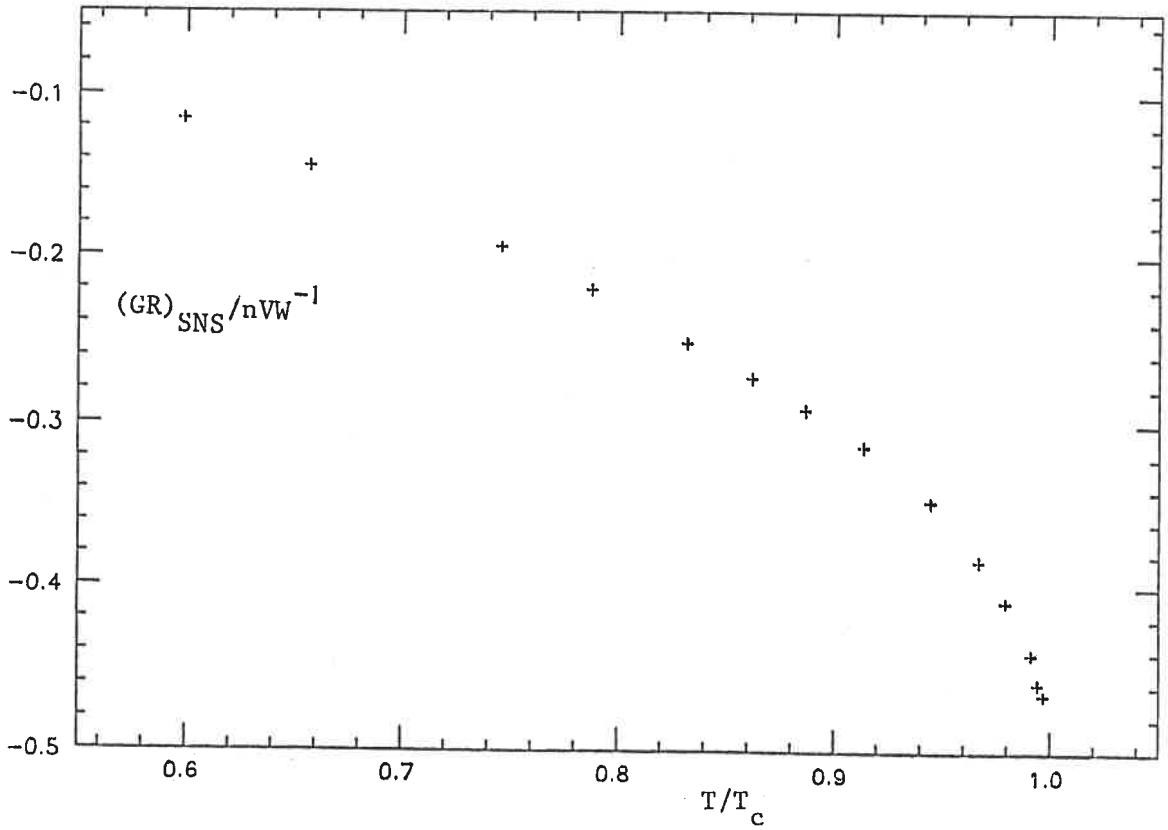

Fig. 8.9 $(GR)_{SNS}$ Curve For Sample with $G_{In}^{N}=+0.14\ V^{-1}$.

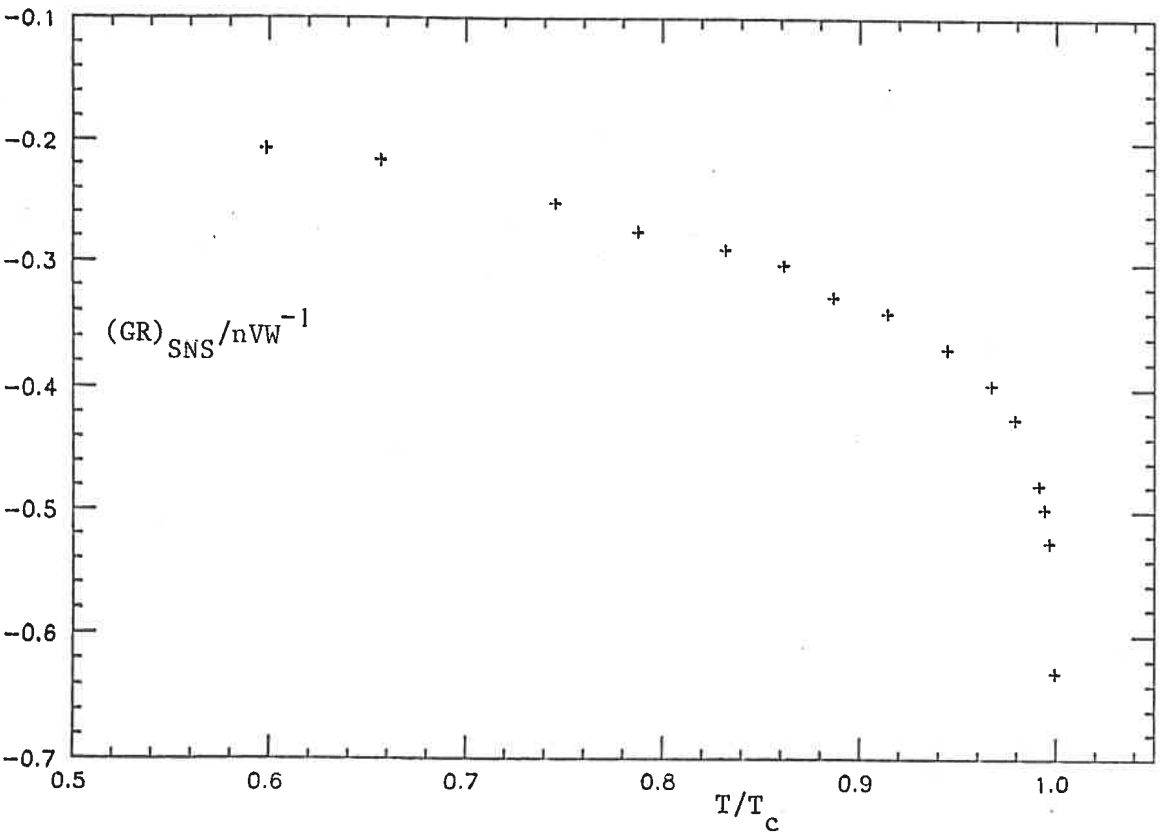

Fig. 8.10 $(GR)_{SNS}$ Curve For Sample with $G_{In}^{N}=-0.14\ V^{-1}$.

from Table 8.1 the results discussed in the last section also imply that G^S is less than G_{In}^N by about 0.7 V^{-1}. One complication which has been ignored so far is that with the thermopower of different samples of In varying so drastically there is no reason to suppose that the casts on the two sides of a given sample had anything like similar properties. However, to a good approximation this does not affect the analysis, since G^S appears linearly in the expression for the interface thermopower, (8.5). One can therefore define effective values of G_{In}^N and G^S by averaging the values in the two casts. This is only approximate because λ_3 will vary from cast to cast (but only as $\sqrt{\rho_s}$). However since no numerical analysis has been done on this data and only the qualitative features are of interest, the problem of the differences between the two casts can be ignored.

8.5 Discussion

The experimental evidence of both the pure and the slightly dirty samples therefore implies that G^S is significantly more negative than G_{In}^N. There are three possible explanations for this. Either there was some systematic error in measuring G_{In}^N, or an unthought of effect contributed an additional divergent thermopower below T_c, or G is for some reason more negative in the superconducting state. These will be discussed in turn.

Systematic errors in measuring G_{In}^N would arise if there were a significant additional positive contribution to the measured G_{SNS} above T_c which was being erroneously ascribed to G_{In}^N. This would be consistent with the fact that the discrepancy is observed to be of roughly the same magnitude independent of the absolute value of G in the case of pure In. The most obvious source of such contributions to G would be the In/Woods Metal joints at the ends of the samples. It is unlikely, however, that these contributions would be large enough to explain the observed

discrepancy, for the normal In casts completely dominate the scattering in the samples. It should be remembered that if the Woods Metal joints and the casts both contribute to G, the overall value of G must be calculated according to the expression:

$$G_{Tot} = (G_c R_c + G_j R_j)/(R_c + R_j) \qquad (8.7)$$

Where G_{Tot} is the total G value measured for the whole sample and subscripts c and j refer to the casts and the Woods Metal joints respectively. It can be seen that the G values are weighted according to the resistance of the part of the sample concerned. The normal resistance of the slightly dirty In casts was around 60nΩ which is much greater than any resistances which are likely to arise at the Woods Metal/In joints. These joints (above T_c of In) are essentially NS interfaces, although it is likely that the In and Woods Metal (which are mutually soluble) interdiffused significantly while the joints were being made. In the case of the very pure In the resistance of the casts was around 10nΩ; in this case the Woods metal joint resistances could conceivably have been significant (but not dominant since that would imply that the resistance ratio of the In was even higher than was assumed which seems very unlikely).

An important point is that (8.7) implies that if the Woods Metal joints were contributing significantly to the observed properties above T_c, the discrepancy observed would be expected to be substantially different for the pure and the slightly dirty samples (becuase R_c differs by about a factor of six). In fact, as mentioned in the last section, the discrepancy is approximately the same in the two cases. A possible explanation would be if the resistance of the joints was proportional to the resistivity of the casts. There is, however, no reason to expect this. The only other conclusion consistent with these observations is that the

resistance of the joints was negligible in both cases as expected from the arguments above. It seems therefore, despite the fact that it would be a simple explanation for the observed discrepancy, that the Woods Metal/In joints were not contributing significantly to G_{In}^{N}.

The other possible source of spurious thermovoltages (as discussed by Battersby (1982)) was the standard resistor. The precautions described by Battersby to avoid possible effects due to conduction of heat to R_{STD} were also employed in the present work. In addition a test for such effects was carried out using a rod of In mounted in the insert instead of a sample. No significant voltages were observed when heat was passed through the superconducting rod which showed that there were no sources of spurious voltage in the voltmeter loop.

A related possibility is that the thermopower of the parts of the casts sampled by the Q* (ie within λ_3 of the interfaces) was not the same as that of the bulk. This could occur if small amounts of oxide or other dirt (in small enough concentrations not to affect the resistance significantly) diffused into the In from the interface. The value of λ_3 at the closest temperatures to T_c at which data was taken (~$0.999T_c$) was still only about 4×10^{-4}m. In order to fit the experimental observations it would have been necessary for the dirt to diffuse a much greater distance from the interface than this. Otherwise, G would have varied significantly over the range of λ_3 in which case the temperature dependence of $(GR)_{SNS}$ in the slightly dirty samples would not have been as expected. In fact, it can be seen in some of the data for samples with pure In casts (Fig.s 8.8 and 8.9) that the points closest to T_c show slight signs of the appearence of a positively diverging term. A problem with this hypothesis is that it is difficult to see how dirt diffusing into the In would give the same discrepancy in both the pure and slightly dirty samples. In the absence of other explanations, however, this sort of hypothesis needs to be considered seriously.

It is possible that below T_c there are extra contributions to the NS interface thermopower. The only effects which would contribute to the discrepancy under consideration here would be those which generate Q* in S and therefore diverge with λ_3 below T_c. For example one possibility, which has been pointed out by Waldram (1986), is that charge imbalance could be generated in S because of the change in the charge of the excitations when they cross the interface. There will be small differences in the charge associated with electrons and holes of the same energy. Unfortunately this effect cannot be the cause of the present discrepancy because close to T_c the excitation spectra on the two sides of the interface become the same. (It is possible, however, that this effect is important some way below T_c).

A similar idea is that significant Q* could be produced at the interface by the small differences between the reflection factors for electrons and holes of the same energy. It turns out, however, that this effect would not produce a divergent Q* at T_c. This is because equal and opposite Q* would be produced on the two sides of the interface which could therefore decay by diffusion of excitations across the interface. This process would be quicker than the bulk Q* relaxation mechanisms close to T_c so a divergence would not be expected.

The other possibility is that the thermopower of the In really does change discontinuously at T_c. Theoretically (Gal'perin, Gurevich and Kozub 1974) it is expected that the thermopower of superconductors is continuous across T_c. Van Harlingen et. al. (1980) have pointed out that this analysis neglects the effect of the superfluid couterflow on the properties of the excitations. This counterflow has a very large velocity close to T_c and could therefore conceivably affect the thermopower. It is, however, difficult to envisage a mechanism which would give an approximately constant jump in G at T_c irrespective of the overall value as is observed in the present work. Any theory to explain these

observations would also have to explain why In is different from Pb (in which the properties have been observed to be continuous at T_c).

As was mentioned in Section 1.5, the previous experimental data on the thermopower of superconductors is mostly inconclusive. Of particular interest to the present work is that of Van Harlingen et. al. (1980) on the thermopower of superconducting In, using the bimetallic ring technique. The results of that experiment, if taken seriously, imply that the thermopower of In below T_c differs from the normal state value by a factor of about $10^3(1-T/T_c)^{-1/2}$. The authors state that this unexpected result could be spurious for a variety of reasons; this seems likely in the light of the more recent work of Van Harlingen (1981a) using SNS sandwiches. With this technique he was able to show that the thermopower of In is constant across T_c to within an order of magnitude (more firm conclusions were not possible because direct measurements of the normal state thermopower were not made). No other data is available on In, and only in the case of Pb (Battersby 1982) is there definite experimental evidence that the thermopower is continuous across the superconducting transition.

In conclusion, the reason for the observed discrepancy between G^S and G_{In}^N is not known. It is difficult to think of systematic errors which would give the observed results although it is possible that G near the interface was different from that of the bulk for some reason. The alternative interpretation, namely that the thermopower of In changes discontinuously at T_c, is in disagreement with presently available theory and with the experimental findings on Pb. Clearly more work needs to be done on this problem.

CHAPTER 9

THERMOPOWER OF DIRTY SNS SANDWICHES

9.1 Introduction.

The subject of this chapter is the thermopower data obtained on the dirty samples whose resistive properties were discussed in Chapters 6 and 7. This area is very poorly understood theoretically; the purpose of this chapter is to present the results obtained and make some general comments about them. Fig. 9.1 shows the $(GR)_{SNS}$ curve of a typical dirty sample compared to the curve for the same sample with pure casts. It can be seen that, as in the case of $R_{SNS}(T)$, there are a number of features to be considered. Section 9.2 considers the shift in the low temperature value of $(GR)_{SNS}$ due to the dirt, analagous to the shift in R_{SNS} considered in Chapter 6. Section 9.3 discusses the divergences below T_c observed in the dirty samples and the temperature dependence at low temperatures is discussed in section 9.4.

9.2 Low Temperature Shift in Thermopower.

As was discussed in Chapter 6, the low temperature electrical resistance of SNS sandwiches is found to increase as dirt is added to S. This is assumed to be due to the increased scattering of the evanescent modes in S. It is natural to ask if there is a similar effect with the thermopower. The effect which has been considered so far is that with dirty superconductors the Andreev reflection process is no longer perfect; some excitations are reflected without change of character. This will clearly cause electrical resistance since while the Andreev reflection process is compatible with electric current flow, normal reflection is not. The effect of this on the thermovoltage in the case where a heat current is flowing is not as clear. Both Andreev and normal reflection are equally incompatible with heat flow which means that the net heat current

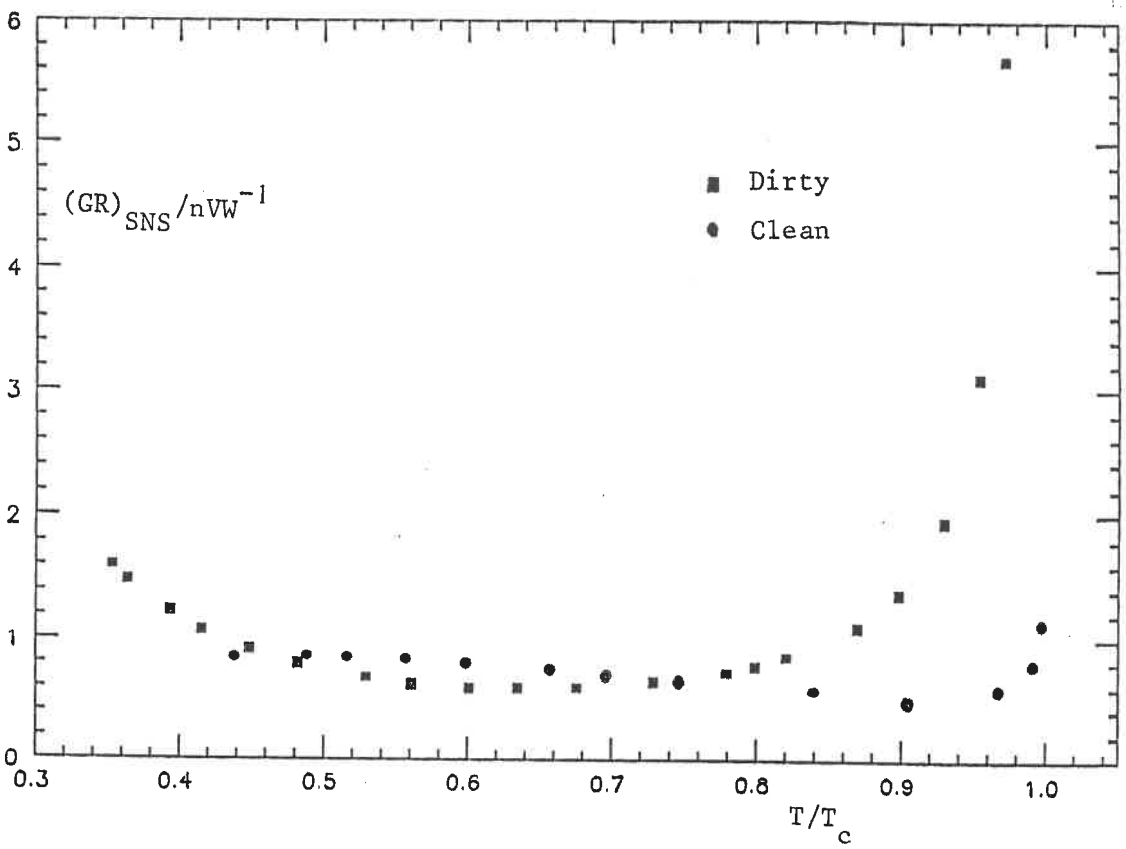

Fig. 9.1 Typical Clean and Dirty $(GR)_{SNS}$ Data.

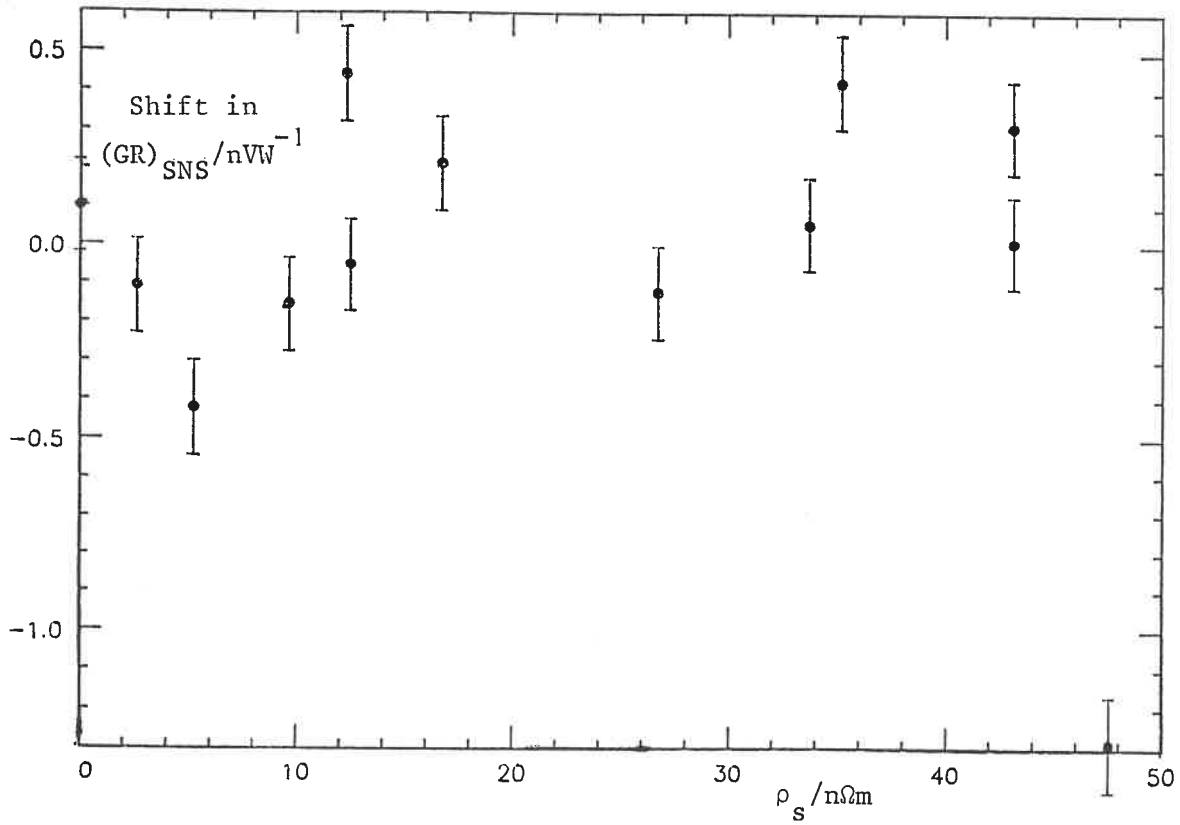

Fig. 9.2 Data for Shift in Minimum Values of $(GR)_{SNS}$ on Recasting.

carried by the low energy excitations will be zero just on the N side of the interface. It is possible that a thermoelectic effect dependent on the concentration of dirt in S could arise from small asymmetries between the scattering of the subgap electrons and holes at the interface. More theoretical work would need to be done in order to determine if an important effect would be expected. It should be remembered that at low temperatures very little heat is carried by the excitations anyway; it would not be surprising if this effect was then not significant.

From Fig. 9.1 it can be seen that another complication is that unlike in the R_{SNS} case $(GR)_{SNS}$ does not appear to tend to a limiting value at low temperatures. In the clean samples $(GR)_{SNS}$ shows signs of falling off as the temperature is reduced whereas in the dirty ones it appears to have a positive divergence. This means that the problem of the limiting thermopower at low temperatures (analagous to the subject of Chapter 6) does not strictly arise. The procedure which was adopted, therefore, was to look at the shift in the value of $(GR)_{SNS}$ at the minima of the curves on recasting. This meant that the temperature at which the dirty interface thermopower was effectively being measured at was $\sim 0.6T_c$ (the temperature at which the minimum occured in the dirty samples). The choice of which points on the curves to use to measure the shift was, of course, fairly arbitrary; as long as they were chosen consistently for all the data any trend should have been visible.

The results obtained in this way are shown in Fig. 9.2. Firstly, it should be noted that the estimated errors are relatively large. These were determined, as in the case of the resistance, by noting the shift in $(GR)_{SNS}$ on recasting with the slightly dirty In, rather than a more dirty alloy (Hence the point at $\rho_S \equiv 0$). There are fewer points on this graph than on Fig. 6.1 because some of the earlier data on that graph was taken using pure In casts initially. It can be seen that there is absolutely no discernable trend in the data, either above or below $\rho \sim 25n\Omega$ (where the

linear trend in the resistance data broke down). The only definite conclusion that can be drawn is that the random errors were larger than the estimate above (also shown as the error bars). It is clear that the thermopower is more sensitive than the resistance to small imperfections on the interface and the changes in these on recasting. In conclusion it can be said that there appears to be no large dependence of the interface thermopower on dirtiness of S at about $0.6T_c$. However in order to reach any definite conclusions it would be necessary to repeat the experiments using a sample preparation method which could be relied on to produce extremely clean and reproducible interfaces.

9.3 Divergence Below T_c.

This section and the next one look at the question, analagous to that discussed in Chapter 7, of the temperature dependence of $(GR)_{SNS}$ when S is dirty. This section looks at the behaviour just below T_c where a divergence is observed as would be expected. The next section looks at the less well understood question of the low temperature divergence which is observed in these samples. Fig. 9.3 shows the $(GR)_{SNS}(T)$ curves obtained just below T_c for a number of dirty samples. Since the present interest is in their divergence, these curves have had constants added or subtracted in order to make their minimum values zero. It can be seen that, as in the case of $R_{SNS}(T)$ the dirty samples have much larger divergences than the pure ones. The size of the divergence, however, was not always seen to increase monatonically with concentration.

These results have been examined in more detail only in terms of the simple theory expressed by (8.5). This theory is more acceptable with dirty superconductors than the corresponding one in the case of the resistance; as discussed in the last section, experimentally there is no obvious subgap contribution to the thermopower from making S dirty. The results were therefore plotted (as in Section 8.3.2) in the form $(GR)_{SNS}$

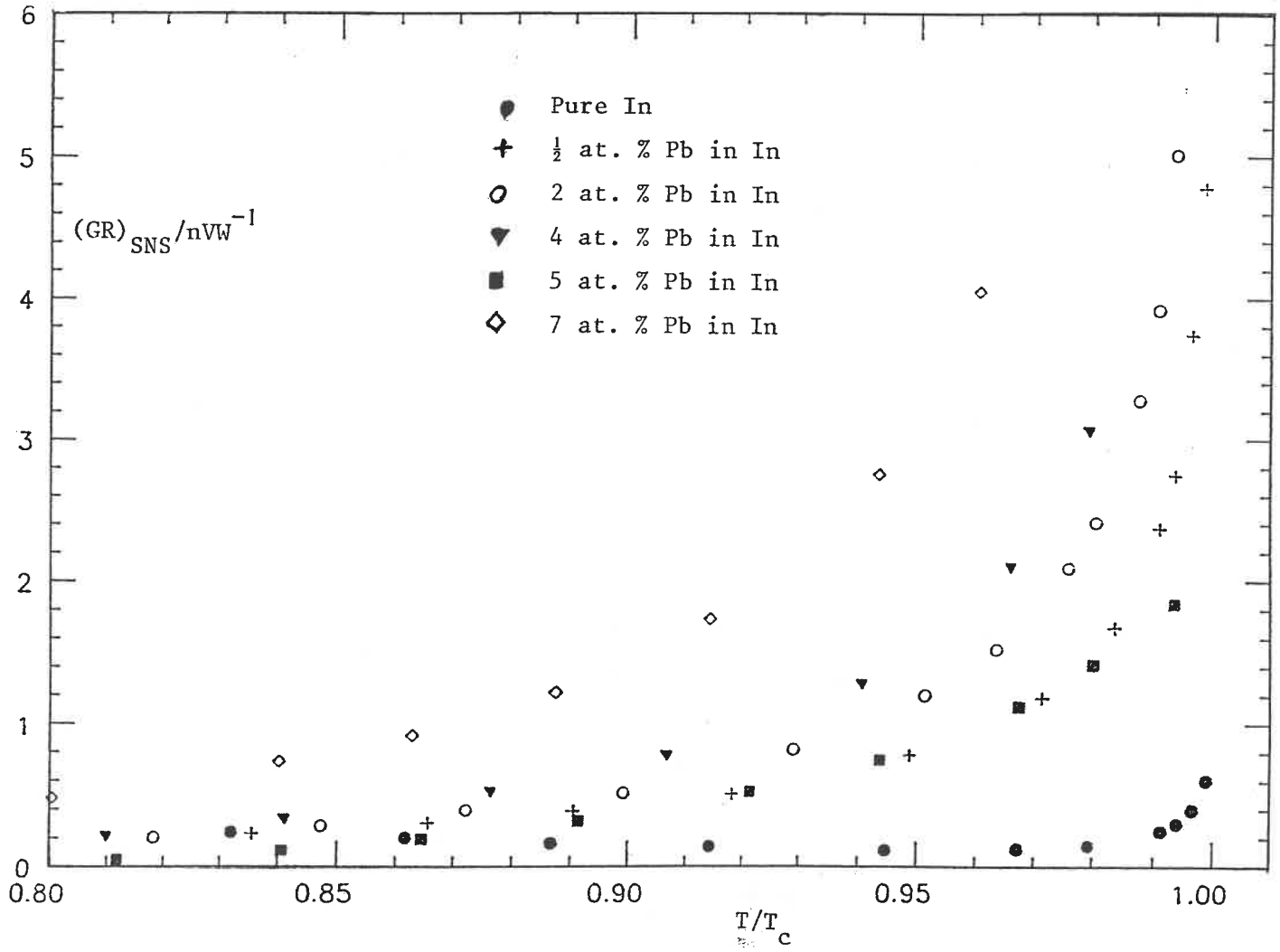

Fig. 9.3 Divergence of Dirty $(GR)_{SNS}$ Curves.

against S(T). Examination of the expression (8.5) while remembering that λ_3 is expected to be proportional to $\sqrt{\rho_s}$ shows that the that the plots are expected to be linear, with gradients proportional to $(\sqrt{\rho_s})G^S$. The results of this analysis are shown in Table 9.1 (The values of G^S given are the measured values of $G_{In}{}^N$ ie the values of G directly measured just above T_c. Any discrepancy between G^S and $G_{In}{}^N$ similar to that discussed in the last chapter is therefore neglected in this approximate treatment).

Table 9.1

% Pb	Sample No	ρ_s/ nΩm	G^S/ nVW^{-1}	Gradient/ nVW^{-1}	Grad/$\sqrt{\rho_s}G^S$ $\Omega^{-0.5}$
0.5	115A	2.55	1.68	1.8	0.68
1	89A	5.37	1.53	2.5	0.71
2	114A	9.77	1.33	3.3	0.78
3	97A	12.50	1.13	3.15	0.79
4	86A	16.28	1.19	(3.0)	(0.62)
5	85A	21.46	1.05	(2.1)	(0.43)
7	99A	35.2	1.23	16.0	2.19

It was not felt worth analysing the data for the two samples which were clearly deviant from the R_p vs ρ_s linear relation. Similarly the data from the high concentration region in which the aforementioned relation was not obeyed were not analysed in detail (although one sample was).The reason in both these cases was that this analysis is, in any case, very speculative and there is little to be gained by using it on samples for which even the resistive behaviour is not understood.

In four of the samples given in Table 9.1 the curve was found to be a good linear relation; an example is shown in Fig. 9.4. The curve for the 0.5% Pb sample was found to be not quite such a good fit (Fig. 9.5). The fits for the 4% and 5% Pb samples were found to be extremely poor (the

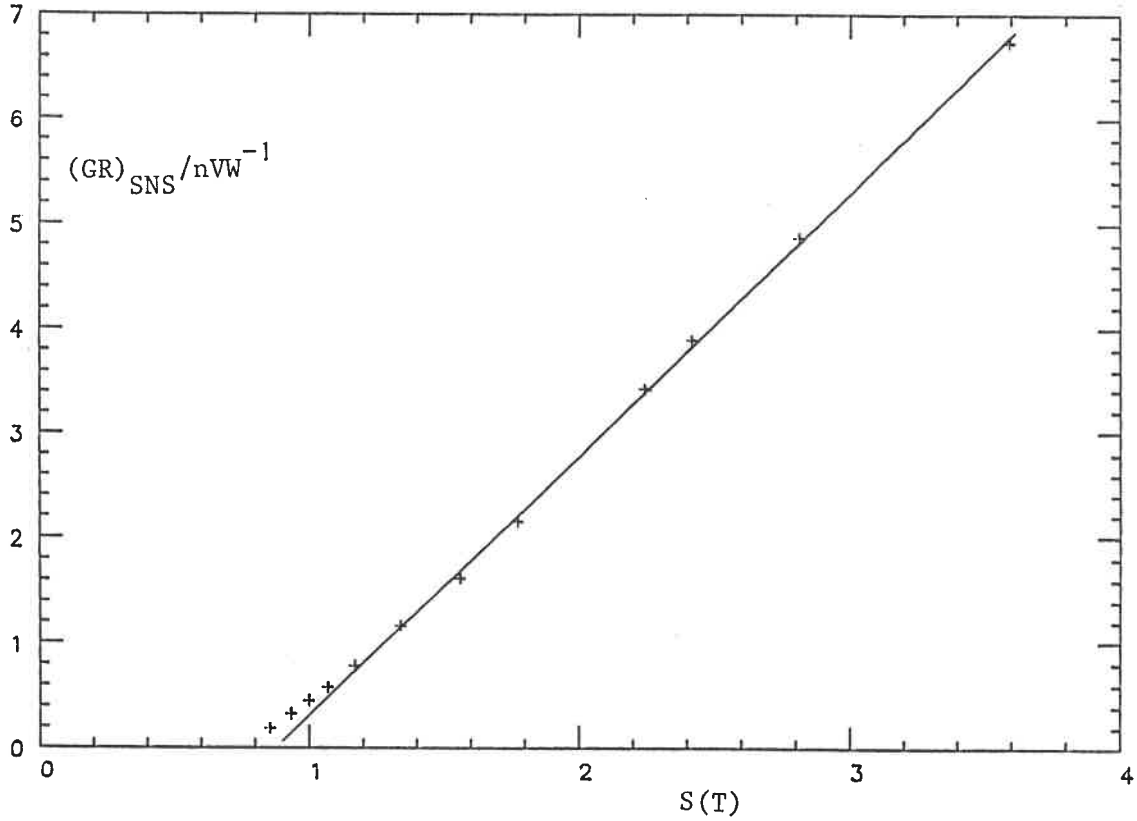

Fig. 9.4 Fit to Theory for $(GR)_{SNS}(T)$ for 1 at.% Pb Sample.

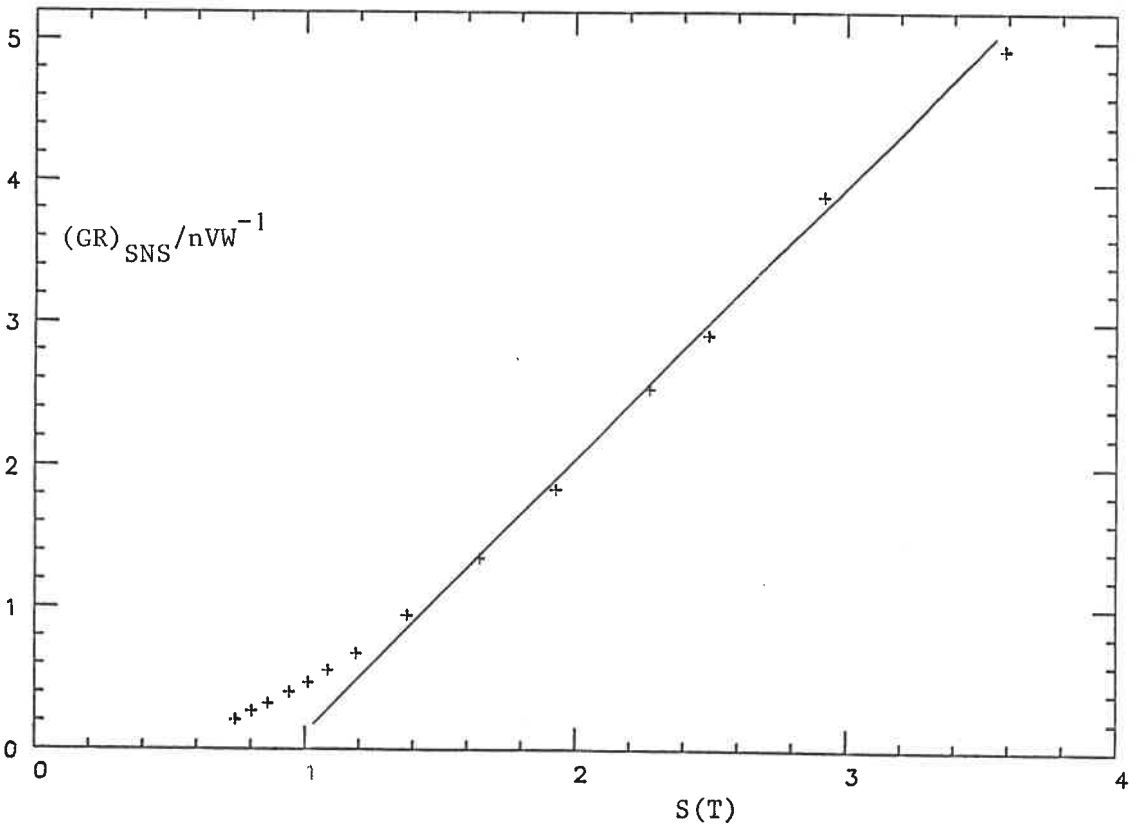

Fig. 9.5 Fit to Theory for $(GR)_{SNS}(T)$ for 1/2 at.% Pb Sample.

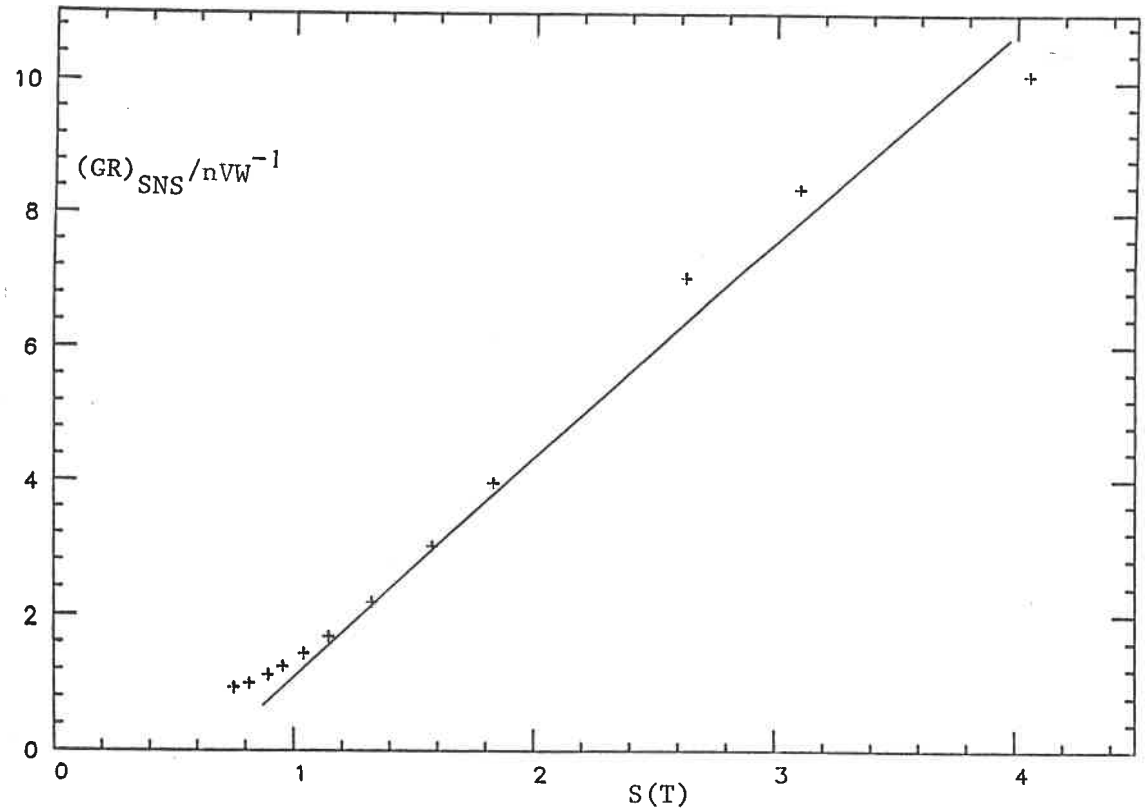

Fig. 9.6 Fit to Theory for $(GR)_{SNS}(T)$ for 4 at.% Pb Sample.

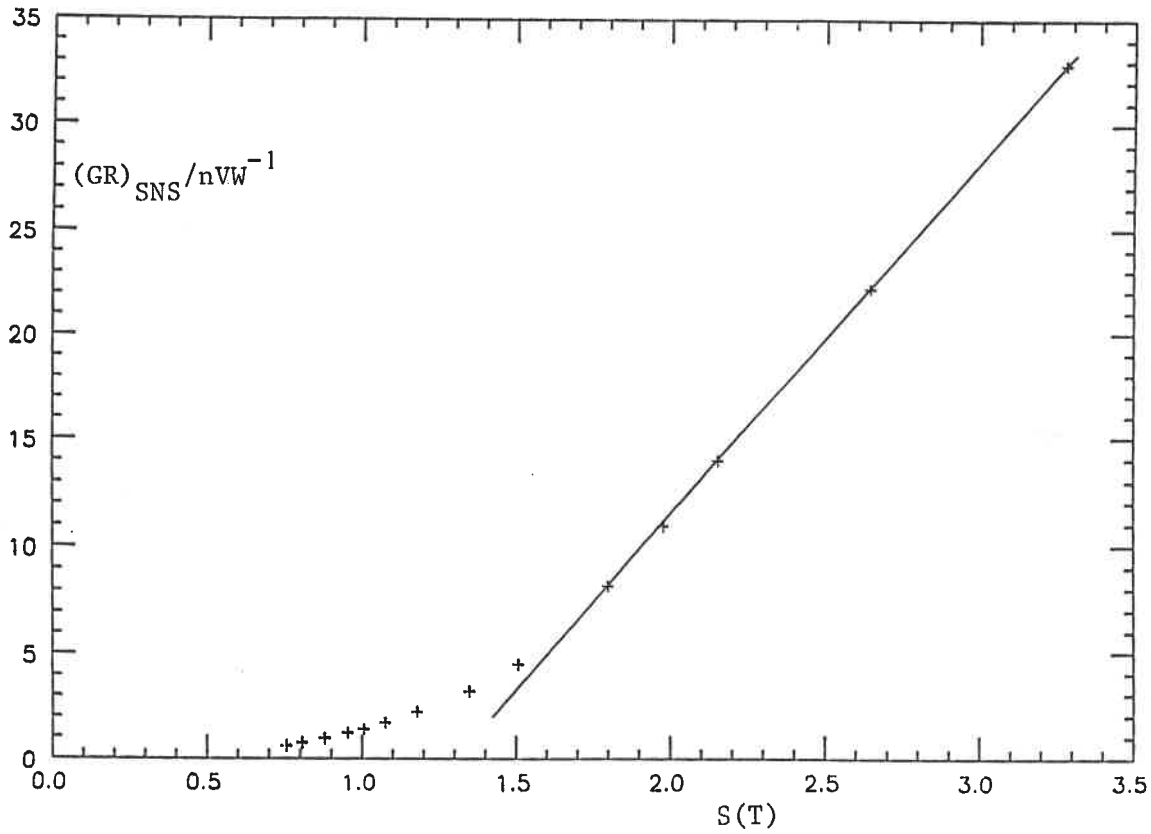

Fig. 9.7 Fit to Theory for $(GR)_{SNS}(T)$ for 7 at.% Pb Sample.

curve for the 4% sample is shown in Fig. 9.6). For this reason the values of the gradients should be treated with caution (and are given in brackets in table 9.1). The parameter (gradient)/$\sqrt{\rho_s G^S}$, which would be constant if the theory was obeyed, can be seen to vary systematically by about 12% between the 0.5 and 3% samples. The fact that this trend breaks down for the 4% and 5% samples is further evidence that these samples are in some way different. It can, therefore, be concluded that the simple theory expressed by (8.5) approximately fits the present data in the range up to about 3% Pb. Above this range there are larger discrepancies.

Not surprisingly the 7% sample was found to have rather different characteristics. The curve (Fig. 9.7) was found to be linear but only relatively close to T_c. The gradient (and consequently (gradient)/$\sqrt{\rho_s G^S}$) was found to be much larger than in the other samples. Since even the resistance data is not understood in this concentration range, no attempt has been made to explain this.

9.4 Behaviour of $(GR)_{SNS}$ at Low Temperatures

It was mentioned in Section 9.2 that in dirty samples, a positive divergence in $(GR)_{SNS}$ is seen to appear at low temperatures. The low temperature behaviour of $(GR)_{SNS}$ for several samples is shown in Fig. 9.8 (the curves have again had constants subtracted to give them a value of zero at the minimum). It can be seen that the 2%, 3% and 4% samples had very similar curves at low temperatures. The divergence is seen to be smaller in both the 0.5% and 7% samples. A similar temperature dependence has been seen by Battersby (1982) in eutectic PbBi/Cu interfaces.

The cause of the apparent divergence at low temperatures is not known. It is necessary to ask what is likely to have such a rapid temperature dependence at temperatures so far below T_c. The obvious answer is that the thermal resistivity of the interface diverges at low temperatures (Andreev 1964). This reflects the reduction in the number of

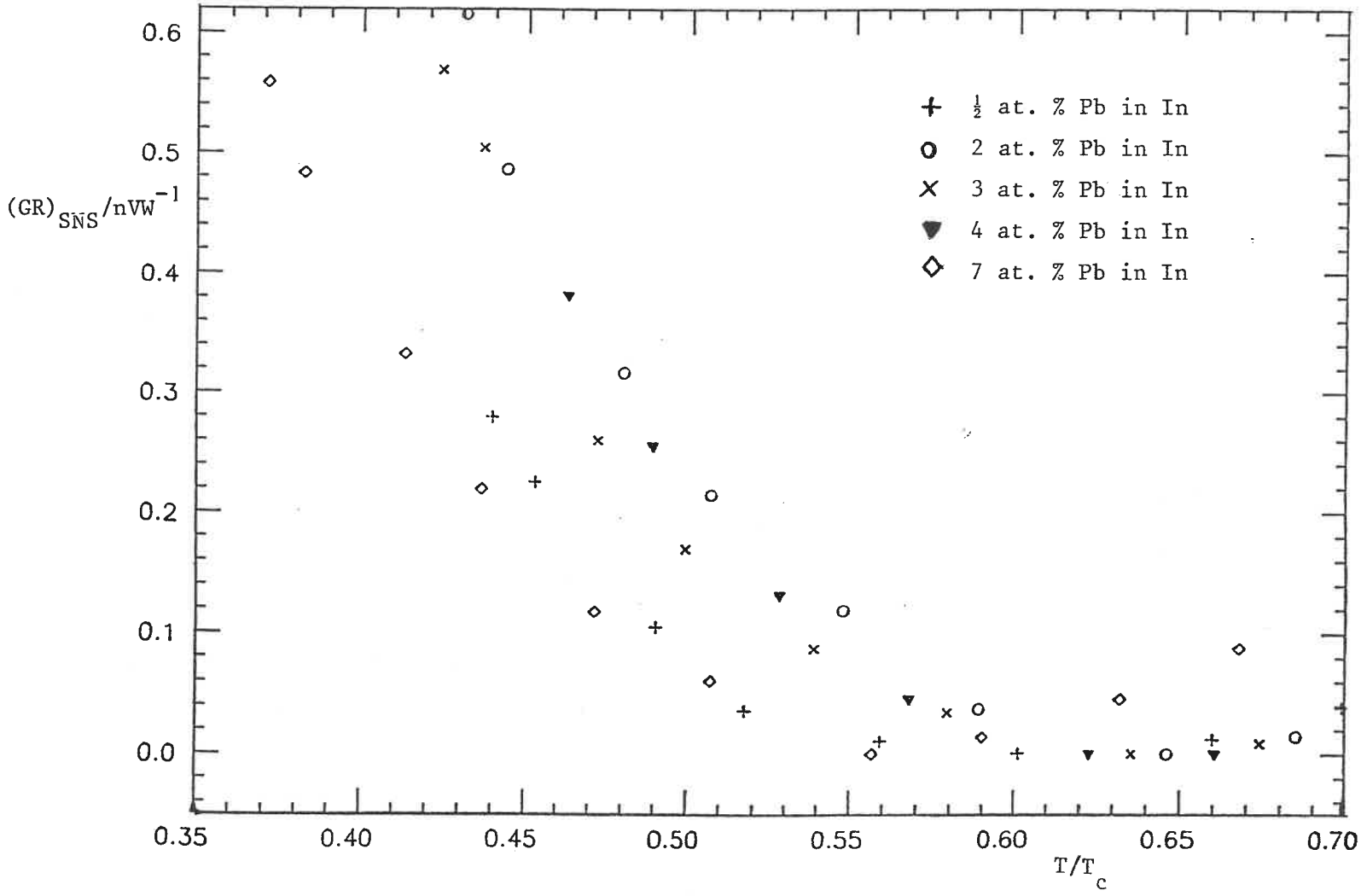

Fig. 9.8 $(GR)_{SNS}(T)$ Curves at Low Temperatures.

supergap excitations as the temperature is reduced. It is in this temperature range that the dominant heat carrying mechanism in S changes from being the excitations to the phonons. It seems very likely that the observed effect in $(GR)_{SNS}$ is related to this transition and is, therefore, outside the scope of the theories discussed above.

CHAPTER 10

CONCLUSIONS

10.1 Introduction.

The purpose of this chapter is to summarise briefly the work so that the reader may obtain an overview of what has been acheived. It will be seen that positive contributions have been made to several problems. There are still unsolved questions, however, especially in the fields of the low temperature resistance of dirty SNS sandwiches and the thermoelectric effect.

10.2 Sample Preparation.

A major part of this work was the lengthy process of developing a suitable sample preparation technique. It was decided to use W for the normal metal and In for S. Several different approaches were tried, but the final preparation technique consisted of melting In onto orange hot W in high vacuum. The important advantage of this method over the others which were tried was that the In coated the W surface while it was orange hot and clean. There was, therefore, no opportunity for the surface to become contaminated after cleaning. This method was found to produce interfaces comparable in quality to those used by previous workers. The resistance and thermopower was measured in the range 1.2-4.2K in both samples with pure In and samples in which the In contained up to 10% Pb.

10.3 Resistance of Clean Samples.

This was the first time that In/W/In sandwiches had been used, most previous workers having used Pb/Cu/Pb. For this reason the first priority was to check that the $R_{SNS}(T)$ data from the clean samples fitted the theory found by previous workers to fit Pb/Cu/Pb just below T_c. The theory used for this was that of Battersby (1982). This is a version of the

general theory of Waldram (1975) which assumes that there is no normal reflection of excitations at the interface. It was found that this theory fitted the data on In/W/In sandwiches, although the more complicated form gave more ambiguous values for the parameters than in the case of Pb/Cu/Pb.

Attempts were made to improve on the simple theory in order to explain the behaviour of $R_{SNS}(T)$ well below T_c. In particular, an explanation was sought of the form of the fall in R_{SNS} observed as T is increased from about 0.3 to $0.8T_c$. It was known from previous work that this feature was related to sources of normal reflection (mismatch, oxide etc.) at the interface. The approach to this problem was to calculate more realistic boundary conditions by solving the Bogoliubov equations with model potentials. Two models were tried in which the interface was represented by a step and a delta function in the normal potential. These models were successful in that they predicted R_{SNS} falling with rising temperature at low temperatures before reaching a minimum around $0.8T_c$. However, it was found that the curvature of the R_{SNS} curve predicted in the range $0.3\text{-}0.6T_c$ was incorrect (it was found experimentally that the gradient of the curve became smaller again at the lowest temperatures whereas the theory predicted it should continue to increase as the temperature was reduced). This problem was solved when the proximity effect was included in the theory; the effect of the energy gap extending some distance into the W was to move the point of reflection further from the imperfections of the interface and therefore to reduce the normal reflection.

10.4 Resistance of Dirty Samples.

Data was taken on dirty samples to determine the effect on $R_{SNS}(T)$ of adding dirt to S. The most important problem investigated was the effect of adding dirt on the low temperature interface resistance. In order to

investigate this a technique was developed of remelting the In in the samples and adding Pb impurity in order to determine the effect on the resistance. A theory of Pippard (1984) proposes that the interface resistance is due to scattering, in S, of the evanescent tails of subgap excitations. It predicts that the resistance will be proportional to the resistivity of the superconductor. The only other previous experimental work on this problem (by Harding (1973) on Pb/Cu/Pb) found an approximately linear dependence as expected but the magnitude of the resistance was about three times less than the theory would suggest. In the present work a good linear dependence was found for Pb concentrations of less than 5% with the data becoming irreproducible for higher concentrations. For the linear portion the resistance was found to be about five times less than that predicted by the theory. The reason for this is not known for certain but it is thought it may be related to mismatch of the Fermi surfaces in the two metals. The reason for the breakdown of the linear dependence above 5% is also not known; it may be related to a known Fermi surface-Brillouin zone interaction at about that concentration or it may be due to some imperfection in the more dirty samples.

The other work on the resistance of dirty samples concerned the form of $R_{SNS}(T)$ of the samples with up to 5% Pb. In order to calculate the expected curve, the form of the subgap boundary conditions inferred from the low temerature behaviour was inserted into the theory of Waldram (1975). The resultant theory was found to be a good fit to the experimental data. This was the first such agreement for this problem. (The only previous attempt (Harding et. al. 1974) to fit similar data (on Pb/Cu/Pb) gave very poor agreement because the phase factor was neglected.)

10.5 Thermopower of Clean Samples.

The thermopower data on the samples with clean In divided into two groups. Most of the samples used In with very small amounts of Pb added to make the thermoelectric properties reproducible. The data from these samples close to T_c, was analysed using the theory of Battersby and Waldram (1984). It was found, in contrast to the findings of Battersby (1982) on Pb, that there appeared to be a discontinuity in the thermopower of In at the superconducting transition temperature. The normal state thermopower appeared to be consistently more positive than that below T_c. The first samples used had very pure In (as supplied by the manufacturer) whose thermopower varied significantly from sample to sample. The results from these samples appeared to be in agreement with the conclusion that the thermopower of the superconductor is more negative than that of the normal metal by a roughly constant amount (irrespective of the overall value). The reason for the apparent discrepancy is unknown, but clearly there must be either some systematic error or a real discontinuity in the thermopower of In at T_c. The former hypothesis seems attractive but when investigated in detail it is difficult to explain the observations. It seems possible therefore that the results imply a discontinuity in the thermopower at T_c which contradicts previous theoretical predictions and the experimental results of Battersby on Pb.

10.6 Thermopower of Dirty Samples.

Finally, there was the data on the thermopower of the dirty samples. This subject is the least well understood theoretically. The obvious question to look at was the problem analagous to the low temperature interface resistance, ie the low temperature interface thermopower as a function of the concentration of Pb in the In. On very simple theoretical grounds it is not clear if an effect is expected (in contrast to the resistance case). Experimentally the question is complicated by the fact

that in the dirty samples the $(GR)_{SNS}$ curve does not appear to tend to a constant value at low temperatures. For this reason an attempt was made to measure the absolute shift of the curves by comparing the minima of the $(GR)_{SNS}$ curves. Unfortunately the experimental errors turned out to be quite large. No definite trend was seen in the shift with concentration within experimental error. Two features are noticable in the $(GR)_{SNS}$ curves of the dirty samples. Firstly, as in the case of the resistance, the divergence below T_c is observed to be much larger in dirty samples and to extend to much lower temperatures. The simple theory, used for the clean samples was also applied to this and was found to fit approximately for samples with 3% Pb or less. Secondly, an apparent divergence was observed in $(GR)_{SNS}$ with falling temperature at the lowest temperatures at which data was taken. The reason for this feature is unknown.

10.7 Suggestions for Further Work.

There is clearly scope for further work (both experimental and theoretical) to attempt to solve the unanswered questions relating to the resistance of the dirty samples and the thermoelectric results. In the opinion of the author the crucial problem to be confronted is that of producing better characterised samples. In several parts of the work described in this thesis the question arose of whether an apparent effect was "real" or whether it was caused by some defect in the samples. The sample preparation techniques used both by Battersby and the author were relatively crude. There was plenty of scope to explain unexpected effects in terms of the sample not being quite the system it was assumed to be in the theory. Using modern U.H.V. and epitaxial growth techniques it would presumably be possible to produce samples in which the detailed nature of the system under study would be known with more certainty. An experimental investigation of the unexplained features of this work would not be worth carrying out unless such facilities were available.

APPENDIX 1

WALDRAM THEORY OF SN INTERFACES

In this appendix the theory of Waldram (1975) is summarised, concentrating on giving the results which are used in this thesis. A modification to the subgap boundary conditions which was suggested by Waldram (1986) is included. The excitations in this theory are described by the functions $g_n(E)$ where $g=f-f_o$ is the deviation of the occupation number from equilibrium and $n=1-4$ is the number of the branch (see Fig. 1.2). By symmetry, in the usual electric carrying state, $g_1=-g_3$ and $g_2=-g_4$. q and j are also introduced defined by $q=g_1-g_2$ and $j=g_1+g_2$. q and j are the contributions to the charge imbalance and the electric current repectively at that energy. J* and Q* are defined as the integrals over E of j and q respectively.

The boundary conditions are specified by

$$q^N = \gamma_{11} q^S + \gamma_{12} j^S$$
$$j^N = \gamma_{21} q^S + \gamma_{22} j^S \qquad \text{(A1.1)}$$

for $E>\Delta$, and

$$-q^N/j^N = P \qquad \text{(A1.2)}$$

for $E<\Delta$

Here q^N and q^N are the values of q just on the normal and superconducting sides of the interface respectively and the same for j. It is important to note that in general all the γs and P are energy dependent. Making reasonable estimates of these quantities is the central problem in constructing theories of SN interfaces.

Waldram distinguishes 3 scattering lengths: ℓ_1 for elastic scattering, ℓ_2 for ordinary inelastic scattering, and ℓ_3 for branch crossing processes in S. The mean free path for any process is denoted simply by ℓ. These are used to construct a Boltzmann equation which is solved subject to the boundary conditions above. Two diffusion lengths are defined: $\lambda_2=[(1/\ell)(1/\ell_2+1/\ell_3)]^{-0.5}$ is a diffusion length for all types of inelelastic scattering, $\lambda_3=(\ell\ell_3)^{0.5}$ is the diffusion length for branch crossing processes. The latter turns out to be important because it is the characteristic length with which Q* decays exponentially into S.

The result derived for the resistance of the interface in terms of number of mean free paths in N, Q_i is

$$Q_i = \frac{W_1^N - Z}{(\ell/\lambda_3)^S W_3^S + (\ell/\lambda_2)^S(1-W_3^S) + (\ell/\lambda_3)^N(1-W_1^N+Z)} \qquad (A1.3)$$

Where Z is defined by

$$Z = \frac{(\ell/\lambda_3)^S - (\ell/\lambda_2)^S}{(\ell/\lambda_2)^N + (\ell/\lambda_2)^S}(W_2^N W_4^S - W_1^N W_3^S) \qquad (A1.4)$$

The W_i are defined by:

$$W_i = (1/f(\Delta))\int_{\Delta}^{\infty} -f'(E)u_i[(\ell/\lambda_2)^N+(\ell/\lambda_2)^S]dE \qquad (A1.5)$$

Where:

$$u_1 = A/D \qquad A = \gamma_{12}(\ell/\lambda_2)^S - \gamma_{11}$$

$$u_2 = u_4 = -1/D \qquad B = \gamma_{22}(\ell/\lambda_2)^S - \gamma_{21} \qquad (A1.6)$$

$$u_3 = C/D \qquad C = \gamma_{12}(\ell/\lambda_2)^N - \gamma_{22}$$

$$D = (\ell/\lambda_2)^N A - B$$

for $E>\Delta$

or:

$$u_1 = \frac{P}{1 + P(\ell/\lambda_2)^N} \qquad (A1.7)$$

$$u_2 = 0$$

For $E<\Delta$

For practical calculations it is also useful to know the relations between the above boundary conditions and the reflection and transmission coefficients. These are easily derived from (A1.1) and (A1.2) to be:

$$\gamma_{11} = \gamma_{22} = (T_N+T_A)/(T_N-T_A)$$
$$\gamma_{12} = -2R_N/(T_N-T_A) \qquad (A1.9)$$
$$\gamma_{21} = -2R_A/(T_N-T_A)$$

$E>\Delta$

And:

$$P = R_N/R_A \qquad (A1.10)$$

$E<\Delta$

APPENDIX 2

BOUNDARY CONDITION FUNCTIONS FOR MISMATCH THEORYS.

A2.1 u Functions for Mismatch Theory

In this section the results for u_{1-4} obtained from (5.6), (5.7), (A1.9) and (A1.6) are given for reference.

For E>Δ :

$$u_1 = X^{-1}[(\ell/\lambda_2)^S 1/2\gamma(\varepsilon/E)(1-\gamma^2)^2 + (1+\gamma^2+2\gamma\varepsilon/E)]$$
$$u_2 = u_4 = X^{-1}[2\gamma+\varepsilon/E+\gamma^2\varepsilon/E]$$
$$u_3 = X^{-1}[(\ell/\lambda_2)^N 1/2\gamma(\varepsilon/E)(1-\gamma^2)^2 + (1+\gamma^2+2\gamma\varepsilon/E)]$$

where $$X = (\ell/\lambda_2)^N(\ell/\lambda_2)^S 1/2\gamma(\varepsilon/E)(1-\gamma^2)^2$$
$$+ [(\ell/\lambda_2)^N+(\ell/\lambda_2)^S](1+\gamma^2+2\gamma\varepsilon/E) + 2(E/\varepsilon)(1-(\varepsilon/E)^2)\gamma$$

For E<Δ:

$$P(E) = (A-1)(1-(\Delta/E)^2) \qquad \text{where } A=(1+\gamma^2)^2/4\gamma^2$$

A2.2 u Functions for Imperfect Interface Theory.

These functions were obtained from (5.10),(5.11),(A1.9) and (A1.6).

For E>Δ:

$$u_1 = Y^{-1}[0.5(\ell/\lambda_2)^S(a^4+4a^2)+2+(2+a^2)(E/\varepsilon)]$$
$$u_2 = u_4 = Y^{-1}[2(1+(E/\varepsilon))+a^2]$$
$$u_2 = Y^{-1}[0.5(\ell/\lambda_2)^N(a^4+4a^2)+2+(2+a^2)(E/\varepsilon)]$$

where $$Y = (\ell/\lambda_2)^N(\ell/\lambda_2)^S 0.5(a^4+4a^2)$$
$$+ [(\ell/\lambda_2)N+(\ell/\lambda_2)S](2+(2+a2)(E/\varepsilon)) + 2((E/\varepsilon)2-1)$$

For $E<\Delta$:

$$P(E) = (4R/(1-R))(1-(\Delta/E)^2) \quad \text{where } R = a^2/(4+a^2)$$

A2.3 Proximity Effect.

In order to take account of the proximity effect (Section 5.8) the subgap boundary conditions are modified to:

$$P(E) = (4R/(1-R))(1-(\Delta/E)^2) \qquad \text{for } \Delta_o/X<E<\Delta_o$$

$$P(E) = (4R/(\theta^2-R/\theta^2))(1-(\Delta/E)^2) \qquad \text{for } 0<E<\Delta_o/X$$

where $X=\Delta_o/\Delta_N$, $\theta=\exp[(\Delta_N K_N^{-1}/hv_F)f(E/\Delta_N)]$

and $f(u) = (1-u^2)^{0.5} - u\cos^{-1}u$

APPENDIX 3

EXPERIMENTS TO MEASURE THERMOPOWER OF W.

This appendix describes the attempts to measure independently the thermopower (and resistance) of the W. The basic approach was to measure G and R along a slice of W by mounting it in the insert in place of a sample. (This was the method used by Battersby (1982) to measure the properties of his Cu). The practical problem which arose was how to mount the slice in such a way that the properties of the W dominated the properties of the total system. The original idea was to mount the slice by clamping with screws and washers. This was unsatisfactory because unacceptably large temperature drops were found to occur across such joints when a heat current was passed along the slice. It was therefore found necessary to use In/W joints prepared in the same way as in sample preparation. The procedure was to coat one side of the W entirely with In as described in Section 3.7. The In was then removed from all of the slice except a blob at either end. The slice was mounted by these blobs between the block and the sample heater with Woods Metal.

The remaining question was where to attach the Nb voltage leads. The initial idea was to attach them at points in the middle of the slice to facilitate a four-terminal measurement. This was tried once using Pb contacts clamped to the slice with screws; these were found to have a resistance of less than 10^{-6} Ω which was low enough. It was difficult to obtain reliable data with this arrangement because the voltage contacts were of necessity too close together so the voltages being measured were very small. In addition there were worries that the superconducting Pb pads would have undesirable effects on the current flow (ideally a π shaped piece of W would have been used). It was also suspected that the heat flowing along the voltage leads and across the NS interfaces of the Pb contacts would complicate matters.

The arrangement finally used was the same as that employed with the samples: voltage leads embedded in the Woods Metal joints. This is illustrated in Fig. A3.1. The fact that this was only a two-terminal measurement was not significant since the joints were superconducting. The problem with this arrangement was that it was still, in effect, an SNS sandwich. By making the blobs of In at either end large it was hoped that the W would completely dominate the measured properties with the interface effects being negligible. (This arrangement also allowed the resistance to be measured as well as the thermoelectric data).

The results obtained using this arrangement for $(GR)_W(T)$ are shown in Fig. A3.2. It can be seen that the results unfortunately were still strongly affected by the In/W interfaces. As would be expected the In transition was strongly evident but some divergence could also be seen below. The effective In/W interface was probably very small in area because the current was constrained to flow along the slice. It was, therefore, difficult to draw any firm conclusions about the thermopower of the W from these measurements. The essential reason why Battersby, in contrast, obtained useful data on his Cu using this approach was that the W slices were both thicker and of higher resistance ratio than the Cu. This meant that, in the present case, it was not possible to ensure that the W slice dominated the properties of the sample.

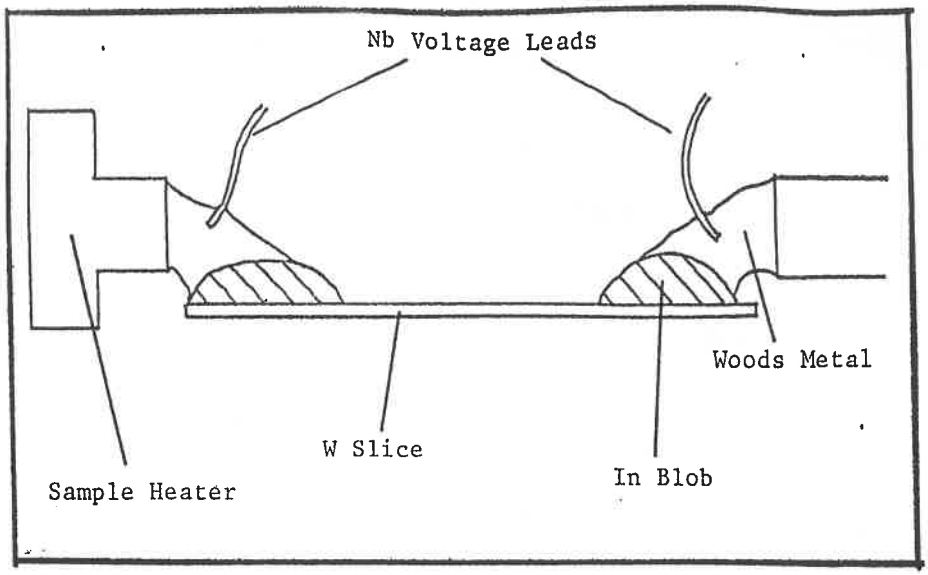

Fig. A3.1 Diagram of Arrangement to Measure Properties of the W.

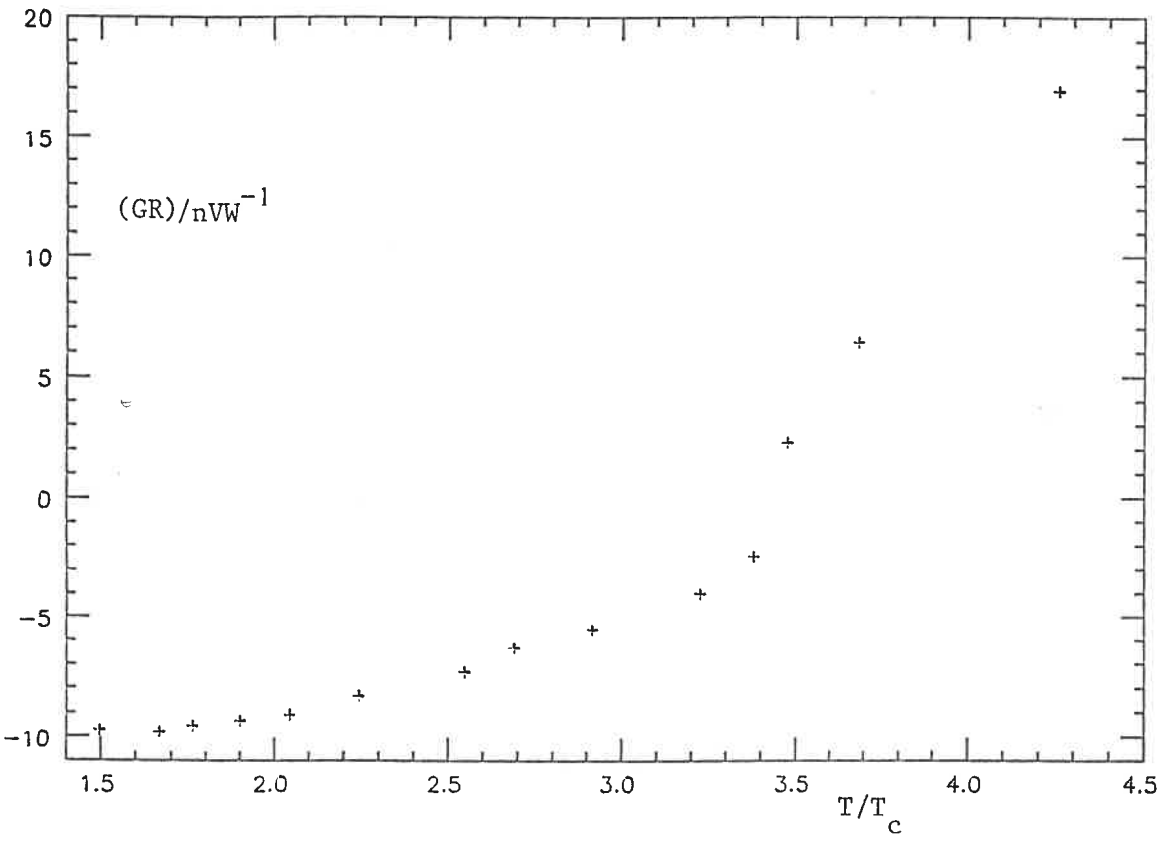

Fig. A3.2 GR(T) for W Slice.

REFERENCES

Adkins C. J. (1961) J. Sci. Instrum., **38**, 305

Andreev A. F. (1964) Sov. Phys. JETP, **19**, 1228

Bardeen J., Cooper L. N., Schrieffer J. R. (1957) Phys. Rev., **108**, 1175

Bardeen J., Rickayzen G., Tewordt L. (1959) Phys. Rev., **113**, 982

Battersby S. J., (1982) Ph.D. thesis, University of Cambridge.

Battersby S. J., Waldram J. R. (1984) J. Phys. F., **14** L109

Battersby S. J., Waldram J. R. (1987) to be published

Blakemore J. S. (1962) Rev. Sci. Instrum., **33**, 106

Bogoliubov N. N. (1958) Nuovo Cim., **7**, 794

Chambers R. G. (1952) Proc. Roy. Soc. Lond. A **215**, 481

Chang J. J. (1979) Phys. Rev. B, **19**, 1420

Chi C. C., Clarke J. (1979) Phys. Rev. B, **19**, 4495

Chi C. C., Clarke J. (1980) Phys. Rev. B, **21**, 333

Clarke J. (1967) Ph.D. thesis, University of Cambridge

Clarke J. (1972) Sol. Stat. Comm., **11**, 689

Clarke J., Freake S. M. (1972) Phys. Rev. Letts., **29**, 588

Dheer P. N. (1960) Proc. Roy. Soc. Lond., **A260**, 333

Ekin J. W., Wagner D. K. (1970) Rev. Sci. Instrum., **41**, 1109

Forgan E. M. (1974) Cryogenics, **14**, 207

Gal'perin Y. M., Gurevich V. L., Kozub V. I. (1974) Sov. Phys. JETP, **39**, 680

Garland J. C., Van Harlingen D. J. (1974a) Phys. Lett., **47A**, 423

Garland J. C., Van Harlingen D. J. (1974b) Phys. Rev. B, **10**, 4825

de Gennes P. D. (1964) Rev. Mod. Phys., **36**, 225

Ginzburg V. L. (1944) Sov. Phys. JETP, **8**, 148

Ginzburg V. L., Zharkov G. F. (1978) Sov. Phys. Usp. **21**, 381

Guenault A. M. (1960) Ph.D. thesis, University of Cambridge

Hansen M. (1958) Constitution of Binary Alloys. McGraw-Hill

Harding G. L. (1973) Ph.D. thesis, University of Cambridge

Harding G. L., Pippard A. B., Tomlinson J. R. (1974) Proc. Roy. Soc. Lond. **A340**, 1

Holland L. (1956) Vacuum Deposition of Thin Films. Chapman and Hall

Hook J. R., Waldram J. R. (1973) Proc. Roy. Soc. Lond., **A334**, 171

Hsiang T. Y., Clarke J. C. (1980) Phys. Rev. B, **21**, 945

McMillan W. L. (1968) Phys. Rev. **175**, 559

Meissner H. (1960) Phys. Rev. **117**, 672

Merriam M. F. (1963) Phys. Rev. Letts., **11**, 321

Merriam M. F. (1964) Rev. Mod. Phys., **36**, 152

Muhlschlegel (1959) Z. Phys., **155**, 313

Pankratov N. A., Zaitsev G. A., Khrebtov I. A. (1971) Cryogenics, **17**, 138

Pethick C. J., Smith H. (1980) J. Phys. C., **13**, 6313

Pippard A. B. (1984) Proc. Roy. Soc. Lond., **A391**, 255

Pippard A. B., Shepherd J. G., Tindall D. A. (1971) Proc. Roy. Soc. Lond., A324, 17

Rosebury F. (1965) Handbook of Electron Tube and Vacuum Technology, Addison Wesley, 298

Selzer P. M., Fairbank W. M. (1974) Phys. Letts., **48A**, 279

Shepherd J. G. (1971) Ph.D. thesis, University of Cambridge

Shoenburg D. (1969) in The Physics of Metals - 1. Electrons, Ziman J. M. ed., Cambridge, 112

Smithells C. J. (1936) Tungsten, a Treatise on its Metallurgy, Properties and Applications. 2nd ed.

Shelankov A. L. (1985) Sov. Phys. Sol. Stat., **27** 965

Sparlin D. M., Marcus J. A. (1966) Phys. Rev., **144**, 484

Tindall D. A. (1971) Ph.D. thesis, University of Cambridge

Tomlinson J. R. (1973) Ph.D. thesis, University of Cambridge

Van Harlingen D. J., Heidel D. F., Garland J. C., (1980) Phys. Rev. B, **21**, 1842

Van Harlingen D. J. (1981a) J. Low Temp. Phys., **44**, 163

Van Harlingen D. J. (1981b) Proc. LT-16.

Wagner D. K., Garland J. C., Bowers R., (1971) Phys. Rev. B, **3**, 3141

Waldram J. R. (1975) Proc. Roy. Soc. Lond., **A345**, 231

Waldram J. R. (1986) Private Communication

Waldram J. R., Pippard A. B., Clarke J. (1970) Phil. Trans. Roy. Soc., **A268**, 265

Welker N. K., Bedard F. D. (1977) SQUID - Superconducting Quantum Interference Devices and their Applications, Hahlbohm H. D., Lubbig H. eds. 200

White K. W. (1968) Experimental Techniques in Low Temperature Physics, Oxford p142